DOCTORAT BIOLOGIE BRETAGNE SANTE LOIRE

ÉCOLE NATIONALE VÉTÉRINAIRE, AGROALIMENTAIRE ET DE L'ALIMENTATION
SANTÉ ET ALIMENTATION AU CŒUR DE LA VIE

THESE DE DOCTORAT DE

ONIRIS

ECOLE DOCTORALE N° 605
Biologie Santé
Spécialité : « *Nutrition et Pathologies Métaboliques* »

Par
Michelle MOUGHAIZEL

Metabolic and cardiovascular effects of nitric oxide-cyclic guanosine monophosphate (NO-cGMP) signaling pathway modulation: Study in the WHHL rabbit as an experimental model of high fructose high fat diet-induced metabolic syndrome.

Thèse présentée et soutenue à Nantes, le 16 décembre 2020
Unité de recherche : Nutrition, PhysioPathologie et Pharmacologie (NP3, 2017.B146)

Rapporteurs avant soutenance :

Valérie Nivet-Antoine — Professeur, UFR Pharmacie Paris Descartes, Paris
Caroline Prouillac — Professeur, VetAgroSup, Lyon

Composition du Jury :

Président : Khadija Ouguerram — Professeur, Faculté des Sciences, Université de Nantes
Examinateurs : Rana Chaaya — Maître de Conférences, Faculté d'agronomie et de Médecine Vétérinaire, Liban

Dir. de thèse : Jean-Claude Desfontis — Professeur, Oniris, Nantes
Co-dir. de thèse : Mohamed Yassine Mallem — Professeur, Oniris, Nantes

Invité(s)
Mickael Théron — Maître de Conférences, Université de Bretagne Occidentale, Brest

DOCTORAT BIOLOGIE BRETAGNE SANTE LOIRE

ÉCOLE NATIONALE VÉTÉRINAIRE, AGROALIMENTAIRE ET DE L'ALIMENTATION
SANTÉ ET ALIMENTATION AU CŒUR DE LA VIE

THESE DE DOCTORAT DE

ONIRIS

ECOLE DOCTORALE N° 605
Biologie Santé
Spécialité : « *Nutrition et Pathologies Métaboliques* »

Par
Michelle MOUGHAIZEL

Metabolic and cardiovascular effects of nitric oxide-cyclic guanosine monophosphate (NO-cGMP) signaling pathway modulation: Study in the WHHL rabbit as an experimental model of high fructose high fat diet-induced metabolic syndrome.

Thèse présentée et soutenue à Nantes, le 16 décembre 2020
Unité de recherche : Nutrition, PhysioPathologie et Pharmacologie (NP3, 2017.B146)

Rapporteurs avant soutenance :

Valérie Nivet-Antoine	Professeur, UFR Pharmacie Paris Descartes, Paris
Caroline Prouillac	Professeur, VetAgroSup, Lyon

Composition du Jury :

Examinateurs :	Khadija Ouguerram	Professeur, Faculté des Sciences, Université de Nantes
	Rana Chaaya	Maître de Conférences, Faculté d'agronomie et de Médecine Vétérinaire, Liban
Dir. de thèse :	Jean-Claude Desfontis	Professeur, Oniris, Nantes
Co-dir. de thèse :	Mohamed Yassine Mallem	Professeur, Oniris, Nantes

Invité(s)

Mickael Théron	Maître de Conférences, Université de Bretagne Occidentale, Brest

Remerciements

Mes plus sincères remerciements vont :

à Mesdames et Messieurs les membres du jury,

Madame Valérie Nivet-Antoine,

Madame Caroline Prouillac,

Madame Khadija Ouguerram,

Madame Rana Chayya,

Monsieur Mikael Theron,

pour avoir accepté de faire partie de ce jury de thèse et d'évaluer mes travaux.

à Monsieur Jean-Claude Desfontis, mon directeur de thèse,

pour son encadrement, sa gentillesse et sa disponibilité. Merci également pour votre confiance et pour m'avoir donné la chance de réaliser cette thèse au sein de votre unité.

à Monsieur Yassine Mallem, mon co-directeur de thèse,

pour son encadrement, sa supervision continue, son organisation, sa disponibilité, sa bienveillance, sa rigueur et son exigence. Merci, de m'avoir accompagnée tout au long de mon parcours pour vos conseils, vos corrections, pour les moments de partage scientifique. Je tiens à exprimer ma reconnaissance envers votre implication inestimable dans ce projet.

à Madame Karine Pichavant et Monsieur Moez Rhimi,

pour avoir accepté de faire partie de mon comité de suivi de thèse et pour m'avoir suivie pendant ces 3 années. Merci pour tous vos conseils et remarques pertinentes qui m'ont permise d'améliorer mon projet.

à tous les membres de l'unité de pharmacologie,

Hervé Pouliquen, Martine Kammerer, Françoise Bodin, Daria Pineau, Sandrine Destrumelle et Valérie Lalanne, pour tous ces moments de partages. Merci également à Valérie pour avoir effectué les dosages de GMPc.

à tous les membres de Laboniris,

Jérôme Abadie, Sophie Lancien, Sophie Labrut, Florence Lezin, Bernard Fernandez, Suzy Calves, Caroline Berder de m'avoir accueillie au sein de votre laboratoire toujours dans la bonne humeur. Merci pour tous ces moments de convivialités partagés avec vous pendant les pauses café et les déjeuners à la cafète. Je tiens aussi à remercier les membres de l'unité LDH de m'avoir permise d'utiliser leurs lecteurs de plaques.

à tous les membres du CRIP,

Je tiens à remercier Monsieur Olivier Gauthier et Madame Gwenola Touzot de m'avoir accueillie au sein du CRIP et pour leur confiance. Je remercie également Madame Ingrid Leborgne et Monsieur Patrice Leroy, pour leur aide leur gentillesse et leur disponibilité permanente.

à Madame Chantal Thorin,

pour votre gentillesse, votre bienveillance et pour vos conseils en analyses statistiques. Merci également pour tous ces moments de convivialités partagés avec vous à la cafète.

à Madame Sylvie Chauvin,

pour son soutien, sa bienveillance et son énergie positive qui m'a permise de décompresser dans un climat humoristique et détendu permanent. Tu es quelqu'un d'exceptionnel ! Je vous souhaite plein de bonheur et de joie à toi et à ta famille.

à Madame Frédérique Sauvaget,

merci pour ton soutien, ta gentillesse, ta bienveillance. Merci également pour nos discussions infinies et nos rigolades dans la cafète et surtout merci pour ton honnêteté et ton caractère juste et humble. Ta présence a rendu les pauses beaucoup plus agréables. Tu es quelqu'un que je respecte, que j'admire énormément. Je te souhaite plein de bonheur et de joie.

à Madame Fanny Kieken,

pour ton soutien et ta gentillesse dans l'organisation de cette thèse. Merci pour ton oreille attentive et tes précieux conseils.

à Madame Anne huet,

pour le travail et les efforts qu'elles effectuent pour faciliter la vie des doctorants. Merci beaucoup pour ta gentillesse et ton soutien.

à Nora Bouhsina,

Merci pour ta gentillesse et ton aide. Ca m'a fait un grand plaisir de travailler avec toi. Bon courage pour la suite.

à Chloé, Maurine, Niki, Floran, petite Chloé et Kévin,

avec qui j'ai partagé dans le bureau des moments inoubliables. Je n'ai pas vu le temps passé à vos côtés. Je vous souhaite une bonne continuation et une vie pleine de bonheur. Vous m'avez tous marqué.

à Yosra,

une collègue et amie. Ensemble, nous avons vécu de nombreuses expériences. Merci pour tes encouragements et pour tous nos bons moments de rigolades. Je te souhaite une très bonne continuation et un futur plein de succès et de bonheur.

à Mohammed, mon stagiaire préféré, (même si tu es le seul)

pour ton aide et ton soutien permanent. Ton optimisme, ta confiance en toi et ta persévérance t'emmènerons très loin. Bravo, je suis très fière de toi ! Bon courage pour la suite. Je serai toujours là pour toi. Surtout, garde ton enthousiasme et ton sourire contagieux !

à Clément,

Clémoun, un vrai ami ! Une personne exceptionnelle ! Merci pour ton humour, pour ton aide et tous les moments drôles que nous avons partagé. Mais surtout merci de m'avoir écoutée et encouragée. Tu m'as toujours soutenue. Je serai toujours là pour toi. A très bientôt.

à Florian, Pichpich, Lydouille, Alicounette et Marinus,

pour tous ces moments partagés, pour nos fous rires pendant nos petites pauses qui m'ont permise de décompresser, ainsi que pour toutes nos soirées et sorties inoubliables (bowling, Lazer game et autres). Mais, surtout pour votre amitié envers les deux libanais expatriés. Ces 3 dernières années ans sont passés beaucoup plus vite à vos côtés.

à Effi et Vasilis,

nos chers amis grecs avec qui nous partageons la culture du bassin méditerranéen. Pour tous les moments de fun que nous avons passé ensemble, pour nos sorties au centre-ville où les gens nous regardaient de travers parce que nous étions les seuls à crier.

à Georges, Anthony et Walid,

qui donne à notre quotidien français un goût d'houmous et de Knéfé. Merci pour tous ces moments de partage et d'échange de recettes libanaises ! A très bientôt.

à Alex,

pour tes conseils précieux, et l'aide que tu m'as apportée, surtout dans les kits de dosage infinis ! Tu es quelqu'un de très admirable qui aime partager sans rien demander en retour. Mais surtout merci de m'avoir écoutée, encouragée et toujours proposée de l'aide. Enfin merci pour ces bons moments passés ensemble avec pleins de gossip ! A très bientôt à Lyon.

à Ophélie,

pour ton soutien, tes encouragements, et tes messages pleins d'amour qui m'ont remontée à chaque fois le moral. Merci pour les longues conversations au téléphone avec pleins de gossip et de rigolades. Tu me manques beaucoup. Le bureau était si vide après ton départ.

à Antoun,

pour ton énergie positive, ton humour et tes idées rebelles et philosophiques (on ne s'ennuie jamais à tes côtés). Merci pour ces moments inoubliables que nous avons passé ensemble. Tu as su ajouter du peps à nos rencontres ! Tu nous manques beaucoup ! Nous avons hâte de visiter l'Est de la France avec toi ! A très bientôt sur Lyon.

à Cindy et Ibrahim,

pour avoir été là pendant les moments heureux et les moments difficiles. Merci pour toutes ces soirées et ces dîners partagés. Merci d'être notre famille nantaise ou plutôt bretonne. Vivement la fin de la thèse pour passer pleins de week-end à Lyon et évidement à Nantes aussi.

à Elsy, Petra, et Yara mes meilleures amies

pour votre amitié. Je suis fière de vous et de votre parcours. Vous me manquez beaucoup.

à mes cousins et cousines,

Maria, Jane, Georges, Dédé, Dona, Wendy, Joy, Johnny et Daniel. Je vous aime.

à ma belle-famille ou plutôt ma seconde famille,

Joseph, Eliane et le frère que je n'ai jamais eu Karl. Merci pour votre soutien continu et merci d'être toujours là pour nous. Merci surtout de m'avoir confiée le plus beau des cadeaux au monde. Je vous aime. A Karl, pour tous nos moments partagés et nos discussions souvent à 1h du matin, après mes longues journées de rédaction.

à ma tante Leila,

mon ange gardien à qui je tiens énormément et qui m'a toujours soutenu. Je t'aime fort.

à ma famille,

mes chers parents, Joseph et Amale pour leurs soutiens constants et leurs encouragements. Sans vos sacrifices, je n'y serais jamais arrivée. Je vous dois beaucoup et j'espère que vous êtes fières de moi.

A mes sœurs Paulina et Marie-Joe, à qui je tiens énormément. Je vous remercie du fond du cœur pour votre écoute et votre soutien permanent. Je serai toujours là pour vous et je sais que je pourrai toujours compter sur vous. Je vous aime très fort ! Vous me manquez énormément ! Fêter Noël ne sera pas pareil sans vous. Je remercie aussi Jessy une personne que je considère comme un membre de notre famille (can't wait guys).

à Elie,

mon meilleur ami, mon confident, mon mari et surtout ma personne préférée. Je suis éternellement reconnaissante pour ton soutien et ton amour qui m'ont apporté un support moral tout au long de mon parcours et m'ont certainement permise d'arriver jusque-là. Sans toi, ce travail n'aurait pas été accompli. Je me considère très chanceuse de t'avoir dans ma vie. Tu étais là pour moi jour et nuit. Je serai là avec toi pour le meilleur et pour le pire. Merci d'avoir pris soin de moi ces derniers mois ! J'ai hâte de commencer notre nouvelle vie ! Sans études et sans stress ! Dans notre nouvel appartement et dans une nouvelle ville ! Je t'aime vraiment, follement et profondément.

Contents

List of figures

List of tables

List of abbreviations

AA	Arachidonic Acid
ACE	Angiotensin converting enzyme
ACEI	ACE inhibitors
ACs	Adenylate cyclase
ADMA	Asymmetric dimethyl-arginine
Akt	Protein kinase B
Ang II	angiotensin II
ANP	Atrial natriuretic peptide
ApoB	Apolipoprotein B
ARBs	Angiotensin receptor blockers
AT1 receptor	Type 1 Angiotensin receptor
BAT	Brown adipose tissue
BH4	Tetrahydrobiopterin
BK	Bradykinin
BP	Blood pressure
CA	Catecholamine
cAMP	Cyclic adenosine monophosphate
CCBs	Calcium channel blockers
CETP	Cholesteryl ester transfer protein
cGMP	Cyclic guanosine monophosphate
CMs	Cardiac myocytes
COX	Cyclooxygenase
CRP	C-reactive protein
CVD	Cardiovascular disease
ED	Endothelial dysfunction
EDHF	Endothelial-derived hyperpolarizing factor
eNOS	Endothelial nitric oxide synthase
ER	Endoplasmic reticulum
ET-1	Endothelin-1

FAD	Flavin adenine dinucleotide
FFAs	Free fatty acids
FMN	Flavin mononucleotide
GLP-1	Glucagon-like peptide 1
HDL	High density lipoprotein
HFFD	High-fructose high-fat diet
HOMA-IR	Homeostatic model assessment of IR
i[Ca^{2+}]	Intracellular calcium concentrations
IL-6	Interleukin-6
IR	Insulin resistance
IRS-1	Insulin receptor substrate 1
LDL	Low density lipoprotein
LDLr	Low density lipoprotein receptor
LTCC	L-type calcium channel
MAPK	Mitogen-activated protein kinase
MetS	Metabolic syndrome
NADPH	Nicotinamide adenine dinucleotide phosphate
NFκB	Nuclear factor kappa B
nNOS	Neuronal NOS
NO	Nitric oxide
NOS	Nitric oxide synthase
NOX	NADPH oxidase
NP	Natriuretic peptide
NPY	Neuropeptide Y
O_2^-	Superoxide anion
$ONOO^-$	Peroxynitrite
PAI-1	Plasminogen activator inhibitor-1
PDE	Phosphodiesterase
pGC	Particulate guanylyl cysclase
PGE_2	Prostaglandin E_2
PGI_2	Prostacyclin

PI3K	Phosphoinositide 3-kinase
PKA	Protein kinase A
PKG	Protein Kinase G
RAAS	Renin angiotensin aldosterone
RAS	Ras protein
RNS	Reactive nitrogen species
ROS	Reactive oxygen species
sAC	Soluble adenylate cyclase
sGC	Soluble guanylyl cyclase
SMCs	Smooth muscle cells
SNS	Sympathetic nervous system
T2DM	Type 2 diabetes mellitus
TGs	Triglycerides
TNF-α	Tumor necrosis factor-α
TxA_2	Thromboxane
VLDL	Very low density lipoprotein
WHHL	Watanabe heritable hyperlipidemic
WAT	White adipose tissue
XO	Xanthine oxidase
$\beta_{1/2/3}$-AR	$\beta_{1/2/3}$-adrenoceptor

Introduction

The metabolic syndrome (MetS), also known as the cardiometabolic syndrome, is a cluster of several risk factors that when combined increase the risk of an individual developing cardiovascular disease (CVD). The MetS associates, abdominal obesity, insulin resistance (IR), dyslipidemia and arterial hypertension. Underlying causes of the MetS are related to a worldwide spread of the western lifestyle, which is characterized by increased consumption of high caloric-low fiber food (fast food) and lack of physical activity (sedentary lifestyle). The MetS has become the major global health hazard of the modern world. Besides being a clinical challenge and its serious impact on the individual's health, it is undeniable that the MetS is also implicated in increasing healthcare costs.

Whether for investigating the pathogenesis or for finding an appropriate treatment, working on suitable animal models of MetS is of utmost importance. In our study, we aimed to develop an animal model of MetS with two main factors, dyslipidemia and IR. In order to induce IR, we used a high-fructose fat-diet (HFFD). As for the animal used in this study, it involves the Watanabe heritable hyperlipidemic (WHHL) rabbit, which, due to a mutation in its low-density lipoprotein receptor (LDLr), develops spontaneous dyslipidemia and atherosclerosis.

Scientific investigation to improve therapeutic and preventive measures to manage the MetS has become essential. Currently most of the treatments used in the management of this syndrome are directed towards each risk factor alone. Therefore, using molecules with pleiotropic effects or that acts on a broad spectrum of tissues and cells, might be more successful in managing this multifactorial complex syndrome. We hypothesized that modulation of nitric oxide-cyclic guanosine 3',5'-monophosphate (NO-cGMP) signaling by pharmacological tools might represent a promising therapeutic modality for treating the MetS and its related cardiovascular pathologies. Our hypothesis was made based upon promising results related to nitric oxide-sGC-cyclic guanosine 3',5'-monophosphate (NO-sGC-cGMP) signaling modulation in metabolic and cardiovascular disease. Thus, we investigated the potential of two different molecules, BAY 41-2272 (a sGC stimulator) and mirabegron (a β_3-adrenoceptor (β_3-AR) agonist), both activators of the NO-sGC-cGMP signaling pathway, as treatments of MetS and its cardiovascular consequences.

This thesis consists of four main sections: literature review, objectives, experimental study and discussion & conclusion. The first section (literature review) is divided into four chapters. In the first chapter, we detailed the definition, etiology and pathophysiology of the MetS. In the second chapter, we reviewed the components and the role of NO-sGC-cGMP pathway in the cardiovascular system. We displayed the main cardiovascular changes/consequences of the MetS in the third chapter. Finally, we portrayed the management (pharmacological and non-pharmacological) of the MetS in the fourth chapter. The third section (experimental study) included two parts, materials & methods and results (represented as three articles).

I. Literatur review

1. Metabolic syndrome

1.1. Definition of the Metabolic Syndrome

The MetS also known as the cardiometabolic syndrome, refers to the co-occurrence of a cluster of metabolic disorders and cardiovascular risk factors. These include IR/glucose intolerance, visceral/central obesity, atherogenic dyslipidemia and arterial hypertension (Zimmet et al. 2005; Rochlani et al. 2017). Defining the MetS has been a subject of debate and controversies due to its complex, inter-dependent, multi-factorial nature (Tune et al. 2017).

Table 1: Definitions of the metabolic syndrome.

	NCEP ATP III (2005 revision)	WHO (1998)	EGIR (1999)	IDF (2005)
Absolutely required	None	Insulin resistance* (IGT, IFG, T2D or other evidence of IR)	Hyperinsulinemia‡ (plasma insulin >75th percentile)	Central obesity (waist circumference§): ≥94 cm (M), ≥80 cm (F)
Criteria	Any three of the five criteria below	Insulin resistance or diabetes, plus two of the five criteria below	Hyperinsulinemia, plus two of the four criteria below	Obesity, plus two of the four criteria below
Obesity	Waist circumference: >40 inches (M), >35 inches (F)	Waist/hip ratio: >0.90 (M), >0.85 (F); or BMI >30 kg/m^2	Waist circumference: ≥94 cm (M), ≥80cm (F)	Central obesity already required
Hyperglycemia	Fasting glucose ≥100 mg/dl or Rx	Insulin resistance already required	Insulin resistance already required	Fasting glucose ≥100 mg/dl
Dyslipidemia	TG ≥150 mg/dl or Rx	TG ≥150 mg/dl or HDL-C: <35 mg/dl (M), <39 mg/dl (F)	TG ≥177 mg/dl or HDL-C <39 mg/dl	TG ≥150 mg/dl or Rx
Dyslipidemia (second, separate criteria)	HDL cholesterol: <40 mg/dl (M), <50 mg/dl (F); or Rx			HDL cholesterol: <40 mg/dl (M), <50 mg/dl (F); or Rx
Hypertension	>130 mmHg systolic or >85 mmHg diastolic or Rx	≥140/90 mmHg	≥140/90 mmHg or Rx	>130 mmHg systolic or >85 mmHg diastolic or Rx
Other criteria		Microalbuminuria†		

WHO: World Health Organization, EGIR: European Group for the study of IR, NCEP ATPIII: National Cholesterol Education Program Adult Treatment Panel III, IDF: International Diabetes Federation. From Huang (2009)

1.2. History & clinical definitions of the Metabolic Syndrome

The concept of MetS was first introduced in 1988 by Dr. Reaven as syndrome X (Reaven 2000). However, it was not until 1998 that the **World Health Organization** (WHO) gave it a definition (Alberti and Zimmet 1998). In the WHO definition, insulin resistance (IR) was considered an essential requirement in addition to any two of the following criteria: obesity, dyslipidemia, hypertension, and microalbuminuria. Then in 1999, the **European Group for the study of IR** (EGIR) modified the WHO definition (Balkau and Charles 1999). Their definition was practically the same as the WHO's, with IR as the main criterion, but did not include microalbuminuria. The other main difference between both definitions involves the obesity

criterion. According to the WHO definition this criterion is characterized, either by waist-to-hip ratio or by body-mass index. As for EGIR it is simply portrayed as waist circumference. In 2001, the **National Cholesterol Education Program (NCEP) Adult Treatment Panel III** (ATPIII) gave a definition to the MetS that was updated in 2005 by the American Heart Association and the National Heart Lung and Blood Institute (Grundy et al. 2005). The NCEP ATP III definition is the most commonly used of all. It incorporates any three of the following five features: hyperglycemia/IR, visceral obesity, atherogenic dyslipidemia and hypertension. Later in 2005, the **International Diabetes Foundation** (IDF) considered that obesity is an essential requirement rather than IR (Grundy et al. 2005) **(Table 1)**.

1.3. Etiology

The main underlying causes of the MetS are mainly unhealthy diet and/or sedentary lifestyle that are practically translated by an imbalance between energy intake and energy expenditure. To a lesser extent genetic predisposition might also lead to the occurrence of this syndrome (Lanktree and Hegele 2017). Over the past decades, the world shift towards global industrialization/modernization has promoted an unhealthy lifestyle. The increased abundance of prepackaged food and easy access to fast-food restaurants/delivery along with a busy every-day life makes it hard for anyone to make healthier food choices. Moreover, maintaining a physical activity has also been a challenge with longer work-shifts, in addition to increased mechanized transportation/technologies (Saklayen 2018).

1.4. Epidemiology

It is well established that the prevalence of the MetS and its components have been rapidly increasing worldwide. In fact, the global prevalence of MetS is currently about 25% with over a billion people affected (Saklayen 2018). However, this increase seems to be widely influenced by the geography and ethnicity. It also seems that the pattern of its related components is different in relation to different regions (Nematy et al. 2014).

The prevalence of the MetS is often linked to the prevalence of obesity. However, with the increased awareness regarding the presence of metabolically healthy obesity, cohorts and meta-analysis studies now proceed more carefully when evaluating the prevalence of the MetS. In a collaborative analysis of ten large cohorts studies across Europe, it was found that the among all

obese subjects, 24% to 65 % women and 43% to 78% men were diagnosed with MetS (van Vliet-Ostaptchouk et al. 2014).

Scuteri et al. (2015) estimated that the overall prevalence of the MetS across Europe reached 24.3% with a prevalence of 23.9% in men versus 24.6% in women. In their study, they observed an age-related increase in the prevalence in all cohorts and described different clusters of risk factors that varies from one country to another.

Data shows that the prevalence of MetS in the United States (US) increased by 35% from 1980s to 2012 (Lanktree and Hegele 2017). According to the 2017 CDC published data, about one third of US adults have MetS (Saklayen 2018). Moreover, it is predicted that by 2030, 86% of US adults will be overweight or obese (Youfa Wang et al. 2008).

1.5. Pathophysiology

1.5.1. Abdominal/visceral obesity

According to the WHO, an individual is considered obese when his body mass index (BMI)[1] is 30 or above. When BMI ranges between 25 to 34.9 kg/m2, sex-specific waist circumference cutoffs are used concomitantly with BMI to identify patients at risk. Man and woman are considered obese when their waist circumference exceeds 102 and 88 cm, respectively (WHO 2020).

The "obesity epidemic" is primarily caused by increased consumption of high calorie food and reduced physical activity that leads to an imbalance between energy intake and energy expenditure and eventually to an excessive weight gain (Drenowatz 2015). In obesity, the balance between adipocytes lipolysis and triglyceride synthesis, that is usually regulated by hormones and autonomic nervous system is disrupted (Kershaw and Flier 2004). Besides its function in energy storage, adipose tissue is an endocrine organ that participates in energy homeostasis and thus responds rapidly and dynamically to alterations in energy. It adapts to nutrient excess through hypertrophy and hyperplasia (Halberg, Wernstedt-Asterholm, and Scherer 2008; Sun, Kusminski, and Scherer 2011; Longo et al. 2019). Due to adipocyte enlargement, the blood supply is reduced

[1] BMI is calculated using the following formula: weight / (height)^2 (kg/m^2). Obesity = BMI is between 30 and 40. Morbid obesity = BMI > 40

subsequently leading to hypoxia (Ellulu et al. 2017). It was proposed that hypoxia then induces necrosis and macrophage infiltration leading to overproduction of adipocytokines including, pro-inflammatory mediators (tumor necrosis factor-α (TNF-α) and interleukin-6 (IL-6)), free fatty acids (FFAs), leptin, plasminogen activator inhibitor-1 (PAI-1), C-reactive protein (CRP), leptin and angiotensinogen (Ye 2009; Chan and Hsieh 2017) **(Figure 1)**. The localized adipose tissue inflammation later spreads to an overall systemic low-grade inflammation, leading to other complications seen in the MetS (Zatterale et al. 2020). Moreover, body fat distribution seems to play an important role in the pathogenesis of the MetS. For instance, visceral adipose tissue accumulation has much more harmful metabolic consequences than peripheral and subcutaneous adiposity (Castro et al. 2014). This is due to the fact that, both, the resistance to the insulin-mediated metabolic effects and the rate of lipolysis are higher in visceral than in peripheral fat (Jensen 1997; Cnop et al. 2002). Moreover, ectopic fat deposition, whether alone or in association with increased visceral adiposity was also found to be incriminated in the development of obesity-induced anomalies especially IR in MetS (Guebre-Egziabher et al. 2013).

1.5.1.1. Role of adipocytokines in the development of obesity-related comorbidities

Free fatty acids

Free fatty acids (FFAs) result from the mobilization of energy stores (triglycerides, TGs) in adipose tissue via lipolysis. During periods of fasting, the latter process is initiated by catecholamines (CAs) which stimulate the release of FFAs under the action of cyclic adenosine monophosphate (cAMP) consecutive to β-adrenergic stimulation. The excessive release of FFAs into the circulation, during obesity, impairs the insulin's anti-lipolytic action, further increasing the FFA release into the circulation (McCracken et al. 2018). In addition, the increased delivery of FFA to the liver and muscle leading to atherogenic dyslipidemia and IR[2] respectively. Moreover, FFAs themselves might cause increases in blood pressure[3].

[2] The responsible mechanisms are detailed in the dyslipidemia and IR sections of chapter 1.
[3] The mechanisms responsible for increased blood pressure are detailed in the hypertension section of chapter 1.

Tumor necrosis factor-α

The pro-inflammatory cytokine, TNF-α is a paracrine mediator that is produced and secreted from the adipose tissue (Makki, Froguel, and Wolowczuk 2013). It increases the release of FFAs to the circulation through stimulating lipolysis. Rodent studies showed that TNF-α in adipose tissue of obese rodents causes IR in skeletal muscle and liver (Hotamisligil et al. 1993). TNF-α affects insulin sensitivity and action through downregulating multiple genes that participate in insulin action (i.e. insulin receptor, insulin receptor substrate 1 and glucose transport (GLUT4) (Rydén and Arner 2007). TNF-α also promotes IR in adipocytes and muscle by inhibiting both the insulin receptor and IRS-1 activity (Kanety et al. 1995; Hotamisligil et al. 1996; Makki, Froguel, and Wolowczuk 2013). TNF-α might raise serum TG levels *via* stimulating very low density lipoprotein (VLDL) production and also may inhibit lipid storage *via* the downregulation of lipoprotein lipase (Fernández-Real and Ricart 2003; Rydén and Arner 2007). Moreover, a positive correlation exists between TNF-α and body weight, waist circumference, and triglycerides (TGs) whereas, TNF-α negatively correlates with high density lipoprotein-cholesterol (HDL-C) (Xydakis et al. 2004).

C-reactive protein

C-reactive protein (CRP) levels are good predictors of future cardiovascular events and are also used as predictors of negative outcomes in MetS patients (Clearfield 2005; Mirhoseini et al. 2018; Hong et al. 2020). CRP is produced by the liver in response to inflammation. Increased CRP levels were found to be associated with increased IR and hyperglycemia (Soto González et al. 2006). It seems that CRP levels increase in obese with IR but, not in obese individuals with normal insulin sensitivity (McLaughlin et al. 2002). In addition, human studies demonstrated that CRP reduces NO release from arterial and venous endothelial cells and endothelial nitric oxide synthase (eNOS) activity leading to endothelial dysfunction (ED). Moreover, clinical and experimental studies points towards a role of CRP as a pro-atherogenic factor (Devaraj, Siegel, and Jialal 2011).

Interleukin-6

Interleukin-6 (IL-6) acts as both an inflammatory and anti-inflammatory agent. It is secreted by both skeletal muscle and adipose tissue (Pedersen et al. 2001; Sandoo et al. 2010; Scheller et al. 2011). In addition, it is mainly produced by visceral rather than subcutaneous adipose tissue (Fried et al. 1998). Besides its ability to control appetite, energy intake and energy expenditure

through its receptors in the hypothalamus, it also seems that IL-6 decreases insulin sensitivity (Yudkin et al. 2000; Senn et al. 2002; Stenlöf et al. 2003; Pazos et al. 2013). In addition, it has been proposed that IL-6 has pro-coagulant effects, stimulates adhesion molecules to the vascular endothelium and increases hepatic production of fibrinogen and CRP. Moreover, IL-6 also stimulates the central and the sympathetic nervous system (SNS) contributing to hypertension (Yudkin et al. 2000). Furthermore, Il-6 appears to be negatively correlated with HDL-C (Zuliani et al. 2007). Finally, increased IL-6 levels predicts cardiovascular mortality (Ridker et al. 2000).

Plasminogen activator inhibitor-1

Plasminogen activator inhibitor-1 (PAI-1) is considered to be an important factor in the MetS. It inhibits the tissue plasminogen activator, a protein involved in the breakdown of blood clots. Thus, it is considered as a marker of an impaired fibrinolysis and athero-thrombosis (Marie Christine Alessi and Juhan-Vague 2006). It is secreted from abdominal adipocytes, platelets, and vascular endothelium (Yoo 2014). Its increased secretion leads to a prothrombotic state, that is often seen in abdominally obese individuals and during inflammation (M. C. Alessi and Juhan-Vague 2004). Besides its role in inducing athero-thrombosis. PAI-1's increased levels are associated with increased adverse cardiovascular outcomes (Kohler and Grant 2000)

Adiponectin

Adiponectin is an anti-inflammatory cytokine. Besides having an anti-inflammatory effect, it also has anti-atherogenic properties (Ukkola and Santaniemi 2002). In fact, adiponectin hinder the development of mature atheroma plaques through inhibiting endothelial activation, reducing the transformation of macrophages into foam cells, and inhibiting smooth muscle (SM) proliferation and arterial remodeling (Matsuzawa et al. 2004). Besides having, a protective effect through antagonizing TNF-α action, adiponectin also seems to exert many beneficial effects on metabolism (Ouchi et al. 2000). It improves insulin sensitivity (Goldstein and Scalia 2004) and also regulates energy balance and both glucose and lipid metabolism through activating the AMP protein kinase (AMPK[4]). This activation stimulates both glucose utilization and fatty-acid oxidation (Yamauchi et al. 2002).

[4] AMPK stimulates switches the cells from an anabolic state to a catabolic state

During obesity, adiponectin levels are decreased, particularly in individuals with abdominal obesity (Guenther et al. 2014). Moreover, low adiponectin plasma concentrations were associated with almost all the risk factors, constituting the metabolic syndrome (Santaniemi et al. 2006).

Leptin

Leptin is synthetized by the adipose tissue and plays a key role in regulating satiety and energy intake (Yoo 2014). Its receptors are expressed in different regions of the brain, i.e. hypothalamus and brain stem. Leptin exerts its effects, through activating these receptors. Its functions involve controlling appetite, energy expenditure (through thermogenesis) and other neuroendocrine functions (Hutley and Prins 2005). Leptin also acts directly on peripheral tissues such as muscle, where it promotes glucose uptake. Obesity often leads to elevated levels of leptin and eventually to a leptin resistance state during which all the beneficial effect of leptin are counteracted. For instance, hyperleptinemia becomes not able to suppress appetite, which explains the hyperphagia often seen in individuals with overweight and obesity (Morton and Schwartz 2011). In addition, leptin is able to induce hypertension through multiple mechanisms[5].

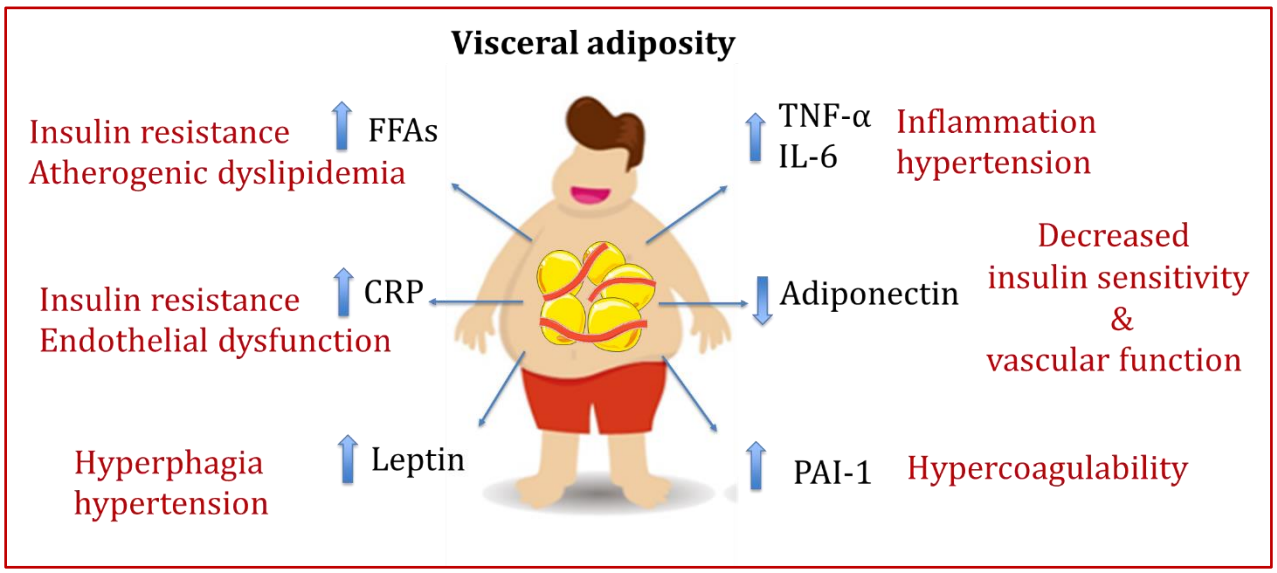

Figure 1: Role of visceral obesity in the development of metabolic syndrome.

[5] More details in hypertension section chapter 1.

CRP: C-reactive protein, FFAs: free fatty acids, PAI-1: plasminogen activator inhibitor-1, TNF-α: tumor necrosis factor-α. Inspired by Huang (2009).

There is substantial evidence that the MetS is associated with increased SNS activity. Central obesity seem to be one of the main metabolic alterations linking these two together (Tune et al. 2017). Animal and human studies have shown that overeating increases the sympathetic activity as an adaptive physiologic response aiming to stabilize body weight through increased thermogenesis and energy expenditure (Landsberg 2001). Even though this response is beneficial in physiologic states, during prolonged overfeeding, chronic thermogenesis leads to sustained β-adrenergic activation in peripheral/resistance vessels and kidneys. The latter, induces a secondary rise in blood pressure and hypertension via sodium retention, glomerular hyperfiltration and renin release (G. W. Lambert et al. 2010). Moreover, it was found that body fat distribution directly affects the degree of overactivity, which is greater in individuals with central obesity rather than subcutaneous obesity (Straznicky et al. 2008). Leptin exerts its effects, i.e. appetite reduction and energy expenditure increase via sympathetic activation. Thus, the chronic hyperleptinemia encountered during obesity, leads to leptin receptors desensitization, which is translated by a decrease in its anorexigenic effect with preserved sympathoexcitation (Mark et al. 2002; Morton and Schwartz 2011).

1.5.2. Insulin resistance

IR is one of the main and essential components of the MetS. It is described as an unresponsiveness of insulin-sensitive tissues to the effect of insulin (Kaur 2014). In an attempt to counterbalance this state, insulin secretion is increased leading to a state of hyperinsulinemia (Liese et al. 1998). Generally, from a biological standpoint of view, it is well documented that IR is characterized by increased levels of insulin (hyperinsulinemia), hyperglycemia and an impaired homeostatic model assessment of IR (HOMA-IR) (Beilby 2004).

Most agree that both abdominal obesity and IR are at the center of the MetS and its remaining components (Cornier et al. 2008; Gallagher, Leroith, and Karnieli 2010). Moreover, it seems that FFAs and inflammatory cytokines, not only, play a central role in the development of IR but are also the link between visceral obesity and IR (S. E. Kahn et al. 2006) (**Figure 3**). However, it is to be noted that some obese individuals are metabolically normal with normal insulin sensitivity; meanwhile, IR can be present in non-obese subjects (Ruderman et al. 1998; Karelis et al. 2005).

Furthermore, metabolically obese individuals but with normal weight are described as a category of individuals that in addition to exhibiting an impaired insulin sensitivity, display higher risks of developing T2DM, CVD and mortality (S. H. Lee et al. 2015).

Metabolic and hemodynamic effects of insulin

Insulin production by the pancreas is stimulated by hyperglycemia. In fact, its role is to maintain glucose homeostasis. It keeps glucose levels in tight control, through glucose usage and storage, in several organs, including, adipose tissue, skeletal muscle and the liver. In purpose of removing glucose from the circulation, insulin stimulates glucose uptake through the translocation of the glucose transporter (GLUT4) to the cell surface, in both skeletal muscle and adipose tissue, where it also inhibits lipolysis. In the skeletal muscle and liver, insulin prevents more glucose influx by stimulating glucose storage as glycogen and inhibiting glycogenolysis (**Figures 2&3**). Meanwhile insulin also inhibits hepatic gluconeogenesis. Insulin may also regulate glucose levels by activating insulin-signaling pathway in the hypothalamus where it exerts anorexigenic effects by inhibiting neuropeptide Y (NPY) (Kaur 2014).

Under physiologic state, Both insulin's vasodilatory and metabolic effect require signaling through insulin receptor substrate 1 (IRS-1)-phosphoinositide 3-kinase (PI3K)-protein kinase B (Akt) pathway (IRS1-PI3K-Akt) (Eringa et al. 2002). Thus, it is believed that insulin, by increasing blood flow is able to control its own access and that of other molecules i.e. glucose (Vincent et al. 2005). Insulin exerts its function by binding to its enzyme-receptor on the cell, through activating two parallel pathways, the IRS1-PI3K-Akt and the Ras protein (RAS)-mitogen-activated protein kinase (Ras-MAPK) pathways (Kim et al. 2006) (**Figure 2**). The activation of the former leads to the metabolic and vasodilatory effects of insulin via endothelial NO synthase (eNOS) and thereby NO production (Clark et al. 2003; Muniyappa et al. 2008). Meanwhile the activation of the latter leads to vasoconstriction via endothelin-1[6] (ET-1) production, expression of adhesion molecules and mitogenic effects on vascular smooth muscle cells (SMCs) (Muniyappa et al. 2008; Muniyappa and Sowers 2013). Akt kinase activates eNOS in endothelial cells and stimulates the translocation of GLUT 4 to the cells surface in both skeletal muscle and adipose tissue (J.-A. Kim

[6] A strong vasoconstrictor

et al. 2006), thereby stimulating glucose uptake, and then it activates downstream pathways of glucose metabolism (Shulman 2004) (**Figures 2&4**).

1.5.2.1. General mechanisms of insulin resistance

In states of IR, all insulin sensitive tissues become non-responsive to the effect of insulin leading to maintained hyperglycemia and to increased orexigenic effects (Kaur 2014). During IR, only the IRS1-PI3K-Akt-NO signaling pathway is reduced, meanwhile the Ras-MAPK-ET1 signaling pathway either remains intact or becomes heightened. This imbalance between both pathways leads to ED due to decreased NO synthesis with unaffected production levels of ET-1 in addition to expression of vascular cell adhesion molecules and vascular SMCs proliferation (Muniyappa and Sowers 2013). In addition, GLUT4 translocation is reduced leading to decreased fat and muscle glucose uptake (Kim et al. 2006) (**Figures 2,3&4**).

Both metabolic and hemodynamic actions of insulin seem to be complementary. Since, in addition to its vasodilatory action[7] via eNOS activation and the subsequent NO production, insulin enhances glucose delivery to target tissue through capillary recruitment[8] (Barrett et al. 2011). During IR, insulin-mediated vasodilation is compromised leading to decreased delivery of glucose and insulin to their target organs. Moreover, the impaired intracellular insulin-mediated glucose and lipid metabolism leads to increased levels of reactive oxygen species (ROS) and reactive nitrogen species (RNS) resulting in greater NO consumption, and then a further decrease in NO availability (Cersosimo and DeFronzo 2006). IR is characterized by metabolic abnormalities that include glucotoxicity, lipotoxicity, contributing to vascular damage and inflammatory response induction (adhesion of monocytes/lymphocytes to endothelial cells)(Janus et al. 2016) and leading to ED (Kim et al. 2006).

During IR, hyperinsulinemia leads to suppressed inhibition of NPY neurons and thereby promotes orexigenic effects via liver sympathetic overactivation, further inducing hepatic IR and glucose production (J. Wang et al. 2001). Hyperinsulinemia also increases sodium reabsorption in

[7] Dilation of larger-resistance vessels increases overall perfusion.
[8] Capillary recruitments occurs within minutes.

response to increased activation of nephron sodium transporters and thereby contributes to increased intravascular volume through fluid retention (Demarco, Aroor, and Sowers 2014).

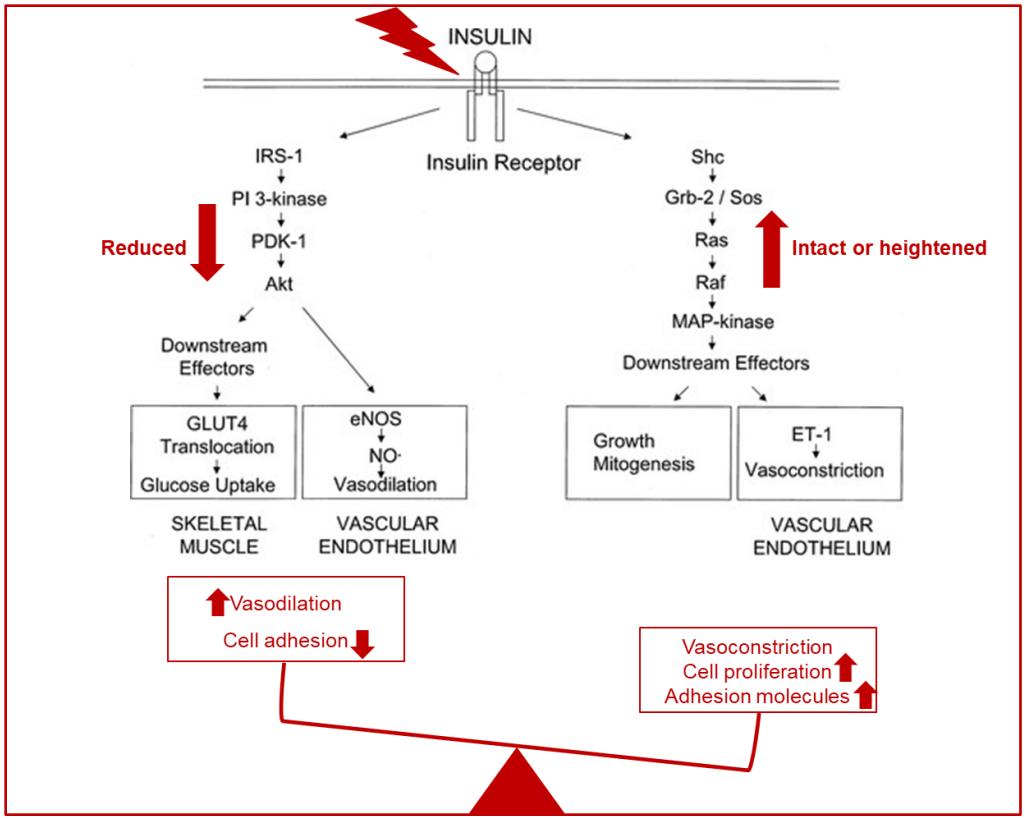

Figure 2: A diagram representing the consequences on an imbalance between, IRS-PI3K-Akt and the Ras protein-mitogen-activated protein kinase (Ras-MAPK) pathways, encountered during insulin resistance.

Akt: protein kinase B, eNOS: endothelial nitric oxide synthase, ET-1 : endothelin 1, GLUT4: glucose transporter 4, IRS1: insulin receptor substrate 1, PDK-1: phosphoinositide dependent-kinase-1, PI3K : phosphoinositide 3-kinase, MAP-Kinase: mitogen-activated protein kinase, NO: nitric oxide, Ras: Ras protein. Modified from (Kim et al. 2006).

1.5.2.2. Role of free fatty acids and inflammatory cytokines in the development of insulin resistance

As mentioned earlier,[9] it is believed that the excessive release of FFAs into the circulation, observed during obesity is an underlying cause of IR. Moreover, high levels of inflammatory cytokines are also thought to participate in the development of IR during MetS (S. E. Kahn et al. 2006; Cornier et al. 2008).

[9] In the abdominal obesity (chapter 1.5.1)

During IR in adipose tissue, levels of FFA are increased. In fact, besides the enlargement and expansion of adipose tissue that results in increased FFA levels, insulin is unable to suppress the release of FFAs through lipolysis, resulting in further increases in FFA liberation into the plasma (Ginsberg 2000)(B. B. Kahn and Flier 2000; Eckel et al. 2005). However, not only IR increases FFA levels but it also seems that FFAs in addition to excessive pro-inflammatory cytokines induce IR and ED (J.-A. Kim et al. 2006). When released from adipocytes these cytokines affect the insulin action in adipose tissue, in a local paracrine manner, and in both skeletal muscle and liver via systemic circulation (i.e. endocrine mechanism) (Cornier et al. 2008) (**Figure 3**).

Hepatic insulin action is impaired in response to increases in FFA flux (Bergman et al. 2007). In fact, the increased levels of circulating FAs reduces insulin signaling in liver through an increased serine phosphorylation of the insulin receptor substrate (IRS-1). When this occurs, the PI3-k's activation is decreased leading to decreased glycogenesis and increased gluconeogenesis in the liver (Copps and White 2012). Moreover, Increased FFAs in the liver stimulates increased hepatic glucose and TG production and release leading to states of hyperglycemia and atherogenic dyslipidemia [10], respectively (Lewis and Steiner 1996; Fujimoto 2000; Ginsberg et al. 2005).

Acute rises in plasma FFAs increase the intramyocellular fatty acid metabolites[11] levels in skeletal muscle (Kirk and Klein 2009). These metabolites inhibit insulin's ability to activate PI3-k's activity by phosphorylating IRS-1 at the serine/threonine sites, thereby decreasing downstream events, including glucose uptake (GLUT4 translocation) (Boden et al. 2001; Itani et al. 2002; Copps and White 2012). Another responsible mechanism is a defective skeletal muscle mitochondrial function, during which, mitochondrial fatty acid oxidation is impaired. This leads to an intracellular fatty acids accumulation, thereby contributing to the impairment of insulin action (Petersen et al. 2004). Moreover, increased levels of intracellular fatty acids leads to over-production of ROS, leading to the activation of the pro-inflammatory nuclear factor kappa B (NFκB) pathway, further increasing IR (Jonk et al. 2007) (**Figure 3**). (see also endothelial dysfunction in chapter 3.1).

[10] Development of atherogenic dyslipidemia is detailed in the dyslipidemia section (chapter 1.5.3.).
[11] These include, long-chain fatty acyl-CoA and diacylglycerol.

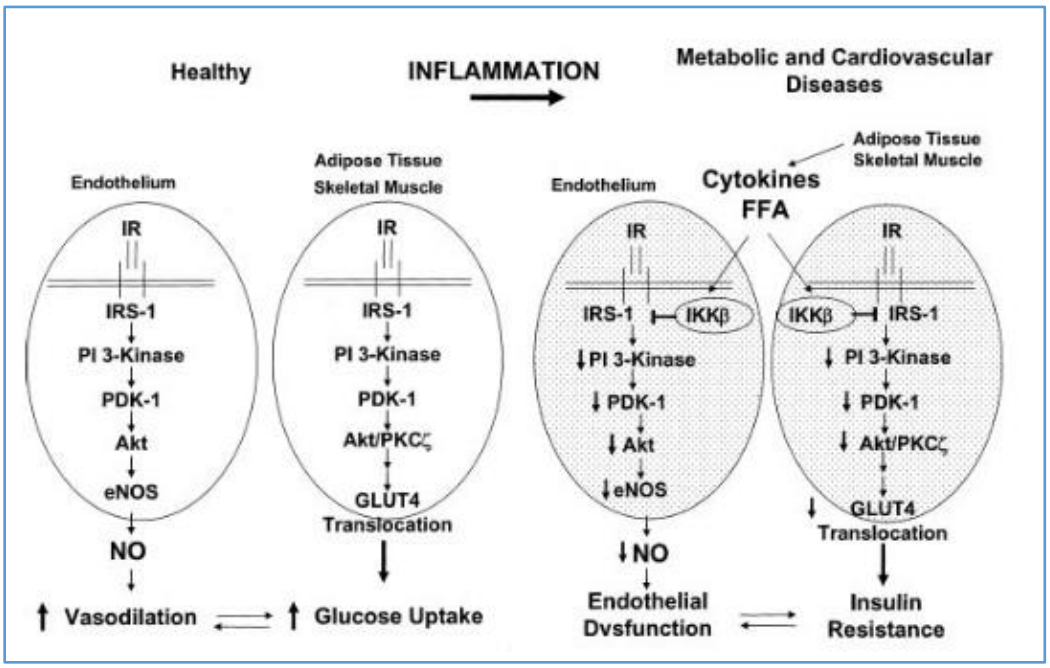

Figure 3: This schematic represents normal insulin signaling (on the left) and parallel impairment in insulin-signaling pathways (in endothelium, adipose tissue and skeletal muscle) under the action of FFA (i.e. increased adiposity) leading to synergistic occurrence of insulin resistance and endothelial dysfunction.

1.5.2.3. Late stage of insulin resistance: hyperglycemia

Clinical hyperglycemia is considered when basal glycemic levels exceeds 120 mg/dl. Increased levels of FFAs stimulates glucose production and release from the liver and impairs glucose uptake by the skeletal muscles (Stumvoll et al. 2005; S. E. Kahn et al. 2006). Taken together both these actions lead to elevated levels of fasting glucose, which is also an important component of MetS (Kurotani et al. 2017). However, clinical hyperglycemia is not encountered before IR reaches an advanced level that is characterized by a decline in pancreatic β-cells function (Stumvoll et al. 2005). During early stages of IR, a state of insulin insensitivity occurs with a maintenance of normal glucose levels. Whereas, increased basal glycaemia only occurs when pancreatic β-cells lose their capacity to secrete insulin (Stumvoll et al. 2005; S. E. Kahn et al. 2006; Ferrannini 2006). Whenever, insulin insensitivity is combined with β-cell failure to secrete insulin in response to glucose, Type 2 diabetes mellitus (T2DM) develops (Goldstein 2002).

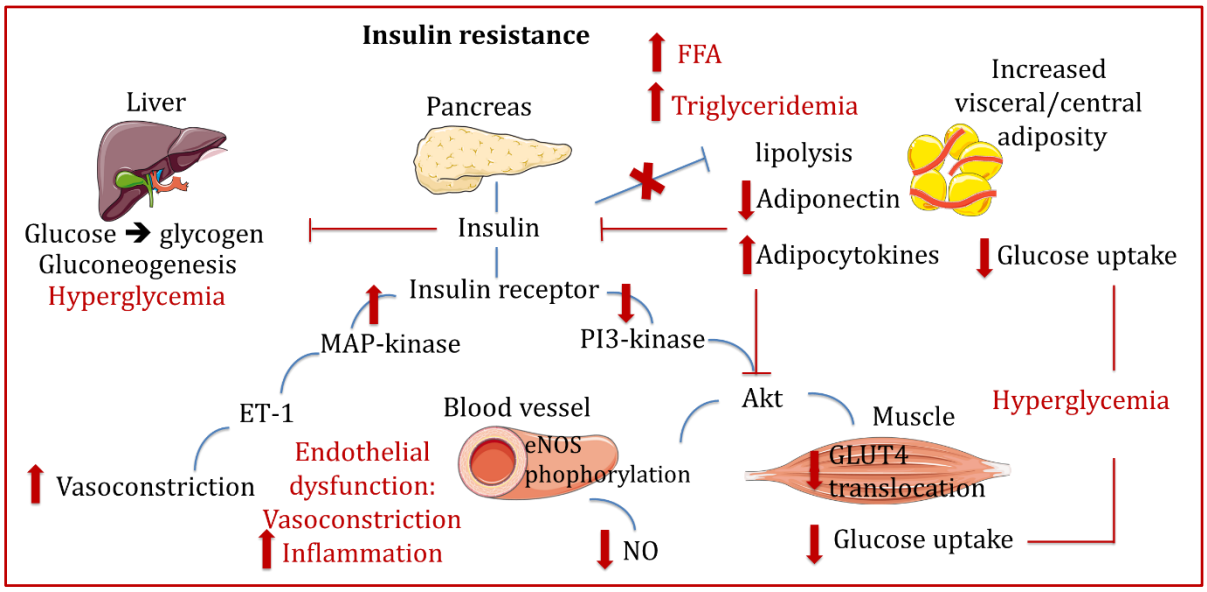

Figure 4: Role of insulin resistance in the pathogenesis of the metabolic syndrome..

Akt: protein kinase B, eNOS: endothelial nitric oxide, ET-1: endothelin-1, FFA: free fatty acids, GLUT4: glucose transporter 4, MAP-kinase: mitogen-activated protein kinase, NO: nitric oxide, PI3-kinase: phosphoinositide 3-kinase. Inspired from a study by Huang (2009).

1.5.3. Dyslipidemia

Dyslipidemia is characterized by an increase in plasma TG levels and in small dense LDL-C and a decrease in HDL-C levels (Grundy 2006). It has been well established that both IR and visceral obesity are associated with atherogenic dyslipidemia (Giannini et al. 2011; Hwang et al. 2016). Under physiological conditions, insulin decreases VLDL triglyceride and apolipoprotein B (apoB) production and secretion and also enhances apoB degradation (Gonzalez-Baró et al. 2007; Sparks et al. 2012).

In normal states, insulin alters apoB through PI3K-dependent pathways and regulates the activity of lipoprotein lipase, leading to decreased production and increased clearance of VLDL, respectively. Since during IR, insulin is unable to perform its effects, both these actions are counteracted, leading to an increase in VLDL levels. Moreover, in states of IR, impaired insulin-signaling results in increased lipolysis and in a subsequent increase in FFA levels (Kaur 2014). Whether resulting from IR itself or from visceral adipose tissue enlargement, increased FFAs flux to the liver leads to increased TG production and storage; meanwhile, excess TG is packaged with the apoB and secreted as VLDL (Lewis et al. 1995; Lewis and Steiner 1996; Ginsberg et al. 2005).

In reverse cholesterol transport, cholesteryl ester transport protein (CETP) stimulates the transfer of TGs from VLDL to HDL in exchange for cholesteryl esters. Thus, Increased TG and VLDL levels result in TG-enriched HDL and cholesteryl ester-enriched VLDL particles (Ginsberg et al. 2005). TG-enriched HDL particles are better substrates for hepatic lipase, which means that they are more subject to clearance. These particles are, then, rapidly cleared from the circulation, leading to decreased HDL plasma concentrations and thereby to atherogenic dyslipidemia (Lamarche et al. 1999; Kaur 2014). In fact, HDL-C is well known for both its anti-atherosclerotic and anti-inflammatory properties (Weverling-Rijnsburger et al. 2003; Sanossian et al. 2007). Thus, its decreased levels are associated with increased cardiovascular risk. Furthermore, even though LDL levels are sometimes unchanged, the fact that TG-enriched LDL particles are small and dense, this facilitates their penetration to the endothelial wall and makes them more susceptible to oxidation, further increasing atherogenecity and cardiovascular risk (Lamarche et al. 1998; Hulthe et al. 2000; Cornier et al. 2008) (**Figure 5**).

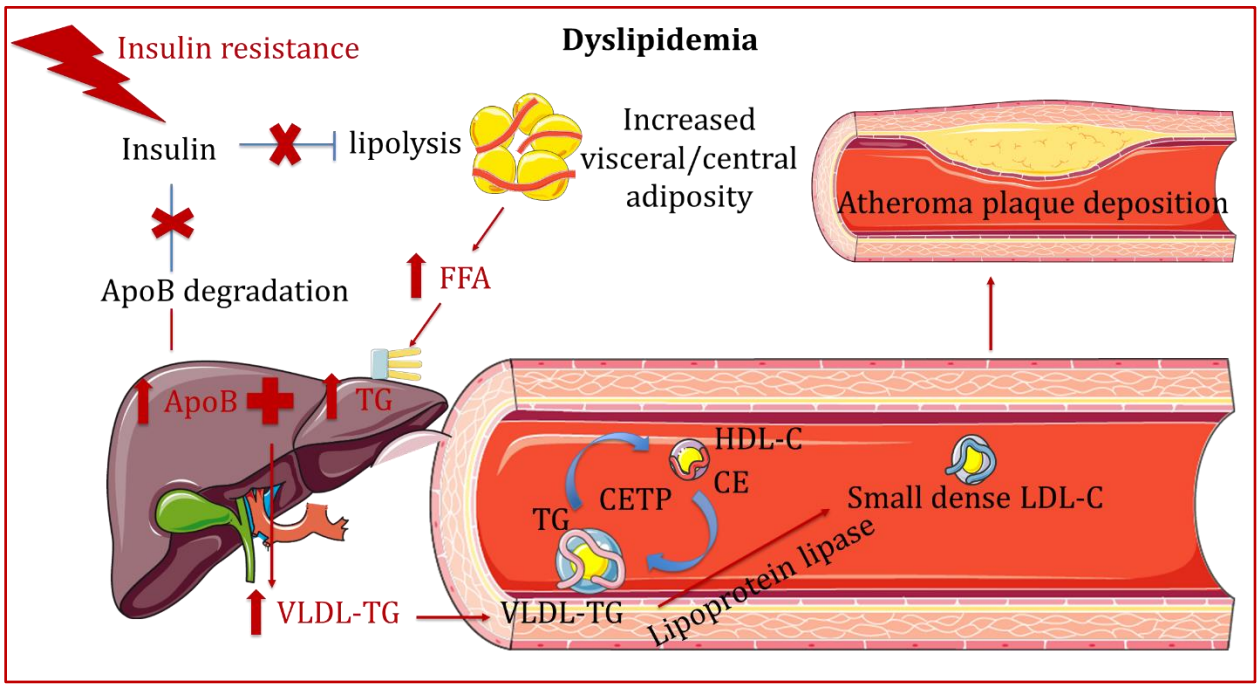

Figure 5: Atherogenic dyslipidemia in the metabolic syndrome.

ApoB: Apolipoprotein B, CE: cholesteryl ester, CETP, cholesteryl ester transfer protein, FFA: free fatty acid, HDL-C: high density lipoprotein–cholesterol, TG: triglyceride, VLDL-TG: very low density lipoprotein-triglyceride. *Inspired from a study by* Huang (2009).

1.5.4. Arterial hypertension

In clinical diagnosis, an individual is considered hypertensive when systolic blood pressure and/or diastolic blood pressure exceed 140 mmHg and 90 mmHg, respectively (Unger et al. 2020).

Hypertension is a classical feature of the MetS. It has been reported that up to 1/3 of hypertensive patients have the MetS (Schillaci et al. 2004; Cuspidi et al. 2004). Increased arterial blood pressure (ABP) during MetS seems to be strongly associated with increased visceral adiposity and IR (Ferrannini et al. 1997; Yanai et al. 2008). Multiple mechanisms underlie the development of hypertension in the MetS, such as activation of renin angiotensin aldosterone (RAAS) and the SNS activity. Moreover, the hypertrophic visceral adipose tissue is responsible for the production and secretion of multiple numbers of adipocytokines, such as TNF-α, IL-6, angiotensinogen, leptin and FFA. These molecules participate in increasing ABP through different pathways (Katagiri et al. 2007) **(Figure 6)**.

One of the main mechanisms responsible for the development of hypertension is the activation of RAAS. In obesity, adipocytes-derived angiotensinogen leads to an increase in blood pressure through the RAAS. Angiotensinogen is converted to angiotensin I, in presence of kidney-secreted renin, to later be hydrolyzed into its active form angiotensin II (Ang II), under the action of angiotensin converting enzyme (ACE). Besides its direct effect on blood pressure through vasoconstriction, Ang II also stimulates the release of aldosterone, which further increases ABP through water and sodium retention. The latter is responsible for increased intravascular fluid which is often seen in obese individuals and which leads to increases in ABP (Flack et al. 2007). The RAAS also seems to be activated during IR states. Hyperinsulinemia increases the expression of angiotensinogen, Ang II and the type 1 angiotensin (AT1) receptor, thereby contributing to the development of hypertension (Malhotra et al. 2001; Kaur 2014). On the other hand, Ang II inhibits insulin-mediated PI3K pathway activation, thereby impairing endothelial NO production and Glut-4 translocation in insulin-sensitive tissues, which results in vascular and systemic IR, respectively (Zhou et al. 2012) **(Figure 6)**.

Insulin is also known for its ability to directly stimulate renal sodium re-absorption. Thus, increased insulin levels in IR also might lead to increased ABP through favoring expansion of extracellular fluid volume (Mendizábal et al. 2013; Demarco et al. 2014). Insulin might also stimulate ET-1 leading to increased vasoconstriction (Pantelis A et al. 2007). While on the other hand, the impairment of PI3K-dependent signaling, in insulin-resistant individuals, causes an imbalance between production of NO and secretion of ET-1, leading to ED **(Figure 6)**. The latter results from both decreased vasodilation and increased vasoconstriction further inducing hypertension (J.-A. Kim et al. 2006). Moreover, both leptin and FFA levels are increased in insulin resistance states and are suspected to augment SNS activation in the MetS (Egan 2003; Florian and Pawelczyk 2010).

The other mechanism responsible for increased ABP levels is the sympathetic overactivity due to the increased release of adipocytokines encountered during obesity. Leptin increases ABP, directly, through activation of the SNS in the hypothalamus and indirectly by increasing renal sympathetic activity, which leads to increased renin release and sodium retention, further inducing hypertension (Carlyle et al. 2002; Eikelis et al. 2003; Kaur 2014) **(Figure 7)**. IL-6 might lead to increased ABP either through stimulation of the central and SNS or through inducing an increase in plasma angiotensinogen and Ang II (Takano et al. 1993; Papanicolaou et al. 1996) (**Figure 6**). Meanwhile, TNF-α in addition to increasing the SNS activity, also stimulates the production of angiotensinogen and ET-1, further increasing ABP (Brasier et al. 1996; Kahaleh and Fan 1997) (**Figure 6**). In addition, FFAs were found to increase ABP through stimulating α1-AR-induced vasoconstriction, ED and increase in oxidant stress (Sarafidis and Bakris 2007). In fact, increased oxidative stress also seems to play a role in inducing hypertension, through altering endothelial function (Roberts et al. 2005a). The responsible mechanisms will be thoroughly reviewed later in the manuscript. Furthermore, high-sensitivity C-reactive protein (hsCRP), a clinical criterion of MetS was found to be positively correlated to hypertension (Sesso et al. 2003).

In normal states, baroreceptors located in the carotid sinus and aortic arch, are able to control blood pressure through their sensitivity towards changes in vessel wall stretch. During increased arterial pressure, baroreflex activity is blunted due to reduced arterial distensibility resulting in a chronic stimulation in peripheral sympathetic outflow (Grassi et al. 2005). Arterial baroreflex

activity also seems to be impaired during other components of the metabolic syndrome, including visceral obesity, insulin resistance and prediabetes (Skrapari et al. 2007; Straznicky et al. 2009).

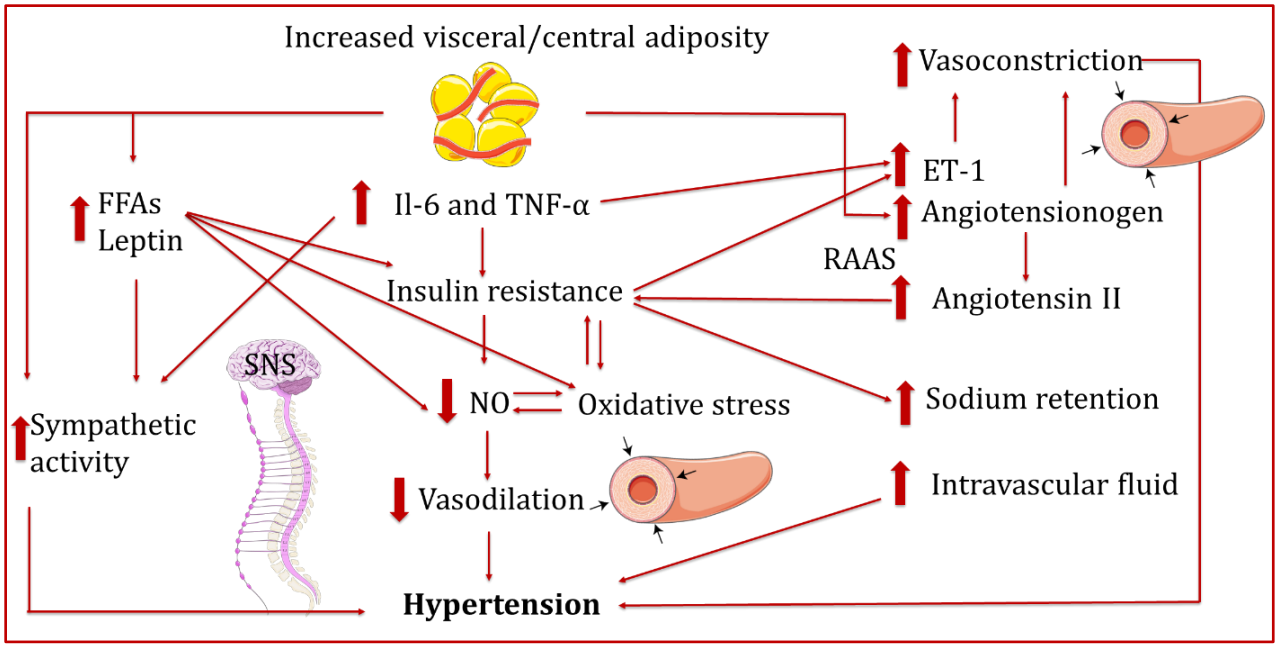

Figure 6: A schematic that represents mechanisms involved in the development of hypertension in the metabolic syndrome.

FFAs: free fatty acids, ET-1: endothelin-1, Il-6: interleukin 6, NO: nitric oxide, TNF-α: tumor necrosis factor-α. Inspired by Yanai et al. (2008).

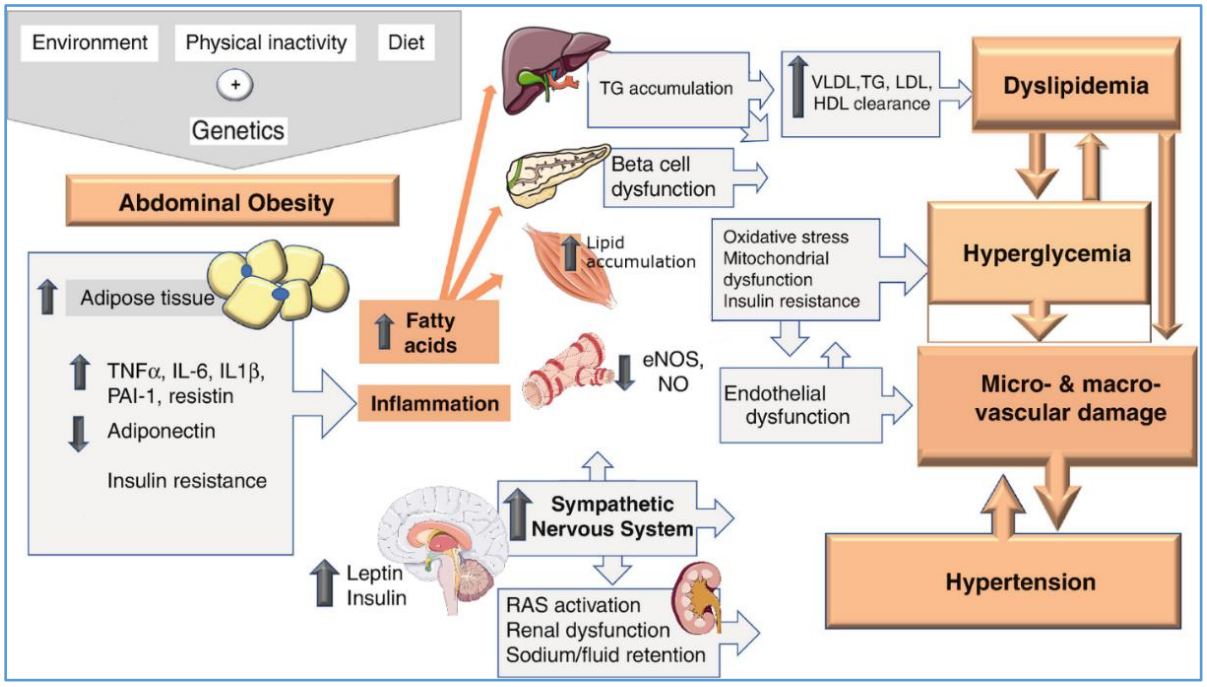

Figure 7: A schematic that recapitulates the etiology, main risk factors and mechanisms involved in the pathophysiology of the metabolic syndrome.

Edited from Dipla et al. (2020)

2. Nitric oxide-soluble guanylyl cyclase- cyclic guanosine monophosphate- protein kinase G signaling pathway: an overview

The NO-cGMP-Protein Kinase G (PKG) is one of the main pathways governing cardiac and vascular functions. This pathway plays a pivotal role in the cardiovascular homeostasis by regulating the vascular tone and cardiac function. It mainly promotes vasodilation, inhibits platelet aggregation (thrombosis), vascular smooth muscle cell growth/and migration and leukocyte endothelial adhesion (inflammation), and also regulates myocardial function and provides cardioprotection (Evgenov et al. 2008; Kadowitz and Nossaman 2013; M. Park at el. 2018).

2.1. Nitric oxide production

2.1.1. Nitric oxide synthases

NO is generated in a vast number of cell types by three different isoforms of NO synthase. The first two, Neuronal NOS (nNOS) and endothelial NOS (eNOS) are both constitutively expressed and continuously produce small amounts of NO. Whereas the third isoform, inducible NOS (iNOS) is highly expressed in inflammatory states and produces large amount of NO. eNOS is typically expressed in the vascular (including coronary) and cardiac endothelium, while nNOS is mainly located in cardiomyocytes. These NOSs catalyze the oxidation of L-arginine to NO, which plays a central role in the regulation of vascular tone and the maintenance of endothelial integrity.

2.1.2. Calcium-dependent nitric oxide production in endothelial cells

In the endothelial cells, eNOS can be activated (phosphorylated) in a calcium/calmodulin-dependent manner, which is induced by receptor-bound agonists, like acetylcholine and β_3-agonists. Its binding to the membrane-bound muscarinic receptors increases intracellular levels of calcium that activate calmodulin, which then binds eNOS, leading to its phosphorylation (Nathan and Xie 1994). One of the major agonists is acetylcholine. This binding facilitates electron flow from nicotinamide adenine dinucleotide phosphate (NADPH) in the reductase domain of eNOS to the heme in the oxygenase domain to flavin adenine dinucleotide (FAD) and flavin mononucleotide (FMN) (Abu-Soud and Stuehr 1993). eNOS uses the amino acid L-arginine as a precursor together with several cofactors, including NADPH and tetrahydrobiopterin (BH4), in a complex oxygen-dependent reaction to generate equimolar amounts of NO and L-citruline (Fö Rstermann and Sessa 2012). In fact, BH4 is a key redox-dependent cofactor that regulates eNOS

activity by promoting and stabilizing eNOS dimerization (active form of eNOS) as well as the binding of L-arginine to its catalytic heme (Levine and Levine 2013). The Akt-mediated phosphorylation of eNOS at serine 1177, which the key regulatory site, enhances its activity. While the activation of the enzyme is further promoted by its interaction with heat shock protein 90 (Pritchard et al. 2001). Once synthetized, NO diffuses to the smooth muscle cells, in a paracrine manner. There, it stimulates the sGC yielding increased levels of cGMP, its downstream effector, leading to vasodilation (**Figure 8**).

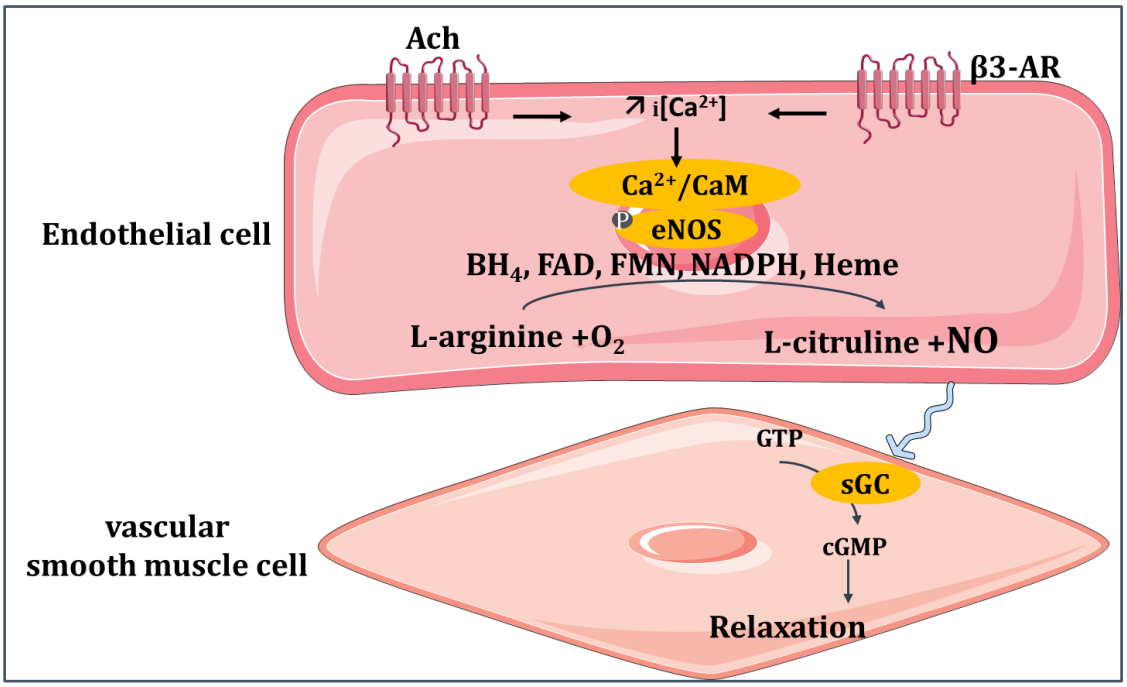

Figure 8: Calcium-dependent NO production and vasorelaxation.

Ach: acetylcholine, β_3-AR: β_3-adrenoceptor, BH4: tetrahydrobiopterin, CAM: calmodulin, cGMP: cyclic guanosine monophosphate, eNOS: endothelial nitric oxide synthase, FAD: flavin adenine dinucleotide FMN: flavin mononucleotide, GTP: guanosine triphosphate, i[Ca^{2+}]: intracellular calcium, NADPH: nicotinamide adenine dinucleotide phosphate, sGC: soluble guanylyl cyclase. Inspired by (Polovina et al. 2014).

2.1.3. Calcium-independent nitric oxide production in endothelial cells

2.1.3.1.Shear stress-mediated vasorelaxation

Shear stress induces calcium-independent receptor-independent eNOS phosphorylation via activating the src kinase/PI3k/Akt (also known as protein kinase B) pathway, leading to NO-sGC-cGMP mediated vasodilation (**Figure 9**).

2.1.3.2.Insulin-mediated vasorelaxation

eNOS activity can also be modulated in a calcium-independent receptor-dependent way, through Insulin. The latter activates its receptor, located on the endothelial membrane. When activated, insulin receptor phosphorylates a number of substrates. Phosphorylation of IRS1 induces the activation of PI3K. This leads to the conversion of phosphatidylinositol(3,4)-biphosphate(PIP2) to the second messenger phosphatidylinositol(3,4,5)-triphosphate(PIP3) which activates Akt via phosphoinositide dependent-kinase-1 (PDK-1). In turn, Akt induces the phosphorylation of eNOS and the subsequent conversion of L-arginine to L-citruline and NO. The release of another endothelium-derived relaxing factor was also found to be stimulated by insulin i.e. PGI2 (Baron 1994) (**Figure 9**).

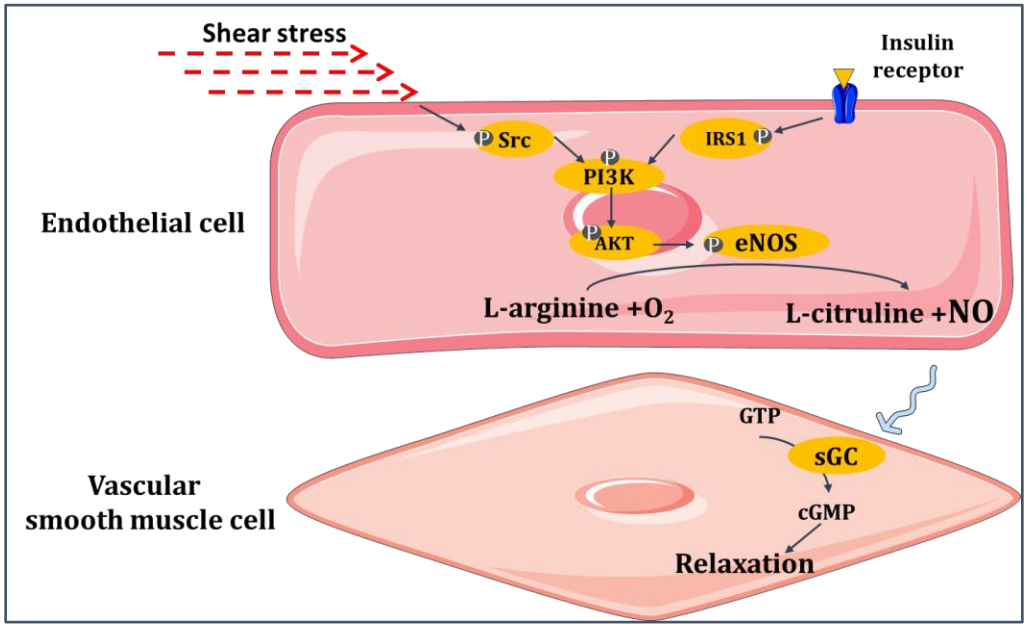

Figure 9: Calcium-independent vasorelaxation.

Akt: protein kinase B, cGMP: cyclic guanosine monophosphate, eNOS: endothelial nitric oxide synthase, GTP: guanosine triphosphate, NO: nitric oxide, IRS1: insulin receptor substrate 1, PI3k: phosphatidylinositol 3-Kinase, sGC: soluble guanylyl cyclase, Src: Src kinase. Inspired by (Auger et al. 2014)

2.2. Nitric oxide in vascular cells

2.2.1. Vascular function of nitric oxide

Besides its major role in maintaining the basal vascular tone through vascular smooth muscle cell vasodilation. Functions of NO also involve restraining thrombosis by inhibiting platelet secretion, activation, adhesion and aggregation, and by promoting platelet disaggregation. NO is

also involved in hindering leukocyte adhesion to the endothelium and thus in reducing inflammation. Finally, NO also inhibits smooth muscle cell migration and proliferation.

Besides all of its previously mentioned functions, NO may also have antioxidant properties through increasing the expression of the extracellular SOD in a cGMP-dependent manner, inhibiting low-density lipoprotein (LDL) oxidation and lowering the production of ROS (Levine and Levine 2013).

2.2.2. Nitric oxide signaling in vascular cells

NO diffuses in a paracrine manner from endothelial cells to the vascular smooth muscle cells (SMCs) where it binds to the reduced heme (Fe^{2+}) moiety of the sGC enzyme, leading to its activation (Evgenov et al. 2006). In fact sGC is a target for gaseous ligands such as NO and is a heterodimer, composed of a larger α-subunit and a smaller heme-binding β-subunit (Kamisaki et al. 1986). sGCα1β1 seems to be the most prevalent sGC isoform (Bork and Nikolaev 2018). sGC activation induces the conversion of GTP to cGMP, a second messenger that in addition to vasodilation. The vasodilatory effect of cGMP is achieved through several mechanisms that decrease the intracellular Ca^{2+} concentrations (i[Ca^{2+}]) in the SMC. These mechanisms mainly involve the inhibition of IP3-mediated calcium release and of extracellular Ca^{2+} influx through voltage-gated Ca^{2+} channels (Tsai and Kass 2009).

Besides causing vasodilation, cGMP generation activates several downstream effector molecules, with cGMP-dependent protein kinases (PKG or cGK) and cGMP-regulated phosphodiesterases (PDEs) predominating in the cardiovascular system.

Once activated, cGMP-dependent PKG phosphorylates several intracellular key target proteins that are involved in controlling i[Ca^{2+}]. In fact, the phosphorylation of these proteins further reduces i[Ca^{2+}] and thus results in smooth muscle relaxation. PKGI seems to be the primary kinase in the cardiovascular system.

As mentioned earlier cGMP is essential for various functions. Thus, its intracellular concentration needs to be kept in tight control. This is the role of PDEs, which are responsible for cyclic nucleotides (i.e. cGMP and cAMP) hydrolization (Friebe et al. 2020) . These enzymes control both the duration and the amplitude of the cyclic nucleotides signaling thereby regulating the NO-sGC-cGMP pathway. PDEs are divided into 11 families (PDE1-PDE11), of which some

are specific to cGMP (e.g. PDE3 & PDE5), some to cAMP and others have dual actions (Takimoto 2012).

It is to be noted that, in addition to the sGC there exists particulate GC (pGC) (also known as Natriuretic Peptide Receptors) that also stimulate cGMP in vascular smooth muscle cells. In contrast to the free cytosolic sGC, these are membrane-bound protein receptors that are activated by natriuretic peptides. However, the NP/pGC/cGMP pathway does not seem to be the predominating signaling pathway involved in smooth muscle cell relaxation (Bork and Nikolaev 2018) (**Figure 10**).

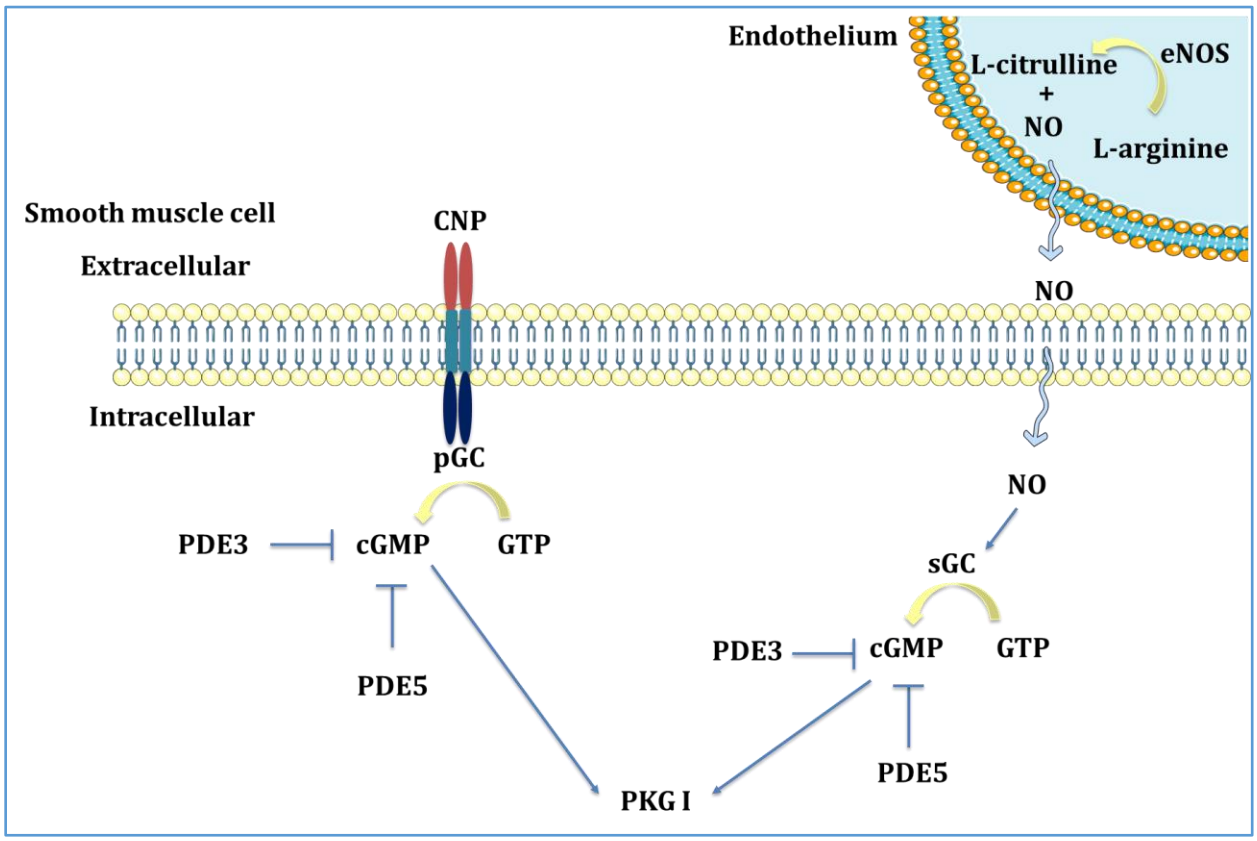

Figure 10: cGMP compartmentation in smooth muscle cells.

CNP: C-type natriuretic peptide, cGMP: cyclic guanosine monophosphate, eNOS: endothelial nitric oxide synthase , GTP: guanosine triphosphate, NO: nitric oxide, NOS: nitric oxide synthase, PDE: phosphodiesterase, pGC: particulate guanylyl cyclase, PKG: protein kinase G. Inspired by Bork et al. (2018).

2.3. Endothelium-derived factors/mediators beyond nitric oxide

The most important endothelium-derived mediators are divided into vasodilatory and vasoconstrictor molecules. Besides NO also known as the endothelial-derived relaxing factor,

other vasodilating prostanoids (prostacyclin (PGI2) & prostaglandin E2 (PGE2), endothelial-derived hyperpolarizing factor (EDHF), bradykinin (BK) are secreted (**Figure 11**). Endothelium-derived vasoconstrictors include endothelin1 (ET1), Ang II and vasoconstricting prostanoids e.g. thromboxane (TxA2). The rest of endothelium-derived factors comprise antithrombotic and prothrombotic factors as well as mediators of inflammatory immune response (P. M. Vanhoutte et al. 2017).

2.4. Endothelial function beyond nitric oxide

PGI2 is produced from arachidonic acid (AA) (produced by the phospholipase A2 (PLA2)) under the action of cyclooxygenase system (COX). PGI2 migrates to the vascular SMC, in a paracrine manner, where it binds to its membrane receptor leading to the activation of soluble adenylate cyclase (sAC) leading to vasodilation through increased cyclic adenosine monophosphate cAMP levels. PGI2's major role seems to be the inhibition of platelet aggregation and adhesion rather than vasodilation (Moncada and Vane 1978; Pellegrin et al. 2009) (**Figure 11**).

Endothelial derived hyperpolarizing factor (EDHF) induces vascular SMC relaxation and vasodilation by activating potassium (K+) current through small and intermediate-conductance calcium (Ca2+)-activated K+ channels, causing endothelial cell hyperpolarization. Endothelial membrane potential hyperpolarization is then transmitted to the vascular SMC through myoendothelial gap junctions. This leads to decreased calcium entry through voltage dependent calcium channels and consequently to vasodilation. The activation of Ca2+- activated K+ channels may also decrease the endothelial intracellular Ca2+ leading to vasorelaxation through the activation of NOS and PLA2 (Ledoux et al. 2006; Auger and Schini-Kerth 2014). In cases of decreased NO bioavailability, it seems that EDHF is able to compensate for the loss of NO-induced vasodilation, particularly in the microcirculation (Deanfield et al. 2007) (**Figure 11**).

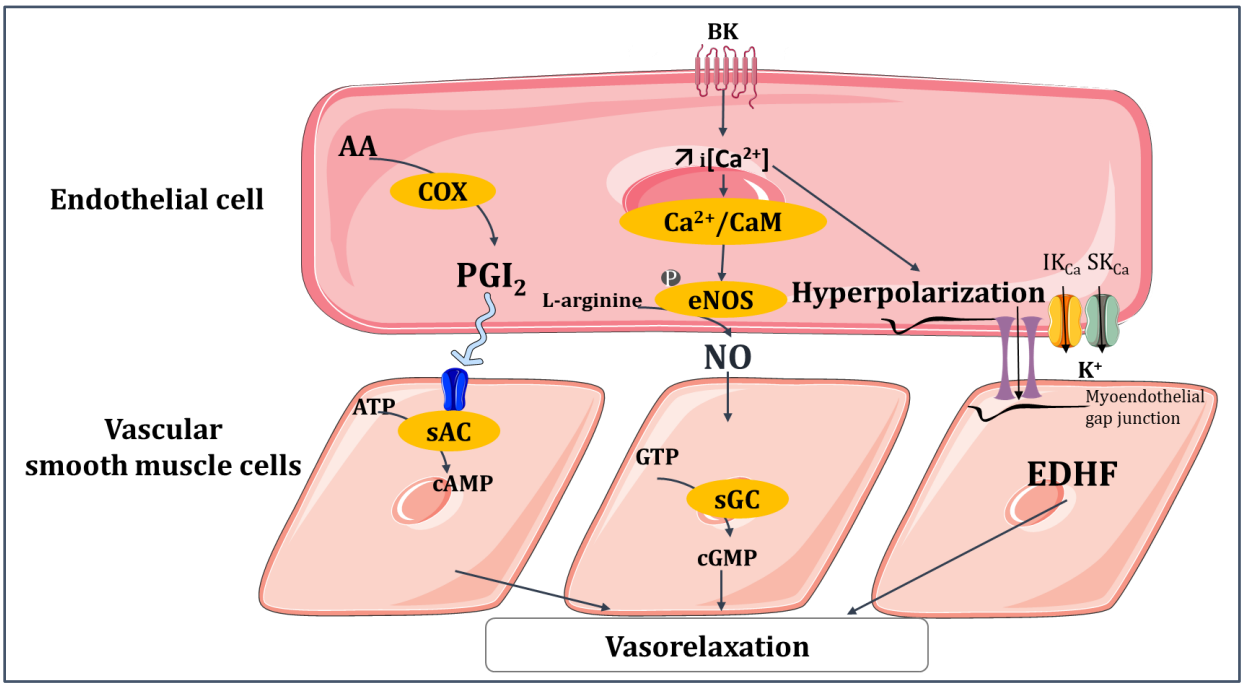

Figure 11: A schematic representing vasorelaxation beyond NO (right and left) and NO-induced vasorelaxation (center)..

AA: arachidonic acid, ATP: adenosine triphosphate, BK: bradykinin, CAM: calmodulin, cAMP: cyclic adenosine monophosphate, cGMP: cyclic guanosine monophosphate , COX: cyclooxygenase, EDHF: endothelium-derived hyperpolarizing factor, eNOS: endothelial nitric oxide synthase, GTP: guanosine triphosphate, i[Ca^{2+}]: intracellular calcium, IK_{ca} & SK_{ca} : calcium activated-potassium channels, PGI_2: prostacyclin, sAC: soluble adenylate cyclase, sGC: soluble guanylyl cyclase. Inspired by (Auger et al. 2014).

2.5. Nitric oxide in the myocardium

2.5.1. Cardiac function of nitric oxide

NO is derived from eNOS and nNOS in cardiomyocytes. Its major role includes regulating myocardial function and conferring cardioprotection. This is achieved by reducing the contractile frequency of cardiomyocytes, attenuating cardiac contractility, accelerating relaxation and increasing distensibility of cardiomyocytes, and finally by improving the efficiency of myocardial oxygen consumption. All these effects occur through a cascade of signaling events, involving cGMP and PKG (Fö Rstermann and Sessa 2012).

2.5.2. Nitric oxide signaling in cardiac myocytes

In cardiac myocytes (CMs), cGMP signaling is involved in the regulation of contractility. As in endothelial cells, both the NP-pGC and NO-sGC lead to cGMP generation. However here the former seems to be predominating. There exists three types of NPs. ANP and BNP are secreted in

the heart, by the atria and ventricles, respectively. Whereas the third, CNP is derived primarily from endothelial cells. These natriuretic peptides exert their biological effects by binding to the cell-membrane localized pGC. Meanwhile, the NO-sGC-cGMP pool is controlled by the β_3-AR at the cell surface caveolae (**Figure 12**). In fact, the β-adrenergic system, an important regulator of myocardial contraction and relaxation. β-adrenergic receptors (β-AR) are important regulators of normal and pathologic cardiac function. The three subtypes of β-ARs are β_1-AR, β_2-AR and β_3-AR, with β_1 and β_2-ARs the most expressed and studied (Cannavo and Koch 2016).

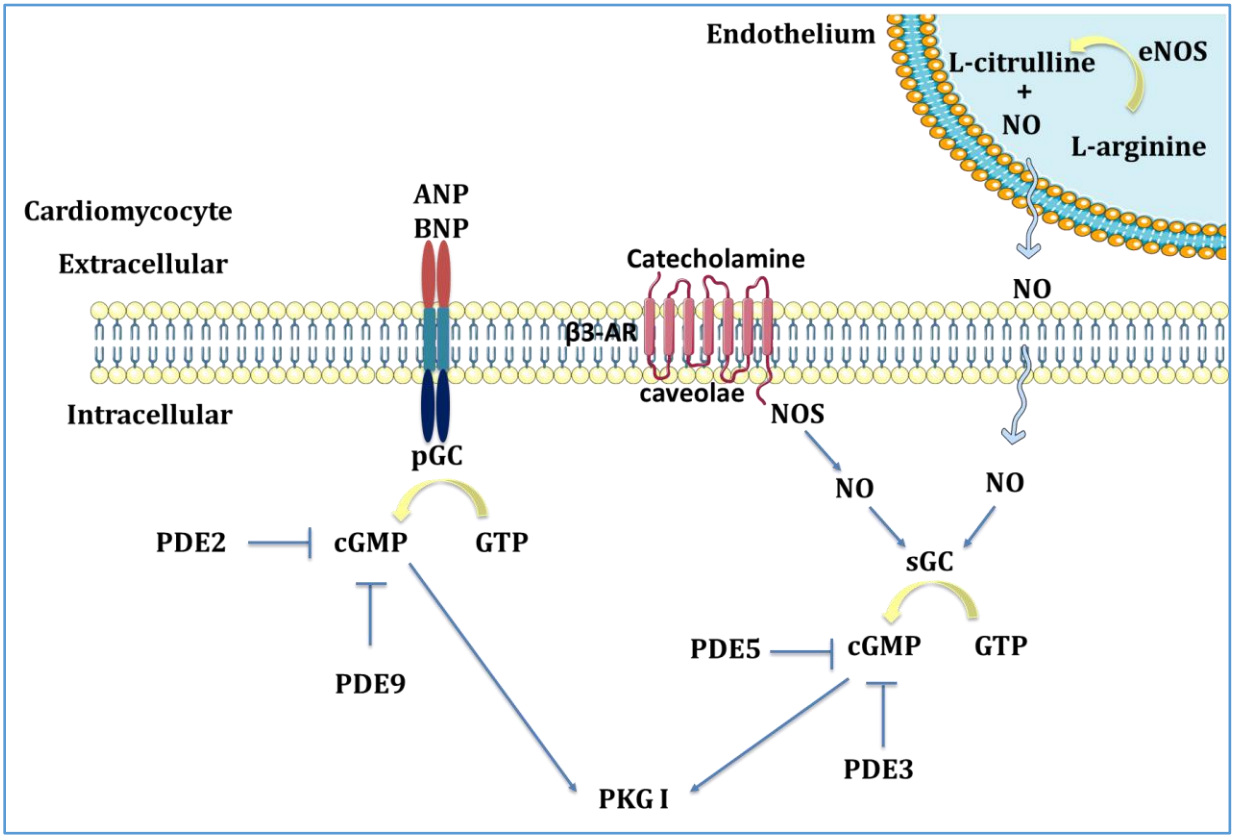

Figure 12: cGMP compartmentation in cardiomyocytes.

ANP: atrial natriuretic peptide, BNP: brain natriuretic peptide, pGC: particulate guanylyl cyclase, NO: nitric oxide, GTP: guanosine triphosphate, cGMP: cyclic guanosine monophosphate, PDE: phosphodiesterase, NOS: nitric oxide synthase, eNOS: endothelial nitric oxide synthase, PKG: protein kinase G, β_3-AR: β_3-adrenergic receptor. Inspired by Tsai and Kass (2009) Bork et al. (2018) & Friebe et al. (2020).

Contraction of cardiac myocytes is induced by catecholamine-β-AR stimulation. ARs are coupled to stimulatory G (sG) proteins, which activate adenylate cyclases (ACs), catalyzing the formation of cyclic adenosine monophosphate (cAMP). This leads to the activation of PKA

subsequently causing the phosphorylation of multiple proteins involved in excitation-contraction coupling. Phosphorylation of L-type calcium channels (LTCC) and ryanodine receptor (RyR), respectively, increase the calcium influx and calcium release from the sarcoplasmic reticulum (SR). Both mechanisms lead to increased intracellular calcium levels and contractile force of cardiomyocytes.

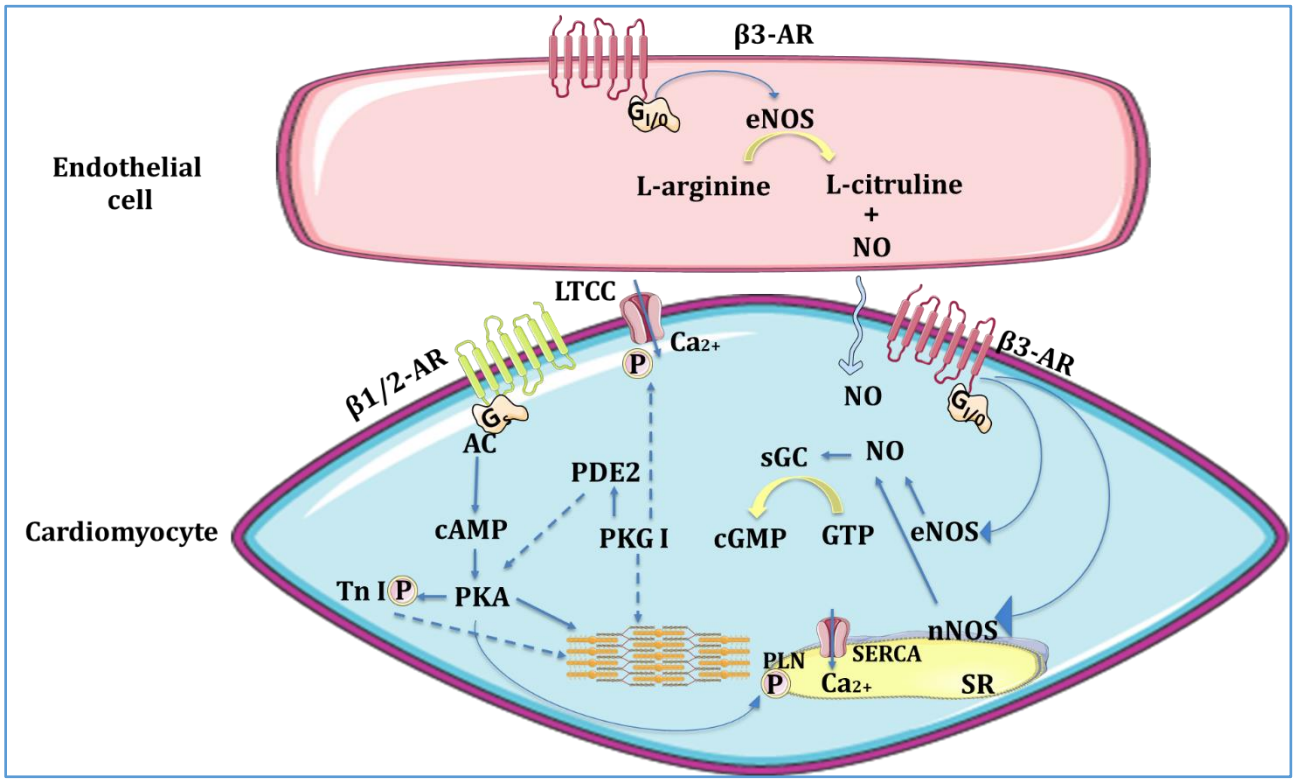

Figure 13: Simplified diagram of the mechanism involved in β_3-AR-dependent cardiomyocyte relaxation.

AC: adenylate cyclase, $\beta_{1/2/3}$-AR: $\beta_{1/2/3}$-adrenergic receptor, cAMP: cyclic adenosine monophosphate, cGMP: cyclic guanosine monophosphate, eNOS: endothelial nitric oxide synthase, Gs: stimulatory G-protein, GI/0: inhibitory G-protein, NO: nitric oxide, GTP: guanosine triphosphate, LTCC: L-type calcium channels, nNOS: neuronal nitric oxide synthase, PDE: phosphodiesterase, PLN: phospholamban, PKA: protein kinase A, PKG: protein kinase G, SR: sarcoplasmic reticulum, SERCA: sarco-endoplasmic reticulum Ca^{2+}-ATPase pump, Tn: troponin. Inspired by (Imbrogno et al. 2015).

Whereas, in cardiac myocyte relaxation, PKA phosphorylates the phospholamban (PLN or PLB) which stimulates the sarco-endoplasmic reticulum Ca2+-ATPase (SERCA) pump leading to increased Ca2+ re-uptake into the SR. PKA also phosphorylates troponin I (TnI) reducing the sensitivity of the contractile apparatus to calcium subsequently accelerating the relaxation. The β3-AR plays an important role in relaxation. In fact, stimulation of β3-ARs leads to increased endothelial eNOS or nNOS activation, increasing NO generation, which then leads to activation

of sGC and to a subsequent production of cGMP and finally to cGMP-dependent protein kinase G (PKG) activation. Activation of β_3AR/NO-cGMP/PKG signaling pathway exerts a cardioprotective mechanism that can be beneficial in failing myocardium (Cannavo and Koch 2016). Then via PKG, cGMP causes negative inotropism through phosphorylation of LTCC (Yang et al. 2007) and troponin I (Lee et al. 2010) and positive lusitropism through phosphorylation of titin (Balligand 2016) (**Figure 13**).

3. Circulatory alterations in relation with the Metabolic Syndrome

The MetS is an independent risk factor for CVD. When combined together, these risk factors increase the rate and severity of CVD (Tune et al. 2017). These include vascular and cardiac changes.

3.1. Vascular changes

3.1.1. Micro- and macro-vascular alterations

Vascular alterations encountered during the MetS involve both micro- and macrovascular blood vessels. These alteration mainly involve ED, a hallmark of MetS-induced vascular complications (Tune et al. 2017). The term ED might be used to describe any alteration in the normal endothelial function. This may involve either its anti-inflammatory, anticoagulant or modulation of vascular growth and remodeling properties. However, this term is generally used to refer to an impairment in endothelium-dependent vasorelaxation caused by decreased NO bioavailability or bioactivity (Cai and Harrison 2000)(Aoqui et al. 2014).

Oxidative stress is an imbalance between production and accumulation of ROS in cells and the antioxidant defenses of the body, that leads to tissue damage (Pizzino et al. 2017). However, in normal states, low levels of ROS participate in several essential and beneficial mechanisms such as intracellular signaling and cytoprotection. However, their levels should be kept in tight control and should not exceed a certain limit. In fact, an antioxidant defense system maintains the balance between the physiological and pathophysiological roles of ROS. The defense against ROS includes endogenous antioxidant enzymes (e.g. superoxide dismutase, SOD), vitamins and minerals and is mainly based on enzymatic inactivation (Levine and Levine 2013). Major sources of ROS are NADPH oxidase (NOX), xanthine oxidase (XO), eNOS uncoupling, and mitochondrial electron transport chain. As much as increased levels of ROS might result from increased NOX, the main ROS-generating pathway, it might also originate from a decrease in ROS-scavenging pathways such as SOD (Labazi and Trask 2017). The mechanisms implicated in oxidative stress causing ED are multifactorial and may differ from one situation to another. ROS might affect eNOS expression and activity while on the other hand it might impair NO bioavailability and signaling. For instance, eNOS activity is diminished during reductions in its phophorylation at Serine 1177. In addition, ROS increase the inhibition of NOS by increasing the plasma levels of asymmetric dimethyl-arginine (ADMA), a competitive inhibitor of NOS, leading to ED (Cooke 2000). FAD, FMN, BH4

and NADPH are all essential eNOS cofactors. During oxidative stress, NOX is activated, leading to an augmentation of ROS levels in the vasculature. Increased ROS levels then leads to the uncoupling of BH4[12] from eNOS, which results in O_2^- formation (instead of NO), and thereby to a decrease in NO bioavailability (Schiffrin 2008). On the other hand, NO is subject to scavenging by superoxide anion (O_2^-) and other reactive oxygen species (ROS). Therefore, increased levels of superoxide (O_2^-) whether resulting from NOX or from uncoupled eNOS, enhances NO scavenging leading to increased peroxynitrite (ONOO−) formation which results in decreased NO activation and bioavailability (Cai 2005). Moreover, ONOO− is a potent pro-oxidant that inhibits eNOS bioactivity and thus leads to a further reduction in NO bioavailability and increase in ROS (Endemann and Schiffrin 2004). Furthermore, both O_2^- and ONOO− potently inhibit sGC, interfering with the eNOS-NO-cGMP signaling pathway (Münzel et al. 2003) (**Figure 14**).

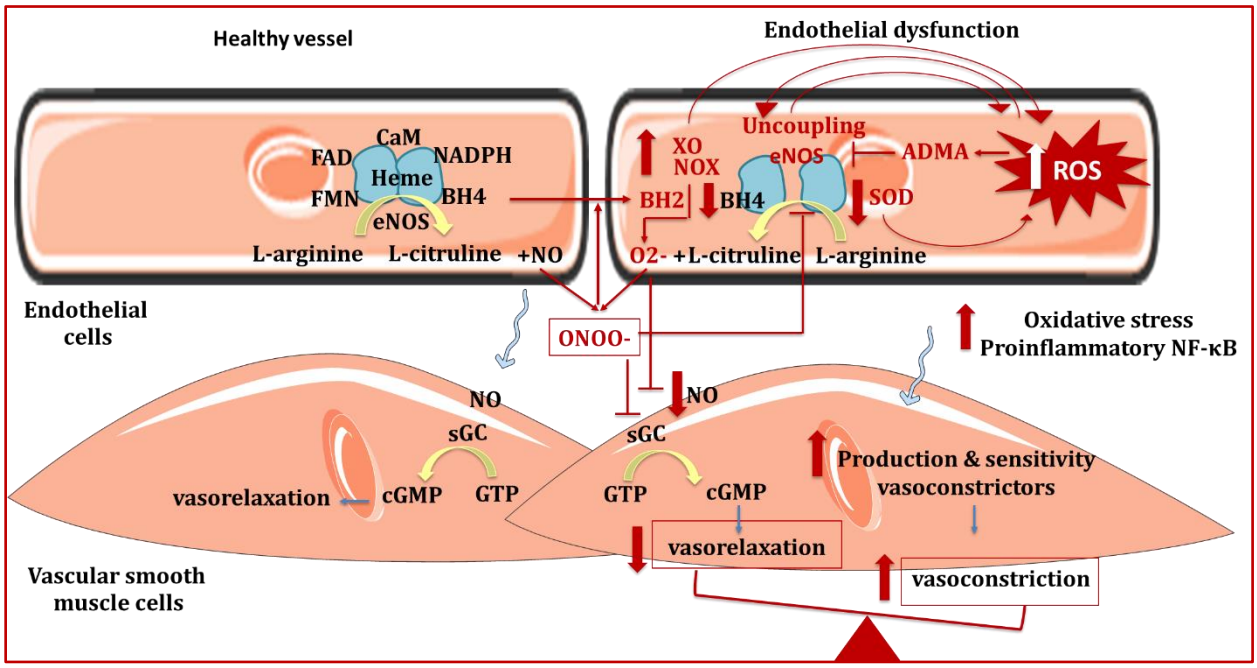

Figure 14: A simplified diagram on the role of oxidative stress in endothelial dysfunction.

ADMA: asymmetric dimethyl-arginine, BH2: dihydrobiopterin, BH4: tetrahydrobiopterin, CaM: calmodulin, cGMP: cyclic guanosine monophosphate, eNOS: endothelial nitric oxide synthase, Fad, flavin adenine dinucleotide, FMN: flavin mononucleotide, NADPH : nicotinamide adenine dinucleotide phosphate, NF-κB: nuclear factor-κB, NOX: nicotinamide adenine dinucleotide phosphate oxidase, O_2^-: superoxide anion, ROS: reactive oxygen species, sGC: soluble guanylate cyclase, SOD: superoxide dismutase, XO: xanthine oxidase.

[12] BH4, exhibits antioxidant properties against ROS of which O_2^-. Thus, Oxidative stress can lead to excessive oxidation and depletion of BH_4 causing eNOS 'uncoupling'.

3.1.1.1. Endothelial dysfunction in Metabolic Syndrome

The mechanisms of ED, associated with the constituents of the MetS, mainly involve decreased production of NO or an imbalance in the homeostasis due to downregulation endothelium-derived relaxing (e.g., NO, PGI2, EDHF) and upregulation of contracting factors (e.g., prostaglandin H2, thromboxane A2, and endothelin-1) (Lerman and Zeiher 2005). Decreased NO might be caused by reduced expression of the eNOS, a lack of substrate or cofactors for eNOS (eNOS uncoupling) and increased/accelerated NO degradation by ROS during oxidative stress (Cai and Harrison 2000). Nevertheless, ED is not only associated with decreased NO but might also involve increased vascular sensitivity or production of endothelial-dependent vasoconstricting factors (Tune et al. 2017). During the metabolic syndrome, the endothelium switches from a functional to a dysfunctional state. This involves the promotion of pro-inflammatory and oxidative stress pathways, via a number of active changes within the vasculature, that are mainly related to ROS production (Deanfield et al. 2007; Aoqui et al. 2014).

During **hyperglycemia**, an impairment of endothelium-dependent vasodilatation occurs in small and large arteries i.e. coronary arterioles, aorta, and mesenteric arteries. This impairment is mainly related to increased O_2^- production and to activation of immune responses that results in decreases in both endothelium-dependent relaxing factors function and insulin regulation (Tran et al. 2020). As much as ED might be a consequence of IR, it also impairs insulin signaling further reducing insulin sensitivity and thereby inducing a vicious cycle in the MetS. For instance, in obese zucker rats, the alteration of insulin signaling (PI3K-Akt-eNOS) impairs the vasodilatation of resistance arteries due to decreased insulin-mediated NO synthesis. The mechanism behind this insulin resistance-induced impairment involves ROS that lead to a degradation of eNOS's precursor, BH4, resulting in decreased NO production and thus, to the alteration of NO-dependent vasodilation (Eringa et al. 2007). In addition, oxidation of BH4 results in decreased interaction between eNOS and BH4 leading to eNOS uncoupling and thereby to O_2^- production instead of NO (Heitzer et al. 2000). In this state eNOS itself becomes a ROS generator, creating a vicious cycle (Mudau et al. 2012). On the other hand, ED impairs insulin action by altering the transcapillary passage of insulin to insulin-sensitive tissues. The decrease in capillary network expansion, accompanied with a compromized microcirculatory blood flow, contributes to the impairment of

insulin-induced glucose uptake and lipid metabolism in metabolically active tissue (Vykoukal and Davies 2011).

Furthermore, advanced Glycation End Products (AGEs) are lipids or proteins that become glycated as a result of exposure to sugars. During hyperglycemia, AGEs are increased, leading to ED in multiple ways. First AGEs might increase the rate of eNOS mRNA degradation (Eringa et al. 2007). AGEs produce ROS and increases oxidative stress either by activating NOX through RAGEs (specific receptors for AGE) or 1,2-diacylglycerol (DAG)/protein kinase C (PKC) pathway (Wautier et al. 2001; Picchi 2010). Another mechanism by which AGE induces ROS generation through direct glycation and inactivation of the antioxidant enzyme, superoxide dismutase (SOD) (Picchi 2010).

All of the above-mentioned mechanisms involve an ED originating from decreased vasodilation. However, it was found that acute hyperglycemia might also promotes vasoconstricting-prostanoid production and thereby to increased vascular SMC contractility and vascular tone leading to ED (Bagi et al. 2003; Okon et al. 2003).

In **dyslipidemia**, endothelial-dependent relaxation is impaired through multiple and sometimes selective pathways. For instance, in hypercholesterolemia, ach-induced vasorelaxation is reduced while BK-induced vasorelaxation remains intact meaning that the alteration of vasorelaxation pathways is selective in response to increased cholesterol levels (Matsumoto et al. 2004; Gendron et al. 2007). In addition, during dyslipidemia, an increase in oxidized LDL (oxLDL) alters the endothelial function. This occurs through attenuation of NO production either by acting on receptors that decrease L-arginine availability or by decreasing eNOS expression (Saraswathi and Hasty 2006; Shi et al. 2014). Moreover, it was found that in dyslipidemia, pro-inflammatory cytokines i.e. Tκα may reduce eNOS activity and thereby impair vasorelaxation through interfering with eNOS mRNA levels (degradation) (Yoshizumi et al. 1993). ADMA, are increased during hypercholesterolemia, leading to decreased NO bioavailability (Sibal et al. 2010).

In **obesity**, the degree of visceral adipose tissue strongly affects the severity of ED, through multiple mechanisms of which, adipocyte hypertrophy, hypoxia and macrophage infiltration (Lobato et al. 2012). Increased visceral adiposity leads to eNOS uncoupling through increasing oxidative stress and changing the pro-inflammatory adipokine profiles. This change involves an

increase of adipokines that are known for having harmful effects and a decrease in those that exert protective effects such as plasminogen activator inhibitor-1 (PAI-1) and adiponectin, respectively (Q. Li et al. 2015). During obesity, NOX is upregulated leading to increased ROS production and thereby to ED in the aorta (Serpillon et al. 2009; Jiang et al. 2011).

MetS is characterized by an obesity-linked state of chronic low-grade inflammation. During this state, levels of circulating inflammatory markers including CRP, TNF-α and IL-6 are elevated. These markers might lead to ED through increasing ROS generation and decreasing NO (NO) bioavailability (Labazi and Trask 2017). The activation of the nuclear factor-κB (NF-κB)-induced pro-inflammatory pathways (production of cytokines and adhesion molecules) also seems to play an important role in the impairment of endothelial-dependent relaxation through increasing ROS and reducing NO production (De Martin et al. 2000; Kobayasi et al. 2010). TNF-α, in particular was found play a major role in ED through inhibiting endothelium-dependent vasorelaxation (Greenberg et al. 1993). In fact, increased levels of TNF-α leads to decreased NO bioavailability through multiple mechanisms. It might reduce NO production either by direct inhibition of eNOS expression and activity or by stimulation of the endogenous NOS inhibitor ADMA (Yoshizumi et al. 1993; Ito et al. 1999; Valerio et al. 2006). TNF-α may also increase the NOX activity in endothelial cells and smooth muscle cells, stimulating O_2^- production and the subsequent NO removal (Griendling et al. 2000)(Didion et al. 2002). Moreover, it was found that TNF-α inhibits the kinase activity in the insulin signaling pathway of insulin-sensitive tissues such as skeletal muscle and adipocytes, leading to decreased NO production (Del Aguila et al. 1999; F. Kim et al. 2001).

ED is not always associated with impaired vasodilation, but might as well be related to increased vasoconstriction. For example, in both the thoracic aorta and the carotid artery vascular dysfunction was found to result from increased thromboxane gene expression and vasoconstrictor prostanoids (Traupe et al. 2002). Moreover, in another study obesity increased ET-1-induced vasoconstriction (Mundy et al. 2007).

A strong link between ED and **hypertension** has been established. On the other hand, a sustained increase in blood pressure has been strongly associated with decreased levels of NO and increased ROS in the vasculature (Konukoglu and Uzun 2016). Thus, Oxidative stress seems to

play a major role in the pathophysiology of hypertension-induced ED. In fact, besides the fact that ROS are able to directly stimulate vasoconstriction and to impair antioxidant production, they decrease NO bioavailability thereby leading to ED (Santilli et al. 2015). The decrease in NO levels in this case might be related to increased NO scavenging to form ONOO− which leads to eNOS uncoupling. In addition, angiotensin II-induced hypertension was found to increase NOX activity, which then increases superoxide, triggering eNOS uncoupling thereby leading to impaired NO/cGMP signaling and to ED (Mollnau et al. 2002; Y. H. Zhang 2017). Moreover, as in hypercholesterolemia, ADMA levels are increased during hypertension leading to decreased NO bioavailability (Sibal et al. 2010). Moreover, in cases of hypertension, levels of Arginase, a competitor of NOS for the substrate L-arginine, are increased resulting in decreased NO production (Toque et al. 2013).

During hypertension, rodents may show increased prostanoids-induced vasoconstriction. However, in humans, the main underlying cause of vascular dysfunction in hypertension is impaired endothelium-dependent vasodilation (Paul M et al. 2008; Paul M et al. 2005).

3.2. Cardiac changes

3.2.1. Functional alterations

Myocardial function has been shown to be impaired in models of MetS. Among the main factors that have been suggested to be responsible for cardiac abnormalities during MetS are alterations in the NO pathway and the β-adrenergic system. Alterations in the β-adrenergic system, may occur at both the receptor or post-receptor intracellular signaling level, i.e. calcium (Ca^{2+}) handling proteins (J. F. Carroll et al. 2002; Lima-Leopoldo et al. 2011). Moreover, myocardial metabolism also seems to be dysregulated during the MetS

3.2.1.1. Alterations in β-adrenergic system

β-adrenergic alteration at the receptor level

Decreases in β-ARs affinity and/or density, also known as β-ARs desensitization, leads to loss of the receptor's activity (Cros 1985). This decrease is associated with catecholamine-induced overstimulation, often originating from chronic SNS activation, encountered during the MetS (Tune et al. 2017). To avoid the deleterious effects of excessive and prolonged sympathetic

stimulation, two types of compensatory mechanisms might be initiated, homologous and heterologous desensitization.

The **homologous desensitization** requires the fixation of a ligand on the β–AR, changing the receptor's conformation and thereby leading to its phosphorylation at the C-terminal level by G protein coupled receptor kinase GRK (Walther and Ferguson 2013). This phosphorylation then allows the recruitment of β-arrestin to the membrane where it binds to the receptor, decreasing its affinity to G proteins, subsequently leading to their uncoupling from one another (Kelly et al. 2008). In addition, β-arrestin is essential for the formation of endocytic vesicles, it allows the receptor internalization and its degradation and/or recycling thereby leading to its downregulation (Kohout and Lefkowitz 2003; Violin et al. 2014).

In contrast to the latter, **heterologous desensitization** does not require the binding of a ligand and even desensitizes the receptor to other ligands; it involves phosphorylation of the receptor at the C-terminal level of the β–AR via the PKA. This phosphorylation causes rapid uncoupling of the G protein from β–AR. Among all the three β–AR subtypes, only β3-AR has low tendency to homologous and heterologous desensitization, since it lacks potential phosphorylation sites, which makes it insensitive to GRK and PKA mediated desensitization, respectively (Rozec and Gauthier 2006)

β-adrenergic alteration at the intracellular signaling level

Alterations in one or more components of the β-receptor–Gs protein–adenylate cyclase–cAMP pathway have been implicated in the reduced contractile response (Joan F. Carroll et al. 1997; J. F. Carroll, Kyser, and Martin 2002). In the intracellular myocardial domain, both cardiac Ca2+ channel/ryanodine receptor (RyR2) and SERCA pump play a key role in the modulation of cardiac excitation–contraction coupling (ECC). The former via Ca2+release and the latter via Ca2+ uptake into internal stores (Fernández-Miranda et al. 2019). Many researchers suggested that the molecular pathways linking the MetS to myocardial dysfunction involve myocardial Ca2+ mishandling and altered signaling due to alteration in sarcoplasmic reticulum function via changes in the functional expression of SERCA pump and ryanodine (RyR2) receptors (Dincer 2011; Okatan, Durak, and Turan 2016). In fact, in a study done by Fernandez et al, They demonstrated that Ca2+ mishandling in MetS heart is due to a decreased functionally active RyRs and to reduced

SERCA pump activity through decreased Ser2814 and Thr17-PLN phosphorylation, respectively (Fernández-Miranda et al. 2019).

As mentioned earlier, during MetS, the SNS is overactivated leading to an increase in circulating catecholamine levels. However, increased exposure to CAs can become harmful through a β-ARs signaling dysfunction, that results in a decreased cardiac function and inotropic reserve due to decreased cardiac β-ARs responsiveness (Lymperopoulos, Rengo, and Koch 2013).

3.2.1.2. Alterations in nitric oxide pathway

In the heart, impaired NO availability and its signalling seems to be associated with many risk factors including those constituting the metabolic syndrome and others (Pechánová et al. 2015). These risk factors include: hyperlipidemia/atheroclerosis, high blood pressure/hypertension, an unbalanced diet, sedentary lifestyle and diabetes (Lundberg et al. 2015).

The pathological remodelling, that occurs during **hypertension**, seems to be related to an imbalance between vasoconstrictor and proliferative activities on one hand and vasodilating and anti-proliferative effects on the other hand. The former mainly involves Ang II, aldosterone or ET-1 meanwhile the latter includes NO, PGI2, BK, or ANP (Pechánová et al. 2015). In fact, in normal states, NO not only antagonizes the effects of Ang II (on vascular tone and renal sodium excretion) but also downregulates the synthesis of AT1 receptor and ACE. Thus during hypertension, Ang II increases oxidative stress thereby leading to a decrease in NO bioavailability and thereby counteracting the NO antagonistic effects (Tirziu and Simons 2008).

As mentioned earlier ROS production is not always harmful as it stimulates the anti-oxidant defense activities and improves NO signaling thus maintaining an equilibrium between oxidative stress and the NO pathway (Dröge 2002). However, in obesity related hypertension, ROS might favor the activation of the pro-inflammatory NF-κB-dependent pathways. This results in increased levels of inflammatory cytokines e.g. TNF-α and IL-6 which leads to a decrease in NOS activity and eventually in NO bioavailability (Belin de Chantemele and Stepp 2012). Moreover, NO-sGC-cGMP is impaired during hypertension. This seems to be related to prolonged ROS formation that leads to eNOS/iNOS uncoupling (J. P. Stasch et al. 2011; Evgenov et al. 2006).

Leptin is an adipocyte-derived hormone that plays an important role in regulating energy balance and metabolism. During **obesity**, disrupted leptin signaling was found to be linked to

nitroso-redox imbalance. The latter involves decreased cardiac expression of nNOS and NO production, with a parallel increase in XO activity and oxidative stress (Saraiva et al., 2007).

In addition, a link between decreased cardiac β_3-AR expression and function and leptin deficiency has been established. Hyperleptinemia might be closely associated with obesity, however it should be noted that it coexists with leptin resistance mimicking leptin deficiency states. This explains leptin's role in obesity-related cardiac hypertrophy and heart failure (Larson et al., 2012). It was also suggested that leptin might impair myocyte function through an upregulation of iNOS that generates large amounts of NO thereby inducing nitrosative/nitrative stress.

Cardiac lipotoxicity related to obesity has been described to be related to impaired NO signaling . For instance, elevation of ceramides levels seem to activate NOX promoting oxidative stress in cardiomyocytes (Zhang et al., 2003). In cardiomyocytes eNOS and caveolin-3's colocalization falicitates both eNOS activation and NO release. Increased ceramide levels in obesity may inhibit eNOS activity by decreasing caveolin-3 expression proteins (Knowles et al., 2013).

Cardiac NO metabolism seem to be strongly affected by **hypercholesterolemia**. Many have reported that besides decreasing NO cardiac levels, increased cholesterol levels blunt the NO signaling through lowering the PKG activity. Some have also found decreased phosphorylated levels of eNOS in the myocardium. However, results regarding eNOS are controversial, since others suggested that decreased levels of NO during hypercholesterolemia are related to increased NO clearance rather than decreased eNOS activity. NO elimination seems to be the result of increased oxidative stress markers i.e. O_2^- originating from elevated XO and NOX activities. Moreover, Increased XO activity was found to be associated with myocardial and coronary ED, in cholesterol-enriched diet-fed guinea pigs. In another study, performed on genetically hypercholesterolemic mice, positive chronotropic effect of atropine was lost. While decreased cardiac contractility and eNOS expression was reported to be decreased in another hypercholesterolemic mice model. Furthermore, besides decreased NO bioavailability, NO-sGC signaling also seems to be impaired during atherosclerosis (Pechánová et al. 2015).

In health, the myocardium uses both glucose and fatty acids (FAs) as main sources of energy to sustain a continuous contractile activity. During MetS, the **myocardial metabolism is dysregulated** due to substrate imbalance. The latter results from an excessive reliance on FA, rather than glucose, as a source of energy. In fact, that chronic fuel shift towards FFAs as substrate

appears to be linked to cardiac dysfunction and increased susceptibility to heart failure (Tune et al. 2017).

In **obesity and IR**, the myocardium exhibits abnormally increased rates of fatty acid uptake and oxidation (Rider et al. 2013). The impaired ability to shift away from this increased FA utilization leads to decreased glycolysis and glucose oxidation (Lopaschuk 2016). Since FFAs require more oxygen for each ATP mole generated, an over-reliance on FA oxidation as a source of energy increases oxygen consumption for contractility (How et al. 2005). In support of this, is that stimulating glucose oxidation and inhibiting fatty acid oxidation increases the cardiac efficiency during heart failure (Lopaschuk et al. 2010).

3.2.2. Structural alterations

3.2.2.1. Cardiac remodeling

Cardiac remodeling is associated with MetS. It is considered as an adaptive response from heart to stress related physiological and pathological conditions i.e. changes in the volume and pressure loads or even metabolic changes (Ferron et al. 2018). Cardiac remodeling encountered during the MetS mainly involves **left ventricular (LV) remodeling** that might be **eccentric** or **concentric** (Grossman 2009). An increase in volume, results in an eccentric LV hypertrophy (LVH) characterized by dilatation of the LV chamber, as a reactive mechanism to compensate for volume overload. Whereas, an increase in pressure, results in a concentric LV hypertrophy characterized by increased LV wall thickness, as a reactive mechanism to compensate for pressure overload (Müller and Dhalla 2013). The increased metabolic demand resulting from **increased adiposity** and augmented mass in obesity leads to an elevated blood volume and subsequently to an increase in **preload** (Vasan 2003). In addition, not only hyperadiposity but also hyperinsulinemia, encountered during **IR** increases sodium reabsorption in response to increased activation of nephron sodium transporters and thereby contributes to intravascular volume expansion, through fluid retention, also leading to increased preload (Demarco et al. 2014). Moreover, **afterload** is also elevated in individuals with **MetS**, e.g. in **obese** and/or in **hypertensive**, due to both augmented peripheral resistance and increased conduit artery stiffness (Vasan 2003; Grossman 2009). LVH has also been reported in rabbits (Joan F. Carroll et al. 1999). In a Multi-Ethnic Study of Atherosclerosis (MESA), **IR** and waist-to-hip ratio were found to be associated with concentric LVH independent of BMI (Shah et al. 2013; Ferron et al. 2018) found

that, rat animal models of diet-induced **dyslipidemia/MetS**, developed cardiac remodeling characterized by LV hypertrophy. In their study (Panchal et al. 2011) showed ventricular dilation, increased systolic volume and increased estimated left ventricular mass in rat models of diet induced MetS.

Whether cardiac changes are structural (LVH) or functional (subclinical impairment of LV systolic and diastolic function), they are believed to be precursors to cardiac dysfunction and heart failure (Abel et al. 2008).

4. Management of the Metabolic Syndrome

4.1. Non-pharmacological interventions

4.1.1. Nutrition

One of the main underlying causes of the MetS is an imbalance between energy intake and energy expenditure that eventually leads to an excessive weight gain (Drenowatz 2015). Therefore, weight control and reduction are considered as the cornerstones in prevention and treatment of the metabolic syndrome (Magkos et al. 2009). Weight reduction could be achieved, either through lowering energy intake or through increasing energy expenditure (Hill, Wyatt, and Peters 2012). The former is often accomplished by consuming a healthier reduced calorie diet meanwhile the latter involves engaging in physical activities and exercise (Strasser 2013). In a prospective study done by Hasegawa et al., it was shown that even modest weight reduction of 5 % can substantially lower blood pressure, improve blood lipid profile, insulin sensitivity and glucose tolerance (Hasegawa et al. 2019).

Eating a healthier diet also has a great impact on the health outcomes. In their prospective cohort study, Wang et al., found that healthy diet interventions promote weight loss and prevent metabolic syndrome, even in individuals with elevated genetic risk for obesity (T. Wang et al. 2018). Healthy diets consist of diets low in saturated fat, high in protein and fiber, rich in fruits and vegetables, and with a low glycemic index (Skerrett and Willett 2010). This type of diet, e.g. Mediterranean diet, is associated with decreased risk of metabolic syndrome, T2DM as well as CVD morbidity and mortality (Sleiman et al. 2015; Estruch et al. 2018; Pallazola et al. 2019). Moreover, in a randomized controlled trial done by babio et al., it was found that Mediterranean diet was associated with reversion of the MetS (Babio et al. 2014). Other types of diets have also been found to be effective in the management of the MetS e.g. vegetarian and Dietary Approaches to Stop Hypertension (DASH) diets. The former has been associated with lower risk of MetS (N. S. Rizzo et al. 2011); meanwhile, the latter has proven to be effective in controlling ABP and improving the lipid profile, glucose metabolism, and other cardiovascular risk factors (Saneei et al. 2013).

There also exists pattern of diets such as intermittent fasting diet that has recently emerged as a beneficial approach in the management of MetS. In their clinical study Wilkinson et al., were

able to show that time restricted feeding (10 hours/day) intervention improves cardiometabolic health for patients with metabolic syndrome (M. J. Wilkinson et al. 2020).

4.1.2. Physical activity

Weight loss (decreases in body mass) is often associated with a decline in metabolism, especially when not associated with physical activity. This often leads to a lack of success in long-term weight loss and maintenance. Therefore, the state of negative energy balance (calorie deficit), needed for weight loss is better achieved through energy expenditure exceeding energy intake, which is reached through increased physical activity (Hill, Wyatt, and Peters 2012).

Physical activity is associated with reduced risk of obesity, T2DM and CVD. There is substantial evidence from several studies that exercise is effective in the treatment of the metabolic syndrome (Misra et al. 2008; Ilanne-Parikka et al. 2010; Conceição et al. 2013; He et al. 2014). Generally, the beneficial effects of exercise include regulating fat and glucose metabolism, improving insulin sensitivity and lowering ABP (Golbidi et al. 2012). The recommendation is around 30–60 min of moderate intensity exercise, including aerobic and work-related activity and muscle strengthening (as tolerated), five days a week but preferably all days of the week (Grundy et al. 2005; Pérez-Martínez et al. 2017). Aerobic exercise, resistance training, and their combination have been reported to be effective in improving hyperglycemia, reducing ABP and upregulating skeletal muscle oxidative capacity (Dipla et al. 2020).

Anderssen et al., found that the Association of both diet and exercise is significantly more effective than either approach alone for the treatment of metabolic syndrome (Anderssen et al. 2007).

4.2. Pharmacological intervention

4.2.1. Anti-obesity agents

Weight loss can be achieved through phramacotherapeutic agents. These either limit the absorption of food either suppress appetite and thus reduce food intake or increase energy expenditure.

4.2.1.1. Agents that limit food absorption

One of the most used is, Orlistat a Food and Drug Administration (FDA) approved medication for the treatment of obesity. It acts by inhibiting gastric and pancreatic lipase leading to decreased

free fatty acid and cholesterol absorption. It can reduce fat absorption by up to 30%. Orlistat should be combined with diet, exercise, and behavior modification to significantly improve weight management. However, Orlistat is associated with gastrointestinal side effects (Furman 2007; G. W. Kim et al. 2014).

4.2.1.2. Agents that reduce the appetite

The hypothalamus, contains two key populations of neurons that stimulate (e.g. NPY) or inhibit (e.g. POMC) food intake (Suzuki et al. 2010). Agents that reduce appetite (anorectic) act by targeting the hypothalamic appetite pathways either through direct stimulation or via dopaminergic or serotoninergic signaling (Jones and Bloom 2015).

Liraglutide is a glucagon-like peptide-1 (GLP-1) mimetic also known as incretin mimetic. This medication is used as an anti-obesity and anti-diabetic agent. GLP-1 directly interacts with the hypothalamic POMC neurons leading to decreased food intake. Several clinical trials have demonstrated that, when adjunct to diet and exercise, liraglutide was associated with reduced body weight (Wadden et al. 2013; Pi-Sunyer et al. 2015; Ard et al. 2016).

These agents might be successful in reducing weight, however care should be taken since their side effects sometimes exceeds their beneficial effects such as in the case of Lorcaserin. This medication is a serotonin receptor agonist that decreases appetite and reduces food intake through stimulation of the anorexogenic POMC neurons (Jones and Bloom 2015). It was withdrawn from the market in 2020 at the request of the FDA, after a clinical trial showed an increased occurrence of cancers including pancreatic, colorectal and lung cancer ("FDA Requests the Withdrawal of the Weight-Loss Drug Belviq, Belviq XR (Lorcaserin) from the Market | FDA" 2020)

Bupropion/Naltrexone bupropion is a dopamine/norepinephrine reuptake inhibitor is used in combination with naltrexone, an opioid receptor antagonist. Combining these two agents leads to reduced appetite the former, stimulates POMC neurons whereas the latter counteracts the autoinhibitory effects of endogenous opioids (Jones and Bloom 2015). In a phase 3 trial, combination of naltrexone/bupropion lead to up to 6.1% of weight loss (Greenway et al. 2010). In another study conducted by Hollander et al., it was shown that naltrexone/bupropion combination leads to more than 5% weight loss, decreases HbA1c and also improves TG and HDL-C levels (Hollander et al. 2013). This combination has been reported to increase blood pressure and suicidality (Jones and Bloom 2015).

4.2.1.3. Agents that increase energy expenditure

Increased energy expenditure (EE) mainly occurs through increased thermogenesis, the dissipation of energy in form of heat. The main organs responsible for adaptive thermogenesis are skeletal muscle, brown adipose tissue (BAT), and white adipose tissue (WAT) (K. Y. Chen et al. 2020).

Sympathomimetic drugs such as ephedrine have been used to increase EE in rodents and humans. Ephedrine is thought to directly activate the β-ARs and to increase EE through activation of skeletal muscle rather than BAT and was also found to decrease appetite. A meta-analysis of 20 clinical trials has found that ephedrine treatment was associated with many adverse effects e.g. cardiovascular side effects as well as other risks. Other agents also exist such as caffeine and nicotine (K. Y. Chen et al. 2020). Combination of phentermine and topiramate has been shown to be efficacious in inducing and maintaining negative energy balance in addition to improved lipid profile and blood pressure (Jordan et al. 2014; Jones and Bloom 2015). These long-term effects suggest an increase in metabolic rate with no effects on BAT thermogenesis.

Activators of brown adipose tissue activity has been described as a target for the treatment of obesity/insulin resistance (Poher et al. 2015). BAT expresses high levels of uncoupling protein-1 (UCP-1), which uncouples mitochondrial substrate utilization from ATP production, leading to energy dissipation as heat (thermogenesis) (Dehvari et al. 2018). BAT is also able to utilize both glucose and fatty acids from TG in mitochondrial metabolism (Townsend and Tseng 2012) and has been postulated to also use cholesterol (Worthmann et al. 2017), thereby releasing the resulting energy in form of heat. Pharmacological activation of β_3-AR expressed on WAT and BAT has proven to be possible (Szentirmai and Kapas 2017a). One of the most promising β_3-AR agonists is **Mirabegron**. It is currently under investigation as an anti-obesity and anti-diabetic agent (O'Mara et al. 2020; Finlin et al. 2020).

4.2.2. Anti-diabetic drugs

4.2.2.1.Glucagon-like peptide-1 mimetics

GLP-1 mimetic such as **Liraglutide** not only stimulates satiety (anorectic) but also enhances postprandial glucose-stimulated insulin release by pancreatic β cells (Murphy and Bloom 2006). GLP-1 is also suspected of stimulating energy utilization via BAT (Beiroa et al. 2014). In their

study, Wadden et al., they showed that Liraglutide, prescribed as 3.0 mg per day, not only leads to weight loss of 6 % but also helps in maintaining weight loss and improves CVD-risk factors (Wadden et al. 2013). Liraglutide has demonstrated improvements in glycaemic control of T2DM patients, associated with amelioration in both β cell function and insulin resistance (Ferdinand et al. 2014).

Despite their success as both anti-obesity and anti-diabetic agents, GLP-1 receptor agonists have been associated with a possible risk of medullary thyroid cancer in mice (Rosol 2013).

4.2.2.2. Antihyperglycaemic drug

Metformin is an oral antidiabetic drug commonly used as a first-line treatment for T2DM. It is also considered as an insulin sensitizer. This medication has been shown to reduce excessive rates hepatic glucose production, decreases intestinal absorption of glucose, and improves insulin sensitivity by increasing extrahepatic peripheral glucose uptake and utilization (Binesh Marvasti and Adeli 2010) (Rena et al. 2017). Metformin was also reported to stimulate glucagon-like peptide 1 (GLP-1) secretion likely leading to prevention of weight gain (Rena et al. 2017).

Metformin does not only exhibit anti-hyperglycemic properties but has also proven to be effective in weight loss and in improving endothelial function, insulin resistance, lipid profiles, and decreased visceral fat (Reinehr et al. 2004; Rojas and Gomes 2013).

4.2.2.3. Insulin-sensitizing agents

Rosiglitazone is PPAR-gamma (peroxisome- proliferator-activated receptor gamma) stimulator used as second-line treatment for T2DM. It does not only exhibit hypoglycaemic effects but also plays an important role in the regulation of cardiovascular functions (Binesh Marvasti and Adeli 2010).

The combination of rosiglitazone and metformin have proven to be very effective in the treatment of T2DM. In a randomized double-blind controlled trial, Zinman et al., were able to show that a low-dose combination therapy of rosiglitazone and metformin prevented the occurrence of T2DM in patients with impaired glucose tolerance with little or no adverse effects (Zinman et al. 2010).

4.2.3. Anti-dyslipidaemic agents

4.2.3.1. Cholesterol lowering agents

Statins are a class of drugs that inhibit HMG-CoA reductase, the enzyme responsible for catalyzing cholesterol biosynthesis pathway. Statins are very effective in the treatment of hypercholesterolemia through reducing both the plasma levels of cholesterol and apoB-containing lipoproteins. They act by upregulating the LDL-receptor expression (increased cholesterol uptake) and by regulating apoB. They either reduce translocation of apoB across the endoplasmic reticulum (ER) membrane or increase their intracellular degradation, leading to diminished lipoprotein assembly. Statins were also found to be effective in reducing plasma TG levels. The most common statins are atrovastatin, simvastatin, and rosuvastatin. Besides their ability to decrease cholesterol and LDL-C levels, these molecules can have additional beneficial effects (Binesh Marvasti and Adeli 2010).

Atrovastatin

In a study conducted, on an animal model of IR (the fructose-fed Syrian golden hamster) treatment with atorvastatin, not only reduced the LDL-C levels, but also ameliorated lipoprotein overproduction and improved hepatic insulin sensitivity and signaling (Binesh Marvasti and Adeli 2010).

Simvastatin

Simvastatin treatment was shown to acutely increase synthesis and secretion of apoA, a major Apo-lipoprotein of HDL particles (Gratl et al. 2002). Even though other statins were also shown to increase HDL levels, simvastatin was the most effective in raising plasma HDL concentrations (Binesh Marvasti and Adeli 2010).

Rosuvastatin

Amongst the statin family rosuvastatin was found to have the highest therapeutic efficacy in reducing LDL-C (Hu and Tomlinson 2013) due to higher interaction with Hydroxymethylglutaryl-coenzyme A (HMG-CoA) reductase (Binesh Marvasti and Adeli 2010). In a randomized trial study by Park et.al, rosuvastatin (10 mg) was found to be more effective than atorvastatin (10 mg) in attaining the NCEP ATP III LDL-C goals. Greater reductions in total cholesterol, HDL-C and apoB levels were observed with rosuvastatin treatment in MetS patients (J. S. Park et al. 2010). Napels et al., also reported an improvement of insulin sensitivity via improved cellular insulin

signal transduction in response to rosuvastatin treatment (Naples et al. 2008). In a recent systematic review and network meta-analyses of 50 Randomized Controlled Trials, rosuvastatin ranked 1st in LDL-C- and ApoB-lowering efficacy and ApoA1-increasing efficacy (Zhang et al. 2020).

Two other statins exist on the market, such as lovastatin that was reported to have a high efficacy in TC- and TG-lowering efficacy and fluvastatin that showed a high efficacy in increasing HDL-C (X. Zhang et al. 2020).

4.2.3.2. Cholesterol absorption inhibitors

Cholesterol absorption inhibitors are a class of medication that decrease the absorption of cholesterol in the small intestine leading to decreased cholesterol delivery to the liver and enhanced cholesterol clearance.

Ezetimib

Ezetimib is one of the most widely used subclasses. It inhibits the intestinal absorption of dietary and biliary cholesterol by binding to the transport protein (NPC1L1) leading to decreased LDL-C levels. It is often combined with statins. Ezetimibe's potency in decreasing LDL-C and apoB substantially increases in combination with statins, leading to a total LDL-C lowering of 34–61% (Vavlukis and Vavlukis 2020). In a double-blind, placebo-controlled trial, conducted by, Pearson et al., it was reported that the combination ezetimibe and statin is more efficient in reducing LDL concentration compared to treatment with statin monotherapy (Pearson et al. 2005). Moreover, In a meta-ananlysis study, Yu et al., found that the addition of ezetimibe to statin is more effective on reducing LDL-C and TC concentrations than using a double dose of statin (Yu et al. 2020).

4.2.3.3. Triglyceride lowering agents

Fibrates or fenofibrates are mainly used to treat high triglyceridemia. They act by both enhancing VLDL-TG catabolism and reducing VLDL-TG production but are also associated with a modest decrease in LDL-C and an increase in HDL-C levels (Staels et al. 1998). These molecules stimulate peroxisome proliferator activated receptor-α (PPARα), a transcription factor that controls the expression of genes mediating triglyceride metabolism. This leads to decreased fatty acids and TG synthesis resulting in decreased hepatic VLDL-TG prodcuction. Fibrates also increase

lipoprotein lipase activation and apo-A1 synthesis promoting TG catabolism (decreased VLDL production) and HDL production, respectively, via PPARα (Simons and Sullivan 2005; N. H. Kim and Kim 2020). Fibrates are often associated with statins (M. Elam et al. 2011; M. B. Elam et al. 2017; Zhu et al. 2020). In a cohort study performed on Mets patients, kim et al., showed that the risk of major cardiovascular events was significantly lower with fenofibrate as add-on to statin treatment than with statin treatment alone in adults with metabolic syndrome (N. H. Kim et al. 2019).

4.2.4. Anti-oxidants agents

Antioxidants are agents that can be benificial due to their direct effect on oxidative stress. An imbalance between ROS production (increased) and antioxidant defense system (decreased) leading to a state of oxidative stress, has been associated with the MetS (Bilbis et al. 2014). Antioxidants are now being considered in the management of MetS due to potential beneficial effects on constituants of the MetS, diabetes and cardiovascular dysfunctions (Bilbis et al. 2014; Martins Gregório et al. 2016). Antioxidants are either found in a wide range of foods or available as supplements. Antioxidants that might be beneficial in the Mets context include flavonoids, arginine, vitamin C, vitamin E, carotenoids, resveratrol and selenium (Martins Gregório et al. 2016). Data from many experimental and clinical studies, performed on animals and humans, indicate that these aformentioned antioxidants have potential benefits against diabetes, insulin resistance, dyslipidemia, obesity, and cardiovascular dysfunctions. Nevertheles, conflicting data have been reported, since some studies found no beneficial effects of antioxidant supplementation.

In their study bilbis et al., investigated the effects of vitamins A, C, and E in the management of metabolic syndrome in rats. They found a significant reduction in blood pressure, total cholesterol, TG, LDL-C, and VLDL-C and an increase in both HDL-C and total antioxidant status compared to the unterated group (Bilbis et al. 2012). Salonen et al., found that supplementation vitamin E and vitamin C slowed down atherosclerotic progression in hypercholesterolemic patients (Salonen et al. 2003). Whereas in a randomized, double-blind, placebo-controlled trial (HOPE), performed on 55 years-old patients with diabetes and vascular disease, Lonn et al. failed to show any improvement in cardiovascular outcomes (Lonn et al. 2005).

4.2.5. Anti-hypertensive agents

First-line pharmacological treatment of hypertension include diuretics, ACE inhibitors or angiotensin receptor blockers (ARBs), beta-blockers, and calcium channel blockers (CCBs). A combination of two antihypertensive medications is commonly used to achieve a certain ABP target and/or to minimize side effects (Nguyen et al. 2010).

Antihypertensive drugs might significantly interfere with glycaemic control, insulin resistance, lipid metabolism, and electrolyte balance (Studyštefan et al. 2017). Therefore, care is taken when choosing an antihypertensive treatment in patients with MetS. On the other hand, some of these molecules, in addition to their effect on ABP, have beneficial cardiometabolic effects and are even recommended during MetS. For instance, ACE inhibitors, are well known for their nephroprotective, angioprotective, cardioprotective and metabolic effects (improve IR) (Israili et al. 2007; Studyštefan et al. 2017). Long-acting CCBs also improve IR. The ARBs are both renoprotective and cardioprotective. The combination of β-blockers to a diuretic to treat hypertension, has been reported to have favorable effect in terms of glucose tolerance and IR in MetS patients (Israili et al. 2007).

4.2.5.1. Diuretics

Diuretics can be divided into 3 groups: thiazides, loop, and potassium-sparing diuretics. Thiazides' mechanism of action involves inhibiting the absorption of Na and Cl in the distal convoluted tubule (Nguyen et al. 2010). Generally, thiazides are the most preferred class of diuretics and were reported as the most commonly used for treatment of MetS (Katsimardou et al. 2019) . Nevertheless, diuretic might induce hypokalemia, leading to hyperglycemia due to an indirect reduction in insulin secretion. Therefore, thiazide diuretics should be used in combination with potassium-sparing diuretics or with potassium supplements (Zillich et al. 2006).

4.2.5.2. Renin-angiotensin system (RAS) inhibitors

ACE inhibitors and ARBs, both result in the blockage of the RAS. A correlation between RAS and IR has been well established (Katsimardou et al. 2019). The mechanism behind this correlation is believed to be related to a state of vasoconstriction induced by the activation of the system, that affects the delivery of glucose and insulin to the skeletal muscle cells and leads to IR.

Therefore, RAS inhibitors not only have positive effect on hypertension but also on glucose metabolism (Henriksen and Prasannarong 2013). In addition, RAS inhibitors are associated with cardioprotection. In a prospective cohort study, conducted by Zreikat et al., it was found that ACE inhibitor/ARB use was associated with a lower risk of cardiovascular events in old hypertensive patients with MetS (Zreikat et al. 2014). In their study by Kintscher et al., showed that treatment with an ARB improved in blood pressure and metabolic risk factors (Kintscher et al. 2007). Takagi et al., also found improvement of metabolic parameters in patients with metabolic syndrome, in response to treatment with an ARB (Takagi et al. 2013). In a meta-analysis by Y. Wang et al., an ARB was found to improves insulin resistance (Yan Wang et al. 2018).

4.2.5.3. Beta blockers

Overactivation of the SNS has been proposed as a key pathophysiologic mechanism, in the pathogenesis of hypertension in MetS (Thorp and Schlaich 2015). Therefore, inhibition of the sympathetic system is expected to be beneficial in the treatment of hypertension. However, some conventional β-blockers were found to induce negative metabolic effects, such as weight gain, glucose intolerance and dyslipidemia in addition to an onset of diabetes (Sharma et al. 2001; Mancia et al. 2006). These adverse effect seem to be mainly related to β_2-AR blockade is associated with inhibition of insulin release (Philipson 2002; Studyštefan et al. 2017) and to vasoconstriction. In contrast, β-blockers, with a simultaneous alpha-adrenergic receptor blocking (vasodilating) effect seem to be associated with a better metabolic profile compared to traditional agents (Katsimardou et al. 2019). In the a prospective, open-label study (YESTONO) study that included hypertensive patients with T2DM three months of treatment with nebivolol improved the metabolic status (fasting blood glucose, HbA1c, total cholesterol, LDL-C, TG, HDL-C)(Bell, Bakris, and McGill 2009). In another study, after 6 months of treatment, in contrast to metoprolol, nebivolol reduced insulin resistance and oxidative stress in patients with hypertension (Celik et al. 2006).

4.2.5.4. Calcium channel blockers.

CCBs are considered safe in the treatment of MetS. They are often used in combination with another antihypertensive medication. CCBs, were found to be associated with a lower incidence of diabetes and resulted in better metabolic and anti-inflammatory effects, when combined to a

ARB, than when combined to a diuretic in hypertensive patients with MetS (Martinez-Martin et al. 2011). In a randomized controlled trial study, conducted by Zanchetti et al., treatment with a CCBs lead to a lower progression of carotid atherosclerosis as well as a lower incidence of new MetS, compared to treatment with a β-blocker (Zanchetti et al. 2007).

4.2.6. Investigational agents (repurposable)

Signaling through the NO-sGC-cGMP-PKG cascade has gained a lot of attention from researchers (M. Park, Sandner, and Krieg 2018) and has emerged as an attractive target in the treatment of metabolic and CVD. This is mainly due to a growing body of evidence that have proven that modulation of the NO-cGMP signaling, by pharmacological tools, could be effective, notably, in metabolic and CVD contexts (J.-P. Stasch et al. 2002; Mitschke et al. 2013; Nossaman and Kadowitz 2013; Pfeifer et al. 2013; Ramirez et al. 2015; M. Park et al. 2018). NO-cGMP signaling is not only a regulator of vascular tone and insulin action but is also a key player in the regulation of energy and fuel homeostasis (Ayala et al. 2007). For instance, sildenafil citrate a PDE 5 inhibitor that leads to increased cGMP levels was proven to be effective in reducing weight, improving glucose tolerance, insulin sensitivity and lipid profiles and reversing ED (Ayala et al. 2007; Behr-Roussel et al. 2008; Salih Sahib et al. 2014; Ramirez et al. 2015). Moreover, what makes activation of the NO-cGMP axis, an appealing target is the fact that it promotes lipolysis and stimulates thermogenic pathways, leading to decreased WAT-mediated fat storage and to increased BAT-mediated energy expenditure (EE), respectively (Cypess and Kahn 2010; G. W. Kim et al. 2014). Pharmacological strategies to increase cGMP include mainly increasing NO, activating soluble guanylate cyclase directly, or decreasing the degradation of cGMP by using a PDE 5 inhibitor (Ramirez et al. 2015).

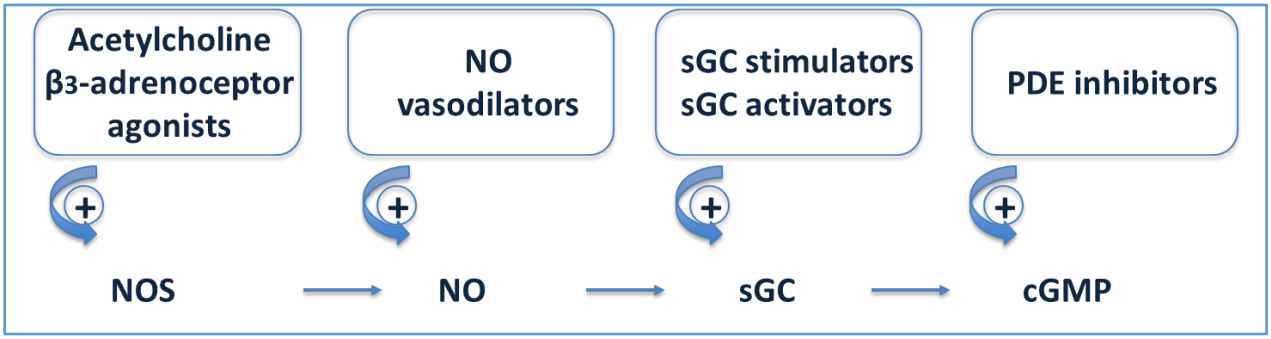

Figure 15: Activation of NO-sGC-cGMP pathway can occur at different levels.

β_3-adrenoceptor agonist stimulate the production of nitric oxide (NO) though activation of nitric oxide synthase (NOS). NO donors, stimulate soluble guanylyl cyclase (sGC). sGC stimulators and activators increase the activity of sGC. Activated sGC stimulates production of cyclic guanosine 3',5'-monophosphate (cGMP). Phosphodiesterases (PDEs) inhibitors, inhibit the break down of cGMP. Inspired by (Kadowitz and Nossaman 2013) .

4.2.6.1. Mirabegron

Mirabegron has been classified as a (β_3-AR) agonist and has been FDA approved for the treatment of overactive bladder (Chapple et al. 2014; Warren et al. 2016; Dehvari et al. 2018). β_3-ARs are expressed in endothelial cells, smooth muscle cells, cardiac myocytes and adipocytes of brown and white adipocytes as well as in other tissues (Cannavo and Koch 2016; Michel and Balligand 2017).

β_3-ARs can activate signaling pathways that may protect the heart, facing myocardial stress (Michel and Balligand 2017). One of the proposed mechanism is that β_3-ARs can act as a brake to prevent β_1 and β_2-ARs overactivation, due to their coupling to Gαi which leads to activation of eNOS/nNOS-NO-sGC- cGMP- PKG pathway. In addition, β_3-ARs stimulation improves cardiac and vascular muscle relaxation by activating the NOS-NO-sGC-cGMP-PKG pathway in the cardiovascular system (Balligand 2016).

β_3-ARs activation is currently one of the best known pharmacological approach for stimulating brown and beige fat (Finlin et al. 2020). The rediscovery of BAT in adult humans in 2009 led to an increased interest in its targeting (Symonds et al. 2018; Alcalá et al. 2019; Kiranmayi and Bhargav 2019). β_3-ARs stimulation leads to activation of mitochondrial protein uncoupling-protein 1 (UCP1) of BAT and of the cAMP-PKA axis of WAT, triggering non-shivering thermogenesis (increased energy expenditure) and lipolysis (reduce fat stores), respectively

(Himms-Hagen et al. 1994; Collins 2012; Cypess et al. 2015; Szentirmai and Kapas 2017a; Clookey et al. 2019). β_3-AR agonism has also been proven to decrease food consumption and weight, to improve glucose tolerance and insulin sensitivity and to even induce browning also known as beiging of WAT (Grujic et al. 1997; Diaz et al. 2014; Cero et al. 2018; Finlin et al. 2020; O'Mara et al. 2020).

4.2.6.2. BAY 41-2272

BAY 41-2272 belongs to a class of drugs called sGC modulators. It is an NO-independent heme-dependent sGC stimulator that directly activate sGC but does so synergistically with NO, potentiating the effect of low levels of NO and elevating the maximal catalytic rate of sGC (Tsai and Kass 2009). Compounds that belong to the same class of drugs are mainly used for the treatment of pulmonary arterial hypertension (PAH), i.e. Riociguat was approved for the treatment of PAH in 2013 (Sandner et al. 2017). sGC activation was proven effective in lowering blood pressure, conferring vasoprotective actions and decreasing cardiac hypertrophy in several animal models. In addition, direct sGC stimulation was reported to be beneficial in thrombogenic and inflammatory disorders, including atherosclerosis (Stasch et al. 2011).

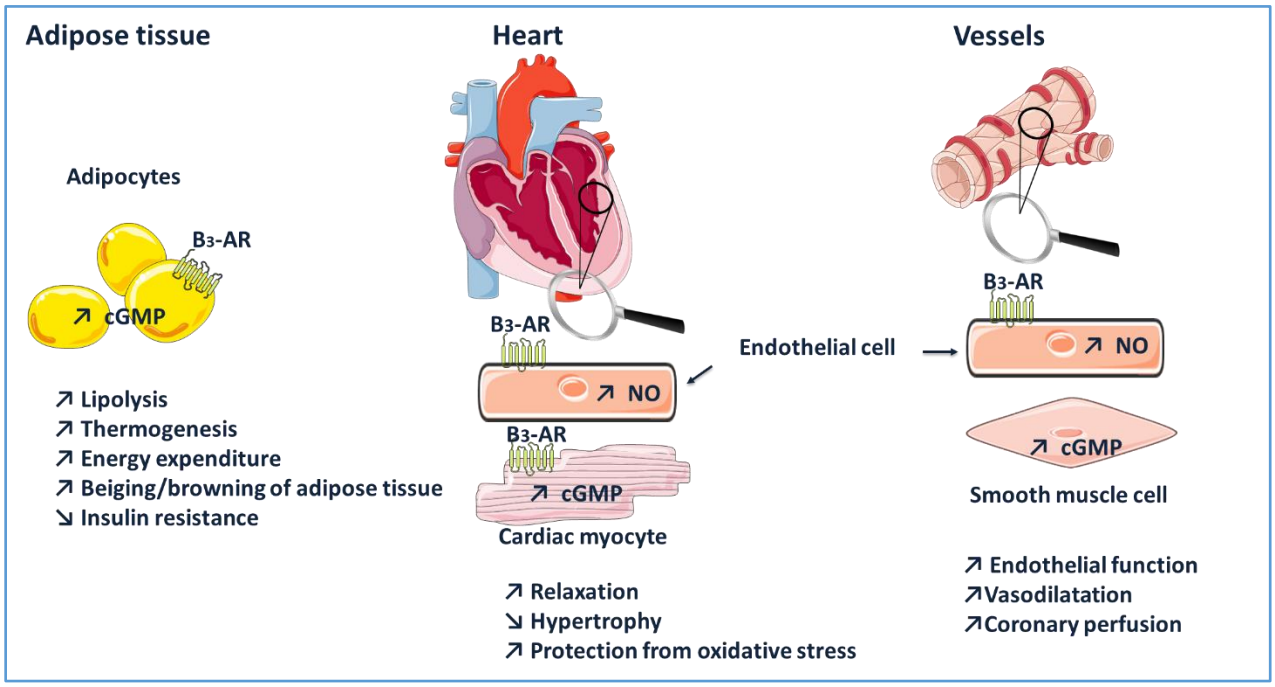

Figure 16: Therapeutic effect of mirabegron and BAY 41-2272 through activation of the NO-cGMP axis in adipose tissue, heart and vessels.

Mirabegron and BAY 41-2272 activate the β_3 adrenergic receptors and sGC-cGMP in adipocytes, respectively (left), resulting in increased lipolysis (WAT), energy expenditure (increased lipolysis and thermogenesis in BAT), adipocyte beiging and browning, and peripheral insulin sensitivity (through transcapillary passage of insulin to target tissues; in cardiac myocytes (center), resulting in antioxidant and cGMP-mediated protective effects against remodeling and improved relaxation; and in endothelial cells of the vasculature (right; including coronary resistance arteries), thereby increasing endothelium-dependent vasodilatation and myocardial perfusion. Inspired by (Balligand 2016) (Pouleur et al. 2018).

4.3. Other interventions

4.3.1. Bariatric surgery

Bariatric surgery is being increasingly used to aid weight loss in patients with severe obesity and to help improve their metabolic status (Frühbeck 2015). In addition, Sjöström et al., showed that bariatric surgery was associated with lower incidence of cardiovascular events in obese adults and reduced number of cardiovascular deaths (Sjöström et al. 2012). Weight regain is not uncommon after conventional weight loss programs especially in severely obese individuals, which is probably due to a lowering of resting EE with weight loss (loss of muscle mass) (K. Y. Chen et al. 2020). Therefore, bariatric surgery might represent a potential procedure that leads to sustained weight loss and long-term health benefits (Jones and Bloom 2015). However, weight-loss surgery is not without risk (Benotti et al. 2014). Therefore, it is often used as the last resort, when behavioral interventions or even pharmacotherapy is unsuccessful or even sometimes not possible. Specific criteria such as BMI (kg/m2) >40 and of 35-40 for patients with comorbid conditions, have been established to select patients for such intervention (Frühbeck 2015). Metabolic complications have been reported. These include protein malnutrition, metabolic bone disease, and deficiency of iron, calcium, and vitamins (e.g. A, B12, D, E, and K). The indication of this surgery requires that the benefits exceed the high risks of obesity-related complications. Thus surgeons remain reluctant in performing these procedures (Mallare et al. 2005).

II. Objectives of the study

MetS is considered a health and economic burden to society due to its association to increased risk of T2DM and CVD. Therefore, scientific investigation to improve therapeutic and preventive measures has become essential.

Growing body of evidence have proven that modulation of the NO-cGMP signaling, by pharmacological tools, could be effective, notably, in metabolic and CVD contexts (J.-P. Stasch et al. 2002; Mitschke et al. 2013; Nossaman and Kadowitz 2013; Pfeifer et al. 2013; Ramirez et al. 2015; M. Park et al. 2018). We hypothesized that chronic pharmacological activation of the NO-sGC-cGMP pathway might represent a promising pharmacological modality for managing the combination of two major components of the MetS, dyslipidemia and IR.

Our first aim was to develop and characterize an experimental animal model of diet-induced MetS with dyslipidemia and IR as main factors.

Our second aim was to investigate the efficacy of a β_3-AR agonist (mirabegron) and a sGC stimulator (BAY 41-2272) in attenuating the metabolic disturbances associated with the dyslipidemia-IR combination, and thereby in preventing the development of metabolic and cardiovascular changes/consequences of the MetS.

In this regard, we worked on WHHL rabbits, animal models of FH and spontaneous dyslipidemia due to a genetic defect in their LDLr. We used a HFFD in order induce IR. Our experimental protocol lasted for 12 weeks, and included four groups of WHHL rabbits: control, HFFD, HFFD with BAY 41-2272 and HFFD with mirabegron.

III. Experimental study

5. Materials and methods

5.1. Animals

Watanabe Heritable Hyperlipidemic Rabbits (male and female) weighing 2.8-3.5 kg were used in all experiments. They were randomly divided into four groups: Control (n=9), HFFD (n=12), HFFD+BAY (n=9) and HFFD+MIR (n=9). These groups respectively received a standard chow diet (3410.PS.S10; SERLAB, France), a high-fructose and high-fat diet[13] (HFFD, modified 3410.PS.S10; SERLAB, France), a HFFD along with BAY 41-2272 (n=9) and a HFFD along with MIRABEGRON (n=9). The pharmacological treatments were orally administrated. The purpose of our study was to induce insulin resistance rather than obesity[14]. Thus, we used a HFFD which, compared to a standard chow diet, is rich in sugar and fat but contains less protein and fibers (Ning et al. 2015). This avoids excessive body weight gain.

5.2. Ethical care of animals

Animals were housed in individual cages, located in a room that was maintained at constant temperature (21°C) and humidity (>45%), under a 12h dark/light cycle with Ad libitum access to food and water. Temperature and humidity were constantly checked to make sure that the animals were always in normal environmental conditions.

To promote animal welfare, a toy, a small tunnel, and a small stick to chew on were placed in each cage. An acclimation period of one week was always respected in order to give animals time to stabilize in their new environment. A food transition was applied at the arrival of the animals to prevent sudden environmental change and diarrhea.

A veterinarian frequently examined animals for any possible concomitant disease. Weight was used as strong indicator of animal health. Thus, animals were constantly weighed. Animals were fasted for maximum 12 hours when blood withdrawal and a glucose tolerance test needed to be performed. An anesthetic cream was applied prior to ear catheterization to prevent animals from feeling pain and distress. The amount of blood withdrawn did not exceed 10% of the animal's total

[13] A 30 % fructose, 10 % coconut oil enriched chow diet.
[14] Might be a confounding factor during results analysis

blood volemia. If another blood withdrawal needed to be performed, an interval of two weeks was respected.

All procedures were performed in accordance with the National Institute of Health Guide for the Use and Care of Laboratory Animals guidelines and they are all conducted with the approval of ONIRIS Ethics Committee of Pays de la Loire (APAFIS n° 10722).

5.3. Study design

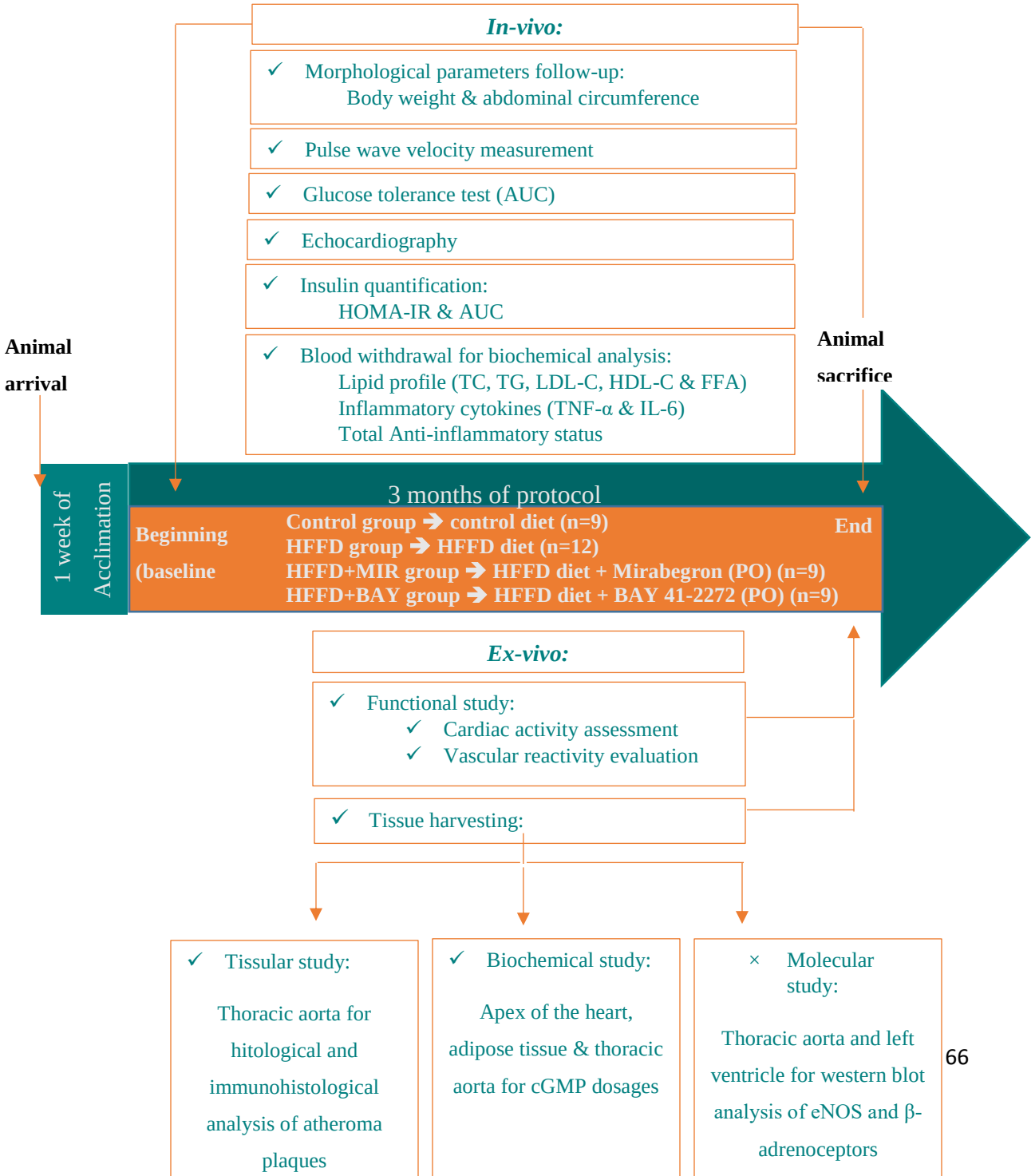

5.4. Blood withdrawal and Intravenous glucose tolerance test

Blood withdrawal and intravenous glucose tolerance test (IVGTT) procedures were performed at baseline and at the end of the protocol. Animals were fasted overnight.

The auricular artery was cannulated (24 G, Vasofix®), 15 min after the topical anesthetic (EMLA™ cream; 2.5% lidocaine, 2.5 prilocaine) was applied. Blood was withdrawn in heparinized tubes. Then, the catheter was fixed to be used during the next two hours. Small blood amounts were drawn at baseline and after 15, 30, 45, 60, 90 and 120 min glucose loading. Samples were collected on ice and later centrifuged (10000g, 15 minutes, 4°C). The plasma was then stored at -80°C for later plasma insulin quantification.

Another 24 G catheter was used to cannulate the anesthetized (with EMLA™ cream) auricular vein of the other ear. Rabbits were intravenously injected with a bolus of glucose solution (0.6 g/kg body weight). Then the catheter was disposed. One drop of whole blood, obtained from the other marginal ear vein, was used to measure glycaemia. This was performed, using a glucose meter (ONETOUCH®VERIO®; © 2012 LifeScan, Inc.), at baseline and 15, 30, 45, 60, 90 and 120 min after the glucose injection (Dimitrova et al. 2008)(Ning et al. 2015).

Two different area under the curve (AUC) were calculated, that of the IVGTT (AUC-GTT) and that of insulin curves (AUC-Insulin). They were calculated by the trapezoidal method[15] using GraphPad PRISM® software (version 8.1) (Antunes et al. 2016).

Homeostasis Model Assessment of basal Insulin Resistance (HOMA-IR) was calculated using the following equation: [(fasting plasma glucose (mmol/l) x fasting plasma insulin (µU/ml))/22.5] (Matthews et al. 1985) (Antunes et al. 2016).

[15] Consists in multiplying the cumulative mean height of glucose (mg.dL^{-1} or g/L) by the time (in hours or min)

Table 2: Li.st of pharmacological substances used in our experiments.

Pharmacological molecule (Supplier)	**Pharmacological properties**	**Concentration/ Solvent**
Phenylephrine hydrochloride (Sigma-Aldrich)	α_1-adrenoceptor agonist	10^{-9}M to 3.10^{-5}M/ Distilled water
Acetylcholine chloride (Sigma-Aldrich)	Muscarinic and nicotinic receptor agonist	10^{-9}M to 3.10^{-5}M/ Distilled water
Sodium nitroprusside (Sigma-Aldrich)	Nitric-oxide (NO) donor	10^{-10}M to 3.10^{-6}M / Distilled water
Human insulin (Sigma-Aldrich)	Insulin receptor agonist	10^{-9}M to 3.10^{-6}M/ Hydrochloric acid (0.01 M)
Isoprenaline hydrocholride (Sigma-Aldrich)	Non-selective β-adrenoceptor agonist (inodilator)	10^{-9}M to 10^{-6}M/ Distilled water + ascorbic acid 1%

5.5. Isolated heart

5.5.1. Generalities

The isolated heart model represents a highly significant tool widely used in cardiovascular research. The Langendorff technique is one type of many isolated perfused heart preparations that serve for investigating physiological and pharmaceutical parameters (Olejnickova, Novakova, and Provaznik 2015). Like any isolated organ experiment, the advantage of the Langendorff isolated heart is that measurements can be achieved without hormonal and neuronal interferences originating from outside of the heart. This allows the investigators to explore specific cardiac drug responses (Dhein 2005).

5.5.2. The Langendorff heart principle

There exists two different setups of the Langendorff isolated heart preparations, one is pressure constant while the other is flow constant. The Langendorff technique involves perfusing the heart via an aortic cannula inserted into the ascending aorta. The cannula delivers the oxygenated perfusion solution to the heart in a retrograde manner, either at a constant pressure or at a constant flow. A constant pressure rate is achieved by controlling the hydrostatic pressure while a constant flow rate is attained by using a peristaltic (roler) pump. During diastole, the perfusion solution flows retrogradely within the aorta and then orthogradely within the coronaries. The retrograde perfusion pressure closes the aortic valve, and thus shunts the perfusate into the coronary ostia at the aortic root. Consequently, the coronary vasculature is perfused and the viability of the heart muscle is maintained. Then, the perfusate enters the right atrium via the coronary sinus and flows out of the heart via the right ventricle and the severed pulmonary artery (Liao et al. 2012) (Skrzypiec-Spring et al. 2007).

5.5.2.1. The Langendorff apparatus

The Langendorff apparatus (**Figure 17**) is a water-jacketed system filled with de-ionized water to help keep all its parts at a physiological temperature 37-38°C. It consists of:

- A perfusion solution bottle/reservoir that contains the perfusion solution **(1)**.
- A heart chamber that covers the heart, avoiding heat loss and evaporation and thus protects and maintains the heart at 37-38°C **(2)**.
- A peristaltic pump that is used to transport the perfusate from the reservoir to the heart **(3)**.
- A bubble trapper that eliminates all the bubbles that might be circulating in the system, thus protecting the heart from embolism **(4)**.
- A thermal circulating pump that pumps the heated de-ionized water throughout the water jacket of the system. Thus, warming and maintaining the system at constant temperature.
- An oxygenation system that involves using fritted glass fused to a glass pipe connected to a carbogen gas tank with a reduction valve and placed in the perfusion solution bottle where it oxygenates the perfusate.

Figure 17: Isolated heart apparatus

5.5.2.2. Perfusion

The perfusion solution (blood, Tyrode, Locke or Krebs-Henseleit) should be propererly oxygeneted using carbogen and kept at a physiological temperature. Carbogen consists of a 95% O2 and 5% CO2 gas mixture. The former is required for oxygenation while the latter is required for correct adjustment of the pH=7.4. The perfusate used in our lab is a krebs solution (table) that was filtered using a bottle top vacuum filtration system with a 0.2 μm PES membrane (VWR). To achieve proper oxygenation and pH the perfusion solution was constantly bubbled with carbogen. This establishes an equilibrium between bicarbonate buffer contained in the solution and the CO2

and allows the stabilization of PCO2 and pH. The perfusion was performed at a constant flow-rate mode (Dhein 2005). The coronary flow was calculated using the following equation: CF = 7.43 × HW0.56 (Döring and Dehnert 1988)(Döring 1990). We estimated the heart weight according to the animal's weight.

Table 3: Composition of krebs solution, with all components needed to simulate the physiological conditions.

Molecule	Concentration (mM)	Major role
NaCl	118.3	Plays a role in osmolarity & in maintaining the membrane potential through a high Na^+ & Cl^- extracellular concentration.
KCl	4.7	Maintains the membrane potential through a high K^+ intracellular concentration. K^+ regulates the potassium channels, affecting the contractile state of small arteries.
$MgSO_47H_2O$	1.2	The Mg^{2+} ion is an important enzyme cofactor.
$NaHCO_3$[16]	20.0	Acid-base buffer. It is the main physiological pH buffer in plasma.
KH_2PO4	1.2	Acid-base buffer.
Glucose	11.1	Energy source.
EDTA	0.016	Chelates metal ions.
$CaCl_2$	2.5	Ca^{2+} is an important enzyme cofactor & Also plays a central role in the molecular mechanism of contraction.

5.5.3. Practical approach

The animal was first anesthetized with an intravenous injection of Sodium Pentobarbital[17] (40 mg/kg). Second, after the nociceptive reflex activity was lost, a thoracotomy was performed and

[16] The bicarbonate ions establish equilibrium with CO2 in the solution & thus control PCO2 & pH
[17] One of the anesthetics that are usually washed out during perfusion & thus do not impair measurements.

the animal was exsanguinated at the abdominal aorta level. Next, the diaphragm was incised and the thorax was opened by cutting both, left and right side. Then, the heart was rapidly freed from the pericardium, excised and transferred into ice-cold filtered Krebs' solution[18] (Lou et al. 2011; L. Wang et al. 2015). The solution was filtered in order to eliminate all the particles and impurities that might either be deleterious to the coronary circulation or falsify the signal (Dhein 2005).

Afterwards, the ex-vivo retrograde heart was connected to an aortic 4 mm cannula (ADInstruments) and perfused at a constant flow-rate (22-28 mL/min) using a peristaltic pump. The freshly prepared and filtered 37-38°C Krebs solution residing in the perfusate reservoir was constantly bubbled with carbogen using a fritted glass pipe. Once, attached to the cannula, the double-walled thermostatic heart chamber was moved upward. A de-ionized water-filled latex balloon connected to a pressure transducer was inserted through the mitral valve into the left ventricle to allow isovolumetric contractions and to continuously record the developed force of the left ventricular pressure (LVP) as an index of cardiac contractility. Then the balloon's volume was adjusted using a water-filled syringe so that the desired end-diastolic pressure (8-10 mmHg) is achieved. The balloon size had to fit the size of the left ventricular cavity. Thus, it was estimated according to the animal's weight. Another pressure transducer located above the aorta recorded the perfusion pressure (PP), an index of coronary vascular tone (Dhein 2005). The heart was allowed to stabilize for 20 minutes before it was infused with different Isoproterenol concentrations (10-10 to 10-5 M), with a 10-12 minutes wash between every two consecutive infusions. We wanted to simulate physical exercise and observe how the heart responds to increased exercise intensity. This is why we used increasing concentrations of isoprenaline or isopoterenol, which is a potent nonselective β-AR agonist. It is a cardiac positive inotrope, chronotrope and lusitrope as well as a vasodilator. The heart responds to this molecule similarly to the way its responds to exercise. This is also called pharmacologic cardiac stress test.

[18] The cold solution induces cardioplagia, reducing the heart's energy consumption.

5.5.3.1. Recorded parameters

Data acquisition and recording were achieved using Powerlab 8/35 LabChart® Pro (ADInstruments, France) Software. Five pharmacodynamic endpoints were studied in order to assess contractility (inotropy), relaxation (lusitropy), heart rate (chronotropy) and coronary vasodilation:

- Inotropy:
  - ✓ LVDP (mmHg): The left ventricular developed pressure is the difference between the maximum pressure in systole and the minimum pressure in diastole.
  - ✓ dP/dT_{max} (mmHg/s): The first derivate of the left ventricular pressure in systole. It reflects the contraction velocity of the left ventricle.
- Chronotropy:
  - ✓ Heart rate (bpm)
- Lusitropy:
  - ✓ dP/dT_{min} (mmHg/s): The first derivate of the left ventricular pressure in diastole. It reflects the relaxation velocity of the left ventricle.
- Coronary vasodilation:
  - ✓ Coronary perfusion pressure.

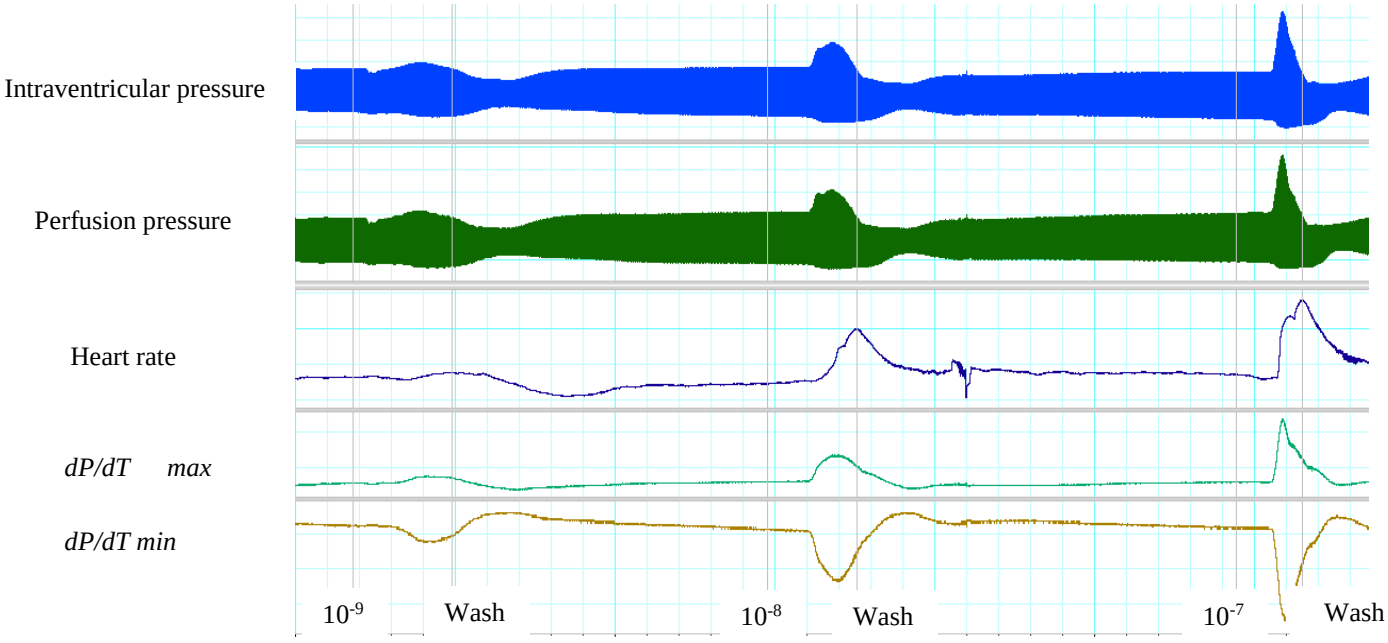

Figure 18: An example of the monitered parameters, recorded during the Langendorff experiment.

5.6. Pulse wave velocity

5.6.1. Generalities

Also known as vitesse d'onde de pouls. Measuring the pulse wave velocity (PWV) is considered to be the in vivo gold standard method for assessing arterial stiffness, given the fact that PWV is a marker of arterial elasticity (Laurent et al. 2001). It is known to be a non-invasive, reproducible and inexpensive procedure, that is readily used in both experimental and clinical settings (Gajdova et al. 2017). In addition, it was shown that measuring the PWV is a very useful technique that is of great clinical importance in the evaluation of cardiovascular risk and thus in the prediction of future cardiovascular events (Barseghian et al. 2019; Mitchell 2009).

5.6.2. Pulse wave velocity principle

The PWV measurement technique allows the study of the arterial wall viscoelasticity. It is based on the following physical principle: the pressure wave propagation in a solid medium is directly proportional to the rigidity of this latter. To put it another way, the arterial pulse wave diffuses along the arteries at a speed that is inversely proportional to the distensibility of the arterial wall. Thus, studying the wave propagation through an arterial segment allows us to indirectly

assess the vascular rigidity of this latter (Greenwald 2002). The pulse pressure wave consists of two components, a forward (incident) wave and a reflected wave (**Figure 19**) at any point along the arterial system. The left ventricle generates the incident wave during systole. Then the reflected wave travels back from the periphery to left ventricle during diastole. When the arterial wall elasticity decreases, the artery loses its distensibility as well as its cushioning function that usually absorbs most of the blood flow pulsatility. This decreased elasticity/increased stiffness, causes the incident wave to travel faster leading to earlier return of the reflected wave (Safar and Frohlich 1995). This is practically perceived, as a decrease in the time interval (Δt) between the two waves and consequently an increase in the PWV value (Gkaliagkousi and Douma 2009). Therefore, this technique allows us to assess the viscoelastic properties of the arteries.

5.6.3. Practical approach

Two sets of PWV measurements were performed: one at the beginning of the protocol and another at the end of the protocol. Animals were kept conscious throughout the experiment and were wrapped in a towel to prevent their movements and to decrease their stress (**Figure 20**). Two piezoelectric sensors (ADInstruments) were placed, one on the auricular artery and another on the caudal one. Recordings of pulse waves were made during 10 min with the software (ADInstruments LabChart v8.1.5). The measurement point (the foot of each pulse wave) was determined using the second derivative of the pulse wave signal. Both the distance between the two sensors and that between the auricular artery and the sternal manubrium, were noted each time. Then, the Δx was calculated by substracting the two distances. The time interval (Δt) between the foot of the auricular waveform and that of the caudal waveform was measured by the software. The PWV is calculated using the formula PWV (m.s-1) = Δx/Δt (**Figure 19**) (Tissier et al. 2016a).

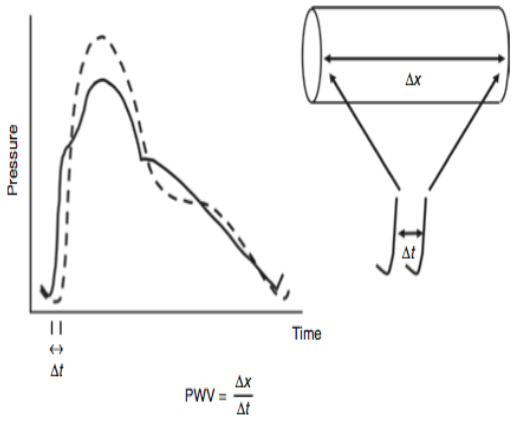

Figure 19: Measurement of PWV between the foot of each pulse wave.

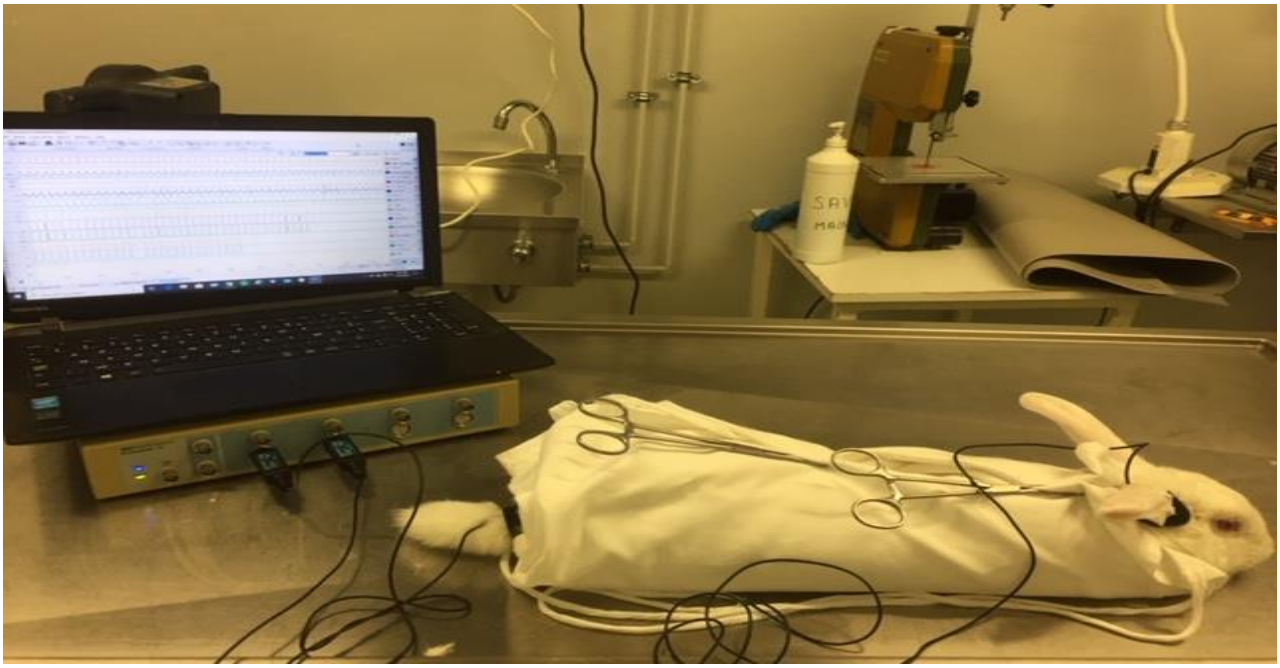

Figure 20: A rabbit during PWV measurement.

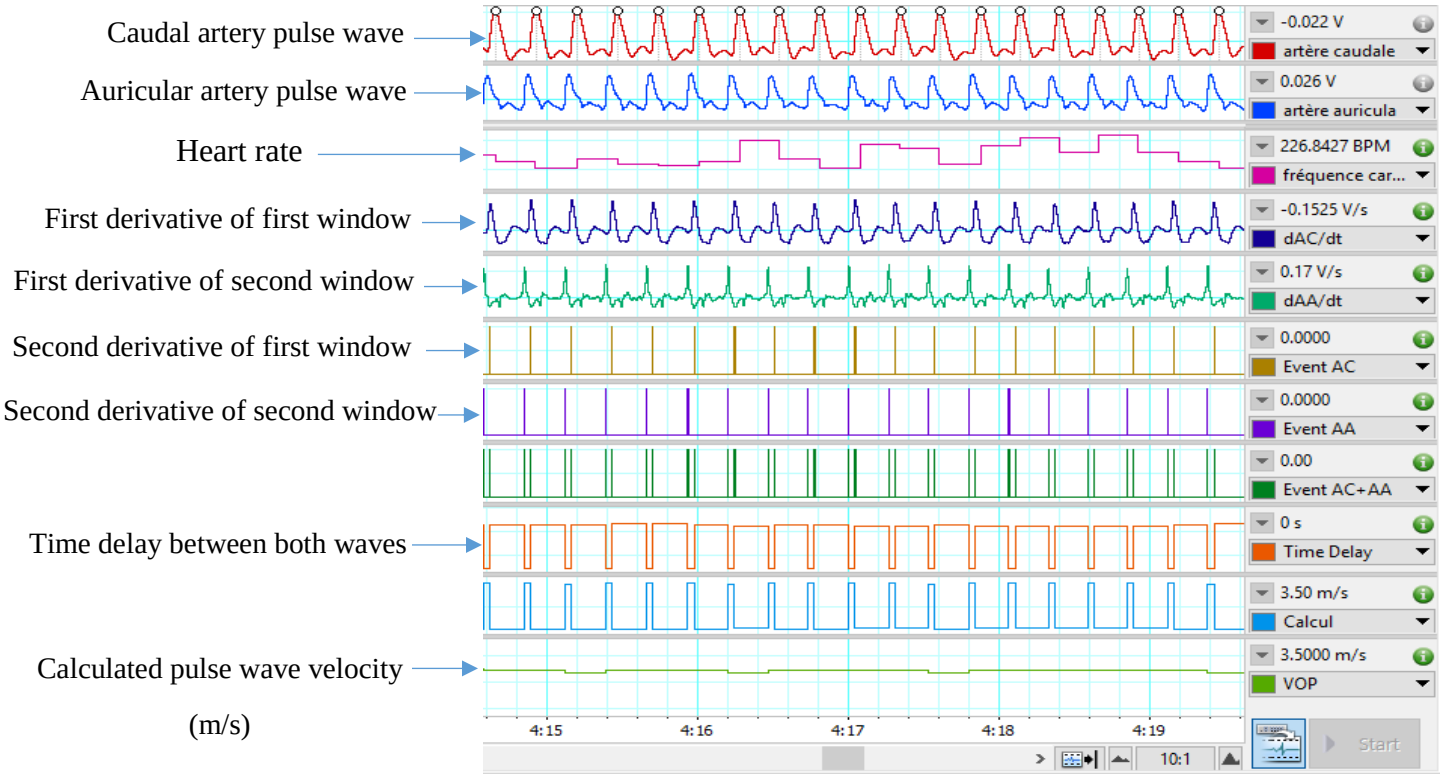

Figure 21: An example of the recordings made during PWV measurement.

5.7. Histochemical and Immuno-histochemical analysis

Immediately after the animal was sacrificed, we evaluated the effect of HFFD on the development and evolution of atherosclerosis in Watanabe rabbits. The cranial thoracic aorta, specifically the area preceding the aortic arch was removed and sampled. These samples were fixed by immersion in neutrally buffered 10% formalin followed by dehydration and paraffin embedding. Then, serial 4µm thick sections were routinely cut and stained.

For histological analysis of thoracic aorta, sections were stained with hematoxylin and eosin, safranin (HES). Green Masson's trichrome and Orcein stains were used to assess collagen and elastic fibers, respectively. Quality of the lesion was evaluated under light microscope.

Immunohistochemistry: In order to study the cellular components of the thoracic aorta, automated immunohistochemistry (Benchmark XT, Ventana Medical Systems, Roche Diagnostics) was performed. The detection systems were the iView DAB detection kit (Ventana Medical Systems, Roche Diagnostics, 760-091) (Other sections were immunohistochemically stained with macrophage antibody (clone RAM11, mouse monoclonal, 1:1200 dilution, Dako Corp, USA) and muscle actin antibody (clone HHF35, mouse monoclonal, 1:50 dilution, Dako Corp, USA), two monoclonal antibodies that detect macrophages and smooth muscle cells (SMCs), respectively.

Using an image analysis system (FIJI), the extent of atherosclerotic lesions in the aorta was expressed as a percentage of the lesion area and the degree of intimal thickening. For determination of average intima thickening, the following equation was used: area of intimal lesion/length of media. The same software was also used for the quantification of elastin fibers, macrophages and SMCs, which was performed by calculating the percentage of immunostaining in lesion area. Finally, an algorithm could not be used for the collagen contents (fibrosis). The latter was graded by a certified veterinary pathologist.

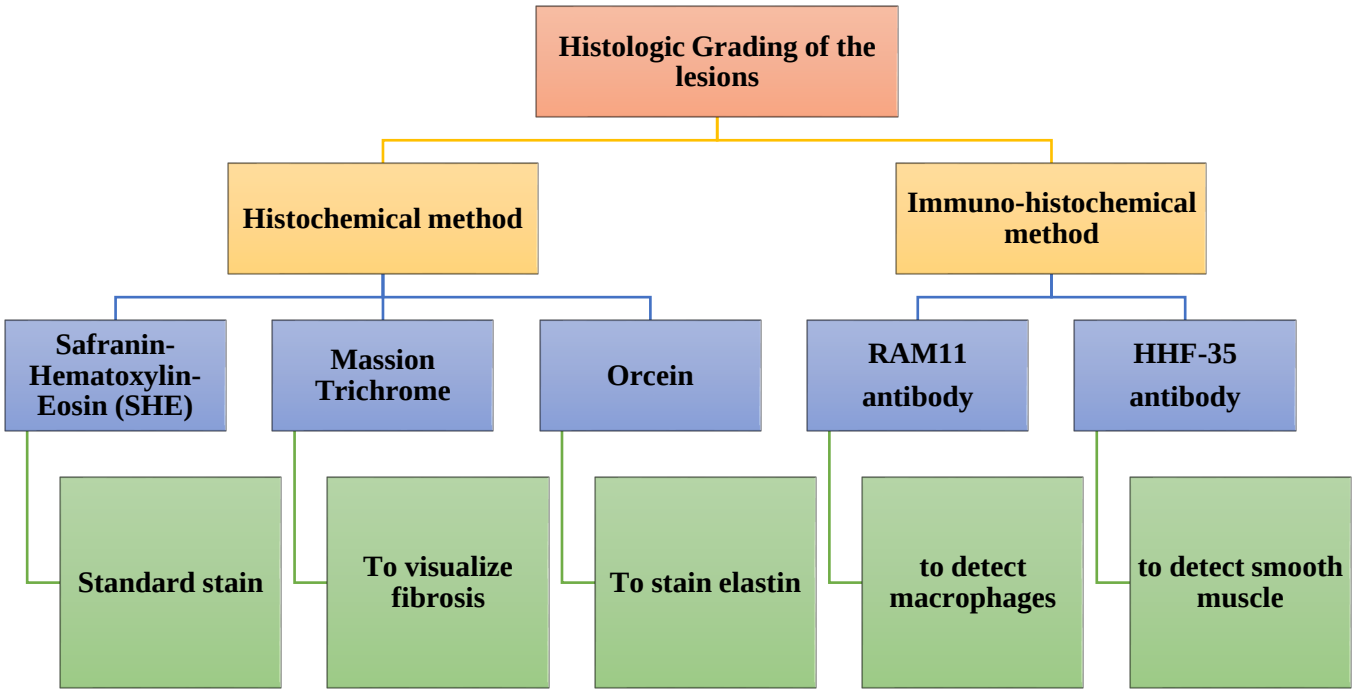

Figure 22: Histochemical and immuno-histochemical methods atheroma lesions grading.

5.8. Vascular reactivity on isolated carotid artery

5.8.1. Generalities

The isolated vessel method is a classical approach that allows investigating the vessel segments function, i.e. of their reactions to the application of vasoactive substances. Under in vivo conditions, vessel responses depend on complex interactions between different cell types[19]and factors[20]. In terms of mechanistic experimental findings, this limits the possibility of appropriate interpretation. Therefore, this in vitro method allows controlling all the confounding factors that might interfere with data interpretation (Schubert 2005).

5.8.2. Principle of isolated vessel approach

The segments are mounted between a triangular steel hook support (fixed) and a triangular movable steel hook (**Figure 24**). The movable hook holding the upper part of the ring segment is

[19] Smooth muscle cells, endothelial cells and various cells in the adventitia
[20] Factors released from nerve endings, metabolites originating from the surrounding tissue, hormones transported by the blood flow, mechanical factors like shear stress and transmural pressure and also the behavior of proximal and distal vessel segments.

attached to a force transducer allowing wall force to be measured. The principle of this method is that whenever a vasoactive substance induces tension variations, a transducer records these changes. These preparations can be investigated either under isotonic[21] or isometric conditions. In our experiment we used the isometric conditions preparation, where the vessel circumference stays constant and where only changes in force are recorded when pharmacological agents take action.

Figure 23: EMKA apparatus used for the vascular reactivity experiment (on the left). A 10ml organ bath with a mounted carotid artery ring and Krebs solution (on the right).

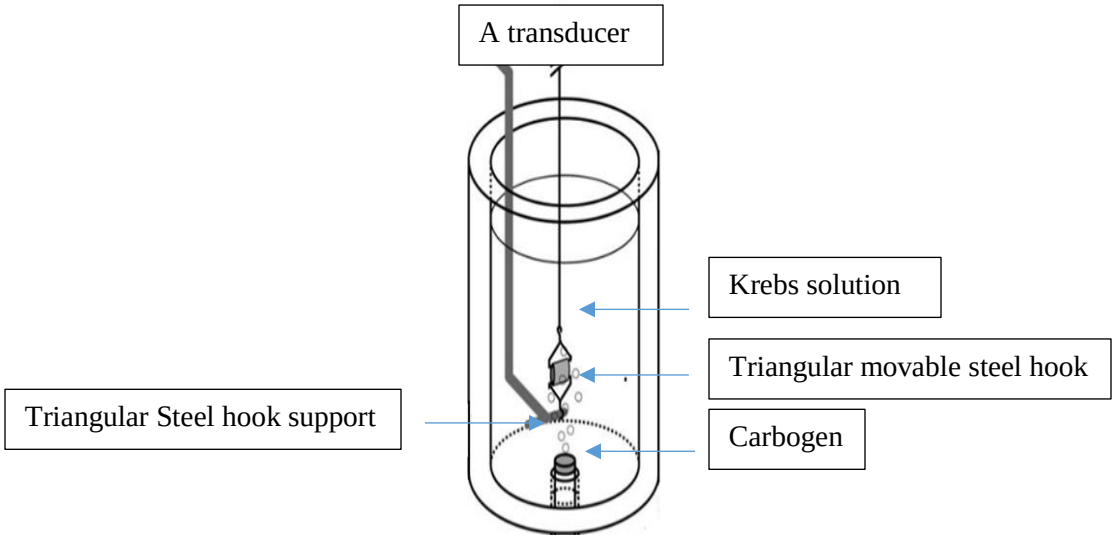

Figure 24: A schematic representation of an organ bath.

[21] The circumference is adjusted during changes in activation in order to achieve a constant force.

5.8.3. Practical approach

Immediately after the heart's excision, a skin incision adjacent (0.5-1cm) to the trachea, showing the underlying fascia and fat tissue, was made. The carotid artery and vagus nerve were exposed through a dissection of the medial side of the internal jugular vein. The carotid artery was removed and placed in ice-cold Krebs'solution (**Table 2**). After being dissected, free of fat and connective tissue the artery was cut into 3-5mm ring segments. These segments were mounted between the two hooks and then suspended in 10-mL organ baths, containing Krebs' solution. To simulate the physiological environment this solution was maintained at 37°C, and constantly gassed with Carbogen. Care was taken not to injure the endothelium during the preparation. The segments were gradually loaded to an initial tension of 2g[22] and allowed to equilibrate for 1 hour. During the equilibration phase the rings were washed four times (one wash every 15 min).

Then, to evaluate the viability of the vessels, the segments were contracted with two different 80 mM KCl injections, separated by a 15 min interval. The maximum tension value reached after the second KCl injection was later used in data analysis. Afterwards, the endothelial integrity was verified by adding Ach[23] (10^{-6} M) to the Phe[24] (3.10^{-6} M) pre-contracted rings. Later, the rings were washed until their resting tension of 2g is reached again. The rings with less than 60% relaxation were considered non-reliant and were later excluded from our data during results analysis.

Next, to asses vascular contractility, cumulative concentration-response curves to Phe (10^{-9} to 3.10^{-5} M) were constructed. The concentration that induced a 70-80% of maximal contraction was later used to induce a pre-contraction before starting the relaxation curves. Again, the rings were washed until their basal tension level of 2g is reached.

Finally, to assess the vascular relaxation, cumulative concentration-relaxation curves (CCRCs), on Phe pre-contracted rings, to four different molecules, were built:

- SNP (10^{-10} to 3.10^{-5} M) to evaluate endothelium-independent relaxation.

[22] A pilot study, using 80mM KCl, was conducted to determine the preload that should be used for the carotid artery of rabbits
[23] A M3 muscarinic receptor agonist in the endothelium.
[24] An AR-α1 agonist.

- Ach (10^{-9} to 3.10^{-5} M) and insulin (Ins, 10^{-9} to 3.10^{-6} M) to evaluate endothelium-dependent relaxation.

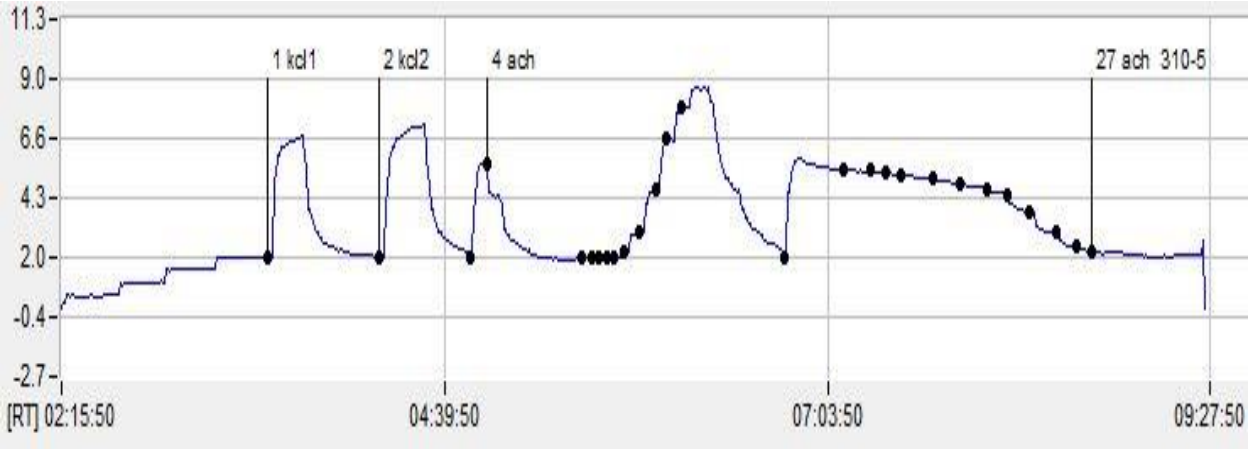

Figure 25: An example of CCRC to phenylephrine and acetylcholine

5.8.3.1. Data acquisition and analysis

Tension was continuously measured with the use of a computerized, automated isometric transducer system (EMKAbath4, EMKA technologies, France) and recorded using a data acquisition software (iox2 version 2.9.5.20). The percentage of contraction and relaxation were calculated relative to the maximal contraction produced by KCl and Phe, respectively. The following equations were used to calculate the percentage of contraction and relaxation, respectively:

Percentage of contraction (%): $\left(\frac{contraction\ value\ reached\ after\ injection - basal\ tension\ (2g)}{value\ of\ 2nd\ KCl\ contraction - basal\ tension\ (2g)}\right) \times 100$

Percentage of relaxation (%): $\left(\frac{value\ of\ Phe\ precontraction - relaxation\ value\ reached\ after\ injection}{value\ of\ Phe\ precontraction - basal\ tension(2g)}\right) \times 100$

5.9. Echocardiography

To assess the left ventricular (LF) global systolic function, transthoracic echocardiography (TTE) was performed at the baseline and at the end of the three months protocol. Conscious animals were restrained in prone (ventral) position without being detained on the table[25]. Since animals were not anaesthetized, this strategy gave the operator an easier access to the

[25] Rabbits were immobilized by being held tight to the chest of the person, with whom animals were familiar.

echocardiographic windows. The Electrocardiographic (ECG) signal recording was obtained by placing three different electrode sensors[26] at different locations on the animal's skin.

5.9.1. Right parasternal approach

5.9.1.1.Two-dimensional (2D) imaging

The echocardiographic examination started with a long axis four-chamber cross-sectional right parasternal view, the linear ultrasound transducer (probe/beam) was held slightly in an oblique position at the 3rd - 4th intercostal space level. It allowed a general evaluation of the heart i.e. visualization of the four chambers, the atrio-ventricular vales, the interventricular and interatrial septa.

5.9.1.2. 2D-guided Motion mode (M-mode) imaging

Then, for a short axis trans-ventricular cross-sectional view also called mushroom view, the ultrasound beam was rotated 90° towards the animal's elbow. For time-motion, recording the M-mode cursor was placed exactly perpendicular to both the interventricular septum and the left ventricular free wall and crossing through the center of the left ventricular cavity. The ECG chart served as a landmark for the measurement of the left ventricular dimensions[27] during systole and diastole. The software automatically calculated both the left ventricular fractional shortening (LVFS) and ejection fraction (LVEF). Two consecutive heart cycles were measured and the average was used for analysis.

$$\text{LVFS} = \frac{\text{LVIDd} - \text{LVIDs}}{\text{LVIDd}} \times 100\%$$

Where, LVIDd = LV internal diameter at end diastole & LVIDs = LV internal diameter at end systole.

$$\text{LVEF} = \frac{\text{LVEDV} - \text{LVESV}}{\text{LVEDV}} \times 100\%$$

[26] The red one, the black one and the yellow one were placed on the lower right side of the thoracic cavity, on the right hind limb and on the lower right of the thoracic cavity, respectively

[27] The measurement of LV dimension when the time cursor is placed at or immediately before the peak of the R-wave in QRS complex is considered as LVIDd. The LV dimension at the end of T-wave in electrocardiogram (ECG) is taken for LVIDs.

Where, LVEDV = LV end-diastolic volume & LVESV = LV end-systolic volume.

5.9.1.3. Doppler imaging: color-flow mapping mode

A short axis modified trans-aortic right parasternal approach was used for the pulmonary flux evaluation. A sectorial probe was used for this part of the examination. The ultrasound probe was kept in same angle position as in the TM mode but was oriented towards the base of the heart. This allowed assessment of the pulmonary artery flow pattern. Since the flow towards the transducer is red, and the one away from the transducer is blue, the pulmonary flux is perceived in blue in color-flow mapping mode. Spectral pulsed-wave Doppler was used to determine the velocity of the pulmonary flow.

5.9.2. Left parasternal approach

5.9.2.1. Doppler imaging: color-flow mapping (CFM) mode

The echocardiographic examination ended with an aortic flux assessment, a long axis five chambers cross-sectional view was used. This allowed the measurements of aortic blood flow direction and velocity. Same, the aortic flux is also perceived in blue.

5.10. Biochemical analysis

5.10.1. Plasma lipid quantification

For the quantitative determination of total cholesterol (TC), triglycerides (TG), free fatty acids (FFA) and HDL-C plasma levels, we used an enzymatic colorimetric method. The dosages and the concentration's determination were performed according to the supplier's instructions (DiaSys enzymatic commercial kits). Meanwhile, low density lipoproteins (LDL-C) levels were calculated using the friedwald's equation. Samples were deposited in a 96-well microplate. Then, after the reagents were added, plate were incubated at 37°C, for 10 min. The absorbance was read at 490 nm using a microplate reader.

5.10.2. Plasma insulin quantification

For the quantitative determination of insulin plasma levels, we used a sensitive Enzyme Linked ImmunoSorbent assay (ELISA) sandwich assay (Rabbit insulin ELISA kit, Crystal Chem High Performance Assays, USA). The latter is based on three main reactions. The first occurs when the samples are deposited in the 96-well microplate. Insulin in the samples bind to the guinea pig anti-

insulin antibody coated on the microplate wells. Then the second reaction occurs when horseradish peroxidase (HRP) (POD)-conjugated anti-insulin antibody is bound to the guinea pig anti-insulin antibody/rabbit insulin complexes immobilized to the microplate wells. Finally, the third reaction which is an enzymatic reaction occurs when bound POD conjugate in the microplate well is detected by the addition of the 3, 3', 5, 5'-tetramethylbenzidine (TMB) substrate solution. The absorbance was read at 450 nm and 630 nm using a microplate reader. The insulin concentration was determined *via* interpolation using the standard curve generated by plotting absorbance (A450-A630) versus the corresponding concentration of rabbit insulin standard.

5.10.3. Plasma tumor necrosis factor-α and interleukin-6 quantification

For the determination of plasma TNF-α and IL-6 plasma levels we used, sandwich ELISA assays (DuoSet® ELISA, R&D Systems Europe, Ltd). In these kits, the primary antibody is deposited in a 96-well microplate and blocked, before the rest of the steps are carried out. The first step is to add plasma samples and standards, once the plate is ready. The latter is washed thoroughly. The second step is to add the detection (secondary) antibody. Another wash is performed at this stage. Then the third step involves adding streptavidin conjugated to HRP. Again another wash is performed, before a color reagent is deposited in the plate. Finally, a stop solution is added. To determine the optical density of each well, the microplate was read at both 450nm and 540nm. Then readings were subtracted (A_{450}-A_{540}) to correct optical imperfections in the plate.

5.10.4. Tissue cGMP quantification

cGMP was quantified in thoracic aorta rings, heart tissue and epididymal/ovarian fat. Immediately after animal sacrifice, these tissue samples were collected, immerged in liquid nitrogen and then stored at -80°C. The day of analysis, samples were thawed, ground and homogenized in a cold solution of 6% trichloroacetic acid (TCA) and then centrifuged at 1500 g for 10 min at 4 ° C. Then, the supernatant fractions were washed three times with a water saturated diethyl ether solution (5 volumes of diethyl ether per 1 volume of supernatant) for the extraction of TCA. The residual diethyl ether was then evaporated by heating the samples at 70 ° C for 5 min. Later, the dried extract was dissolved in an adequate volume of assay buffer. The cGMP concentrations of each sample was measured by using a colorimetric enzyme immunoassay kit (Cayman Chemical Company). The absorbance of each sample was read at 405 nm using a microplate reader. The cGMP value was calculated related to the total cell protein concentrations

previously measured using a protein assay reagent kit (micro-BCA, Pierce Biotechnology, Rockford , USA).

Table 4: List of kits used for biochemical analysis.

kit	Supplier	Method
Rabbit insulin ELISA kit	Crystal Chem High Performance Assays, USA	Sandwich ELISA
DuoSet® ELISA kit, TNF-α	R&D Systems Europe Ltd	Sandwich ELISA
DuoSet® ELISA kit, IL-6	R&D Systems Europe Ltd	Sandwich ELISA
Total Cholesterol FS Kit	Diasys France SAS	colorimetric detection and quantification of Total Cholesterol
Triglyceride FS Kit	Diasys France SAS	colorimetric detection and quantification of Triglyceride
NEFA FS (Non-esterified fatty acids) Kit	Diasys France SAS	colorimetric detection and quantification of free fatty acids
HDL-C	Diasys France SAS	colorimetric detection and quantification of free fatty acids
TAS kit	Randox laboratories Ltd	colorimetric detection and quantification of Total antioxidant status
Micro BCA protein assay kit	Pierce Biotechnology, Rockford , USA	colorimetric detection and quantification of total protein
cGMP kit	Cayman Chemical Company	colorimetric detection and quantification of cGMP

6. Results

nutrients

MDPI

Article 1

Article

Long-term high-fructose high-fat diet feeding elicits insulin resistance, exacerbates dyslipidemia and induces gut microbiota dysbiosis in WHHL rabbits.

Michelle Moughaizel [1]*, Elie Dagher [2], Chantal Thorin [1], Jean-Claude Desfontis [1] and Yassine Mallem [1]*

1 Nutrition, PathoPhysiology and Pharmacology (NP3) Unit, Oniris, Nantes Atlantic College of Veterinary Medicine, Food Science and Engineering, Nantes, France; chantal.thorin@oniris-nantes.fr(CT), jean-claude@oniris-nantes.fr (J-CD).
2 Laboniris, Oniris, Nantes Atlantic College of Veterinary Medicine, Food Science and Engineering, Nantes, France; elie_dagher@hotmail.com (ED).
* Correspondence: m_moughaizel@hotmail.com (MM), yassine.mallem@oniris-nantes.fr (YM).

Abstract: The metabolic syndrome (MetS) had become a global public health burden due to its link to cardiovascular disease and diabetes mellitus. The present study was designed to characterize the metabolic and cardiovascular disturbances, as well as changes in gut microbiota associated with high-fructose high-fat diet-induced (HFFD) MetS in Watanabe heritable hyperlipidemic (WHHL) rabbits. Twenty-one Watanabe rabbits were assigned to a control (n=9) and HFFD (n=12) groups, receiving a chow diet and a HFFD, respectively. During a 12-week protocol, morphological parameters were monitored; plasma fasting levels of lipids, glucose and insulin were measured and a glucose tolerance test (GTT) was performed. HOMA-IR was calculated. Cardiac function and vascular reactivity were evaluated using the Langendorff isolated heart and isolated carotid arteries methods, respectively. 16S rRNA sequencing of stool samples was used to determine gut microbial composition and abundance. HFFD-fed Watanabe rabbits exhibited increased fasting insulin, HOMA-IR, area under the curve (GTT), triglycerides, TC, LDL-C and shifts in intestinal microbial composition and diversity. Our results suggest that HFFD induces insulin resistance and gut microbiota dysbiosis and accentuates dyslipidemia; and that, when subjected to HFFD, Watanabe rabbits might become a potential diet-induced MetS animal models with two main features, dyslipidemia and insulin resistance.

Keywords: Cardiovascular disease, Metabolic Syndrome, Dyslipidemia, Insulin resistance, Watanabe rabbits, High-Fructose High-Fat Diet, Gut dysbiosis.

Introduction

The metabolic syndrome (MetS) includes abdominal (central/visceral) adiposity, insulin resistance (IR), impaired glucose tolerance, arterial hypertension, and dyslipidemia [1]. It has been associated with increased risks of type 2 diabetes and cardiovascular disease. The MetS has become the major global health hazard of the modern world due to a worldwide shift towards a western lifestyle [2,3]. It is estimated that over 1 billion people worldwide are affected by this syndrome [2]. The continuous and rapid rise in the global prevalence of MetS are attributed to increased consumption of food and beverages that are rich in energy, fat, and added sugar, on one hand and to decreased physical activity/sedentary lifestyle, on the other hand [2–5]. It has been demonstrated that chronic consumption of a western diet, rich in sugar and saturated fat, increases the risk of developing IR [6,7], dyslipidemia and obesity [8,9], three main components of MetS [10,11].

The gut microbiota plays an important role in the regulation of host metabolic functions and in the control of energy homeostasis through modulating energy absorption, gut motility, appetite, glucose and lipid metabolism, as well as hepatic fatty storage [12,13]. However, available evidence from both human and animal models studies also suggest that gut microbiota exerts a significant role in the pathogenesis of the MetS i.e. obesity, glucose intolerance, IR, dyslipidemia and arterial hypertension [13–16]. It is believed that the link between intestinal microbiota and the development of the MetS is related to its involvement in host metabolism [12]. Moreover, it was found that germ-free animals are resistant to high-fat diet-induced obesity and IR indicating that gut microbiota likely participates in the development of the MetS [17]. Nevertheless, the exact key mechanisms underlying the implication of gut microbiota dysbiosis in metabolic diseases are just yet starting to be delineated and are still to be thoroughly investigated.

The pathogenesis of the MetS is not fully understood due to its complexity and to the interconnection between its components [18]. Working on suitable animal models that mimic human MetS is of utmost importance to gain a deeper insight into the development of this syndrome. Even though numerous animal models of MetS have been established, those combining dyslipidemia and IR without obesity as a main component, are scarce. Accordingly, data on the association between dyslipidemia and IR in the MetS are less available, and whether this association is independent of other components of the MetS, has not been reported. Similarly, to date most existing studies have linked the intestinal dysbiosis to obesity but few have investigated its association with IR and dyslipidemia.

The aims of the present study were 1) to investigate the relationship between the combination IR-dyslipidemia and metabolic and cardiovascular disturbances and 2) to explore gut microbiota compositional changes that are associated with this combination, independently from other components of the MetS, i.e. obesity.

Materials and methods

Animals and diets

Twenty-one Watanabe heritable hyperlipidemic (WHHL) rabbits (male and female) weighing 3.0-3.5 kg (at the end of the protocol) were used in all experiments. Rabbits (CEGAV, France) were housed individually in a room maintained at constant temperature of 21°C and humidity (>45%), under a 12h dark/light cycle with free access to water and food. Rabbits were randomly divided into two groups, a control group (n=9) fed a standard chow diet (3410.PS.S10; SERLAB, France) and a HFFD group (n=12) fed a chow diet that is supplemented with 30 % fructose and 10 % coconut oil (91% saturated fatty acids) (SERLAB, France). In order to avoid the excessive weight gain, we used a diet that is rich in sugar and fat but with less protein and fibers, compared to a standard chow [19].

Morphological parameters

Weight and abdominal circumference were weekly measured to monitor the animal's weight gain and growth.

Measurement of plasma lipids, glucose and insulin levels

After an overnight fasting, cannulation of the auricular artery (24 G, Vasofix®) and blood withdrawal were performed under local anesthesia (EMLA cream; 2.5% lidocaine, 2.5% prilocaine) at the beginning and end of the protocol. Samples were centrifuged (10000g, 15 minutes, 4°C) and the plasma was stored at -80°C. We used an enzymatic colorimetric method for the quantitative determination of total cholesterol (TC), triglycerides (TG), free fatty acids (FFA) and high-density lipoprotein cholesterol (HDL-C) plasma levels. The dosages were performed according to the supplier's instructions (DiaSys enzymatic commercial kits). Meanwhile, low-density lipoprotein (LDL-C) levels were calculated using the Friedewald's equation, LDL cholesterol (g/L) = Total cholesterol – HDL-cholesterol – (Triglycerides/5) [20]. We used a sensitive rabbit insulin ELISA kit sandwich assay (Crystal Chem High Performance Assays, USA) for the quantitative determination of insulin plasma levels.

Intravenous glucose tolerance test

To examine the effects of HFFD on glucose metabolism and insulin response, an intravenous glucose tolerance test (IVGTT) was performed, at the beginning and end of the protocol. After an overnight fasting, cannulation of the auricular vein (24 G, Vasofix®) was performed under local anesthesia (EMLA cream; 2.5% lidocaine, 2.5 prilocaine). An intravenous glucose solution (0.6 g/kg body weight) was then injected. Blood samples were taken and glucose was measured at 0, 15, 30, 45, 60, 90 and 120 min, post glucose injection. Blood glucose levels were measured using one drop of whole blood, from the marginal ear vein via a glucose meter (ONETOUCH®VERIO®; © 2012 LifeScan, Inc.). Samples were stored on ice and centrifuged (10000g, 15 minutes, 4°C) to later measure plasma insulin concentrations using rabbit insulin ELISA kit (Crystal Chem High Performance Assays, USA). The area under the curves (AUC_{Glu} and AUC_{Ins}) were calculated using GraphPad

PRISM® software (version 8.1). Meanwhile, Homeostasis Model Assessment of basal Insulin Resistance (HOMA-IR) was calculated using the following equation: [(fasting plasma glucose (mmol/l) x fasting plasma insulin (μU/ml))/22.5] [21].

Gut microbiota analysis

Fecal samples were collected at the beginning and end of the protocol. Upon their collection, samples were immediately immerged in liquid nitrogen and were then stored at -80°C. The genomic DNA (gDNA) was extracted from the samples. The V3-V4 region of the purified DNA was amplified during 30 amplification cycles, at 65°C, using the forward primer F343 (CTTTCCCTACACGACGCTCTTCCGATCTACGGRAGGCAGCAG) and the reverse primer R784 (GGAGTTCAGACGTGTGCTCTTCCGATATTACCACC). The 510 bp amplicons were, then purified and all non-specific primers were removed. A second 12 cycles PCR was performed by adding a home-made 6 bp index to the reverse primer R784 (AATGATACGGCGACCACCGAGATCTACACTCTTTCCCTACACGAC) and by using a modified reverse primer (CAAGCAGAAGACGGCATACGAGAT-index-GTGACTGGAGTTCAGACGTGT) via the IlluminaMiseq® technology. The purification and loading of the resulting products onto the Illumina MiSeq cartridge were performed according to the manufacturer's instructions. PhiX was used to check the quality of the run.

Isolated Langendorff heart preparation

After the animal was anesthetized using an intravenous Sodium Pentobarbital injection (40 mg/kg), the thorax was cut and opened. The animal was sacrificed by exsanguinating the abdominal aorta. The heart was rapidly excised and transferred into ice-cold filtered (using a filter funnel) Krebs' solution, containing (mM): NaCl 118.3, NaHCO3 20.0, KCl 4.7, MgSO47H2O 1.2, KH2PO4 1.2, glucose 11.1, EDTA 0.016 and CaCl2 2.5. Afterwards, the heart was cannulated (4 mm aortic cannula, ADinstruments) and perfused at a constant flow-rate (22-28 mL/min) with a Krebs solution that was constantly bubbled with 95% O2 and 5% CO2 at 37 °C. A pressure transducer located above the aorta recorded the perfusion pressure (PP), considered as an index of coronary vasodilation. Then a de-ionized water-filled latex balloon connected to another pressure transducer was inserted through the mitral valve into the left ventricle to record the left ventricular pressure (LVP) as an index of cardiac contractility. The heart was allowed to stabilize for 20 minutes before performing non-cumulative concentration-response curves (non-CCRCs) to isoproterenol (10^{-9} to 10^{-6} M), a nonselective β-adrenergic agonist. Data acquisition and recording was achieved using Powerlab 8/35 and LabChart 7.0 software (ADInstruments). The left ventricular pressure (LVP) and coronary perfusion pressure (PP) were continuously measured during the experiment. The left ventricular developed pressure (LVDevP) was calculated as follows: LV systolic pressure - LV end-diastolic pressure.

Vascular reactivity

Immediately after the animal was sacrificed by exsanguination, the carotid artery was removed and dissected free of fat and connective tissue and placed in a cold Krebs' solution (see composition above). The artery was cut into 4-5mm ring segments, that were then mounted and suspended in 10 mL organ baths containing Krebs' solution, upheld at 37°C and constantly bubbled with carbogen (95% O2 and 5% CO2). The isometric tension was continuously measured using an automated isometric transducer system (EMKAbath4, EMKA technologies, France). Data were recorded using an acquisition software (iox version 2.9.5.20). The arterial rings were gradually loaded to an initial 2 g tension and allowed to equilibrate for 60 minutes. The viability of the vessels was evaluated using an 80 mM KCl solution. Then, the presence of intact endothelium was verified by adding acetylcholine (Ach, 10^{-6} M) to phenylephrine(Phe, 3.10^{-6} M)-precontracted rings. The rings with less than 60% relaxation were considered non-reliant and thus, were eliminated. Cumulative concentration-response curves (CCRCs) to Phe, an α_1-adrenoceptor agonist (10^{-9} to 3.10^{-5} M) were constructed. CCRCs to Ach, a muscarinic receptor agonist (10^{-9} to 3.10^{-5} M) and to insulin (Ins, 10^{-9} to 3.10^{-6} M) were built on Phe-precontracted rings. The contraction and relaxation percentages were calculated in relation to the maximal response from the precontraction produced by KCl- and Phe-precontractions, respectively.

Histology and Immunohistochemistry

We evaluated the effect of HFFD on the development and evolution of atherosclerosis in Watanabe rabbits. Immediately after animal sacrifice, the area preceding the aortic arch of the cranial thoracic aorta was removed and fixed in 10% neutrally buffered formalin. After fixation, samples were dehydrated, embedded in paraffin and cut into serial 4µm thick sections before they finally underwent staining.

For histological analysis, sections were stained with hematoxylin and eosin safranin (HES) and with Green Masson's trichrome and Orceine to detect collagen and elastic fibers, respectively. Other sections were immunohistochemically stained with macrophage antibody (clone RAM11, mouse monoclonal, 1:1200 dilution, Dako) and muscle actin antibody (clone HHF35, mouse monoclonal, 1:50 dilution, Dako) to detect macrophages (Mφ) and smooth muscle cells (SMCs), respectively.

To determine the extent of atherosclerotic lesions both the percentage of the lesion area and the degree of intimal thickening were determined using an image analysis system (FIJI, Image J®). The average intima thickening was calculated as follows: the area of intimal lesion was divided by the length of media. Lesions were classified, by a certified veterinary pathologist, into different types (I, II, III, IV, V and VI) according to the guidelines of the American Heart Association [22]. In order to compare the stage of lesions, type II and III plaques were classified as early lesions whereas type IV and V plaques were classified as advanced lesions.

The FIJI software was also used to quantify elastin fibers, macrophages and SMCs, by calculating the percentage of immunostaining in lesion area. An algorithm could not be used for the collagen deposition (fibrosis). The latter was graded, by a veterinary pathologist, along with the presence of

extracellular lipid, fibrous cap, mineralization and lipid core. The grading was performed using a semi-quantitative scale from 0 to 4 in order to better characterize the different types of plaques as previously described [31].

Statistical analyses

Data were expressed as a mean ± SEM. All graphs were performed using PRISM® software (version 8.0.1). We used repeated measures Two-way ANOVA for multiple group comparisons. Linear Mixed effect (LME) model was used to analyze data from non-CCRCs (isolated heart) and CCRCs to insulin. Meanwhile, Non-linear Mixed Effect model (NLME) was used to assess data from CCRCs to Phe and Ach [23]. Contraction and relaxation were expressed as the percentage relaxation of the KCl- and Phe-induced precontraction, respectively. The efficacy (E_{max}) and the potency (pD_2), respectively, representing the maximum effects and the negative logarithm of the concentration producing 50% of the maximum effect were determined for each of the CCRCs.

Mann Whitney statistical test with a p value correction according to the Benjamini and Hochberg was used to study the composition of the fecal microbiota. Comparative analysis of the microbial composition and abundance were performed at the phylum, family and genus levels.

R software was used to evaluate data from CCRCs, non-CCRCs and from gut microbiota analyses. A p value of less than 0.05 was considered statistically significant for all results.

Result

Effect of HFFD on body weight and abdominal circumference

After 12 weeks of HFFD-feeding, the body weight significantly increased in the both the control and HFFD groups when comparing 12th week values to baseline values ($p < 0.0001$ and $p < 0.01$, respectively). Whereas, at the 12th week of the protocol there was not any significant difference in body weight when comparing the two groups together. Similarly, after 12 weeks of the protocol, the increase in weight was significant in both the control and the HFFD groups when comparing 12th week values to baseline values ($p < 0.0001$ and $p < 0.001$, respectively) but not between the two groups (HFFD vs. Control) at the end of the protocol (12th week) (Table 1).

Effect of HFFD on lipid profile

We additionally examined lipid profile modifications (Table 1). Both TC and LDL-C significantly increased in the HFFD group but remained unchanged in the control group when comparing 12th week values to baseline values ($p < 0.02$). These levels also significantly increased when comparing the two groups together (HFFD vs. Control) at the end of the protocol ($p < 0.01$ for TC and $p < 0.001$ for LDL-C). TG levels significantly increased in the HFFD group, but not in the control group, when comparing 12th week levels to baseline levels (12th week vs. Baseline, $p < 0.05$).

Meanwhile, no change was observed in terms of HDL and FFAs neither when comparing the 12th week levels to the baseline levels nor when comparing the two groups to each other at the end of the protocol.

Table 1 Results of weight, abdominal circumference, glycaemia, insulin and plasma lipids.

	Groups			
Measurements	**Control (n=9)**		**HFFD (n=12)**	
	Baseline	**12th week**	**Baseline**	**12th week**
Weight (Kg)	2 ± 0.1	2.97 ± 0.1 $\$\$\$\$	2.3 ± 0.05	2.7 ± 0.12 $\$\$
Abdominal circumference (cm)	31.78 ± 1.17	38.78 ± 0.76 $\$\$\$\$	31.81 ± 0.88	36.45 ± 0.62 $\$\$\$
Fasting glycaemia (mg/dl)	98 ± 1.88	96 ± 3.06	101 ± 6.6	106 ± 7.54
Fasting insulinemia (ng/ml)	0.37 ± 0.08	0.31 ± 0.07	0.3 ± 0.04	1.15 ± 0.45$
Triglycerides(g/L)	1.4 ± 0.3	1.75 ± 0.35	1.76 ± 0.3	2.65 ± 0.39 $
TC (g/L)	6.72 ± 0.5	6.53 ± 0.8	7.4 ± 0.5	11.05 ± 0.88 $\$\$$ **
HDL-C (g/L)	0.21 ± 0.03	0.22 ± 0.03	0.19 ± 0.02	0.26 ± 0.03
LDL-C (g/L)	6.23 ± 0.45	5.96 ± 0.7	6.87 ± 0.5	10.25 ± 0.85 $\$\$$ ***
FFA (mmol/L)	0.83 ± 0.2	0.65 ± 0.1	1.02 ± 0.21	0.70 ± 0.11

TC = total cholesterol, HDL-C = high-density lipoprotein, LDL-C = low-density lipoprotein, FFA = free fatty acids. Data are represented as mean ± SEM. $ $p < 0.05$, $\$\$ $p < 0.01$, $\$\$\$ <0.001 and $\$\$\$\$ $p < 0.0001$ vs. Baseline. ** $p < 0.01$, *** $p < 0.001$ vs. Control.

Effect of HFFD on glucose and insulin metabolism

Fasting insulinemia significantly increased in the HFFD group (12th week vs. Baseline, $p < 0.03$) and almost significantly increased when comparing the two groups together at the end of the protocol (HFFD vs. Control, $p = 0.0504$). The HOMA-IR significantly increased amongst individuals of the HFFD group (12th week vs. Baseline, $p < 0.02$) and when comparing the two groups together at the end of the protocol (HFFD vs. Control, $p < 0.03$) (Figure 1E). Moreover, fasting plasma glucose levels did not show any significant change (Table 1). However, the AUCGlu from the IVGTT significantly increased when comparing the HFFD to the control group at the end of the protocol ($p < 0.02$) (Figure 1B). The Glycaemic levels obtained 2h after glucose injection also significantly increased in the HFFD group along time (12th week vs. Baseline, $p < 0.05$) and when comparing the HFFD to the control group at the end of the protocol ($p < 0.02$) (Figure 1D). In terms of AUCIns, no difference was found when comparing HFFD group to the control group (Figure 1C).

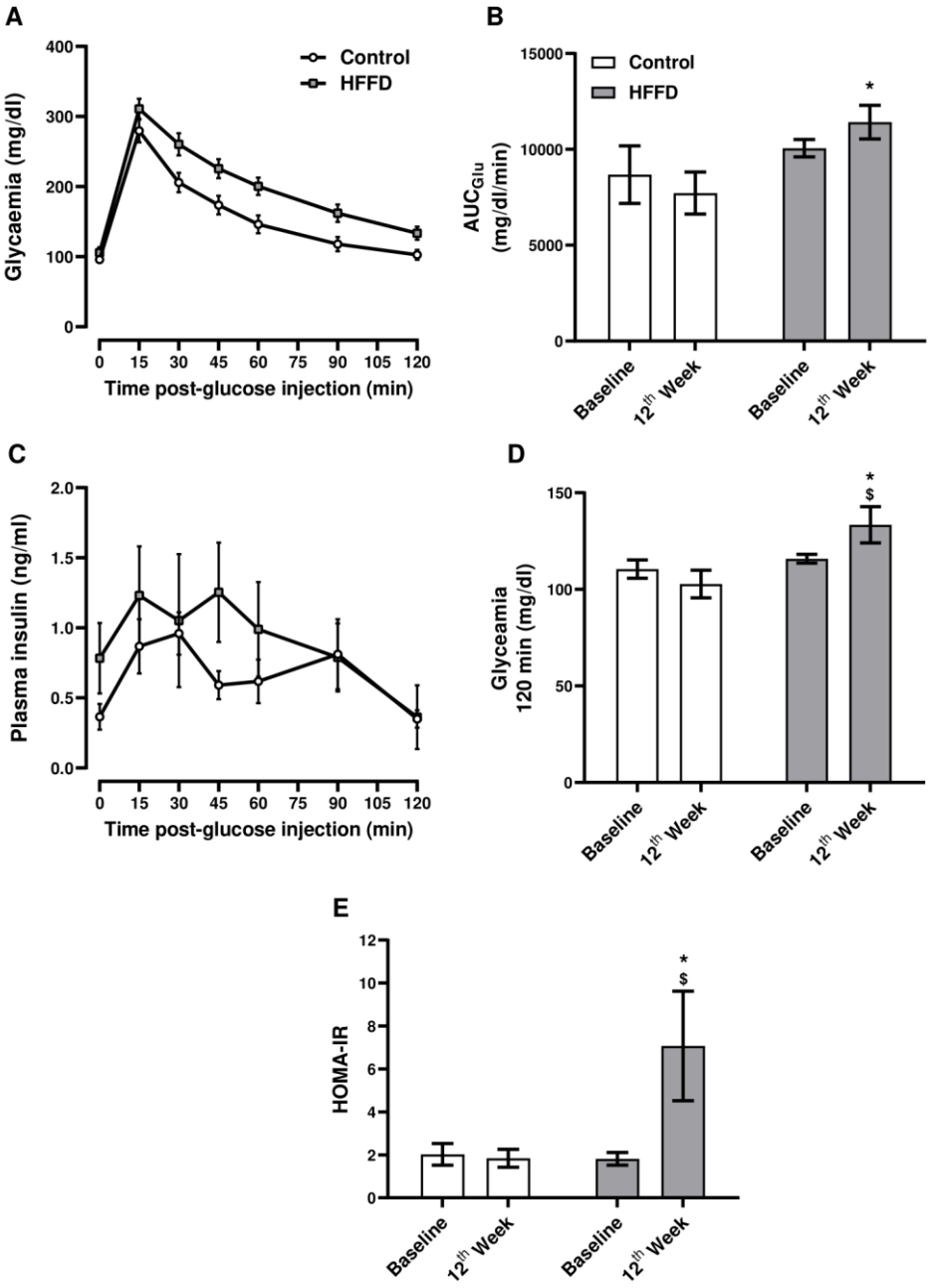

Figure 1 Effect of HFFD feeding on glucose and insulin metabolism. Glucose metabolism was evaluated by: (A) an IVGTT, performed after 12 weeks of HFFD feeding. As described in the method, at the end of the protocol, rabbits were intravenously injected with a glucose bolus, then plasma (B) glucose and (C) insulin levels were evaluated. (B) The AUCGlu of each curve from the IVGTT was calculated to compare the differences between the two groups. (D) Changes in plasma glucose levels 2 hours after the bolus were determined. (E) Insulin metabolism was assessed by calculating the Homeostasis model assessment of insulin resistance (HOMA-IR). Data were expressed as the mean ± SEM. ** $p < 0.01$ or * $p < 0.05$ HFFD vs. control group. $$ $p < 0.01$ or $ $p < 0.05$ 12th week vs. baseline (n=9 for control and n=12 for HFFD).

Cardiovascular function assessment

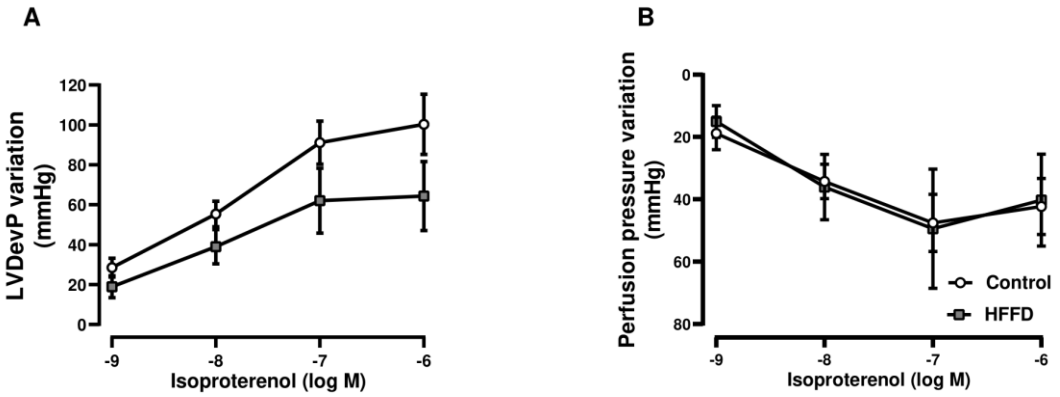

Figure 2 Effects of ß-adrenoceptor stimulation on cardiac function. Cardiac parameters were assessed after ß-adrenoceptor stimulation by building non-CCRCs to isoproterenol (10^{-9} to 10^{-6} M). The (A) LVDevP and (B) perfusion pressure, reflecting cardiac inotropy and coronary vasodilation, respectively, were evaluated. Data are represented as mean ± SEM and are analyzed using LME analysis (n=6 for Control and n=6 for HFFD).

To determine the effects of ß-adrenoceptor stimulation on cardiac inotropy and coronary vasodilation, non-CCRCs to isoproterenol were constructed (Figure 2). Our results showed that isoproterenol-induced positive inotropy exhibited a strong decreasing trend in HFFD-fed rabbits (p = 0.08) compared to the control group (Figure 2A). In terms of coronary vasodilation, we observed no difference between groups (Figure 2B).

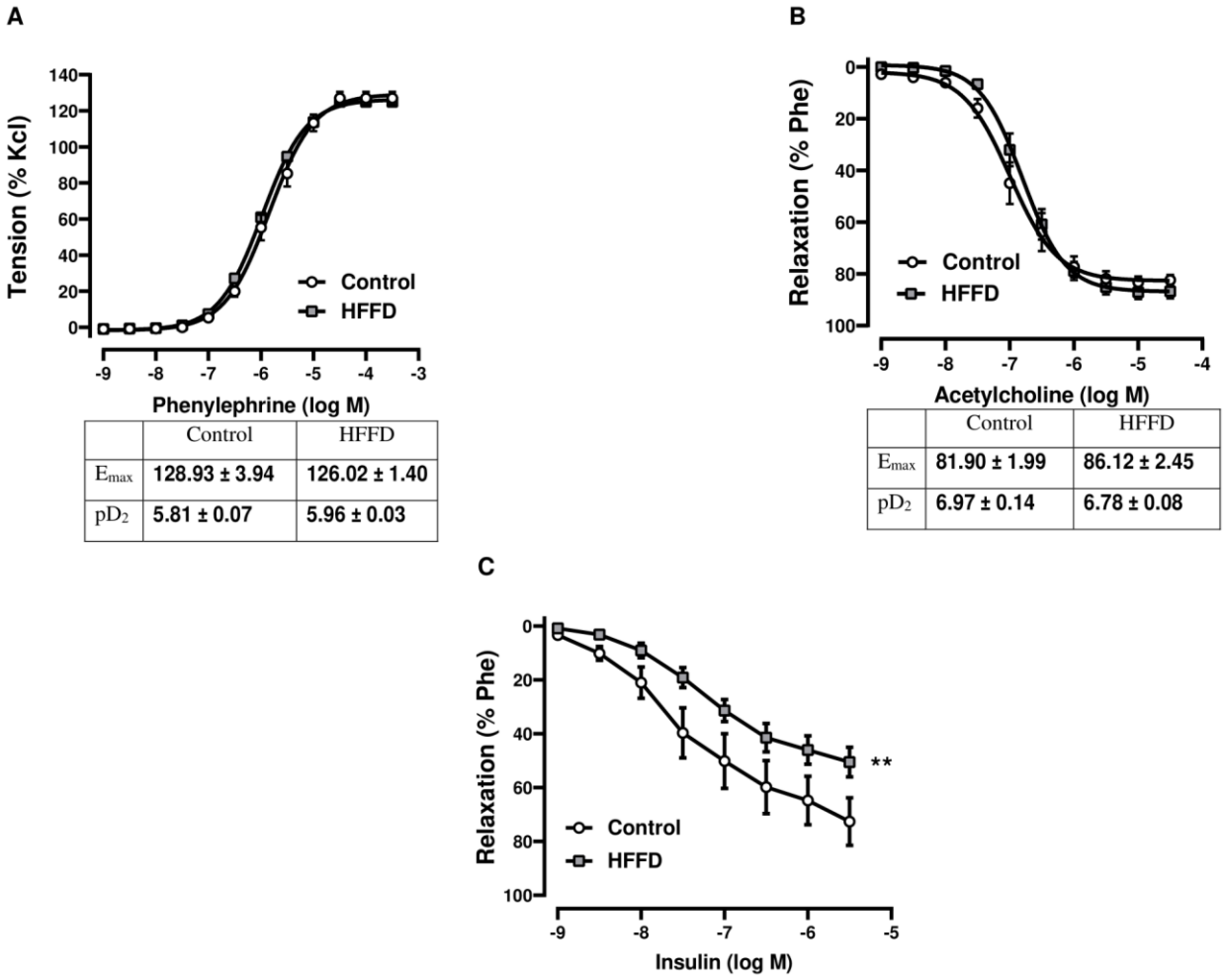

	Control	HFFD
E_{max}	128.93 ± 3.94	126.02 ± 1.40
pD_2	5.81 ± 0.07	5.96 ± 0.03

	Control	HFFD
E_{max}	81.90 ± 1.99	86.12 ± 2.45
pD_2	6.97 ± 0.14	6.78 ± 0.08

Figure 3 Effect of HFFD feeding on carotid vasoreactivity. CCRCs to (A) Phe, (B) Ach and (C) Ins were used to assess the vascular reactivity. (A) Carotid contractile response was evaluated using Phe (10^{-10} to 3.10^{-5}). Meanwhile, relaxant responses were assessed by constructing CCRCs to: (B) Ach (10^{-9} to 3.10^{-5} M) and (C) Ins (10^{-9} to 3.10^{-6} M) on Phe-precontracted carotid rings. The calculated contraction and relaxation percentages are relative to the maximal changes from KCl (contraction) and Phe (precontraction), respectively. Emax and pD2 represent the maximal contractile response and the potency, respectively. Data are expressed as mean ± SEM and analyzed using NLME for Phe and Ach and LME for Ins. * $p < 0.05$, ** $p < 0.01$ HFFD vs. Control (n=9 for Control and n=12 for HFFD).

To assess the vascular reactivity (vasoconstriction and vasorelaxation), CCRCs were built (Figure 3). We observed no change in terms of Phe-induced contraction (Figure 3A). The endothelium-dependent Ins-induced vasorelaxation was significantly lower in the HFFD group ($p < 0.01$ vs. Control) (Figure 3C). On the other hand, we observed no difference neither in terms of E_{max} nor in terms of pD_2 values, corresponding to endothelium-dependent Ach-induced relaxation (Figure 3B) and endothelium-independent relaxation response to SNP (10^{-10} to 3.10^{-5} M) (data not shown).

Aortic atheroma plaques evaluation

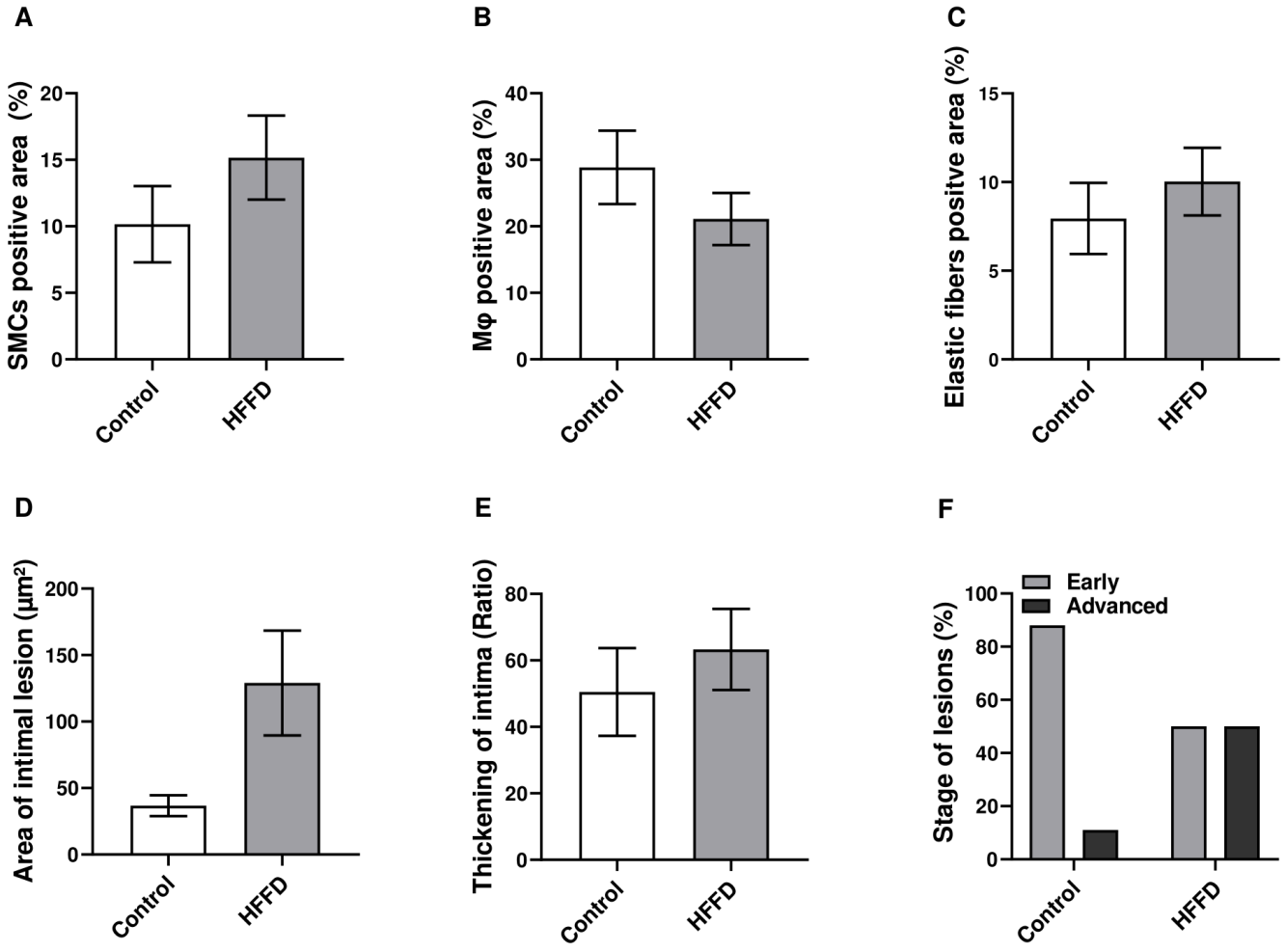

Figure 4 Quantification of aortic atherosclerosis following 12 weeks of HFFD feeding. Positively immuno-stained area of: (A) SMCs (detected using an anti-HHF35 antibody), (B) Mφ (detected using an anti-RAM11 antibody) and (C) elastic fibers (detected using the Orceine stain), were quantified using an image analysis system as described in the method. The same image analysis system was used to determine, (D) the intimal lesion area. Whereas, (E) the thickening of intima was determined by dividing the area of intimal lesion by the length of media. (F) Plaques were classified into early (type II and III plaques) and advanced (type IV and V plaques) stage lesions. Data in all graphs are represented as the mean ± SEM except for the stage of lesions, which was expressed in percentages. Statistical analysis was performed using one-way Anova for all parameters except for stage of lesions, for which a Chi square test was used (n=9 for Control and n=12 for HFFD).

We observed no change regarding the average thickening of the intima. The area of intimal lesion increased in the HFFD group compared to the control group; however, the increase was not significant. SMCs, Mφ and elastic fibers were not significantly different when comparing the HFFD to

the control group. We observed a clear trend towards advanced lesions in the HFFD ($p = 0.0614$ vs. Control) when evaluating the stage of lesions (Figure 4).

Table 2 Classification of atheroma plaques.

Histologic parameter evaluated	Classification	Control (n=9)	HFFD (n=12)	*p* value Control vs. HFFD
Extracellular lipids	**Absence**	3 (33.3%)	4 (33.3%)	0.0567
	Grade 1	5 (55.6%)	1 (8.3%)	
	Grade 2	1 (11.1%)	3 (25.0%)	
	Grade 3	0	4 (33.3%)	
	Grade 4	0	0	
Fibrous cap	**Absence**	7 (77.8%)	6 (50.0%)	0.0502
	Grade 1	2 (22.2%)	0	
	Grade 2	0	5 (41.7%)	
	Grade 3	0	1 (8.3%)	
	Grade 4	0	0	
Mineralization	**Absence**	8 (88.9%)	9 (75.0%)	0.43
	Grade 1	1 (11.1%)	3 (25.0%)	
	Grade 2	0	0	
	Grade 3	0	0	
	Grade 4	0	0	
Lipid core	**Absence**	6 (66.7%)	5 (41.7%)	0.2753
	Grade 1	2 (22.2%)	1 (8.3%)	
	Grade 2	1 (11.1%)	4 (33.3%)	
	Grade 3	0	2 (16.7%)	
	Grade 4	0	0	
Collagen deposition	**Absence**	1 (11.1%)	0	0.1888
	Grade 1	1 (11.1%)	0	
	Grade 2	4 (44.4%)	2 (16.7%)	
	Grade 3	2 (22.2%)	7 (58.3%)	

	Grade 4	1 (11.1%)	3 (25.0%)	
Type of plaque	**No plaque**	1 (11.1%)	0	0.09
	Type II	4 (44.4%)	4 (33.3%)	
	Type III	3 (33.3%)	2 (16.7%)	
	Type IV	1 (11.1%)	0	
	Type V	0	6 (50.0%)	

A semi-quantitative scale from 0 to 4 was used to grade the presence of extracellular lipid, fibrous cap, mineralization, lipid core in addition to collagen's deposition (detected using green Masson's trichrome stain). Types of plaques were classified according to the guidelines of the American Heart Association. The results were expressed as frequency and percentage. Statistical analysis was performed using a Chi-square test.

We found an almost significant increase in the presence of extracellular lipid deposition and fibrous cap ($p = 0.0567$ and $p = 0.0502$, respectively) in the HFFD group (vs. Control). Regarding the extent of mineralization, lipid core severity and collagen deposition, there was no statistically significant difference between the two groups. Nevertheless, we did frequently observe marked and severe collagen deposition in the HFFD group and rarely in the control group. In terms of plaques types, most of plaques observed in the control group were either classified as type II (4/9) or as type III (3/9) with none type V plaques. In contrast, 50% of the plaques (6/12) were classified as type V plaques in the HFFD group. In the current study, only type II, III, IV and V lesions were observed (absence of type I and VI) (Table 2).

Gut microbiota analysis

When comparing the UF and WUF distances between the two microbial communities of the control and HFFD groups, the differences were highly significant ($p < 0.001$ and $p < 0.001$, respectively). This means that samples from the same group of rabbits (control) clustered together and separately from samples belonging the other group of rabbits (HFFD) in the plot, indicating dissimilarities between communities belonging to the control and those belonging to the HFFD group (Figures 5A & 5B). The overall microbial composition analysis revealed a significant decrease of the alpha diversity in the HFFD group compared to the control group, as measured by the Observed, Shannon and Simpson indexes ($p < 0.001$, $p < 0.0001$ and $p < 0.01$, respectively) (Figure 5C). When we evaluated the microbial composition at the phylum level, three main phyla were present, with *Firmicutes* as the most abundant followed by *Bacteroidetes* and *Actinobacteria* (Data not shown). The abundance of Firmicutes, the dominant bacterial phylum, significantly increased ($p < 0.01$); whereas, the abundance of Bacteroidetes and that of Proteobacteria significantly decreased ($p < 0.01$ and $p < 0.05$, respectively) in the HFFD group compared to the control group (Figure 5D). We also

evaluated the microbial composition at the Family level. We found a significant decrease in the abundance of *Rikenellaceae* ($p < 0.05$) and bacteroidaceae ($p < 0.05$) on one hand; and a significant increase in *Ruminococcaceae* ($p < 0.05$), on the other hand (Figure 5E). At the genus level, *Ruminococcus* and *Bacteroides* significantly increased ($p < 0.02$) and decreased ($p < 0.03$) in the HFFD group compared to the control group, respectively (Figure 5F).

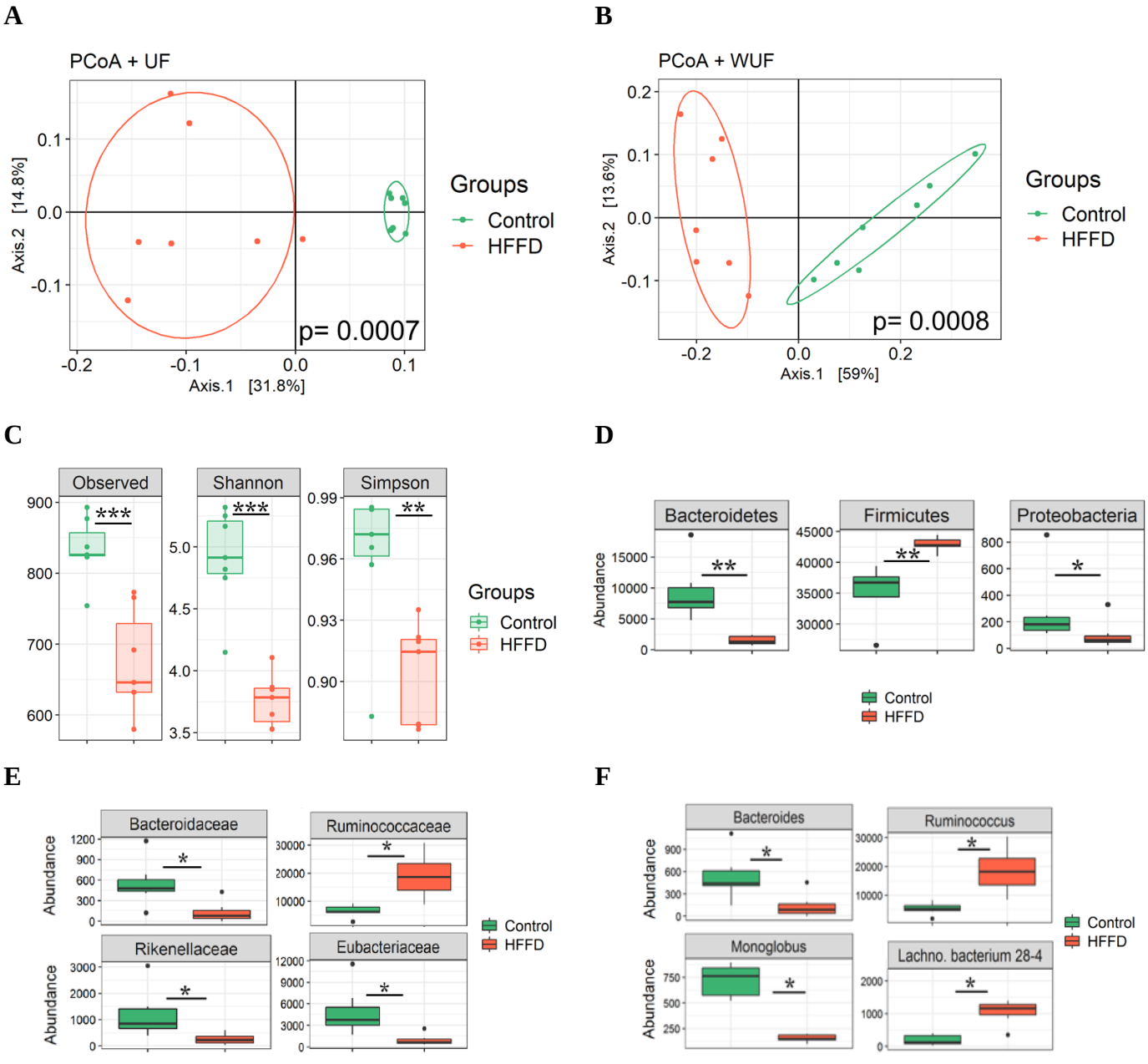

Figure 5 Gut bacterial community analysis by 16S rRNA gene high-throughput sequencing. Principle coordinate analysis (PCoA) based on A) Unifrac (UF) and B) weighted Unifrac (WUF) distance matrices, reveals useful information about the phylogenetic relationship and composition of bacterial microbiota in the different animal groups. C) Alpha

diversity, which takes into account the community richness and evenness, was measured by three different indexes: Observed number of OTUs, Shannon and Simpson. Abundance of bacterial taxa at the D) Phylum, E) Family and F) Genus levels. Data are represented as box plots. * $p < 0.05$, ** $p < 0.01$ and *** $p < 0.001$ (n=6 for Control and n=6 for HFFD

Discussion

In the current study, we explored the changes in metabolic and cardiovascular parameters, as well as in gut microbiota composition, related to a combination of two main factors of the metabolic syndrome, dyslipidemia and IR. To produce this combination, we subjected the Watanabe rabbit, an animal model of dyslipidemia and atherosclerosis, to a HFFD, known for its ability to induce IR; as performed by a previous study, by Ning et al., in which authors aimed at investigating the effect of diet-induced IR on the development of atherosclerosis [19]. Since our purpose was to induce IR rather than obesity (which might be a confounding factor), the HFFD that we used contained the same amount of calories (isocaloric) as the control diet (normal chow). The latter is protein- and fiber-rich, whereas the HFFD is rich in sugar and fat, but reduced in protein and fibers.

Consequently, we found no difference neither in terms of weight gain nor in terms of abdominal circumference, between control and HFFD individuals. Even though both the weight and abdominal circumference parameters significantly increased in both groups (12^{th} week vs. Baseline), the increase was not higher in the HFFD compared to control. Thus, increases in these two parameters were probably age-dependent and not specifically related to the HFFD feeding.

HFFD feeding significantly increased both the fasting plasma levels of insulin and HOMA-IR, two indicators of IR. These results along with the absence of increased weight and abdominal circumference are in consistence with several studies, that have demonstrated that consuming a normal number of calories, whether of a high fructose diet or of a high fructose-fat diet, induces IR without obesity in rabbit models [19,24]. In another study, Baena et al. demonstrated that development of IR in fructose-fed rats is specifically related to fructose feeding and not to the amount of calories ingested. In the same study they also found that fructose supplementation leads to an abnormal GTT [25]. These results are in accordance with our findings regarding the impaired glucose tolerance in our HFFD-fed rabbits. As shown in Figure 1, when challenged with a glucose bolus, HFFD-fed rabbits exhibited delayed capacity for clearing glucose from the circulation. This was confirmed by a significant increase in both the AUC_{Glu} from the IVGTT and the glycaemic levels 2-hours post-glucose injection, compared to the standard chow diet-fed group. The HFFD-induced IR state is related to the fact that fructose is a highly lipogenic nutrient. It has been demonstrated that a high fructose level stimulates visceral adipose deposition leading to an increased FA flux and lipid accumulation in insulin sensitive tissues and thereby to impaired insulin signaling through the IRS1-PI3K-Akt (insulin receptor substrate 1-phosphoinositide 3-kinase-protein kinase B) pathway [7,26]. Then, the impaired insulin signaling results in decreased translocation of GLUT 4 to the cell surface and thereby to reduced glucose uptake, in

insulin sensitive tissues i.e. skeletal muscle and adipose tissue [25,27]. This explains our results regarding the decrease in glucose tolerance in the HFFD-fed group.

It has been shown that the exposure of the liver to high fructose concentrations leads to enhanced rate of de novo lipogenesis in animal models and humans [25]. A high fructose flux, to the liver, increases TG synthesis and/or decreases TG clearance ultimately leading to increased production of very low density lipoprotein (VLDL) particles (TG is packaged with Apo-B in the liver and secreted as VLDL) [28,29]. Moreover, not only fructose but also fat induces lipogenesis; the former stimulates endogenous lipogenesis, whereas the latter increases the availability of exogenous lipids [30]. This explains our results regarding the increased TG levels found in the HFFD group, in agreement with the findings of other studies [31]. The excess of VLDL secretion then delivers higher levels of FAs and TG to skeletal muscle and adipose tissue, further inducing IR [32], which in turn explains our results in regards to the decrease in insulin sensitivity (increased insulinemia and HOMA-IR).

It has been described that, in states of obesity, fasting leads to mobilization of energy stores (TG) in adipose tissue via lipolysis, resulting in increased FFA levels [33] and that abdominal subcutaneous adipose tissue is the only significant site of FFA liberation; meanwhile, only a small and insignificant proportion arises from visceral adipose tissue [34]. Therefore, the stable unchanged FFA levels might be explained by the absence of both, excessive weight gain and increased abdominal circumference in the HFFD-fed subjects.

Even though control Watanabe rabbits spontaneously develop hypercholesterolemia due a mutation in their LDLr [35,36]; we still found that 12 weeks of HFFD feeding leads to an extensive hypercholesterolemia, when compared to the control group. This might be explained by an increase in TG-enriched VLDL production (as described above) due to the long-term HFFD-feeding. These VLDL particles would then undergo lipolysis yielding higher levels of LDL-C particles and subsequently higher cholesterol levels in the circulation. It is highly probable that in Watanabe rabbits, the reduced clearance of lipoproteins (mutated LDLr) lead to a further increase in blood cholesterol levels.

It has been well established that an individual is diagnosed with MetS when presenting three out of five risk factors: increased waist circumference (central or abdominal obesity), elevated triglyceride levels, reduced high-density lipoprotein cholesterol (HDL-C), high blood pressure and elevated fasting glycaemia [37,38]. We found impaired glucose tolerance (increased AUC_{Glu} and 2h glycaemia), hyperinsulinemia and increased HOMA-IR, all indicators of IR. Rabbits also exhibited increased TG levels and low HDL-C. These results point out that Watanabe rabbits developed MetS following 12 weeks of HFFD feeding.

In general and unlike rodents, rabbits have a humanoid lipoprotein metabolism (higher LDL than HDL) and therefore represent the best candidates in terms of animal models for the study of lipid/lipoprotein metabolism and atherosclerosis [35,39,40]. Moreover, the WHHL rabbit, in particular, is an animal model of human familial hypercholesterolemia (FH) due to a genetic defect in its low-density lipoprotein receptor (LDLr); that leads to a delayed clearance of LDL particles from the circulation and consequently to hyperlipidemia and spontaneous atherosclerosis [35,36]. Our results combined together with the aforementioned findings, confirm the development of an animal model of MetS.

Watanabe rabbits are well known for their ability to spontaneously develop atherosclerosis. Therefore, our aim was not to assess the effect of combined dyslipidemia-IR on the induction/establishment of atherosclerosis but rather on its progression under these conditions. Thus, we evaluated the evolution of aortic atherosclerotic plaques in terms of quality and quantity. We observed a qualitative amplification of atherosclerosis in individuals with combined dyslipidemia-IR that is likely due to increased hypercholesterolemia in the HFFD group. Moreover, IR, per se, has been found to increase plasma lipid levels [41]. Under physiological conditions, insulin decreases VLDL-TG and apo-lipoprotein B (apoB) production and enhances apoB degradation [42]. During IR states, insulin's physiological effects are counteracted leading to increased production and secretion of lipids [43]. Hence, it is plausible that IR together with elevated plasma lipids exhibit combinational roles in the worsening of atherosclerosis by making the lesions become more vulnerable and more susceptible to complications, in HFFD-fed WHHL rabbits [19].

It has been proposed that the hyperinsulinemia (encountered during IR) and dyslipidemia lead to sympathetic nervous system (SNS) overdrive [44,45]; which thereby leads to decreased myocardial contractile response to β-stimulation [46]. We evaluated the effects of β-adrenergic stimulation on cardiac inotropy and coronary vasodilation. As reported by Park et al. IR might lead to cardiac dysfunction and remodeling [47] and, as proven by Mazumder et al., cardiac IR reduces the metabolic efficiency of the heart, leading to contractile dysfunction in mice [48]. Our results showed a strong decreasing trend in the positive inotropy in HFFD-fed Watanabe rabbits, indicating a likelihood implication of IR and/or dyslipidemia. Our findings also suggest that the alteration mainly concerns β_1-ARs and not β_2-ARs [49,50] , since no change was observed in terms of coronary vasodilation. Alterations in the β-adrenergic system may occur either at the receptor or post-receptor intracellular signaling level, i.e. calcium (Ca^{2+}) handling proteins [51–54]. Whether the prolonged HFFD-feeding induced-IR impaired cardiac contractility through modification in β-AR expression or β-ARs-linked mechanisms remains to be determined.

A strong link between IR and endothelial dysfunction (ED) has been well established [55]. Thus, we evaluated the reactivity of the carotid

artery. The HFFD did not affect relaxation to SNP (data not shown) nor to Ach, meaning that neither endothelium-independent nor Ach-induced endothelium-dependent vasorelaxation were affected. In contrast, other studies found that high fructose and/or high fat feeding leads to impaired Ach-induced vasorelaxation [56]. It has been found that westernized diet-induced oxidative stress results in reduced NO production and/or increased NO sequestration and inactivation thereby leading to ED [56]. Meanwhile, our results showed that HFFD diminished insulin-mediated vasorelaxation, known to be mainly endothelium-dependent [57]. This is most probably related to a HFFD-induced IR state. Our results are in accordance with the findings of Kim et al. who found that diet-induced IR impaired insulin-mediated vasodilation with no effect on Ach- or SNP-induced vasodilation [58]. In physiologic states, insulin stimulates NO release from the vascular endothelium through PI3K-Akt-mediated phosphorylation of eNOS, leading to vasorelaxation. During IR, signaling through this pathway is downregulated leading to a compromised vasorelaxant effect of insulin [59]. Moreover, vascular IR contributes to the impairment of overall insulin-stimulated glucose uptake, which explains our results regarding the decreased glucose tolerance. In fact vasodilatory actions of insulin are well known for their contribution to insulin delivery and glucose-uptake in skeletal muscle [60]. Then the decreased glucose-uptake, probably stimulated insulin production leading to a hyperinsulinemic state that further induced hepatic TG-rich VLDL production [43].

Evidence from human and animal studies support a link between the gut microbiome and several components of the MetS [12,61]. Moreover, it is believed that changes in diet and activity patterns alter the gut microbiome composition/diversity, leading to changes in the metabolic profile of microbiota and thereby to the onset of disease e.g. MetS [5,62]. Thus, we explored the gut microbial changes that occurred following long term HFFD-feeding to Watanabe rabbits. It is noteworthy that, so far, most of gut microbiota studies have been performed on rodents (mouse and rat models) and rarely on rabbits.

Our results showed that 12 weeks of HFFD-feeding led to a shift in overall intestinal microbial composition, characterized by changes in abundance of dominant bacterial Phyla, and diversity (richness and evenness); indicating a strong impact of dietary fat and carbohydrates on the gut microbiota. In consistence with our results, it has been demonstrated that low richness in gut microbiota, reflecting a reduced microbial diversity correlates with several components of the MetS, namely, IR and dyslipidemia [63].

In the current study, HFFD-fed rabbits exhibited an increased *Firmicutes* abundance and a decreased *Bacteroidetes* abundance. Similar changes in microbiota composition have been observed in mice fed a "Western" diet (high-fat/high-sugar), by Turnbaugh et al. [64]. In another study by the same authors, a decrease in Bacteroidetes abundance was reported, upon a dietary shift to a "Western" diet, in germfree mice colonized with human microbiota [65]. The *Firmicutes* to *Bacteroidetes* ratio, used as a relevant marker/hallmark of metabolic dysfunction [62,66], increased from R= 3.39 in the control group

to R= 28.24 in the HFFD group (data not shown). This is in agreement with a recent study by Horne et al., who found an increase in the *Firmicutes*/*Bacteroidetes* ratio in high-fructose/high-fat diet-fed hamsters [66]. *Firmicutes* were proposed as more effective in extracting energy from food than *Bacteroidetes* [67] which could have contributed to the state of IR in the HFFD-fed group. Even though no apparent/overall obesity was observed in individuals from the HFFD group, these rabbits still developed a state of IR indicating the presence of visceral obesity.

Moreover, *Bacteroidetes* were suggested to have a protective or balancing role against metabolic impairment in rodents and human studies; and more specifically the *Rikenellaceae* Family, was found to point towards more healthy metabolic states [68]. furthermore, in another study decreased *Rikenellaceae* abundance was found to be associated with a negative metabolic outcome e.g. increased BMI [69]. In accordance with those studies, we found a decreased abundance of the *Rikenellaceae* Family in the HFFD group which is most likely related to the altered metabolic state in rabbits belonging to the HFFD group. Our results also showed that HFFD-feeding leads to decreased abundance in another Family belonging to *Bacteroidetes* Phylum, *Bacteroidaceae* which, according to Lippert et al., inversely correlates with visceral obesity [68]. As mentioned earlier, in the present study, rabbits from the HFFD group likely exhibited excessive visceral (rather than subcutaneous) fat accumulation, associated with the IR state that that occurred following 12 weeks of HFFD-feeding. On the other hand, Zeng et al reported a negative correlation between *bacteroides* genus and serum lipids (TC, LDL-C and TG levels) [70]. Accordingly, the decrease in the *bacteroides* genus (Family *Bacteroidaceae*), found in our study, might be explained by the significant increase in the aforementioned lipid levels in the HFFD group.

In their study, Ciubotaru et al. found that *Ruminococcaceae* Family (Phylum *Firmicutes*) were significantly higher in subjects with dyslycaemia, i.e. impaired glucose tolerance and/or impaired fasting glycaemia. In the same study, *Ruminococcus* genus (Family *Ruminococcaceae*) was also found to correlate with dysglycemia [71]. Hence, in the current study, both the increased *Ruminococcaceae* and *Ruminococcus* abundances in individuals from the HFFD group are most likely related to the glucose intolerance/IR state.

In contrast to our findings, consumption of diets rich in fat and sugars was found to increase the number of *Proteobacteria* Phylum [72,73]. Nonetheless, in another study it was reported that subjects with unfavorable lipid profiles/dyslipidemia, had low microbial diversity and lower abundance of many taxa from phyla *Proteobacteria* and *Bacteroidetes*. This is in line with our findings, in regards to the decreased microbial diversity and abundance of both these phyla [74], which is most probably related to the worsening of dyslipidemia in response to the 12-week HFFD feeding.

Conclusions

We demonstrated that long-term HFFD-feeding leads to the development of MetS by inducing an IR state and exacerbating dyslipidemia, and to a shift in overall intestinal microbial composition in WHHL rabbits. We also showed that, independently from obesity, combined IR-

dyslipidemia exhibits atherogenic (worsened aortic atherosclerosis) and deleterious cardiovascular effects (decreased cardiac contractility and reduced insulin-mediated vasorelaxation) and induces gut microbiota dysbiosis. The current study confirms that (isocaloric) HFFD-fed WHHL rabbit represents a promising diet based and time efficient experimental model of MetS, without obesity as a main factor. This model can be further developed to explore new therapeutic strategies in the management of the MetS and its associated cardiovascular disorders.

Supplementary Materials: The following are available online at www.mdpi.com/xxx/s1, title, Table S1: Composition of the standard chow and the high-fructose high-fat diets.

Author Contributions: MM, J-CD and YM conceived and designed the experiments. ED carried out the histological and immunohistochemical analysis of the atheroma plaques. CT helped in statistical analysis. MM and YM drafted the manuscript. All authors read and approved the final manuscript.

Funding: "This research received no external funding"

Institutional Review Board Statement: "The study was conducted in accordance with the National Institute of Health Guide for the Use and Care of Laboratory Animals guidelines and they are all conducted with the approval of the Ethics Committee of Pays de la Loire (APAFIS n° 10722).

Acknowledgments: The authors express their gratitude to the technicians in histopathology (Laboniris) Mr. Bernard Fernandez, Mrs. Florence Lezin, and Mrs. Suzie Calvez. They would also like to express their appreciation to Dr. Julien Pichon and Dr. Alex Moinard (Oniris) for their precious advice in methodology and data interpretation and to Dr. Moez Rhimi (Micalis Inrae) for his participation in data representation and statistical analysis of the gut microbiota part of the study.

Conflicts of Interest: "The authors declare no conflict of interest."

Refrences

1. Rochlani, Y.; Pothineni, N. V.; Kovelamudi, S.; Mehta, J. L. Metabolic syndrome: pathophysiology, management, and modulation by natural compounds. *Ther. Adv. Cardiovasc. Dis. Rev.* **2017**, 11, 215–225.

2. Saklayen, M. G. The Global Epidemic of the Metabolic Syndrome. *Curr. Hypertens. Rep.* **2018**, 20, 1–8.

3. Kopp, W. How western diet and lifestyle drive the pandemic of obesity and civilization diseases. *Diabetes, Metab. Syndr. Obes. Targets Ther.* **2019**, 12, 2221–2236.

4. Misra, A.; Singhal, N.; Khurana, L. Obesity, the metabolic syndrome, and type 2 diabetes in developing countries: Role of dietary fats and oils. *J. Am. Coll. Nutr.* **2010**, 29, 289S-301S.

5. Gildner, T. E. Links between metabolic syndrome and the microbiome. *Evol. Med. Public Heal.* **2020**, 2020, 45–46.

6. Elliott, S. S.; Keim, N. L.; Stern, J. S.; Teff, K.; Havel, P. J. Fructose, weight gain, and the

insulin resistance syndrome. *Am. J. Clin. Nutr.* **2002**, 76, 911–922.

7. Dekker, M. J.; Su, Q.; Baker, C.; Rutledge, A. C.; Adeli, K. Fructose: A highly lipogenic nutrient implicated in insulin resistance, hepatic steatosis, and the metabolic syndrome. *Am. J. Physiol. - Endocrinol. Metab.* **2010**, 299, 685–694.

8. Welsh, J. A.; Sharma, A.; Abramson, J. L.; Vaccarino, V.; Gillespie, C.; Vos, M. B. Caloric sweetener consumption and dyslipidemia among US adults. *JAMA - J. Am. Med. Assoc.* **2010**, 303, 1490–1497.

9. Ludwig, D. S. Dietary glycemic index and obesity. *J. Nutr.* **2000**, 130, 280–283.

10. Lustig, R. H. Metabolic syndrome and the "western diet": Science and politics. *Pediatr. Adolesc. Med.* **2015**, 19, 137–147.

11. Drake, I.; Sonestedt, E.; Ericson, U.; Wallström, P.; Orho-Melander, M. A Western dietary pattern is prospectively associated with cardio-metabolic traits and incidence of the metabolic syndrome. *Br. J. Nutr.* **2018**, 119, 1168–1176.

12. Mazidi, M.; Rezaie, P.; Kengne, A. P.; Mobarhan, M. G.; Ferns, G. A. Gut microbiome and metabolic syndrome. *Diabetes Metab. Syndr. Clin. Res. Rev.* **2016**, 10, S150–S157.

13. Festi, D.; Schiumerini, R.; Eusebi, L. H.; Marasco, G.; Taddia, M.; Colecchia, A. Gut microbiota and metabolic syndrome. *World J. Gastroenterol.* **2014**, 20, 16079–16094.

14. Lecomte, V.; Kaakoush, N. O.; Maloney, C. A.; Raipuria, M.; Huinao, K. D.; Mitchell, H. M.; Morris, M. J. Changes in gut microbiota in rats fed a high fat diet correlate with obesity-associated metabolic parameters. *PLoS One*. **2015**, 10, 1–22.

15. Zhang, X.; Shen, D.; Fang, Z.; Jie, Z.; Qiu, X.; Zhang, C.; Chen, Y.; Ji, L. Human Gut Microbiota Changes Reveal the Progression of Glucose Intolerance. *PLoS One*. **2013**, 8, 1–11.

16. Li, J.; Zhao, F.; Wang, Y.; Chen, J.; Tao, J.; Tian, G.; Wu, S.; Liu, W.; Cui, Q.; Geng, B.; Zhang, W.; Weldon, R.; Auguste, K.; Yang, L.; Liu, X.; Chen, L.; Yang, X.; Zhu, B.; Cai, J. Gut microbiota dysbiosis contributes to the development of hypertension. *Microbiome*. **2017**, 5, 1–19.

17. Bäckhed, F.; Manchester, J. K.; Semenkovich, C. F.; Gordon, J. I. Mechanisms underlying the resistance to diet-induced obesity in germ-free mice. *Proc. Natl. Acad. Sci. U. S. A.* **2007**, 104, 979–984.

18. Cornier, M. A.; Dabelea, D.; Hernandez, T. L.; Lindstrom, R. C.; Steig, A. J.; Stob, N. R.; Van Pelt, R. E.; Wang, H.; Eckel, R. H. The metabolic syndrome. *Endocr. Rev.* **2008**, 29, 777–822.

19. Ning, B.; Wang, X.; Yu, Y.; Waqar, A. B.; Yu, Q.; Koike, T.; Shiomi, M.; Liu, E.; Wang, Y.; Fan, J. High-fructose and high-fat diet-induced insulin resistance enhances atherosclerosis in Watanabe heritable hyperlipidemic rabbits. *Nutr. Metab.* **2015**, 12, 1–11.

20. Ibrahim, M.; Ahmed, I. A.; Mikail, M. A.; Ishola, A. A.; Draman, S.; Isa, M. L. M.; Yusof,

A. M. Baccaurea angulata fruit juice reduces atherosclerotic lesions in diet-induced Hypercholesterolemic rabbits. *Lipids Health Dis.* **2017**, 16, 2–8.

21. Helfenstein, T.; Fonseca, F. A.; Ihara, S. S.; Bottós, J. M.; Moreira, F. T.; Pott, H.; Farah, M. E.; Martins, M. C.; Izar, M. C. Impaired glucose tolerance plus hyperlipidaemia induced by diet promotes retina microaneurysms in New Zealand rabbits. *Int. J. Exp. Pathol.* **2011**, 92, 40–49.

22. Stary, H. C.; Chandler, A. B.; Dinsmore, R. E.; Fuster, V.; Glagov, S.; Insull, W.; Rosenfeld, M. E.; Schwartz, C. J.; Wagner, W. D.; Wissler, R. W. A Definition of Advanced Types of Atherosclerotic Lesions and a Histological Classification of Atherosclerosis. *Circulation*. **1995**, 92, 1355–1374.

23. Thorin, C.; Mallem, M. Y.; Noireaud, J.; Gogny, M.; Desfontis, J.-C. Nonlinear mixed effects models applied to cumulative concentration-response curves. *J. Pharm. Pharmacol.* **2010**, 62, 339–345.

24. Waqar, A. B.; Koike, T.; Yu, Y.; Inoue, T.; Aoki, T.; Liu, E.; Fan, J. High-fat diet without excess calories induces metabolic disorders and enhances atherosclerosis in rabbits. *Atherosclerosis*. **2010**, 213, 148–155.

25. Baena, M.; Sangüesa, G.; Dávalos, A.; Latasa, M. J.; Sala-Vila, A.; Sánchez, R. M.; Roglans, N.; Laguna, J. C.; Alegret, M. Fructose, but not glucose, impairs insulin signaling in the three major insulin-sensitive tissues. *Sci. Rep.* **2016**, 6, 1–15.

26. Stanhope, K. L.; Havel, P. J. Fructose consumption: Potential mechanisms for its effects to increase visceral adiposity and induce dyslipidemia and insulin resistance. *Curr. Opin. Lipidol.* **2008**, 19, 16–24.

27. Kim, J. A.; Montagnani, M.; Kwang, K. K.; Quon, M. J. Reciprocal relationships between insulin resistance and endothelial dysfunction: Molecular and pathophysiological mechanisms. *Circulation*. **2006**, 113, 1888–1904.

28. Basciano, H.; Federico, L.; Adeli, K. Fructose, insulin resistance, and metabolic dyslipidemia. *Nutr. Metab.* **2005**, 2, 1–14.

29. Tranchida, F.; Tchiakpe, L.; Rakotoniaina, Z.; Deyris, V.; Ravion, O.; Hiol, A. Long-term high fructose and saturated fat diet affects plasma fatty acid profile in rats. *J. Zhejiang Univ. Sci. B.* **2012**, 13, 307–317.

30. Namekawa, J.; Takagi, Y.; Wakabayashi, K.; Nakamura, Y.; Watanabe, A.; Nagakubo, D.; Shirai, M.; Asai, F. Effects of high-fat diet and fructose-rich diet on obesity, dyslipidemia and hyperglycemia in the WBN/Kob-Leprfa rat, a new model of type 2 diabetes mellitus. *J. Vet. Med. Sci.* **2017**, 79, 988–991.

31. Toklu, H. Z.; Muller-Delp, J.; Sakarya, Y.; Oktay, S.; Kirichenko, N.; Matheny, M.; Carter, C. S.; Morgan, D.; Strehler, K. Y. E.; Tumer, N.; Scarpace, P. J. High dietary fructose does not exacerbate the detrimental consequences of high fat diet on basilar artery function. *J. Physiol. Pharmacol.* **2016**, 67, 205–216.

32. Choi, S. H.; Ginsberg, H. N. Increased very low density lipoprotein (VLDL) secretion,

hepatic steatosis, and insulin resistance. *Trends Endocrinol. Metab.* **2011**, 22, 353–63.

33. McCracken, E.; Monaghan, M.; Sreenivasan, S. Pathophysiology of the metabolic syndrome. *Clin. Dermatol.* **2018**, 36, 14–20.

34. Jensen, M. D. Adipose tissue and fatty acid metabolism in humans. *J. R. Soc. Med. Suppl.* **2002**, 95, 3–7.

35. Kobayashi, T.; Ito, T.; Shiomi, M. Roles of the WHHL rabbit in translational research on hypercholesterolemia and cardiovascular diseases. *J. Biomed. Biotechnol.* **2011**, 2011, 1–10.

36. Shiomi, M.; Ito, T. The Watanabe heritable hyperlipidemic (WHHL) rabbit, its characteristics and history of development: a tribute to the late Dr. Yoshio Watanabe. *Atherosclerosis*. **2009**, 207, 1–7.

37. Sperling, L. S.; Mechanick, J. I.; Neeland, I. J.; Herrick, C. J.; Després, J. P.; Ndumele, C. E.; Vijayaraghavan, K.; Handelsman, Y.; Puckrein, G. A.; Araneta, M. R. G.; Blum, Q. K.; Collins, K. K.; Cook, S.; Dhurandhar, N. V.; Dixon, D. L.; Egan, B. M.; Ferdinand, D. P.; Herman, L. M.; Hessen, S. E.; Jacobson, T. A.; Pate, R. R.; Ratner, R. E.; Brinton, E. A.; Forker, A. D.; Ritzenthaler, L. L.; Grundy, S. M. The CardioMetabolic Health Alliance Working Toward a New Care Model for the Metabolic Syndrome. *J. Am. Coll. Cardiol.* **2015**, 66, 1050–1067.

38. Wang, H. H.; Lee, D. K.; Liu, M.; Portincasa, P.; Wang, D. Q. H. Novel insights into the pathogenesis and management of the metabolic syndrome. *Pediatr. Gastroenterol. Hepatol. Nutr.* **2020**, 23, 189–230.

39. Fan, J.; Kitajima, S.; Watanabe, T.; Xu, J.; Zhang, J.; Liu, E.; Chen, Y. E. Rabbit models for the study of human atherosclerosis: From pathophysiological mechanisms to translational medicine. *Pharmacol. Ther.* **2015**, 146, 104–119.

40. Trajkovska, K. T.; Topuzovska, S. High-density lipoprotein metabolism and reverse cholesterol transport: Strategies for raising HDL cholesterol. *Anatol. J. Cardiol.* **2017**, 18, 149–154.

41. Biddinger, S. B.; Hernandez-Ono, A.; Rask-Madsen, C.; Haas, J. T.; Alemán, J. O.; Suzuki, R.; Scapa, E. F.; Agarwal, C.; Carey, M. C.; Stephanopoulos, G.; Cohen, D. E.; King, G. L.; Ginsberg, H. N. N.; Kahn, C. R. Hepatic Insulin Resistance Is Sufficient to Produce Dyslipidemia and Susceptibility to Atherosclerosis. *Cell Metab.* **2008**, 7, 125–134.

42. Sparks, J. D.; Sparks, C. E.; Adeli, K. Selective Hepatic Insulin Resistance, VLDL Overproduction, and Hypertriglyceridemia ATVB in Focus New Developments in Hepatic Lipoprotein Production and Clinical Relevance. *Arter. Thromb Vasc Biol*. **2012**, 32, 2104–2112.

43. Czech, M. P. Insulin action and resistance in obesity and type 2 diabetes. *Nat. Med.* **2017**, 23, 804–814.

44. Thorp, A. A.; Schlaich, M. P. Relevance of sympathetic nervous system activation in obesity and metabolic syndrome. *J. Diabetes Res.* **2015**, 2015, 1–11.

45. Lambert, E.; Straznicky, N.; Sari, C. I.; Eikelis, N.; Hering, D.; Head, G.; Dixon, J.; Esler, M.; Schlaich, M.; Lambert, G. Dyslipidemia is associated with sympathetic nervous activation and impaired endothelial function in young females. *Am. J. Hypertens.* **2013**, 26, 250–256.

46. Lymperopoulos, A.; Rengo, G.; Koch, W. J. Adrenergic nervous system in heart failure: Pathophysiology and therapy. *Circ. Res.* **2013**, 113, 739–753.

47. Park, S. Y.; Cho, Y. R.; Kim, H. J.; Higashimori, T.; Danton, C.; Lee, M. K.; Dey, A.; Rothermel, B.; Kim, Y. B.; Kalinowski, A.; Russell, K. S.; Kim, J. K. Unraveling the temporal pattern of diet-induced insulin resistance in individual organs and cardiac dysfunction in C57BL/6 mice. *Diabetes*. **2005**, 54, 3530–3540.

48. Mazumder, P. K.; O'Neill, B. T.; Roberts, M. W.; Buchanan, J.; Yun, U. J.; Cooksey, R. C.; Boudina, S.; Abel, E. D. Impaired cardiac efficiency and increased fatty acid oxidation in insulin-resistant ob/ob mouse hearts. *Diabetes*. **2004**, 53, 2366–2374.

49. Xu, B.; Li, J.; Gao, L.; Ferro, A. Nitric oxide-dependent vasodilatation of rabbit femoral artery by β_2-adrenergic stimulation or cyclic AMP elevation *in vivo*. *Br. J. Pharmacol.* **2000**, 129, 969–974.

50. Lu, Z.; Qu, P.; Xu, K.; Han, C. β-Adrenoceptors in Endothelium of Rabbit Coronary Artery and Alteration in Atherosclerosis. *Neurosignals*. **1995**, 4, 150–159.

51. Carroll, J. F.; Kyser, C. K.; Martin, M. M. β-adrenoceptor density and adenylyl cyclase activity in obese rabbit hearts. *Int. J. Obes.* **2002**, 26, 627–632.

52. Lima-Leopoldo, A. P.; Leopoldo, A. S.; Sugizaki, M. M.; Bruno, A.; Nascimento, A. F.; Luvizotto, R. A. M.; Junior, S. A. O.; Castardeli, E.; Padovani, C. R.; Cicogna, A. C. Myocardial dysfunction and abnormalities in intracellular calcium handling in obese rats. *Arq. Bras. Cardiol.* **2011**, 97, 232–240.

53. Lima-Leopoldo, A. P.; Leopoldo, A. S.; Da Silva, D. C. T.; Do Nascimento, A. F.; De Campos, D. H. S.; Luvizotto, R. A. M.; De Deus, A. F.; Freire, P. P.; Medeiros, A.; Okoshi, K.; Cicogna, A. C. Long-term obesity promotes alterations in diastolic function induced by reduction of phospholamban phosphorylation at serine-16 without affecting calcium handling. *J. Appl. Physiol.* **2014**, 117, 669–678.

54. Ferron, A. J. T.; Jacobsen, B. B.; Sant'Ana, P. G.; De Campos, D. H. S.; De Tomasi, L. C.; Luvizotto, R. D. A. M.; Cicogna, A. C.; Leopoldo, A. S.; Lima-Leopoldo, A. P. Cardiac dysfunction induced by obesity is not related to β-adrenergic system impairment at the receptor-signalling pathway. *PLoS One*. **2015**, 10, 1–18.

55. Kim, J. A.; Montagnani, M.; Kwang, K. K.; Quon, M. J. Reciprocal relationships between insulin resistance and endothelial dysfunction: Molecular and pathophysiological mechanisms. *Circulation*. **2006**, 113, 1888–1904.

56. Roberts, C. K.; Barnard, R. J.; Sindhu, R. K.; Jurczak, M.; Ehdaie, A.; Vaziri, N. D. A high-fat, refined-carbohydrate diet induces endothelial dysfunction and oxidant/antioxidant imbalance and depresses NOS protein expression. *J. Appl. Physiol.* **2005**, 98, 203–210.

57. Muniyappa, R.; Sowers, J. R. Role of insulin resistance in endothelial dysfunction. *Rev. Endocr. Metab. Disord.* **2013**, 14, 5–12.

58. Kim, J. A.; Jang, H. J.; Hwang, D. H. Toll-like receptor 4-induced endoplasmic reticulum stress contributes to impairment of vasodilator action of insulin. *Am. J. Physiol. - Endocrinol. Metab.* **2015**, 309, E767–E776.

59. DeBoer, M. P.; Meijet, R. I.; Wijnstok, N. J.; Jonk, A. M.; Houben, A. J.; Stehouwer, C. D.; Smulders, Y. M.; Eringa, E. C.; Serne, E. H. Microvascular Dysfunction: A Potential Mechanism in the Pathogenesis of Obesity-associated Insulin Resistance and Hypertension. *Microcirculation*. **2012**, 19, 5–18.

60. Kubota, T.; Kubota, N.; Kumagai, H.; Yamaguchi, S.; Kozono, H.; Takahashi, T.; Inoue, M.; Itoh, S.; Takamoto, I.; Sasako, T.; Kumagai, K.; Kawai, T.; Hashimoto, S.; Kobayashi, T.; Sato, M.; Tokuyama, K.; Nishimura, S.; Tsunoda, M.; Ide, T.; Murakami, K.; Yamazaki, T.; Ezaki, O.; Kawamura, K.; Masuda, H.; Moroi, M.; Sugi, K.; Oike, Y.; Shimokawa, H.; Yanagihara, N.; Tsutsui, M.; Terauchi, Y.; Tobe, K.; Nagai, R.; Kamata, K.; Inoue, K.; Kodama, T.; Ueki, K.; Kadowaki, T. Impaired insulin signaling in endothelial cells reduces insulin-induced glucose uptake by skeletal muscle. *Cell Metab.* **2011**, 13, 294–307.

61. Wang, P. X.; Deng, X. R.; Zhang, C. H.; Yuan, H. J. Gut microbiota and metabolic syndrome. *Chin. Med. J. (Engl).* **2020**, 133, 808–816.

62. Magne, F.; Gotteland, M.; Gauthier, L.; Zazueta, A.; Pesoa, S.; Navarrete, P.; Balamurugan, R. The firmicutes/bacteroidetes ratio: A relevant marker of gut dysbiosis in obese patients?. *Nutrients*. **2020**, 12, 1–17.

63. Le Chatelier, E.; Nielsen, T.; Qin, J.; Prifti, E.; Hildebrand, F.; Falony, G.; Almeida, M.; Arumugam, M.; Batto, J. M.; Kennedy, S.; Leonard, P.; Li, J.; Burgdorf, K.; Grarup, N.; Jørgensen, T.; Brandslund, I.; Nielsen, H. B.; Juncker, A. S.; Bertalan, M.; Levenez, F.; Pons, N.; Rasmussen, S.; Sunagawa, S.; Tap, J.; Tims, S.; Zoetendal, E. G.; Brunak, S.; Clément, K.; Doré, J.; Kleerebezem, M.; Kristiansen, K.; Renault, P.; Sicheritz-Ponten, T.; De Vos, W. M.; Zucker, J. D.; Raes, J.; Hansen, T.; Bork, P.; Wang, J.; Ehrlich, S. D.; Pedersen, O.; Guedon, E.; Delorme, C.; Layec, S.; Khaci, G.; Van De Guchte, M.; Vandemeulebrouck, G.; Jamet, A.; Dervyn, R.; Sanchez, N.; Maguin, E.; Haimet, F.; Winogradski, Y.; Cultrone, A.; Leclerc, M.; Juste, C.; Blottière, H.; Pelletier, E.; Lepaslier, D.; Artiguenave, F.; Bruls, T.; Weissenbach, J.; Turner, K.; Parkhill, J.; Antolin, M.; Manichanh, C.; Casellas, F.; Boruel, N.; Varela, E.; Torrejon, A.; Guarner, F.; Denariaz, G.; Derrien, M.; Van Hylckama Vlieg, J. E. T.; Veiga, P.; Oozeer, R.; Knol, J.; Rescigno, M.; Brechot, C.; M'Rini, C.; Mérieux, A.; Yamada, T. Richness of human gut microbiome correlates with metabolic markers. *Nature*. **2013**, 500, 541–546.

64. Turnbaugh, P. J.; Bäckhed, F.; Fulton, L.; Gordon, J. I. Diet-Induced Obesity Is Linked to Marked but Reversible Alterations in the Mouse Distal Gut Microbiome. *Cell Host Microbe*. **2008**, 3, 213–223.

65. Turnbaugh, P. J.; Ridaura, V. K.; Faith, J. J.; Rey, F. E.; Knight, R.; Gordon, J. I. The effect of diet on the human gut microbiome: A metagenomic analysis in humanized gnotobiotic mice. *Sci. Transl. Med.* **2009**, 1, 6ra14.

66. Horne, R. G.; Yu, Y.; Zhang, R.; Abdalqadir, N.; Rossi, L.; Surette, M.; Sherman, P. M.; Adeli, K. High fat-high fructose diet-induced changes in the gut microbiota associated with dyslipidemia in Syrian hamsters. *Nutrients*. **2020**, 12, 1–20.

67. Krajmalnik-Brown, R.; Ilhan, Z. E.; Kang, D. W.; DiBaise, J. K. Effects of gut microbes on nutrient absorption and energy regulation. *Nutr. Clin. Pract.* **2012**, 27, 201–214.

68. Lippert, K.; Kedenko, L.; Antonielli, L.; Kedenko, I.; Gemeier, C.; Leitner, M.; Kautzky-Willer, A.; Paulweber, B.; Hackl, E. Gut microbiota dysbiosis associated with glucose metabolism disorders and the metabolic syndrome in older adults. *Benef. Microbes*. **2017**, 8, 545–556.

69. Fu, J.; Bonder, M. J.; Cenit, M. C.; Tigchelaar, E. F.; Maatman, A.; Dekens, J. A. M.; Brandsma, E.; Marczynska, J.; Imhann, F.; Weersma, R. K.; Franke, L.; Poon, T. W.; Xavier, R. J.; Gevers, D.; Hofker, M. H.; Wijmenga, C.; Zhernakova, A. The gut microbiome contributes to a substantial proportion of the variation in blood lipids. *Circ. Res.* **2015**, 117, 817–824.

70. Zeng, Q.; Li, D.; He, Y.; Li, Y.; Yang, Z.; Zhao, X.; Liu, Y.; Wang, Y.; Sun, J.; Feng, X.; Wang, F.; Chen, J.; Zheng, Y.; Yang, Y.; Sun, X.; Xu, X.; Wang, D.; Kenney, T.; Jiang, Y.; Gu, H.; Li, Y.; Zhou, K.; Li, S.; Dai, W. Discrepant gut microbiota markers for the classification of obesity-related metabolic abnormalities. *Sci. Rep.* **2019**, 9, 1–10.

71. Ciubotaru, I.; Green, S. J.; Kukreja, S.; Barengolts, E. Significant differences in fecal microbiota are associated with various stages of glucose tolerance in African American male veterans. *Transl. Res.* **2015**, 166, 401–411.

72. Zhang, C.; Zhang, M.; Pang, X.; Zhao, Y.; Wang, L.; Zhao, L. Structural resilience of the gut microbiota in adult mice under high-fat dietary perturbations. *ISME J.* **2012**, 6, 1848–1857.

73. Do, M. H.; Lee, E.; Oh, M. J.; Kim, Y.; Park, H. Y. High-glucose or-fructose diet cause changes of the gut microbiota and metabolic disorders in mice without body weight change. *Nutrients*. **2018**, 10, 1–14.

74. Wang, Z.; Koonen, D.; Hofker, M.; Fu, J. Gut microbiome and lipid metabolism: From associations to mechanisms. *Curr. Opin. Lipidol.* **2016**, 27, 216–224.

Article 2

Effect of chronic mirabegron treatment on metabolic and cardiovascular parameters of WHHL rabbits with high-fructose high-fat diet-induced insulin resistance.

Michelle Moughaizel[1*], Elie Dagher[2], Nora Bouhsina[3], Valérie Lalanne[1], Chantal Thorin[1], Jean-Claude Desfontis[1] and Yassine Mallem[1]

[1] Nutrition, PathoPhysiology and Pharmacology (NP3) Unit, Oniris, Nantes Atlantic College of Veterinary Medicine, Food Science and Engineering, Nantes, France

[2] Laboniris, Oniris, Nantes Atlantic College of Veterinary Medicine, Food Science and Engineering, Nantes, France

[3] Department of Diagnostic Imaging, Oniris, Nantes Atlantic College of Veterinary Medicine, Food Science and Engineering, Nantes, France

* Correspondance:

Michelle Moughaizel

m_moughaizel@hotmail.com

Abstract

Background and aim: Metabolic syndrome (MetS) is a global health and economic burden. Finding a suitable pharmacological approach for managing this syndrome is crucial. We explored the therapeutic potential of mirabegron (MIR), a β_3-adrenoceptor (β_3-AR) agonist, as a repurposed agent for the treatment of MetS and its cardiovascular consequences.

Methods: Thirty Watanabe heritable hyperlipidemic rabbits (WHHL) were randomly assigned to control, high-fructose high-fat diet (HFFD) and HFFD+MIR groups that, respectively, received a chow diet, HFFD and HFFD with MIR treatment. The protocol lasted for 12 weeks, during which weight and abdominal circumference were monitored; plasma fasting levels of lipids, glucose and insulin were measured and an intravenous glucose tolerance test (IVGTT) was performed. Homeostasis model assessment of insulin resistance (HOMA-IR) was calculated. Cardiac function was evaluated using *in-vivo* and *ex-vivo* approaches. Vascular reactivity and arterial stiffness were assessed on isolated carotid arteries and by determining the pulse wave velocity, respectively.

Results: HFFD-fed rabbits exhibited a significant increase in fasting insulin, HOMA-IR, area under the curve of the IVGTT, triglycerides (TGs), total cholesterol, LDL-C and α_1-adrenoceptor sensitivity and a decrease in cardiac contractility compared to the control group. Treatment with MIR stabilized weight, abdominal circumference, fasting insulin, HOMA-IR and TG levels and significantly decreased α_1-adrenoceptor sensitivity and increased cardiac inotropy and lusitropy compared to the HFFD group.

Conclusion: Long-term treatment with MIR stabilized weight gain and TG levels, improved insulin sensitivity and enhanced cardiac and endothelial function of a rabbit animal model of combined dyslipidemia and IR.

Keywords: Metabolic syndrome, insulin resistance, dyslipidemia, Watanabe heritable hyperlipidemic rabbit, high-fructose high-fat diet, mirabegron.

Introduction

The metabolic syndrome (MetS) has become a global public health and economic burden due to its increased incidence and prevalence rates [1],[2]. The MetS, also known as the cardiometabolic syndrome, is a cluster of several risk factors that when combined increase the risk of an individual

developing cardiovascular disease [3]. It includes abdominal obesity, insulin resistance (IR), impaired glucose tolerance, arterial hypertension, and dyslipidemia [4]. Targeting each risk factor individually could not always be an effective treatment due to the multifactorial nature of this syndrome. The main underlying etiology of this syndrome includes increased energy intake and/or lack of physical activity and to a lesser extent, genetic predisposition [5]. Even though behavioral interventions such as lifestyle changes might be beneficial, these haven't always been successful, especially on a long-term basis [6]. Thus, a complementary suitable pharmacological approach should be implemented for best results in the prevention and or/curative management of this syndrome.

Cell signaling through the nitric oxide-soluble guanylyl cyclase-cyclic guanosine monophosphate (NO-sGC-cGMP) cascade has emerged as an appealing target in the treatment of metabolic and cardiovascular disease. This is mainly due to a growing body of evidence that have proven that pharmacological modulation of the NO-cGMP signaling could be effective, notably, in metabolic and cardiovascular disease contexts [7]–[9]. Mirabegron (MIR) has been classified as a β_3-AR agonist and has been food and drug administration (FDA)-approved for the treatment of overactive bladder [10]. In addition, β_3-ARs stimulation activates NOS-NO-sGC-cGMP pathway in the cardiovascular system leading to improved cardiac and vascular muscle relaxation and reduced tissue remodeling [11]. β_3-ARs agonism could also represent a novel potential strategy for treatment of metabolic diseases. This is mainly due to its ability to activate lipolysis in white adipocytes and thermogenesis in brown adipocytes and to improve insulin sensitivity and glucose tolerance in humans and rodents [12],[13]. Furthermore a selective β_3-AR agonist CL316,243 was shown to stimulate brown adipose tissue (BAT) activity, further preventing fat accumulation, improving dyslipidemia and attenuating the development of atherosclerosis [14].

Therefore, we hypothesized that chronic treatment with mirabegron, a β_3-AR agonist, might represent a promising pharmacological tool for treating the combination of two major components of the MetS, dyslipidemia and IR. Our aim was to investigate the ability of MIR to attenuate the metabolic disturbances associated with the dyslipidemia-IR combination, and thereby to prevent the development of metabolic and cardiovascular changes/consequences of the MetS. Our experimental protocol lasted for 12 weeks, during which Watanabe heritable hyperlipidemic

(WHHL) rabbits, animal model of spontaneous dyslipidemia, received a high-fructose high-fat diet (HFFD), known for its ability to induce IR [15].

Materials and methods

Experimental design

Thirty WHHL rabbits (male and female; 9-12 weeks of age) weighing 3.0-3.5 kg were used in all experiments. Rabbits were housed individually in a room maintained at constant temperature (21°C) and humidity (>45%), under a 12h dark/light cycle with free access to water and food. Rabbits were randomly divided into three groups: a control group (n=9), a HFFD group (n=12) and a HFFD+MIR group (n=9). These groups, respectively, received a standard chow diet (3410.PS.S10; SERLAB, France), a high-fructose high-fat diet (HFFD, SERLAB, France) and a HFFD along with oral administration of MIR (3mg/kg/d). The HFFD consisted of a chow diet, supplemented with 30 % fructose and 10 % coconut oil (91% saturated fatty acids).

All procedures were performed in accordance with the National Institute of Health Guide for the Use and Care of Laboratory Animals guidelines and they are all conducted with the approval of the institutional ethics Committee of Pays de la Loire, France (APAFIS n° 10722).

Morphological parameters

Weight and abdominal circumference were measured every two weeks to monitor the animal's weight gain and growth.

Measurement of plasma lipids, glucose and insulin levels

Blood withdrawal was performed after overnight fasting. Total cholesterol (TC), triglycerides (TG), free fatty acids (FFA) and high-density lipoprotein cholesterol (HDL-C) plasma levels were quantified, using enzymatic calorimetric kits, according to the supplier's instructions (DiaSys). Meanwhile, low-density lipoprotein cholesterol (LDL-C) levels were calculated using the Friedewald's equation [16]. For the quantitative determination of insulin plasma levels, we used a sensitive rabbit insulin ELISA kit sandwich assay (Crystal Chem High Performance Assays, USA).

Intravenous glucose tolerance test

An IVGTT was performed at the beginning and the end of the protocol, as previously described [17]. After an overnight fasting, rabbits were injected with an intravenous glucose solution (0.6 g/kg body weight). Then glucose measurements were performed before and 15, 30, 45, 60, 90 and 120 min after the glucose loading. Blood glucose was measured via a glucose meter (ONETOUCH®VERIO®; © 2012 LifeScan, Inc.), using one drop of whole blood. The area under the curve (AUC) was calculated using PRISM® software (version 8.0.1). Homeostasis Model Assessment of basal Insulin Resistance (HOMA-IR) was calculated using the following equation: [(fasting plasma glucose (mmol/l) x fasting plasma insulin (µU/ml))/22.5] [18].

Pulse wave velocity

To assess the arterial stiffness, two sets of pulse wave velocity (PWV) measurements were performed, one at the beginning and another, at the 12^{th} week of the protocol. Two piezoelectric sensors (ADInstruments) were placed, one on the auricular artery and another on the caudal one, of conscious animals. Recordings of pulse waves were made during 10 min with the software (ADInstruments LabChart v8.1.5). The measurement point (the foot of each pulse wave) was determined using the second derivative of the pulse wave signal. Both the distance between the two sensors and that between the auricular artery and the sternal manubrium, were noted each time. Then, the Δx was calculated by substracting the two distances. The time interval (Δt) between the foot of the auricular waveform and that of the caudal waveform was measured by the software. The PWV was calculated using the formula PWV ($m.s^{-1}$) = $\Delta x/\Delta t$ [19].

Echocardiographic measurements of cardiac function

To assess *in vivo* cardiac geometry and left ventricular (LV) global systolic function, transthoracic echocardiography (TTE) was performed on conscious animals, at both baseline and at the end of experimental protocol (12^{th} week). A high frequency ultrasound imaging system (Esaote Mylab 70 XVG, 9 MHz microconvex transducer) was used to record both two-dimensional and Motion mode (M-mode) imaging. The left ventricular end-diastolic diameter (LVEDd), left ventricular end-systolic diameter (LVESd) left ventricular fractional shortening (LVFS), left ejection fraction (LVEF), interventricular septal thickness (IVS) and left ventricular posterior wall thickness

(LVPW) were determined using through a right parasternal short axis view of the heart. FS and EF were respectively calculated using the formulas LVFS = [(LVIDd − LVIDs)/ LVIDd] × 100 and EF = [(LVEDV − LVESV)/ LVEDV] × 100. Two consecutive heart cycles were measured and the average was used for analysis. Using Doppler imaging, color-flow mapping mode, the pulmonary and aortic flow were determined, through a short axis-right parasternal and left long axis- five chambers approaches, respectively (Esaote Mylab 70 XVG, 8 MHz sector transducer).

Isolated Langendorff heart preparation

Animals were anaesthetized with an intravenous Sodium Pentobarbital (40 mg/kg). The animal was sacrificed by exsanguinating the abdominal aorta. The heart was rapidly excised and transferred into ice-cold filtered (using a filter funnel) Krebs' solution. The latter, contained (mM): NaCl 118.3, $NaHCO_3$ 20.0, KCl 4.7, $MgSO_47H_2O$ 1.2, KH_2PO4 1.2, glucose 11.1, EDTA 0.016 and $CaCl_2$ 2.5. Afterwards, the heart was cannulated (4 mm aortic cannula, ADinstruments, France) and perfused at a constant flow-rate (22-28 mL/min) with a Krebs solution that is constantly bubbled with 95% O2 and 5% CO2 at 37 °C. The left ventricular pressure (*LVP*) and the perfusion pressure (*PP*), indexes of cardiac contractility and coronary vasodilation, respectively, were recorded using pressure transducers. After stabilization of the heart, non-cumulative concentration-response curves to isoproterenol (10^{-9} to 10^{-6} M), a nonselective β-AR agonist, were built. Left ventricular pressure (*LVP*), coronary perfusion pressure (*PP*), the first derivative of the left ventricular pressure in systole (*dP/dTmax*) (maximum contraction velocity) and first derivative of the left ventricular pressure in diastole (*dP/dTmin*) (maximum relaxation velocities) were measured. The left ventricular developed pressure (*LVDevP*) was calculated as the difference between left ventricular systolic pressure and left ventricular end-diastolic pressure. Data acquisition and recording were achieved using Powerlab 8/35 and LabChart 7.0 software (ADInstruments, France).

Vascular reactivity

Immediately after animal sacrifice by exsanguination the carotid artery was removed, dissected free of fat and connective tissue and placed in a cold Krebs' solution (see composition above). The artery was cut into 5mm ring segments that were mounted on triangular wire supports and suspended in 10 mL organ baths containing Krebs' solution, maintained at 37°C, and gassed with

95% O_2 and 5% CO_2. Isometric tension was continuously measured using a computerized automated isometric transducer system (EMKAbath4, EMKA technologies, France) and recorded with a data acquisition software (iox version 2.9.5.20). The segments were initially loaded to a 2 g tension and allowed to equilibrate for 60 minutes. Then cumulative concentration-response curves (CCRCs) to phenylephrine (Phe), an α_1-adrenoceptor agonist (10^{-9} to 3.10^{-5} M), acetylcholine (Ach), a muscarinic receptor agonist (10^{-9} to 3.10^{-5} M), sodium nitroprusside (SNP), an NO donor (10^{-10} to 3.10^{-5} M) and insulin (Ins) (10^{-9} to 3.10^{-6} M) were constructed. The CCRCs to Ach, SNP and Ins were built on the Phe pre-contracted rings. The calculated contraction and relaxation percentages are relative to the maximal the pre-contraction produced by KCL and Phe, respectively.

Histology and Immunohistochemistry

We evaluated the effect of HFFD on the development and evolution of atherosclerosis in Watanabe rabbits. Samples from the aortic arch were fixed by immersion in neutrally buffered 10% formalin and then dehydrated and paraffin embedded. Then, serial 4µm thick sections were routinely cut and stained.

For histological analysis of thoracic aorta, sections were stained with hematoxylin and eosin, safranin (HES). Green Masson's trichrome and Orceine stains were used to assess collagen and elastic fibers, respectively. The lesions were evaluated under light microscope. In order to study the cellular components of the thoracic aorta, automated immunohistochemistry (Benchmark XT, Ventana Medical Systems, Roche Diagnostics) was performed. The detection systems were the iView DAB detection kit (Ventana Medical Systems, Roche Diagnostics, 760-091) (Other sections were immunohistochemically stained with macrophage antibody (clone RAM11, mouse monoclonal, 1:1200 dilution, Dako Corp, USA) and α-smooth muscle actin antibody (clone HHF35, mouse monoclonal, 1:50 dilution, Dako Corp, USA), two monoclonal antibodies that detect macrophages (Mφ) and smooth muscle cells (SMCs), respectively.

Using an image analysis system (FIJI), the extent of atherosclerotic lesions in the aorta was expressed as a percentage of the lesion area and the degree of intimal thickening. For determination of average intima thickening, the following equation was used: area of intimal lesion/length of media. The same software was also used for the quantification of elastin fibers, macrophages and

SMCs, which was performed by calculating the percentage of immunostaining in lesion area. Conversely, collagen could not be quantified using the same software. Therefore, a semi-quantification was performed microscopically.

Lesions were classified by a certified veterinary pathologist, according to the guidelines of the American Heart Association [20]. According to their classification:

- Type I (initial) lesion contain atherogenic lipoprotein that elicit an increase in macrophages numbers and scattered macrophage foam cell formation,

- Type II lesions consist of layers of macrophage foam cells and lipid-laden smooth muscle cells and comprise lesions grossly designated as fatty streaks,

- Type III lesions are the intermediate stage between type II and IV lesions (atheroma). In addition to the lipid-laden cells present in type II lesions, type III lesions contain scattered collections of extracellular lipid droplets and particles,

- Type IV lesions contain larger, confluent, and more disruptive core of extracellular lipid,

- Lesions comprising a lipid core might also contain thick layers of fibrous connective tissue characterizing type V lesions and/or fissure, hematoma, and thrombus characterizing type VI lesion.

In addition, the presence of extracellular lipid, fibrous cap, mineralization, lipid core and collagen's deposition (using green Masson's trichrome stain) were graded using a semi-quantitative scale from 0 to 4 in order to be able to better characterize the different types of plaques [31]. In order to compare the stage of lesions type II and III plaques were classified as early lesions whereas type IV and V plaques were classified as advanced lesions.

Tissue cGMP quantification

cGMP was quantified in thoracic aorta rings, heart tissue and epididymal/ovarian fat. Immediately after animal sacrifice, samples were collected, immerged in liquid nitrogen and then stored at -80°C. The day of analysis, cGMP concentrations were measured using a colorimetric enzyme immunoassay kit (Cayman Chemical Company). The absorbance of each sample was read at 405 nm using a microplate reader. The cGMP value was calculated related to the total cell protein

concentrations previously measured using a protein assay reagent kit (micro-BCA, Pierce Biotechnology, Rockford, USA).

Plasma inflammatory cytokines and total antioxidant status

Plasma tumor necrosis factor-alpha (TNF-α) and interleukin-6 (IL-6) were measured using ELISA kits according to the manufacturer's instructions (DuoSet® ELISA kit, TNF-α/IL-6**,** R&D Systems Europe Ltd). Plasma total antioxidant status (TAS) was quantified using a colorimetric kit (TAS kit, Randox laboratories Ltd).

Statistical analyses

Data were expressed as a mean ± SEM. All graphs have been performed using PRISM® software (version 8.0.1). We used repeated measures two-way ANOVA, mixed effects analysis for multiple group comparisons (biochemical parameters and PWV measurements) and one-way ANOVA for cGMP analysis. R software was used to evaluate data from non-cumulative concentration response curves (isolated heart and CCRC to insulin) by a linear mixed effect (LME) model. Relaxation was expressed as the percentage relaxation of the phenylephrine-induced precontraction. CCRCs to Ach were compared using a non-linear mixed effect model (NLME) [21], also using R software. The efficacy (E_{max}) and the potency (pD_2) representing the maximum effects and the negative logarithm of the concentration producing 50% of the maximum effect, respectively were determined for each CCRC [21]. Chi square test was used for analyzing the classification of atheroma plaques. A *p* value of less than 0.05 was considered statistically significant for all results.

Results

Effect of HFFD and treatment with Mirabegron on weight and abdominal circumference

After 12 weeks of the protocol, the body weight similarly increased in both the control and HFFD groups. This increase was significant in control (12^{th} week vs. Baseline, $p<0.0001$) and HFFD (12^{th} week vs. Baseline, $p=0.0042$) groups but not in HFFD+MIR-treated group. The same pattern was observed in abdominal circumference comparisons. After 12 weeks of protocol, similar increases were witnessed in the control and HFFD. The increase was significant in control (12^{th} week vs.

Baseline, p<0.0001) and HFFD (12th week vs. Baseline, p<0.0001) groups but not in the HFFD+MIR-treated group (Table1).

Table 1. Results of weight, abdominal circumference, glycaemia, insulin and plasma lipids

Measurements	Groups					
	Control (n=9)		HFFD (n=12)		HFFD+MIR (n=9)	
	Baseline	12th week	Baseline	12th week	Baseline	12th week
Weight (Kg)	2 ± 0.1	2.97 ± 0.1 $\$\$\$\$$	2.3 ± 0.05	2.7 ± 0.12 $\$\$$	3.07 ± 0.17	3.1 ± 0.16
Abdominal circumference (cm)	31.78 ± 1.2	38.78 ± 0.76 $\$\$\$\$$	31.81 ± 0.88	36.45 ± 0.62 $\$\$\$\$$	36.11 ± 0.89	35.66 ± 0.91
Fasting glycaemia (mg/dl)	98 ± 1.88	96 ± 3.06	101 ± 6.6	106 ± 7.54	96.67 ± 4.51	98.33 ± 2.95
Fasting insulinemia (ng/ml)	0.37 ± 0.08	0.31 ± 0.07	0.3 ± 0.04	1.15 ± 0.45 $\$$ *	0.59 ± 0.12	0.44 ± 0.07
Triglycerides(g/L)	1.4 ± 0.3	1.75 ± 0.35	1.76 ± 0.3	2.65 ± 0.39 $\$$	2 ± 0.34	2.12 ± 0.26
TC (g/L)	6.72 ± 0.5	6.53 ± 0.8	7.4 ± 0.5	11.05 ± 0.88 $\$\$$ ***	7.77 ± 0.8	10.8 ± 0.8 $\$\$$ ***
HDL-C (g/L)	0.21 ± 0.03	0.22 ± 0.03	0.19 ± 0.02	0.26 ± 0.03	0.2 ± 0.03	0.17 ± 0.016
LDL-C (g/L)	6.23 ± 0.45	5.96 ± 0.7	6.87 ± 0.5	10.25 ± 0.85 $\$\$$ ***	6.85 ± 0.75	9.75 ± 0.67 $\$\$$ **
FFA (mmol/L)	0.83 ± 0.2	0.65 ± 0.1	1.02 ± 0.21	0.70 ± 0.11	1 ± 0.2	0.82 ± 0.1

TC = total cholesterol, HDL-C = high-density lipoprotein cholesterol, LDL-C = low-density lipoprotein cholesterol, FFA = free fatty acids. Data are expressed as mean ± SEM. A two-way ANOVA test was used for statistical analysis. **** p<0.0001, *** p< 0.001, ** p< 0.01 and * p< 0.05 for HFFD or HFFD+MIR vs. the Control group. $\$\$\$\$ p<0.0001, $\$\$\$ p<0.001, $\$\$ p< 0.01 and $\$ p<0.05 12th week vs. Baseline of the protocol.

Effect of HFFD and treatment with mirabegron on glucose and insulin levels

Our data showed that basal insulinemia significantly increased in the HFFD group (12th week vs. Baseline, p=0.0133) and when comparing the HFFD to the control group at the 12th week

(p=0.0176) but did not change in the HFFD+MIR compared to the control group. We observed no change in the fasting glycaemia **(Table1)**.

Effect of HFFD on lipid profiles

We further examined modifications in lipid profiles **(Table 1)**. We found a significant increase in TC when comparing the 12th week to the baseline levels of both HFFD and HFFD+MIR groups (p=0.0072 and p=0.004, respectively) and when also comparing each of the HFFD and HFFD+MIR to the control group at the end of the protocol (p=0.0002 and p=0.0007, respectively). Similarly, we found a significant increase in LDL-C when comparing the 12th week to the baseline levels of both HFFD and HFFD+MIR groups (p=0.0086 and p=0.0057, respectively) and when also comparing each of the HFFD and HFFD+MIR to the control group at the end of the protocol (p=0.0001 and p=0.0014, respectively). TG levels were significantly increased in the HFFD group when comparing the 12th week to the baseline levels (p=0.0389) but did not change in control nor in MIR-treated groups. Meanwhile, no increase was found in HDL nor in FFAs neither when comparing the 12th week to the baseline levels nor when comparing each of the HFFD and HFFD+MIR to the control group, at the end of the protocol **(Table 1)**.

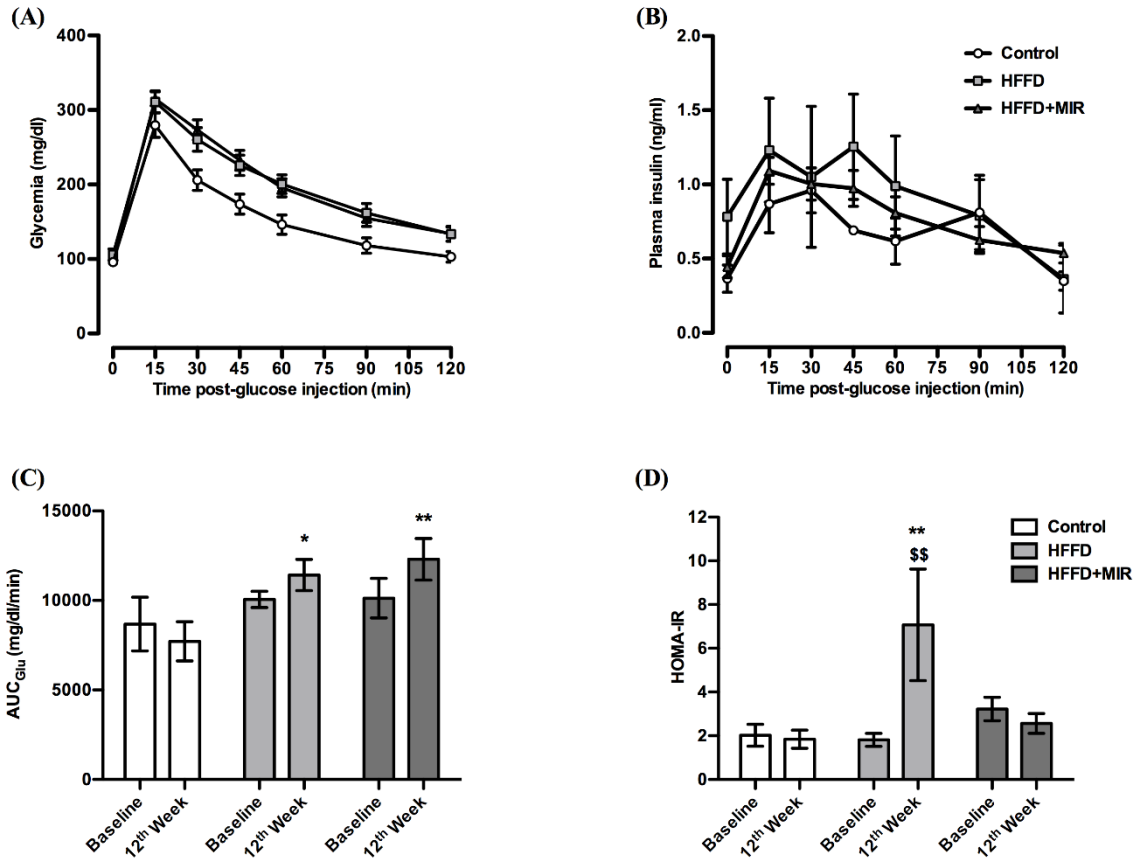

Figure 1. Effect of HFFD feeding and long-term treatment with mirabegron on glucose and insulin metabolism. Glucose metabolism was evaluated by an IVGTT, performed at the end of the protocol. After a glucose bolus, both plasma glucose (A) and insulin levels (B) were measured. AUC_{Glu} from the IVGTT was calculated (C). Insulin metabolism was assessed by calculating the Homeostasis model assessment of insulin resistance (HOMA-IR) (D). Data were expressed as the mean ± SEM. A two-way Anova test was used for statistical analysis. n=9 for Control, n=12 for HFFD and n=9 for HFFD+MIR. ** $p< 0.01$ and * $p< 0.05$ for HFFD vs. Control group. $$ $p< 0.01$ and $ $p<0.05$ 12th week vs. Baseline.

The AUC_{Glu} from the IVGTT significantly increased when comparing the HFFD and the HFFD+MIR to the control group at the end of the protocol (p=0.0205 and p=0.0069, respectively). The glycaemia 2h post glucose injection also significantly increased at the 12th week, in both the HFFD and the HFFD+MIR (p=0.0204 and p= 0.0289, respectively) compared to the control group Meanwhile, we found no difference when comparing the AUC_{Ins} of all groups. On the other hand, HOMA-IR significantly increased amongst individuals of HFFD group (12th week vs. Baseline, p=0.0059) and when comparing both the HFFD and control groups at the 12th week (p=0.0078);

however, no change was observed amongst individuals of the HFFD+MIR (12th week vs. Baseline) nor when compared to the control group **(Figure 1)**.

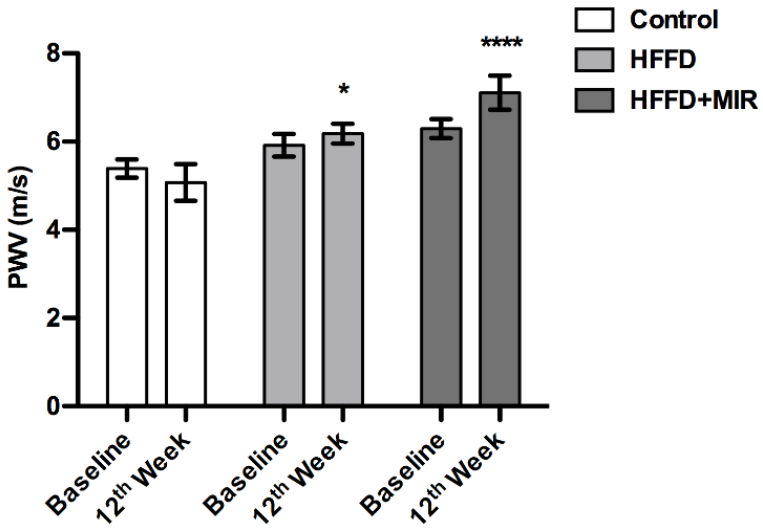

Figure 2. Effect of the HFFD and treatment with mirabegron on the aortic elasticity. The PWV was measured at the beginning and end of the protocol in order to assess the arterial vascular elasticity. It was calculated using the following formula: PWV (m/s) = $\Delta x/\Delta t$. Data are expressed as mean ± SEM. Repeated measures two-way Anova test was used for statistical analysis. n=9 for control, n=12 for HFFD and n=9 for HFFD+MIR. * $p<0.05$, **** $p<0.0001$ vs. Control.

Pulse wave velocity measurements were performed to functionally assess the aortic stiffness. Statistical analysis showed a significant difference between the control and HFFD group and between the control and HFFD+MIR group, specifically at the end of the protocol (12th week, $p=0.0154$, $p<0.0001$) **(Figure 2)**.

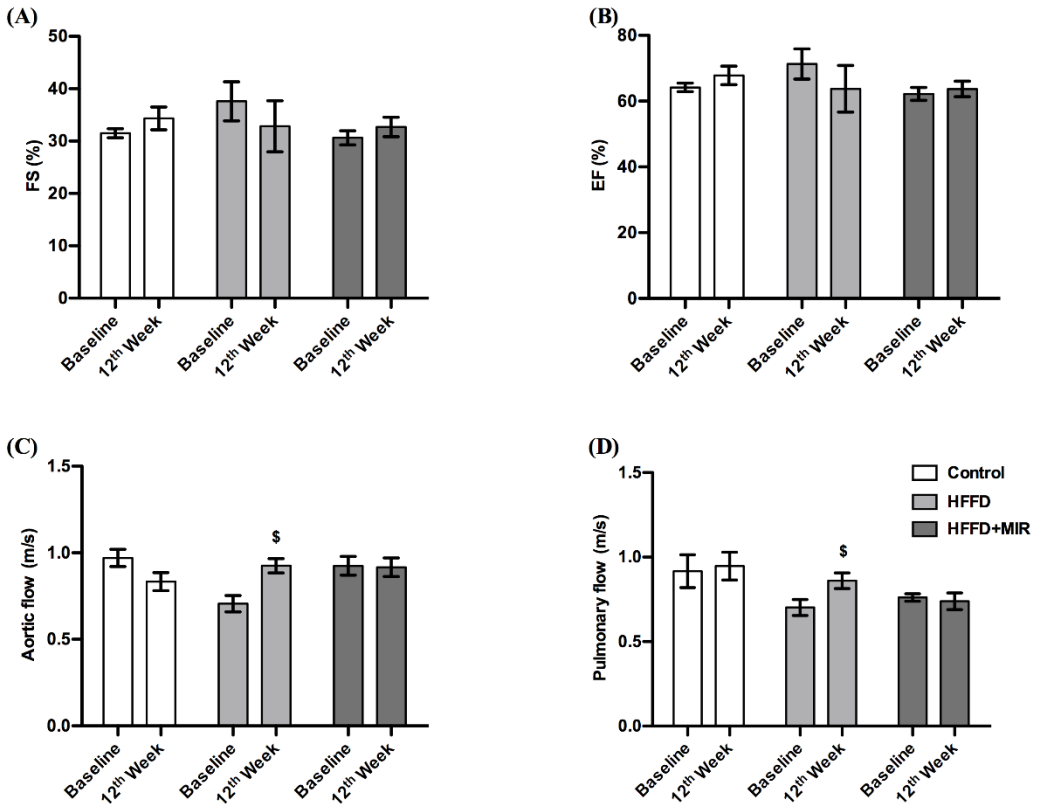

Figure 3. Effect of HFFD and treatment with mirabegron on LV systolic function, blood flow and LV dilation. Fractional shortening (A), ejection fraction (B), aortic flow (C), pulmonary flow (D). Values are expressed as mean ± SEM. a two-way Anova test was used for statistical analysis. n=3 for Control, n=6 for HFFD and n=9 for HFFD+MIR. $ $p<0.05$ 12th week vs. Baseline.

To evaluate the effect of HFFD-feeding and long-term treatment with mirabegron on cardiac contractility, we performed echocardiography **(Figure 3)**. Data indicated no modification in EF and FS nor in end-systolic and end-diastolic diameters (data not shown) indicating no change in LV systolic function nor in LV dilation. Conversely, the pulmonary and aortic flow velocities were both significantly increased in the HFFD group (12th week vs. Baseline, p=0.022 and p=0.0163, respectively) but remained unchanged in the control and mirabegron-treated group.

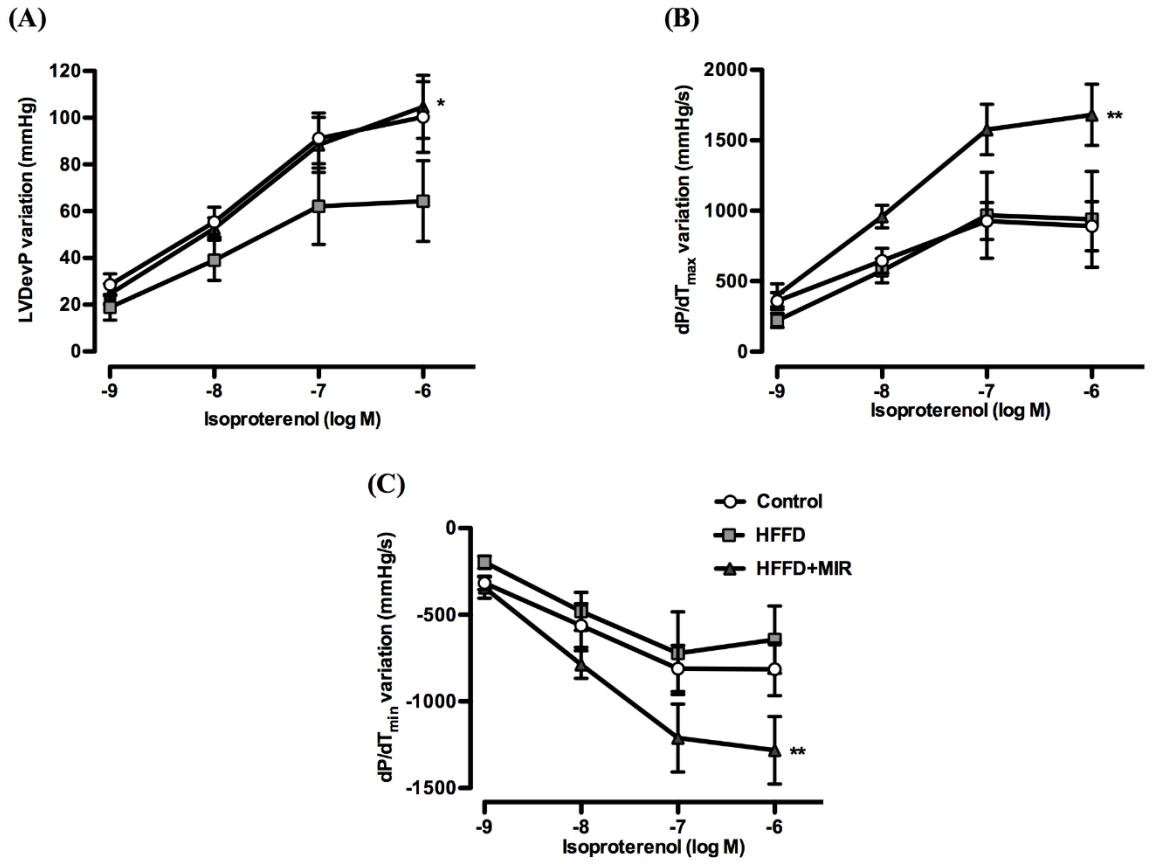

Figure 4. Cardiac parameters were assessed after ß-adrenoceptor stimulation by building non-cumulative concentration response-curves to isoproterenol (10^{-9} to 10^{-6}). The LVDevP (A) and dP/dT_{max} (B), reflecting cardiac inotropy and dP/dT_{min} (C), reflecting cardiac lusitropy, were evaluated. Data are represented as mean ± SEM. n=6 for Control, n=6 for HFFD and n=6 for HFFD+MIR. * $p<0.05$, ** $p<0.01$ vs. HFFD and determined using LME.

To determine the effects of β-AR stimulation on cardiac contractility and relaxation, non-cumulative concentration response-curves to isoproterenol were constructed **(Figure 4)**. The LVDevP was decreased in the HFFD group compared to the control group and significantly increased in the HFFD+MIR-treated group compared to the HFFD-fed group ($p= 0.0179$) but not to the control group. This suggests an alteration of the β-AR-mediated response due to HFFD-feeding that was counteracted in response to long-term treatment with mirabegron. Meanwhile the dP/dT_{max} and dP/dT_{min} were not affected in response to the HFFD-feeding but both significantly increased in the HFFD+MIR compared to the HFFD group ($p=0.0049$ and $p=0.0039$, respectively). This indicates that treatment with mirabegron prevented the decrease of the LVdevP and

ameliorated both the contraction (dP/dT_{max}) and relaxation (dP/dT_{min}) rates. In terms of coronary vasodilation, no change was observed (data not shown).

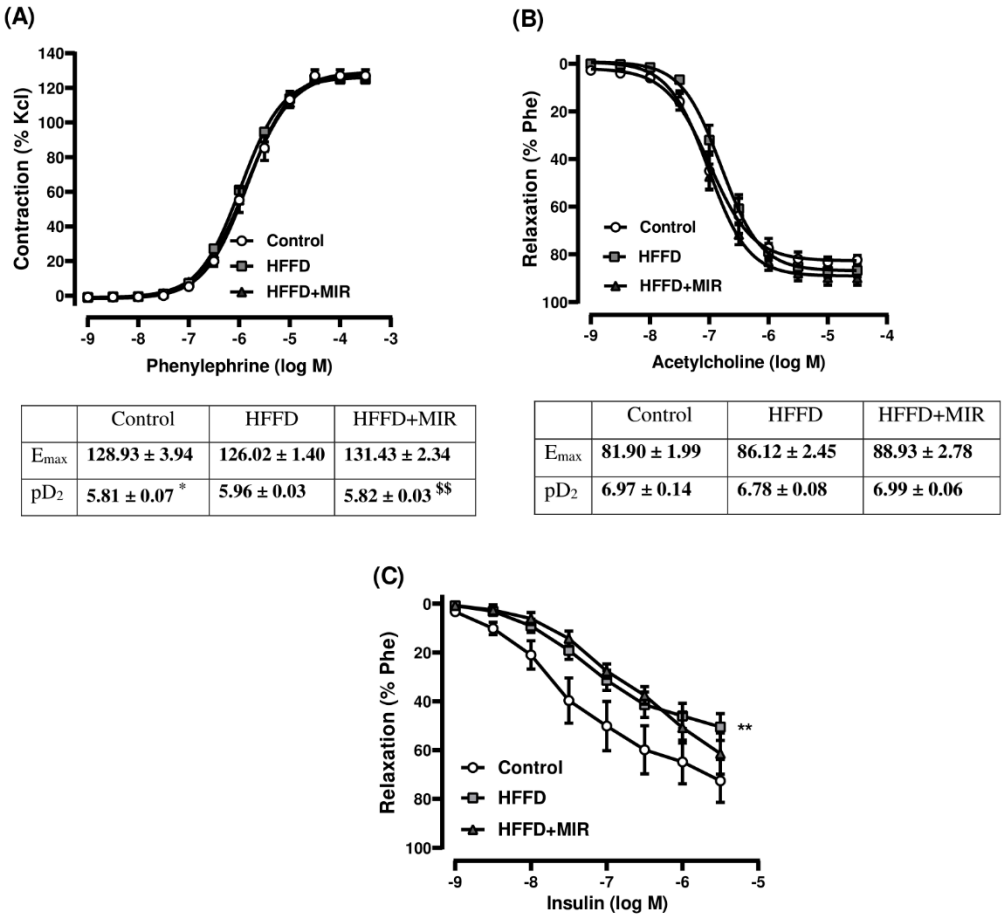

	Control	HFFD	HFFD+MIR
E_{max}	**128.93 ± 3.94**	**126.02 ± 1.40**	**131.43 ± 2.34**
pD_2	**5.81 ± 0.07** *	**5.96 ± 0.03**	**5.82 ± 0.03** $$

	Control	HFFD	HFFD+MIR
E_{max}	**81.90 ± 1.99**	**86.12 ± 2.45**	**88.93 ± 2.78**
pD_2	**6.97 ± 0.14**	**6.78 ± 0.08**	**6.99 ± 0.06**

Figure 5. Effect of HFFD feeding and treatment with mirabegron on carotid vasoreactivity. CCRCs were built to evaluate the carotid contractile using phenylephrine (Phe, 10^{-10} to 3.10^{-5}) (A) and relaxation responses using acetylcholine (Ach, 10^{-9} to 3.10^{-5} M) (B) and insulin (Ins, 10^{-9} to 3.10^{-6} M) (C). The calculated contraction and relaxation percentages are relative to the maximal changes from the pre-contraction produced by KCL and Phe, respectively. Data are expressed as mean ± SEM and determined using NLME for Phe and Ach and LME for Ins. n=9 for Control, n=12 for HFFD and n=9 for HFFD+MIR. * p<0.05, **< 0.01 Control vs. HFFD; $ p<0.05 HFFD+MIR vs. HFFD

To assess the carotid reactivity, CCRCs were built **(Figure 5)**. Even though there was no change in the Phe-induced maximal contractile response (E_{max}); the CCRC significantly shifted to the left (significantly higher pD_2, p=0.019) in the HFFD compared to the control group. Indicating a higher α_1-AR sensitivity. Meanwhile treatment with mirabegron prevented this shift. The pD_2 was

significantly lower in the HFFD+MIR group compared the HFFD group (p=0.0069). We observed no difference neither in the maximal response nor in pD_2 values corresponding to the Ach curves. However, the HFFD group showed a significantly lower Ins-induced vasorelaxation (p=0.001 vs. control). Moreover, an increasing trend in Ins-mediated vasorelaxation was observed in response to treatment with mirabegron (p=0.08 vs. HFFD).

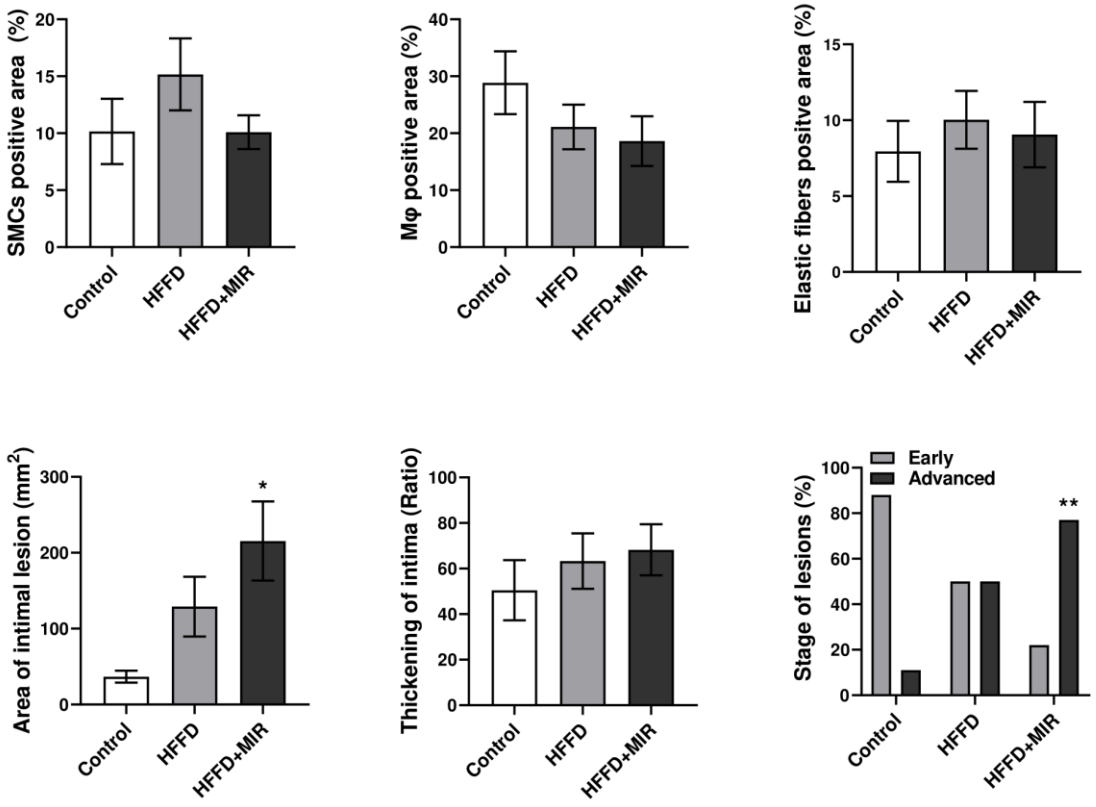

Figure 6. Quantification of aortic atherosclerosis, 12 weeks after HFFD feeding and treatment with mirabegron. Data in all graphs are represented as the mean ± SEM except for the stage of lesions, which was expressed in percentages. Statistical analysis was performed using one-way Anova for all parameters except for stage of lesions, for which a Chi square test was used. n=9 for Control, n=12 for HFFD and n=9 for HFFD+MIR. * p<0.05, ** p<0.01 HFFD+MIR vs. Control.

No difference between groups was observed regarding the average thickening of the intima (Area of intimal lesion/length of media). The area of intimal lesion increased in both the HFFD and the HFFD+MIR groups compared to the control group. However, the increase was only significant in the HFFD+MIR (p=0.0237 vs. Control). SMCs (evaluated using an anti-HHF35 antibody), Mφ (evaluated using an anti-RAM11 antibody) and elastic fibers (evaluated using the Orceine stain)

were not significantly different neither when comparing the HFFD to the control group nor when comparing the HFFD+MIR to the HFFD group. When comparing early versus advanced lesions, the difference was only significant in the HFFD+MIR (p=0.0044 vs. Control). Nevertheless, we also observed a clear trend towards advanced lesions in the HFFD (p=0.0614 vs. Control) **(Figure 6)**.

Table 2. Classification of atheroma plaques.

Histologic parameter evaluated	**Classification**	**Control (n=9)**	**HFFD (n=12)**	**HFFD+MIR (n=9)**	***p* value Control vs. HFFD**	***p* value HFFD+MIR vs. HFFD**
Extracellular lipids	Absence	3 (33.3%)	4 (33.3%)	1 (11.1%)	0.0567	0.4691
	Grade 1	5 (55.6%)	1 (8.3%)	0		
	Grade 2	1 (11.1%)	3 (25.0%)	3 (33.3%)		
	Grade 3	0	4 (33.3%)	5 (55.6%)		
	Grade 4	0	0	0		
Fibrous cap	Absence	7 (77.8%)	6 (50.0%)	2 (22.2%)	0.0502	0.19
	Grade 1	2 (22.2%)	0	2 (22.2%)		
	Grade 2	0	5 (41.7%)	5 (55.6%)		
	Grade 3	0	1 (8.3%)	0		
	Grade 4	0	0	0		
Mineralization	Absence	8 (88.9%)	9 (75.0%)	3 (33.3%)	0.43	0.1252
	Grade 1	1 (11.1%)	3 (25.0%)	5 (55.6%)		
	Grade 2	0	0	0		
	Grade 3	0	0	1 (11.1%)		
	Grade 4	0	0	0		
Lipid core	Absence	6 (66.7%)	5 (41.7%)	2 (22.2%)	0.2753	0.7223
	Grade 1	2 (22.2%)	1 (8.3%)	1 (11.1%)		
	Grade 2	1 (11.1%)	4 (33.3%)	5 (55.6%)		

	Grade 3	0	2 (16.7%)	1 (11.1%)		
	Grade 4	0	0	0		
Collagen deposition	Absence	1 (11.1%)	0	0	0.1888	0.2338
	Grade 1	1 (11.1%)	0	1 (11.1%)		
	Grade 2	4 (44.4%)	2 (16.7%)	1 (11.1%)		
	Grade 3	2 (22.2%)	7 (58.3%)	2 (22.2%)		
	Grade 4	1 (11.1%)	3 (25.0%)	5 (55.6%)		
Type of plaque	No plaque	1 (11.1%)	0	0	0.09	0.4299
	Type II	4 (44.4%)	4 (33.3%)	1 (11.1%)		
	Type III	3 (33.3%)	2 (16.7%)	1 (11.1%)		
	Type IV	1 (11.1%)	0	1 (11.1%)		
	Type V	0	6 (50.0%)	6 (66.7%)		

The presence of extracellular lipid, fibrous cap, mineralization, lipid core and collagen's deposition (using green Masson's trichrome stain) were graded using a semi-quantitative scale from 0 to 4. Type of plaques were classified according to the guidelines of the American Heart Association. The results were expressed as frequency and percentage. Statistical analysis was performed using a Chi-square test.

Extracellular lipid deposition and Fibrous cap presence were almost significantly increased (p=0.0567 and p=0.0502, respectively) in the HFFD group compared to the control group. No significant difference was observed in terms of extent of mineralization, lipid core severity collagen deposition between the HFFD group and the control group. Nevertheless, frequency of marked and severe collagen deposition was higher in HFFD than in control group. Additionally, more advanced grades were observed in the HFFD group. Regarding the type of plaques, most of the plaques in the control group were either type II (4/9) or type III (3/9) with no type V. In contrast, in the HFFD group, 50% of the plaques (6/12) were type V plaques. In the current study, only type II, III, IV and V lesions were observed. There was no significant difference between the HFFD group and the mirabegron-treated group in regards to extracellular lipid deposits, fibrous cap presence, the extent of mineralization, lipid core presence and severity, collagen deposition and plaque types **(Table 2)**.

Table 3. cGMP levels determination in thoracic aorta, heart and adipose tissue.

	Groups		
cGMP	Control (n=9)	HFFD (n=12)	HFFD+MIR (n=9)
Thoracic aorta (pmol/mg of protein)	3.27 ± 1.07	5.69 ± 1.58	1.56 ± 0.21
Heart tissue (pmol/mg of protein)	1.34 ± 0.30	1.79 ± 0.35	1.42 ± 0.26
Adipose tissue (fmol/mg of protein)	0.0506 ± 0.0050	0.0465 ± 0.0089	0.0457 ± 0.0848

Data are expressed as mean ± SEM. One-way ANOVA test was used for statistical analysis.

cGMP intracellular concentrations were determined in thoracic aorta, heart and adipose tissue samples. No difference between the groups was observed (**Table 3**).

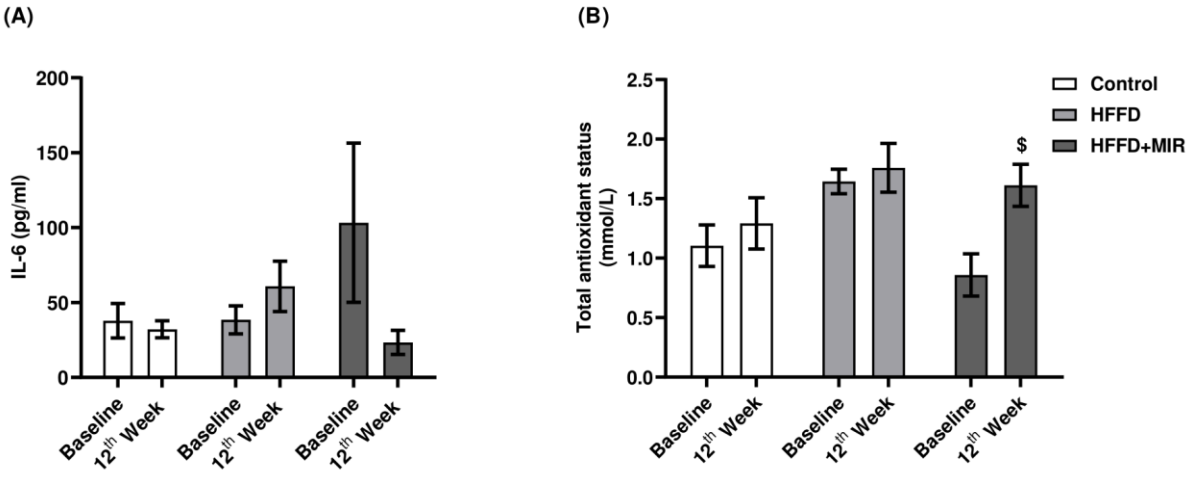

Figure 7. Interleukin-6 (A) and total antioxidant status (B) measurements. Data are expressed as mean ± SEM. A two-way Anova test was used for statistical analysis. n=9 for Control, n=12 for HFFD and n=9 for HFFD+MIR. $ $p<0.05$ 12^{th} Week vs. Baseline.

We assessed the levels of interleukin-6 (IL-6), a main inflammatory cytokine. We also measured the total antioxidant status (TAS). Even though, we observed a strong decline in the Il-6 concentrations of the mirabegron-treated group, this decrease was not statistically significant.

Meanwhile, the TAS level significantly increased in the mirabegron treated group ($p=0.0127$, 12^{th} week vs. Baseline) **(Figure 7**).

Discussion

In the current study, we investigated whether chronic treatment with mirabegron would counteract or prevent metabolic and cardiovascular disturbances that are associated with the combination of two main components of the MetS, dyslipidemia-IR. We were able to produce this combination by feeding a HFFD (to induce IR), to a spontaneously dyslipidaemic rabbit model. Our purpose was to induce IR rather than obesity, which might be a confounding factor. Thus we used a HFFD that, compared to the standard chow, is rich in sugar and fat but contains less protein and fibers [15]. To our knowledge, most of studies that intended to explore MIR as a treatment for metabolic disease were either performed on rodents or on humans but not on rabbits.

We showed that, after 12 weeks of HFFD feeding, WHHL rabbits exhibited increased fasting insulin levels, HOMA-IR, TG and cholesterol (TC and LDL-C) levels as well as impaired glucose tolerance, compared to their counterparts in the control group. We were also able to show that 12 weeks of MIR treatment exhibited global improvement of the metabolic status and cardiovascular function of these rabbits.

Both weight and abdominal circumference similarly increased in the HFFD and control groups. Therefore, this increase is probably not related to the HFFD-feeding, which might be explained by the fact that the HFFD that we used is rich in fat and sugar but with less protein and fibers. Whereas treatment with MIR along with HFFD-feeding did not lead to any increase in weight nor in abdominal circumference, suggesting that MIR prevented this increase. These results are in consistence with several studies that demonstrated that β_3-AR agonists decrease weigh gain [22],[23]. Meanwhile, both CL-316,243 and MIR have been found to increase lipolysis in white adipose tissue (WAT) and thermogenesis in BAT leading to increased energy expenditure (EE) [24],[25]. Berbeé et al. proposed that β_3-AR-stimulation reduces weight gain, through activation of uncoupling-protein 1 (UCP1) of BAT, which induces lipolysis and thermogenesis leading to increased EE [14]. Finlin et al. found that MIR causes the induction of beige adipose tissue in human subcutaneous WAT [26]. The Improvement in weight and abdominal circumference

parameters could also be related to activation of NO-cGMP axis. Signaling through the latter has been found to be essential for brown adipocyte development and function [27] and has been proven to induce lipid uptake into BAT and increase whole-body EE [28]. Moreover, Mitschke et al. demonstrated that increased cGMP promotes healthy expansion and browning of WAT [7]. Therefore, we determined the cGMP levels in the adipose tissue; however, we found no difference between groups, indicating that weight stabilization is possibly related to other mechanisms or pathways that require further investigation.

In addition, we found that individuals that were subjected to the HFFD exhibited hyperinsulinemia, increased HOMA-IR, decreased glucose tolerance, compared to both their baseline levels and their counterparts in the control group. Whereas those that were additionally treated with MIR showed no increase in their fasting insulin nor in their HOMA-IR levels. This indicates that MIR was able to counteract the decreased insulin sensitivity induced by HFFD feeding. This result is in agreement with the findings of a study, done by Hao et al. who found that treatment with MIR improved insulin sensitivity and prevented high-fat diet-induced obesity in mice [29]. During IR, endothelial-mediated vasodilation is compromised leading to decreased delivery of glucose and insulin to their target organs as reviewed by Barrett et al. [30]. Therefore, one of the mechanisms behind improved insulin sensitivity, could be related to β_3-NO-cGMP-stimulated vasodilation (enhanced blood flow) and translocation of glucose transporter 4 to the cell membrane, that lead to improved glucose and insulin delivery to peripheral tissues and increased glucose uptake, respectively [31],[32]. Moreover, a recent clinical study showed that chronic treatment with MIR improves insulin sensitivity in humans [13].

It has been well established that low-grade inflammation plays an important role in mediating insulin resistance during MetS. Therefore, we measured levels of IL-6, an inflammatory cytokine that was proven to decrease insulin sensitivity [33]. Our results revealed that mirabegron exhibited a tendency to decrease IL-6 levels, which might explain the improved insulin sensitivity.

Our results showed that TG levels were significantly increased in the HFFD group but not in control nor in HFFD+MIR groups. This indicates that treatment with MIR prevented the increase of TG levels. It has been well established that MIR has the ability to activate BAT and thermogenesis and to increase lipolysis in WAT in humans and rodents [24],[26]. One of the

proposed mechanisms for decreased TG levels is chronic stimulation of BAT that leads to increased triglyceride-rich lipoproteins consumption [14],[34]. Whereas, others studies attributed this decrease to increased lipolysis [35]. Even though our results showed no changes in FFA levels, it has been documented that increased plasma FFA levels are only transient following β_3-ARs-stimulated WAT lipolysis due to increased energy cost during BAT-induced thermogenesis [36].

Our results showed that HFFD feeding significantly increased TC and LDL-C levels and that MIR did not counteract this increase. Several studies found that BAT activation reduces hypercholesterolemia and protects from atherosclerosis through stimulating cholesterol uptake [34],[37]. Whereas, others showed that BAT activation enhances the selective fatty acids-uptake from triglyceride-rich lipoproteins, leaving behind cholesterol rich remnants [14]. In animals with defective ApoE-LDLr axis, these particles are likely to accumulate in the circulation leading to increased cholesterol levels. This explains why MIR-treated Watanabe rabbits (LDLr-mutated) showed no improvement in cholesterol levels. In agreement with our findings, β_3-agonist induced BAT activation, in *Apoe*$^{-/-}$ and LDL receptor$^{-/-}$ (*Ldlr*$^{-/-}$) mice was either found to have no impact on hypercholesterolemia and atherosclerosis [14] or to increase plasma levels of both LDL-C and VLDL-C remnants, accelerating atherosclerotic plaque growth and instability [35]. The authors of the latter study did not observe any significant difference of HDL between MIR-treated and control mice, which also agrees with our results. Even though other studies found otherwise, those studies were not performed on models with an ApoE-LDLr defective axis. For instance, treatment with BRL37344, a preferential β_3-AR agonist and MIR were shown to increase HDL-C levels [13],[38].

In the present study, MIR-treated rabbits displayed larger and more advanced atherosclerotic lesions, compared to the control group but showed almost similar lesions as the HFFD-fed group. These results are consistent with the findings of Sui et al. who found that treatment with MIR does not improve atherosclerosis. They even found that mirabegron excarebates atherosclerotic plaque development particularly in animals with defective ApoE-LDLr axis. In their study, they attributed this effect to the activation of brown fat-mediated lipolysis that leads to an increase in plasma levels of both LDL-C and VLDL-C remnants and thereby to an acceleration of plaque growth and instability [35]. Moreover, Berbeé et al. demonstrated that activation of BAT using a β_3-agonist, in *Apoe*$^{-/-}$ and *Ldlr*$^{-/-}$ mice does not attenuate hypercholesterolemia and atherosclerosis [14].

Increased arterial stiffness was proven to be correlated to the MetS in humans and experimental animal models [39]. However, in this study we found no change in the PWV values. Even though PWV values significantly increased in both the HFFD and HFFD+MIR groups compared to the control group, we could not consider these results, given that the PWV almost did not change amongst individuals of both the HFFD and HFFD+MIR group. In contrast, Bhatta et al. found that PWV increases in an animal model of diet-induced metabolic syndrome [40]. However, in our study, rabbits were young and the protocol only lasted for 12 weeks. Conversely, our echocardiographic data showed an increase in both the aortic and pulmonary flow velocities, only in individuals from the HFFD group. This increase could not be ascribed to increased LV systolic function since both the LVFS and LVEF were not increased. Thus, this increase in aortic flow velocities is more likely related to a decrease in vascular arterial compliance/arterial stiffness [41]. Treatment with mirabegron prevented this increase probably through the activation of NO-signaling pathway in endothelial cells. Indeed, treatments that lead to vasodilation have been reported to reduce arterial stiffness [42].

It has been well established that the sympathetic nervous system is over-activated during the MetS, leading to decreased contractile responsiveness to β-stimulation [43]. We evaluated the effects of *ex-vivo* β-AR stimulation on cardiac inotropy. We showed a strong decreasing trend in positive inotropy in response to isoproterenol but not in coronary vasodilation (data not shown) in the HFFD group, suggesting that the alteration likely concerns β_1-ARs and not β_2-ARs. Our *ex vivo* findings also revealed that mirabegron increased both isoproterenol-induced inotropic and lusitropic effects. This increase likely involves an improvement of β_1-AR reactivity (*i.e.* modification in β-AR expression and/or β-ARs-linked mechanisms). This is possibly related to a cross-talk between β_1-ARs and β_3-ARs. Several studies reported a cross-regulation between β_1-ARs and β_3-ARs involving intracellular mechanisms in cardiomyocytes [44],[45].

Our *ex-vivo* results regarding the isoproterenol-mediated effects are not in accordance with our echocardiographic findings. The LVFS and LVEF remained unchanged between the groups and when comparing the baseline to the 12^{th} week levels. The discrepancy has already been documented [46]. In their study, Bundgaard et al. found that MIR significantly increased the LVEF compared to patients given placebo. However, they also documented that MIR was only beneficial in patients with reduced LVEF [47].

One of the cardiovascular disturbances associated with the MetS is endothelial dysfunction. We evaluated the vascular reactivity of the carotid artery. HFFD-feeding increased the α_1-AR sensitivity in the HFFD group. This increase was counteracted in response to treatment with mirabegron, since the pD_2 was significantly decreased compared to the HFFD group. This suggests that MIR prevented the Phe-induced hyper-responsiveness to HFFD-feeding probably *via* a change in NO-cGMP intracellular levels [48], that antagonized the vasoconstrictor effects of Phe [49]. In this regard, we determined the tissular aortic cGMP levels, but found no significant difference between groups. Further investigation is needed in support of this hypothesis.

In contrast to several studies on animal models of MetS [40],[50], we found that Ach-mediated vasorelaxation was not affected in the HFFD group; however, the insulin-induced vasorelaxation was significantly impaired, indicating a selective impairment of endothelium-dependent vasorelaxation involving the PI3K-Akt signaling. This is likely due to the IR state that compromised the vasorelaxant effect of insulin as described by others [51],[52]. We also found that treatment with MIR improved Ins-induced vasorelaxation. This improvement probably occurs through increased NOS signaling.

Enhanced α_1-AR responsiveness and decreased insulin-mediated vasorelaxation encountered in the HFFD group might be due to an imbalance between oxidative stress and NO bioavailability [53],[54]. Accordingly, we evaluated the TAS levels, which did not change in the HFFD group but was significantly increased in response to treatment with mirabegron. It has been demonstrated that β_3-AR stimulation exerts antioxidant effects in a rabbit model of hyperglycemia and in an *in-vitro* experiment [55],[56].

Conclusion

In the current study, we demonstrated that HFFD feeding (with no excess in calories) induces IR without obesity and accentuates dyslipidemia in WHHL rabbit (LDLr mutated animal models). Chronic treatment with mirabegron showed a promising improvement in the metabolic status of HFFD-fed WHHL rabbits. It decreased weight gain, improved insulin sensitivity and stabilized TG levels. Our results support the investigation of MIR as a pharmacological mean for the management of MetS.

Conflict of interest

The authors declare that there is no conflict of interest.

Acknowledgments

The authors express their gratitude to the technicians in histopathology Mr. Bernard Fernandez, Mrs. Florence Lezin, and Mrs. Suzie Calvez. They would also like to express their appreciation to both Dr. Julien Pichon and soon to be Dr. Alex Moinard for their precious advice in methodology, data interpretation and analysis.

Author's contribution

MM, JCD and YM conceived and designed the experiments. ED carried out the histological and immunohistochemical analysis of the atheroma plaques. NB performed the echocardiography. VL quantified the cGMP levels. CT helped in statistical analysis. MM and YM drafted the manuscript. All authors read and approved the final manuscript.

References

[1] S. O'Neill and L. O'Driscoll, "Metabolic syndrome: a closer look at the growing epidemic and its associated pathologies," *Obes. Rev.*, vol. 16, no. 1, pp. 1–12, Jan. 2015, doi: 10.1111/obr.12229.

[2] M. G. Saklayen, "The Global Epidemic of the Metabolic Syndrome," *Current Hypertension Reports*, vol. 20, no. 2. Current Medicine Group LLC 1, Feb. 01, 2018, doi: 10.1007/s11906-018-0812-z.

[3] A. Alkerwi, A. Albert, and M. Guillaume, "Cardiometabolic Syndrome," in *Cardiovascular Risk Factors*, 2012, pp. 161–189.

[4] Y. Rochlani, N. V. Pothineni, S. Kovelamudi, and J. L. Mehta, "Metabolic syndrome: pathophysiology, management, and modulation by natural compounds," *Ther. Adv. Cardiovasc. Dis. Rev.*, vol. 11, no. 8, pp. 215–225, 2017, doi: 10.1177/1753944717711379.

[5] M. B. Lanktree and R. A. Hegele, "Metabolic Syndrome," in *Genomic and Precision*

Medicine: Primary Care: Third Edition, Elsevier Inc., 2017, pp. 283–299.

[6] M. D. Jensen, D. H. Ryan, C. M. Apovian, J. D. Ard, A. G. Comuzzie, *et al.*, "2013 AHA/ACC/TOS guideline for the management of overweight and obesity in adults: A report of the American College of cardiology/American Heart Association task force on practice guidelines and the obesity society," *Circulation*, vol. 129, no. 25 SUPPL. 1. Lippincott Williams and Wilkins, pp. S102–S138, Jun. 24, 2014, doi: 10.1161/01.cir.0000437739.71477.ee.

[7] M. M. Mitschke, L. S. Hoffmann, T. Gnad, D. Scholz, K. Kruithoff, *et al.*, "Increased cGMP promotes healthy expansion and browning of white adipose tissue," *FASEB J.*, vol. 27, no. 4, pp. 1621–1630, Apr. 2013, doi: 10.1096/fj.12-221580.

[8] C. E. Ramirez, H. Nian, C. Yu, J. L. Gamboa, J. M. Luther, *et al.*, "Treatment with Sildenafil Improves Insulin Sensitivity in Prediabetes: A Randomized, Controlled Trial," *J. Clin. Endocrinol. Metab.*, vol. 100, no. 12, pp. 4533–4540, Dec. 2015, doi: 10.1210/jc.2015-3415.

[9] M. Park, P. Sandner, and T. Krieg, "cGMP at the centre of attention: emerging strategies for activating the cardioprotective PKG pathway," *Basic Research in Cardiology*, vol. 113, no. 4. Dr. Dietrich Steinkopff Verlag GmbH and Co. KG, Jul. 01, 2018, doi: 10.1007/s00395-018-0679-9.

[10] N. Dehvari, E. D. da Silva Junior, T. Bengtsson, and D. S. Hutchinson, "Mirabegron: potential off target effects and uses beyond the bladder.," *Br. J. Pharmacol.*, vol. 175, no. 21, pp. 4072–4082, Nov. 2018, doi: 10.1111/bph.14121.

[11] J.-L. Balligand, "Cardiac salvage by tweaking with beta-3-adrenergic receptors," *Cardiovasc. Res.*, vol. 111, no. 2, pp. 128–133, Jul. 2016, doi: 10.1093/cvr/cvw056.

[12] C. CERO, A. O'MARA, J. W. JOHNSON, A. S. BASKIN, J. D. LINDERMAN, *et al.*, " Stimulation of the ß 3 -Adrenergic Receptor via Mirabegron Induces Lipolysis and Thermogenesis in Human Adipocytes ," *Diabetes*, vol. 67, no. Supplement 1, pp. 2049-P, May 2018, doi: 10.2337/db18-2049-p.

[13] A. E. O'Mara, J. W. Johnson, J. D. Linderman, R. J. Brychta, S. McGehee, *et al.*, "Chronic mirabegron treatment increases human brown fat, HDL cholesterol, and insulin sensitivity," *J. Clin. Invest.*, vol. 130, no. 5, pp. 2209–2219, May 2020, doi: 10.1172/JCI131126.

[14] J. F. P. Berbeé, M. R. Boon, P. P. S. J. Khedoe, A. Bartelt, C. Schlein, *et al.*, "Brown fat activation reduces hypercholesterolaemia and protects from atherosclerosis development," *Nat. Commun.*, vol. 6, no. 1, pp. 1–11, Mar. 2015, doi: 10.1038/ncomms7356.

[15] B. Ning, X. Wang, Y. Yu, A. B. Waqar, Q. Yu, *et al.*, "High-fructose and high-fat diet-induced insulin resistance enhances atherosclerosis in Watanabe heritable hyperlipidemic rabbits," *Nutr. Metab.*, vol. 12, no. 1, p. 30, Dec. 2015, doi: 10.1186/s12986-015-0024-3.

[16] M. Ibrahim, I. A. Ahmed, M. A. Mikail, A. A. Ishola, S. Draman, *et al.*, "Baccaurea angulata fruit juice reduces atherosclerotic lesions in diet-induced Hypercholesterolemic rabbits," *Lipids Health Dis.*, vol. 16, no. 1, p. 134, Jul. 2017, doi: 10.1186/s12944-017-0526-2.

[17] O. J. Arias-Mutis, V. G. Marrachelli, A. Ruiz-Saurí, A. Alberola, J. M. Morales, *et al.*, "Development and characterization of an experimental model of diet-induced metabolic syndrome in rabbit," pp. 1–18, 2017, doi: 10.1371/journal.pone.0178315.

[18] T. Helfenstein, F. A. Fonseca, S. S. Ihara, J. M. Bottós, F. T. Moreira, *et al.*, "Impaired glucose tolerance plus hyperlipidaemia induced by diet promotes retina microaneurysms in New Zealand rabbits," *Int. J. Exp. Pathol.*, vol. 92, no. 1, pp. 40–49, Feb. 2011, doi: 10.1111/j.1365-2613.2010.00753.x.

[19] F. Tissier, Y. Mallem, C. Goanvec, R. Didier, T. Aubry, *et al.*, "A non-hypocholesterolemic atorvastatin treatment improves vessel elasticity by acting on elastin composition in WHHL rabbits," *Atherosclerosis*, vol. 251, pp. 70–77, Aug. 2016, doi: 10.1016/j.atherosclerosis.2016.05.039.

[20] H. C. Stary, A. B. Chandler, R. E. Dinsmore, V. Fuster, S. Glagov, *et al.*, "A Definition of Advanced Types of Atherosclerotic Lesions and a Histological Classification of Atherosclerosis," *Circulation*, vol. 92, no. 5, pp. 1355–1374, Sep. 1995, doi: 10.1161/01.CIR.92.5.1355.

[21] C. Thorin, M. Y. Mallem, J. Noireaud, M. Gogny, and J.-C. Desfontis, “Nonlinear mixed effects models applied to cumulative concentration-response curves,” *J. Pharm. Pharmacol.*, vol. 62, no. 3, pp. 339–345, Mar. 2010, doi: 10.1211/jpp.62.03.0008.

[22] C. Xiao, M. Goldgof, O. Gavrilova, and M. L. Reitman, “Anti-obesity and metabolic efficacy of the β3-adrenergic agonist, CL316243, in mice at thermoneutrality compared to 22°C,” *Obesity*, vol. 23, no. 7, pp. 1450–1459, Jul. 2015, doi: 10.1002/oby.21124.

[23] S. L. Clookey, R. J. Welly, D. Shay, M. L. Woodford, K. L. Fritsche, *et al.*, “Beta 3 adrenergic receptor activation rescues metabolic dysfunction in female estrogen receptor alpha-null mice,” *Front. Physiol.*, vol. 10, no. FEB, 2019, doi: 10.3389/fphys.2019.00009.

[24] A. M. Cypess, L. S. Weiner, C. Roberts-Toler, E. F. Elía, S. H. Kessler, *et al.*, “Activation of human brown adipose tissue by a β3-adrenergic receptor agonist,” *Cell Metab.*, vol. 21, no. 1, pp. 33–38, Jan. 2015, doi: 10.1016/j.cmet.2014.12.009.

[25] E. Szentirmai and L. Kapas, “The role of the brown adipose tissue in β3-adrenergic receptor activation-induced sleep, metabolic and feeding responses,” *Sci. Rep.*, vol. 7, no. 1, pp. 1–14, Dec. 2017, doi: 10.1038/s41598-017-01047-1.

[26] B. S. Finlin, H. Memetimin, A. L. Confides, I. Kasza, B. Zhu, *et al.*, “Human adipose beiging in response to cold and mirabegron,” *JCI insight*, vol. 3, no. 15, Aug. 2018, doi: 10.1172/jci.insight.121510.

[27] A. Pfeifer, A. Kilić, and L. S. Hoffmann, “Regulation of metabolism by cGMP,” *Pharmacology and Therapeutics*, vol. 140, no. 1. Elsevier Inc., pp. 81–91, Oct. 01, 2013, doi: 10.1016/j.pharmthera.2013.06.001.

[28] L. S. Hoffmann, J. Etzrodt, L. Willkomm, A. Sanyal, L. Scheja, *et al.*, “Stimulation of soluble guanylyl cyclase protects against obesity by recruiting brown adipose tissue,” *Nat. Commun.*, vol. 6, May 2015, doi: 10.1038/ncomms8235.

[29] L. Hao, S. Scott, M. Abbasi, Y. Zu, M. S. H. Khan, *et al.*, “Beneficial metabolic effects of mirabegron in vitro and in high-fat diet-induced obese mice,” *J. Pharmacol. Exp. Ther.*, vol. 369, no. 3, pp. 419–427, 2019, doi: 10.1124/jpet.118.255778.

[30] E. J. Barrett, H. Wang, C. T. Upchurch, and Z. Liu, “Insulin regulates its own delivery to skeletal muscle by feed-forward actions on the vasculature.,” *Am. J. Physiol. Endocrinol. Metab.*, vol. 301, no. 2, pp. E252-63, Aug. 2011, doi: 10.1152/ajpendo.00186.2011.

[31] A. A. Arce-Esquivel, K. A. Bunker, R. C. Mikus, and M. H. Laughlin, “Insulin Resistance and Endothelial Dysfunction: Macro and Microangiopathy,” in *Type 2 Diabetes*, InTech, 2013.

[32] D. Roy, M. Perreault, and A. Marette, “Insulin stimulation of glucose uptake in skeletal muscles and adipose tissues in vivo is NO dependent,” *Am. J. Physiol. - Endocrinol. Metab.*, vol. 274, no. 4 37-4, 1998, doi: 10.1152/ajpendo.1998.274.4.e692.

[33] P. Pazos, L. Lima, F. F. Casanueva, C. Diéguez, and M. C. García, “Interleukin 6 Deficiency Modulates the Hypothalamic Expression of Energy Balance Regulating Peptides during Pregnancy in Mice,” *PLoS One*, vol. 8, no. 8, p. 72339, Aug. 2013, doi: 10.1371/journal.pone.0072339.

[34] G. Hoeke, S. Kooijman, M. R. Boon, P. C. N. Rensen, and J. F. P. Berbeé, “Role of Brown Fat in Lipoprotein Metabolism and Atherosclerosis,” *Circulation Research*, vol. 118, no. 1. Lippincott Williams and Wilkins, pp. 173–182, Jan. 08, 2016, doi: 10.1161/CIRCRESAHA.115.306647.

[35] W. Sui, H. Li, Y. Yang, X. Jing, F. Xue, *et al.*, “Bladder drug mirabegron exacerbates atherosclerosis through activation of brown fat-mediated lipolysis,” *Proc. Natl. Acad. Sci. U. S. A.*, vol. 166, no. 22, pp. 10937–10942, May 2019, doi: 10.1073/pnas.1901655116.

[36] J. M. Olsen, A. Åslund, M. H. Bokhari, D. S. Hutchinson, and T. Bengtsson, “Acute β-adrenoceptor mediated glucose clearance in brown adipose tissue; a distinct pathway independent of functional insulin signaling,” *Mol. Metab.*, vol. 30, pp. 240–249, Dec. 2019, doi: 10.1016/j.molmet.2019.10.004.

[37] A. Worthmann, C. John, M. C. Rühlemann, M. Baguhl, F. A. Heinsen, *et al.*, “Cold-induced conversion of cholesterol to bile acids in mice shapes the gut microbiome and promotes adaptive thermogenesis,” *Nat. Med.*, vol. 23, no. 7, pp. 839–849, Jul. 2017, doi: 10.1038/nm.4357.

[38] X. Cao and Y. Li, “β3-Adrenergic receptor regulates hepatic apolipoprotein A-I gene expression,” *J. Clin. Lipidol.*, vol. 11, no. 5, pp. 1168–1176, Sep. 2017, doi: 10.1016/j.jacl.2017.07.007.

[39] W. R. P. Lopes-Vicente, S. Rodrigues, F. X. Cepeda, C. P. Jordão, V. Costa-Hong, *et al.*, “Arterial stiffness and its association with clustering of metabolic syndrome risk factors,” *Diabetol. Metab. Syndr.*, vol. 9, no. 1, p. 87, Oct. 2017, doi: 10.1186/s13098-017-0286-1.

[40] A. Bhatta, L. Yao, Z. Xu, H. A. Toque, J. Chen, *et al.*, “Obesity-induced vascular dysfunction and arterial stiffening requires endothelial cell arginase 1,” *Cardiovasc. Res.*, vol. 113, no. 13, pp. 1664–1676, Nov. 2017, doi: 10.1093/cvr/cvx164.

[41] S. J. Goldberg, N. Wilson, and D. F. Dickinson, “Increased blood velocities in the heart and great vessels of patients with congenital heart disease. An assessment of their significance in the absence of valvular stenosis,” *Br. Heart J.*, vol. 53, no. 6, pp. 640–644, 1985, doi: 10.1136/hrt.53.6.640.

[42] I. B. Wilkinson, S. S. Franklin, and J. R. Cockcroft, “Nitric oxide and the regulation of large artery stiffness: From physiology to pharmacology,” *Hypertension*, vol. 44, no. 2. Lippincott Williams & Wilkins, pp. 112–116, Aug. 01, 2004, doi: 10.1161/01.HYP.0000138068.03893.40.

[43] A. Lymperopoulos, G. Rengo, and W. J. Koch, “Adrenergic nervous system in heart failure: Pathophysiology and therapy,” *Circ. Res.*, vol. 113, no. 6, pp. 739–753, 2013, doi: 10.1161/CIRCRESAHA.113.300308.

[44] E. Montaudon, L. Dubreil, V. Lalanne, M. Vermot Des Roches, G. Toumaniantz, *et al.*, “Cardiac effects of long-term active immunization with the second extracellular loop of human β1- and/or β3-adrenoceptors in Lewis rats,” *Pharmacol. Res.*, vol. 100, pp. 210–219, 2015, doi: 10.1016/j.phrs.2015.08.006.

[45] C. Ufer and R. Germack, “Cross-regulation between β 1- and β 3- adrenoceptors following chronic β-adrenergic stimulation in neonatal rat cardiomyocytes,” *Br. J. Pharmacol.*, vol. 158, no. 1, pp. 300–313, Sep. 2009, doi: 10.1111/j.1476-5381.2009.00328.x.

[46] N. A. P. Franken, J. A. J. Camps, F. J. M. Van Ravels, A. Van Der Laarse, E. K. J. Pauwels, *et al.*, "Comparison of in vivo cardiac function with ex vivo cardiac performance of the rat heart after thoracic irradiation," *Br. J. Radiol.*, vol. 70, no. OCT., pp. 1004–1009, 1997, doi: 10.1259/bjr.70.838.9404203.

[47] H. Bundgaard, A. Axelsson, J. Hartvig Thomsen, M. Sørgaard, K. F. Kofoed, *et al.*, "The first-in-man randomized trial of a beta3 adrenoceptor agonist in chronic heart failure: the BEAT-HF trial," *Eur. J. Heart Fail.*, vol. 19, no. 4, pp. 566–575, Apr. 2017, doi: 10.1002/ejhf.714.

[48] J. N. Trochu, V. Leblais, Y. Rautureau, F. Bévérelli, H. Le Marec, *et al.*, "Beta 3-adrenoceptor stimulation induces vasorelaxation mediated essentially by endothelium-derived nitric oxide in rat thoracic aorta," *Br. J. Pharmacol.*, vol. 128, no. 1, pp. 69–76, 1999, doi: 10.1038/sj.bjp.0702797.

[49] T. S. Cunha, M. J. C. S. Moura, C. F. Bernardes, A. P. Tanno, and F. K. Marcondes, "Vascular sensitivity to phenylephrine in rats submitted to anaerobic training and nandrolone treatment.," *Hypertension*, vol. 46, no. 4, pp. 1010–1015, Oct. 2005, doi: 10.1161/01.HYP.0000174600.51515.e7.

[50] H. M. El-Bassossy, N. Dsokey, and A. Fahmy, "Characterization of vascular complications in experimental model of fructose-induced metabolic syndrome," *Toxicol. Mech. Methods*, vol. 24, no. 8, pp. 536–543, Dec. 2014, doi: 10.3109/15376516.2014.945109.

[51] M. A. Vincent, M. Montagnani, and M. J. Quon, "Molecular and physiologic actions of insulin related to production of nitric oxide in vascular endothelium," *Current Diabetes Reports*, vol. 3, no. 4. Current Science Ltd, pp. 279–288, 2003, doi: 10.1007/s11892-003-0018-9.

[52] M. P. DE BOER, R. I. MEIJER, N. J. WIJNSTOK, A. M. JONK, A. J. HOUBEN, *et al.*, "Microvascular Dysfunction: A Potential Mechanism in the Pathogenesis of Obesity-associated Insulin Resistance and Hypertension," *Microcirculation*, vol. 19, no. 1, pp. 5–18, Jan. 2012, doi: 10.1111/j.1549-8719.2011.00130.x.

[53] E. R. Duncan, P. A. Crossey, S. Walker, N. Anilkumar, L. Poston, *et al.*, "Effect of

endothelium-specific insulin resistance on endothelial function in vivo," *Diabetes*, vol. 57, no. 12, pp. 3307–3314, 2008, doi: 10.2337/db07-1111.

[54] V. Conti, G. Russomanno, G. Corbi, V. Izzo, C. Vecchione, *et al.*, "Adrenoreceptors and nitric oxide in the cardiovascular system," *Frontiers in Physiology*, vol. 4 NOV. 2013, doi: 10.3389/fphys.2013.00321.

[55] K. K. Galougahi, C.-C. Liu, A. Garcia, C. Gentile, N. A. Fry, *et al.*, "b3 Adrenergic Stimulation Restores Nitric Oxide/Redox Balance and Enhances Endothelial Function in Hyperglycemia," vol. 5, no. 2, 2016, doi: 10.1161/JAHA.115.002824.

[56] L. Sichrovska, I. Malik, E. Sedlarova, J. Csollei, and J. Muselik, "In vitro antioxidant properties of novel β3-adrenoceptor agonists bearing benzenesulfonamide fragment," *Dhaka Univ. J. Pharm. Sci.*, vol. 12, no. 1, pp. 23–28, 2013, doi: 10.3329/dujps.v12i1.16296.

Article 3

Article number three: Effect of long-term treatment with BAY 41-2272, a soluble guanylyl cyclase stimulator, on the metabolic and cardiovascular parameters of an animal model of dyslipidemia and insulin resistance.

Michelle Moughaizel[1*], Elie Dagher[2], Nora Bouhsina[3], Valérie Lalanne[1], Chantal Thorin[1], Jean-Claude Desfontis[1] and Yassine Mallem[1]

[1] Nutrition, PathoPhysiology and Pharmacology (NP3) Unit, Oniris, Nantes Atlantic College of Veterinary Medicine, Food Science and Engineering, Nantes, France

[2] Laboniris, Oniris, Nantes Atlantic College of Veterinary Medicine, Food Science and Engineering, Nantes, France

[3] Department of Diagnostic Imaging, Oniris, Nantes Atlantic College of Veterinary Medicine, Food Science and Engineering, Nantes, France

* Correspondance:

Michelle Moughaizel

m_moughaizel@hotmail.com

Abstract

Background and aim: The metabolic syndrome (MetS) is associated with increased risk of type 2 diabetes and cardiovascular disease. Given the multifactorial nature of this syndrome, its management necessitates a pharmacological therapeutic approach with pleotropic effects. We explored the ability of a cyclic guanosine monophosphate (cGMP) modulator, BAY 41-2272 (BAY), to prevent the development of MetS and its cardiovascular consequences.

Methods: Thirty male and female Watanabe heritable hyperlipidemic rabbits (WHHL) were randomly assigned to control (n=9), high fructose high fat diet (HFFD, n=12) and HFFD+BAY (n=9) groups that, respectively, received a chow, HFFD and HFFD along with BAY treatment (3mg/kg, PO). The protocol lasted for 12 weeks, during which weight and abdominal circumference were monitored; plasma fasting levels of lipids, glucose and insulin were measured and an intravenous glucose tolerance test (IVGTT) was performed. Homeostasis model assessment of insulin resistance (HOMA-IR) was calculated. Cardiac function was evaluated using *in-vivo* (Echocardiography) and *ex-vivo* (Langendorff isolated heart) approaches. Vascular reactivity and arterial stiffness were assessed on isolated carotid arteries and by determining the pulse wave velocity (PWV), respectively.

Results: HFFD-fed rabbits exhibited a significant increase in fasting insulin, HOMA-IR, area under the curve of the IVGTT, triglycerides (TG), total cholesterol, in the sensitivity to phenylephrine and a significant decrease of the insulin-mediated vasorelaxation, compared to the control group. Treatment with BAY prevented the increase in fasting insulin, HOMA-IR, TG levels and the phenylephrine hypersensitivity induced by the HFFD.

Conclusion: In the WHHL rabbit model of combined dyslipidemia and IR, long-term treatment with BAY stabilized weight gain and TG levels and improved insulin sensitivity and endothelial function.

Keywords: Metabolic syndrome, insulin resistance, dyslipidemia, Watanabe heritable hyperlipidemic rabbit, high-fructose high-fat diet, BAY 41-2272.

Introduction

The metabolic syndrome (MetS) combines multiple risk factors that include central/abdominal obesity, insulin resistance (IR), dyslipidemia and arterial hypertension [1]. The increased interest in this syndrome is related to its association with increased risk of type 2 diabetes (T2D) and cardiovascular disease (CVD) [2]–[4]. Lifestyle interventions remain the primary tools for good management of the MetS. However, when lifestyle changes are not successful [5] or simply cannot be established [6], a pharmacological therapeutic approach should be implemented. Currently most of the treatments used in the management of this syndrome are directed towards each risk factor alone. Therefore, using molecules with pleiotropic effects or that acts on a broad spectrum of tissues and cells, might be more successful in managing a multifactorial disease such as the MetS [6].

Animal and clinical trial studies have revealed that modulation of the solube guanylyl cyclase-cyclic guanosine monophosphate-protein kinase G (sGC-cGMP-PKG) pathway exhibits promising metabolic and cardiovascular outcomes. For instance, sildenafil citrate, a phosphodiesterase 5 (PDE_5) inhibitor that leads to increased cGMP levels was reported to be effective in reducing weight, improving glucose tolerance, insulin sensitivity and lipid profiles and reversing endothelial dysfunction [7]–[11]. Moreover, activation of the NO-cGMP axis has been described to promote lipolysis and to stimulate thermogenic pathways, in humans and mice, leading to decreased white adipose tissue-mediated fat storage and to increased brown adipose tissue-mediated energy expenditure (EE), respectively [12]–[14]. Other studies proposed that browning of white adipose tissue is also possible through this pathway in humans and mice [14]–[16]. Collectively, the aforementioned findings suggest that the increased signaling through the NO-sGC-cGMP pathway have the potential to treat metabolic and cardiovascular disorders [17]–[20]. Modulation of this pathway could be achieved by increasing the bioavailability of the intracellular second messenger of NO, the cGMP, either through decreasing its catabolism (PDE inhibitors) or through increasing its biosynthesis (natriuretic peptide, sGC modulators or sGC stimulators) [17], [21], [22]. BAY 41-2272 belongs to a class of compounds called sGC stimulators that directly activate the sGC and work synergistically with NO, yielding increased cGMP levels [23].

Our aim was to investigate the ability of BAY 41-2272 in attenuating the metabolic disturbances associated with the dyslipidemia-IR combination, and thereby in preventing the development of metabolic and cardiovascular changes/consequences of the MetS. We chose to work on Watanabe rabbits, animal models that spontaneously develop dyslipidemia, due to a mutation in their LDLr. These rabbits were subjected to 12 weeks of HFFD feeding, in purpose of inducing IR [24]. The HFFD that we used is rich in sugar and fat but with less protein and fibers [24]. In fact, our purpose was to avoid excessive weight gain-related confounding factors e.g. mechanical inflammatory and cardiometabolic effects of obesity.

Materials and methods

Experimental design

30 Watanabe heritable hyperlipidemic (WHHL) rabbits (male and female; 9-12 weeks of age) weighing 3.0-3.5 kg were used in all experiments. Rabbits were housed individually in a room maintained at constant temperature (21°C) and humidity (>45%), under a 12h dark/light cycle with free access to water and food. Rabbits were randomly divided into three groups a control group (n=9), a HFFD group (n=12) and a HFFD+BAY group (n=9). These group, respectively, received a standard chow diet (3410.PS.S10; SERLAB, France), a high fructose fat diet (HFFD, SERLAB, France) and a HFFD along with oral administration of BAY 41-2272 (BAY, 3mg/kg/d). The HFFD consisted of a chow diet, supplemented with 30 % fructose and 10 % coconut oil (91% saturated fatty acids)(Additional file).

All procedures were performed in accordance with the National Institute of Health Guide for the Use and Care of Laboratory Animals guidelines and they are all conducted with the approval of the institutional ethics Committee of Pays de la Loire (APAFIS n° 10722).

Morphological parameters

Weight and abdominal circumference were measured every two weeks to monitor the animal's weight gain and growth.

Measurement of plasma lipids, glucose and insulin levels

Blood withdrawal was performed at the baseline and 12th week of the experimental protocol. After overnight fasting, blood was withdrawn in heparinized tubes. Samples were centrifuged (10000g, 15 minutes, 4° C) and the plasma was stored at -80° C. For the quantitative determination of total cholesterol (TC), triglycerides (TG), free fatty acids (FFA) and high-density lipoprotein cholesterol (HDL-C) plasma levels, we used an enzymatic colorimetric method. The dosages were performed according to the supplier's instructions (DiaSys enzymatic commercial kits). Meanwhile, low-density lipoprotein (LDL-C) levels were calculated using the Friedewald's equation, LDL cholesterol (g/L) = total cholesterol – HDL-cholesterol – (triglycerides/5) [25]. For the quantitative determination of insulin plasma levels, we used a sensitive rabbit insulin ELISA kit sandwich assay (Crystal Chem High Performance Assays, USA).

Intravenous glucose tolerance test

An IVGTT was performed at the end of the protocol, as previously described [26]. After an overnight fasting, rabbits were injected with an intravenous glucose solution (0.6 g/kg body weight). Then glucose measurements were performed before and 15, 30, 45, 60, 90 and 120 min after the glucose loading. Blood glucose was measured via a glucose meter (ONETOUCH®VERIO®; © 2012 LifeScan, Inc.), using one drop of whole blood, obtained from the marginal ear vein. The area under the curve (AUC) was calculated using PRISM® software (version 8.0.1). Homeostasis Model Assessment of basal Insulin Resistance (HOMA-IR) was calculated using the following equation: [(fasting plasma glucose (mmol/l) x fasting plasma insulin (µU/ml))/22.5] [27].

Pulse wave velocity

To assess the arterial stiffness, two sets of pulse wave velocity (PWV) measurements were performed, one at the beginning and another, at the 12th week of the protocol. Two piezoelectric sensors (ADInstruments, France) were placed, one on the auricular artery and another on the caudal one of conscious animals. Recordings of pulse waves were made during 10 min with the software (ADInstruments LabChart v8.1.5, France). The measurement point (the foot of each pulse wave) was determined using the second derivative of the pulse wave signal. Both the distance between

the two sensors and that between the auricular artery and the sternal manubrium, were noted each time. Then, the Δx was calculated by substracting the two distances. The time interval (Δt) between the foot of the auricular waveform and that of the caudal waveform was measured by the software. The PWV was calculated using the formula PWV ($m.s^{-1}$) = Δx/Δt [28].

Echocardiographic measurements of cardiac function and geometry

To assess *in vivo* cardiac geometry and left ventricular (LV) global systolic function, transthoracic echocardiography (TTE) was performed on conscious animals, at both baseline and at the end of experimental protocol (12^{th} week). A high frequency ultrasound imaging system (Esaote Mylab 70 XVG, 9 MHz microconvex transducer) was used to record both two-dimensional and Motion mode (M-mode) imaging. The left ventricular end-diastolic diameter (LVEDd), left ventricular end-systolic diameter (LVESd) left ventricular fractional shortening (LVFS), left ejection fraction (LVEF), interventricular septal thickness (IVS) and left ventricular posterior wall thickness (LVPW) were determined using through a right parasternal short axis view of the heart. FS and EF were respectively calculated using the formulas LVFS = [(LVIDd − LVIDs)/ LVIDd] × 100 and EF = [(LVEDV − LVESV)/ LVEDV] × 100. Two consecutive heart cycles were measured and the average was used for analysis. Using Doppler imaging, color-flow mapping mode, the pulmonary and aortic flow were determined, through a short axis-right parasternal and left long axis- five chambers approaches, respectively (Esaote Mylab 70 XVG, 8 MHz sector transducer).

Isolated Langendorff heart preparation

Ex vivo retrograde heart perfusion was performed at a constant flow-rate mode. Under anesthesia with intravenous Sodium Pentobarbital (40 mg/kg) the thorax was opened. The animal was sacrificed by exsanguinating the abdominal aorta. The heart was rapidly excised and transferred into ice-cold filtered (using a 0,2 μm filter funnel) Krebs' solution. The latter, contained (mM): NaCl 118.3, $NaHCO_3$ 20.0, KCl 4.7, $MgSO_47H_2O$ 1.2, KH_2PO4 1.2, glucose 11.1, EDTA 0.016 and $CaCl_2$ 2.5. Afterwards, the heart was cannulated (4 mm aortic cannula, ADinstruments) and perfused at a constant flow-rate (22-28 mL/min) with a Krebs solution that is constantly bubbled with 95% O_2 and 5% CO_2 at 37 °C. Then, a de-ionized water-filled latex balloon, connected to a pressure transducer, was inserted into the left ventricle to allow isovolumetric contractions and continuously record the left ventricular pressure (*LVP*) as an index of cardiac contractility. Another

pressure transducer located above the aorta recorded the perfusion pressure (*PP*), as an index of coronary vasodilation. The heart was allowed to stabilize for 20 minutes before non-cumulative concentration response curves to isoproterenol (10^{-9} to 10^{-6} M), a potent nonselective β-adrenergic agonist, were built. Four pharmacodynamic endpoints, left ventricular pressure (*LVP*), coronary perfusion pressure (*PP*), the first derivative of the left ventricular pressure in systole (*dP/dTmax*) and first derivative of the left ventricular pressure in diastole (*dP/dTmin*), were measured and monitored continuously throughout the experiment. The left ventricular developed pressure (*LVDevP*) was calculated as the difference between left ventricular systolic pressure and left ventricular end-diastolic pressure. *dP/dTmax* and *dP/dTmin* reflect the maximum contraction and relaxation velocities, respectively. Data acquisition and recording were achieved using Powerlab (8/35) and LabChart 7.0 software (ADInstruments, France).

Vascular reactivity

Immediately after animals were sacrificed by exsanguination, the carotid artery was removed and dissected free of fat and connective tissue and placed in a cold Krebs' solution of the following composition (mM): NaCl 118.3, KCl 4.7, $MgSO_47H_2O$ 1.2, KH_2PO4 1.2, $NaHCO_3$ 20.0, glucose 11.1, EDTA 0.016, $CaCl_2$ 2.5, pH 7.4. The artery was cut into 5mm ring segments that were mounted on triangular wire supports and suspended in 10 mL organ baths containing Krebs' solution, maintained at 37°C, and gassed with 95% O_2 and 5% CO_2. Isometric tension was continuously measured using a computerized automated isometric transducer system (EMKAbath4, EMKA technologies, France) and recorded with a data acquisition software (iox version 2.9.5.20). The segments were initially loaded to a 2 g tension and allowed to equilibrate for 60 minutes (during which, they were washed four time). Care was taken not to injure the endothelium during the preparation. Firstly, the viability of the vessels was evaluated through an 80 mM KCl solution. Then, the presence of intact endothelium was verified by adding acetylcholine (Ach, 10^{-6} M) to phenylephrine (Phe 3.10^{-6} M) pre-contracted rings. The rings with less than 60% relaxation were considered non-reliant and thus, were eliminated. Cumulative concentration-response curves (CCRCs) to Phenylephrine, an α1-adrenoceptor agonist (Phe, 10^{-9} to 3.10^{-5} M), Acetylcholine, a muscarinic receptor agonist (Ach, 10^{-9} to 3.10^{-5} M), sodium nitroprusside, a NO donor (SNP, 10^{-10} to 3.10^{-5} M), insulin (Ins, 10^{-9} to 3.10^{-6} M) were constructed. The cumulative concentration-relaxation curves (Ach, SNP and Ins) were built on the Phe-

precontracted rings, using: The calculated relaxing percentages are relative to the maximal changes from the pre-contraction produced by phenylephrine in each ring.

Histology and Immunohistochemistry

We evaluated the effect of HFFD on the development and evolution of atherosclerosis in Watanabe rabbits. The cranial thoracic aorta, specifically the area preceding the aortic arch was removed and sampled. These samples were fixed by immersion in neutrally buffered 10% formalin followed by dehydration and paraffin embedding. Then, serial 4μm thick sections were routinely cut and stained.

For histological analysis of thoracic aorta, sections were stained with hematoxylin and eosin, safranin (HES). Green Masson's trichrome and Orceine stains were used to assess collagen and elastic fibers, respectively. The lesions were evaluated under light microscope. In order to study the cellular components of the thoracic aorta, automated immunohistochemistry (Benchmark XT, Ventana Medical Systems, Roche Diagnostics) was performed. The detection systems were the iView DAB detection kit (Ventana Medical Systems, Roche Diagnostics, 760-091) (Other sections were immunohistochemically stained with macrophage antibody (clone RAM11, mouse monoclonal, 1:1200 dilution, Dako Corp, USA) and α-smooth muscle actin antibody (clone HHF35, mouse monoclonal, 1:50 dilution, Dako Corp, USA), two monoclonal antibodies that detect macrophages and smooth muscle cells (SMCs), respectively.

Using an image analysis system (FIJI). The extent of atherosclerotic lesions in the aorta was expressed as a percentage of the lesion area and the degree of intimal thickening. For determination of average intima thickening, the following equation was used: area of intimal lesion/length of media. The same software was also used for the quantification of elastin fibers, macrophages and SMCs, which was performed by calculating the percentage of immunostaining in lesion area. Conversely, collagen could not be quantified using the same software. Therefore, a semi-quantification was performed microscopically. Lesions were classified by a certified veterinary pathologist, according to the guidelines of the American Heart Association [29]. According to their classification:

- Type I (initial) lesion contain atherogenic lipoprotein that elicit an increase in macrophages numbers and scattered macrophage foam cell formation,

- Type II lesions consist of layers of macrophage foam cells and lipid-laden smooth muscle cells and comprise lesions grossly designated as fatty streaks,

- Type III lesions are the intermediate stage between type II and IV lesions (atheroma). In addition to the lipid-laden cells present in type II lesions, type III lesions contain scattered collections of extracellular lipid droplets and particles,

- Type IV lesions contain larger, confluent, and more disruptive core of extracellular lipid,

- Lesions comprising a lipid core might also contain thick layers of fibrous connective tissue characterizing type V lesions and/or fissure, hematoma, and thrombus characterizing type VI lesion.

In addition, the presence of extracellular lipid, fibrous cap, mineralization, lipid core and collagen's deposition (using green Masson's trichrome stain) were graded using a semi-quantitative scale from 0 to 4 in order to be able to better characterize the different types of plaques [31]. In order to compare the stage of lesions type II and III plaques were classified as early lesions whereas type IV and V plaques were classified as advanced lesions.

Tissue cGMP quantification

cGMP was quantified in thoracic aorta rings, heart tissue and epididymal/ovarian fat. Immediately after animal sacrifice, samples were collected, immerged in liquid nitrogen and then stored at -80°C. The day of analysis, samples were thawed, ground and homogenized in a cold solution of 6% trichloroacetic acid (TCA), and then centrifuged at 1500 g for 10 min at 4 ° C. Then, the supernatant fractions were washed three times with a water saturated diethyl ether solution (5 volumes of diethyl ether per 1 volume of supernatant) for the extraction of TCA. The residual diethyl ether was then evaporated by heating the samples at 70 ° C for 5 min. Later, the dried extract was dissolved in an adequate volume of assay buffer. The cGMP concentrations of each sample was measured by using a colorimetric enzyme immunoassay kit (Cayman Chemical Company). The absorbance of each sample was read at 405 nm using a stectrophotometer. The

cGMP value was calculated related to the total cell protein concentrations previously measured using a protein assay reagent kit (micro-BCA, Pierce Biotechnology, Rockford , USA).

Plasma inflammatory cytokines and total antioxidant status

Plasma tumor necrosis factor–alpha (TNF-α) and interleukin-6 (IL-6) were measured using ELISA kits according to the manufacturer's instructions (DuoSet® ELISA kit, TNF-α/IL-6**,** R&D Systems Europe Ltd). Plasma total antioxidant status (TAS) was quantified using a colorimetric kit (TAS kit, Randox laboratories Ltd).

Statistical analysis

Data were expressed as a mean ± SEM. All graphs have been performed using PRISM® software (version 8.0.1). We used repeated measures two-way ANOVA, mixed effects analysis for multiple group comparisons (biochemical parameters and PWV measurements) and one-way ANOVA for cGMP analysis. R software was used to evaluate data from non-cumulative concentration response curves (isolated heart and CCRC to insulin) by a linear mixed effect (LME) model. Relaxation was expressed as the percentage relaxation of the phenylephrine-induced precontraction. CCRCs to Ach were compared using a non-linear mixed effect model (NLME) [30], also using R software. The efficacy (E_{max}) and the potency (pD_2) representing the maximum effects and the negative logarithm of the concentration producing 50% of the maximum effect, respectively were determined for each CCRC [30]. Chi square test was used for analyzing the classification of atheroma plaques. A *p* value of less than 0.05 was considered statistically significant for all results.

Results

Effect of HFFD and treatment with BAY 41-2272 on weight and abdominal circumference

After 12 weeks of the protocol, the body weight similarly increased in both, the control and HFFD groups. This increase was significant in control (12^{th} week vs. Baseline, $p<0.0001$) and HFFD (12^{th} week vs. Baseline, $p=0.0057$) groups but not in the HFFD+BAY-treated group. The same pattern was observed in abdominal circumference comparisons. After 12 weeks of protocol, similar increases were witnessed in the control and HFFD. The increase was significant in control (12^{th} week vs. Baseline, $p<0.0001$) and HFFD (12^{th} week vs. Baseline, $p<0.0001$) groups but not in the HFFD+BAY-treated group. It is to be noted that both diets contained an equal amount of calories.

In fact, even though the HFFD is rich in fat and sugar, it consisted of relatively less protein and fibers (additional file).

Table 1: Results of weight, abdominal circumference, glycaemia, insulin and plasma lipids.

	Groups					
Measurements	Control (n=9)		HFFD (n=12)		HFFD+BAY (n=9)	
	Baseline	12th week	Baseline	12th week	Baseline	12th week
Weight (Kg)	2.00 ± 0.1	2.97 ± 0.1 $$$$	2.30 ± 0.05	2.70 ± 0.12 $$	3.27 ± 0.14	3.02 ± 0.08
Abdominal circumference (cm)	31.78 ± 1.2	38.78 ± 0.76 $$$$	31.81 ± 0.88	36.45 ± 0.62 $$$$	37.34 ± 1.03	36.00 ± 0.91
Fasting glycaemia (mg/dl)	98 ± 1.88	96 ± 3.06	101 ± 6.6	106 ± 7.54	92 ± 2.95	95 ± 4.30
Fasting insulinemia (ng/ml)	0.37 ± 0.08	0.31 ± 0.07	0.3 ± 0.04	1.15 ± 0.45 $ *	0.56 ± 0.15	0.57 ± 0.12
Triglycerides(g/L)	1.4 ± 0.3	1.75 ± 0.35	1.76 ± 0.3	2.65 ± 0.39 $	1.87 ± 0.35	1.68 ± 0.27
TC (g/L)	6.72 ± 0.5	6.53 ± 0.8	7.4 ± 0.5	11.05 ± 0.88 $$ ***	8.65 ± 0.86	10.7 ± 0.94 **
HDL-C (g/L)	0.21 ± 0.03	0.22 ± 0.03	0.19 ± 0.02	0.26 ± 0.03	0.195 ± 0.03	0.186 ± 0.03
LDL-C (g/L)	6.23 ± 0.45	5.96 ± 0.7	6.87 ± 0.5	10.25 ± 0.85 $$ ***	8.09 ± 0.82	10.09 ± 0.86 $ **
FFA (mmol/L)	0.83 ± 0.2	0.65 ± 0.1	1.02 ± 0.21	0.70 ± 0.11	1.26 ± 0.22	0.88 ± 0.06

TC = total cholesterol, HDL-C = high-density lipoprotein cholesterol, LDL-C = low-density lipoprotein cholesterol, FFA = free fatty acids. Data are expressed as mean ± SEM. A two-way ANOVA test was used for statistical analysis. ****p<0.0001, ***p< 0.001, ** p< 0.01 and *p< 0.05 for HFFD or HFFD+BAY vs. the Control group. $$$$p<0.0001, $$$p<0.001, $$ p< 0.01 and $p<0.05 12th week (end) vs. Baseline (beginning) of the protocol.

Effect of HFFD and treatment with BAY 41-2272 on glucose and insulin levels

Our data showed that basal insulinemia, significantly increased in the HFFD group (12th week vs. Baseline, p=0.021) and when comparing the HFFD to the control group at the 12th week (p=0.020)

but did not change in the HFFD+BAY compared to the control group. Even though HFFD feeding significantly increased the plasma levels of insulin, it did not change the fasting plasma glucose in any of the groups **(Table 1)**.

Effect of HFFD and treatment with BAY 41-2272 on lipid profiles

We further examined modifications in lipid profiles **(Table 1)**. We found a significant increase in TC when, comparing the 12^{th} week to the baseline levels, of the HFFD group (p=0.007) and when also comparing each of the HFFD and HFFD+BAY to the control group at the end of the protocol (p=0.0004 and p=0.0016, respectively). The increase of TC levels was almost significant in the HFFD+BAY, when comparing 12^{th} week to the baseline levels (p=0.0538). The same pattern was observed in the LDL-C levels. We found a significant increase in TC and LDL-C when comparing the 12^{th} week to the baseline levels of both the HFFD and HFFD+BAY groups (p=0.008 and p=0.04, respectively) and when also comparing each of the HFFD and HFFD+BAY to the control group at the end of the protocol (p=0.0003 and p=0.0009, respectively). TG levels were significantly increased in the HFFD group when comparing the 12^{th} week to the baseline levels (p=0.01) but did not change in the control nor in the BAY-treated group. Meanwhile, no increase was found in HDL nor in FFAs neither when comparing the 12^{th} week to the baseline levels nor when comparing each of the HFFD and HFFD+MIR to the control groups, at the end of the protocol.

The AUC_{Glu}, from the IVGTT, significantly increased when comparing the HFFD and the HFFD+BAY to the control group at the end of the protocol (p=0.007 and p=0.041, respectively). The glycaemia 2h post glucose injection also significantly increased, at the 12^{th} week, in both the HFFD and the HFFD+BAY (p=0.0052 and p= 0.0265, respectively) compared to the control group Meanwhile, we found no difference when comparing the AUC_{Ins} of all groups. On the other hand, HOMA-IR significantly increased amongst individuals of HFFD group (12^{th} week vs. Baseline, p=0.0075) and when comparing the HFFD to the control group at the 12^{th} week (p=0.0086); however, no change was observed amongst individuals of the HFFD+BAY (12^{th} week vs. Baseline) nor when compared to the control group **(Figure 1)**.

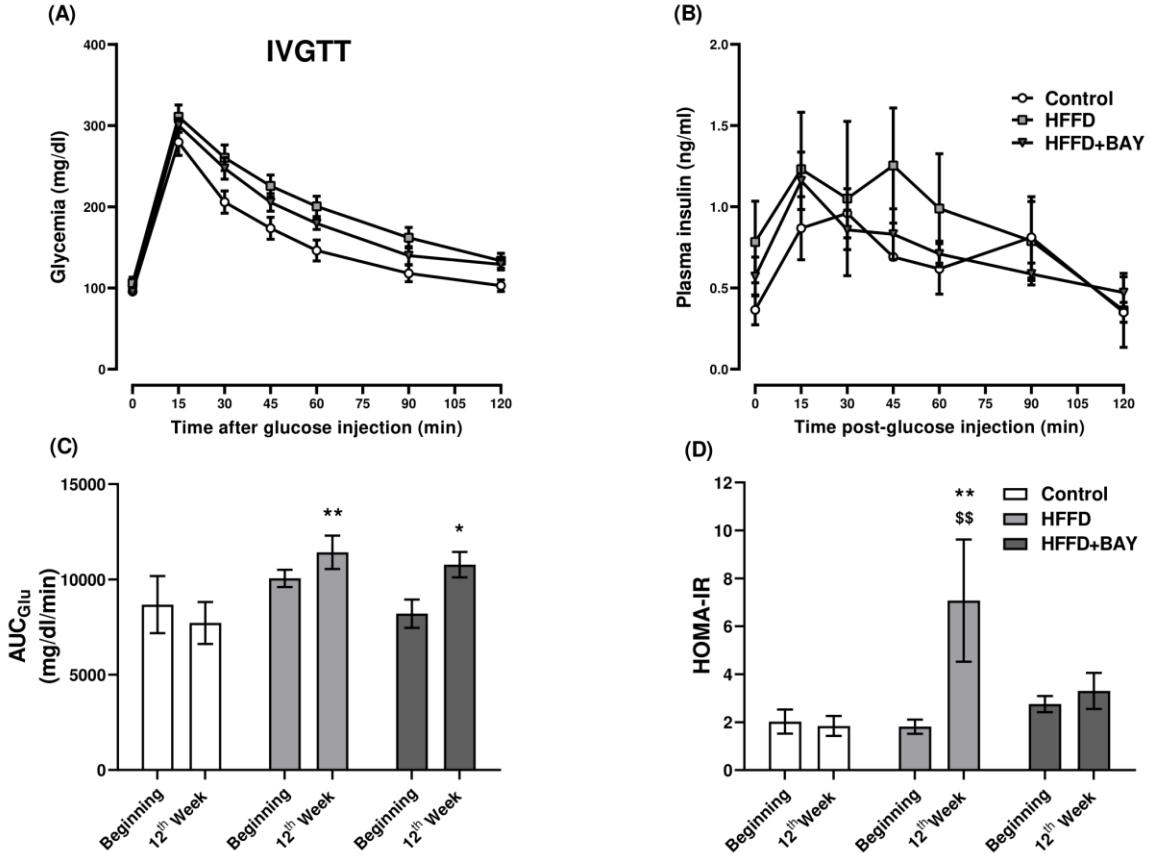

Figure 1: effect of HFFD feeding and long-term treatment with BAY 41-2272 on glucose and insulin metabolism. Glucose metabolism was evaluated by an IVGTT, performed at the end of the protocol (A). After 12 weeks of the protocol, rabbits were intravenously injected with a glucose bolus, both plasma glucose and insulin levels (B) were evaluated, as described in the Methods. AUC_{Glu} of each curve from the IVGTT was calculated to be able to compare the differences between the groups (C). Insulin metabolism was assessed by calculating the homeostasis model assessment of insulin resistance (HOMA-IR) (D). Data were expressed as the mean ± SEM. A two-way Anova test was used for statistical analysis. n=9 for Control, n=12 for HFFD and n=9 for HFFD+BAY. **p< 0.01 and *p< 0.05 for HFFD vs. Control group. $$ p< 0.01 and $p<0.05 12^{th} week vs. Baseline of the protocol.

PWV measurements were performed, to assess the aortic stiffness **(Figure 2)**. Statistical analysis showed a significant difference between the control and HFFD group and between the control and HFFD+BAY group, specifically at the end of the protocol (12^{th} week, p=0.0118, p<0.0032). However, this difference cannot be taken into consideration given that the PWV almost did not increase amongst individuals of both, the HFFD and HFFD+BAY group (no difference between the baseline and the 12^{th} week values).

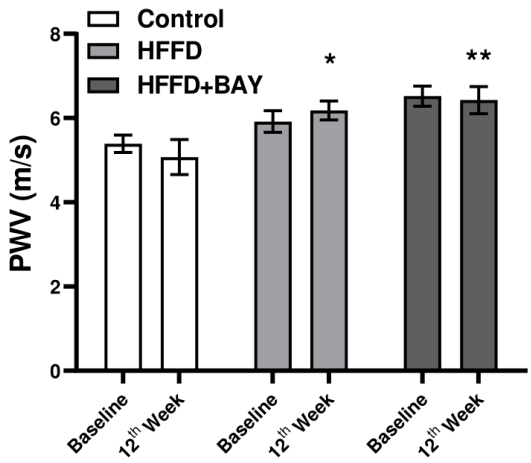

Figure 2: Effect of the HFFD and treatment with BAY 41-2272 on the aortic stiffness. The PWV was measured at the beginning and end of the protocol in order to assess the arterial vascular elasticity. It was calculated using the following formula: PWV (m/s) = $\Delta x/\Delta t$. Data are expressed as mean ± SEM. Repeated measures two-way Anova test was used for statistical analysis. n=9 for control, n=12 for HFFD and n=9 for HFFD+MIR. * $p<0.05$, **$p<0.01$ vs. Control.

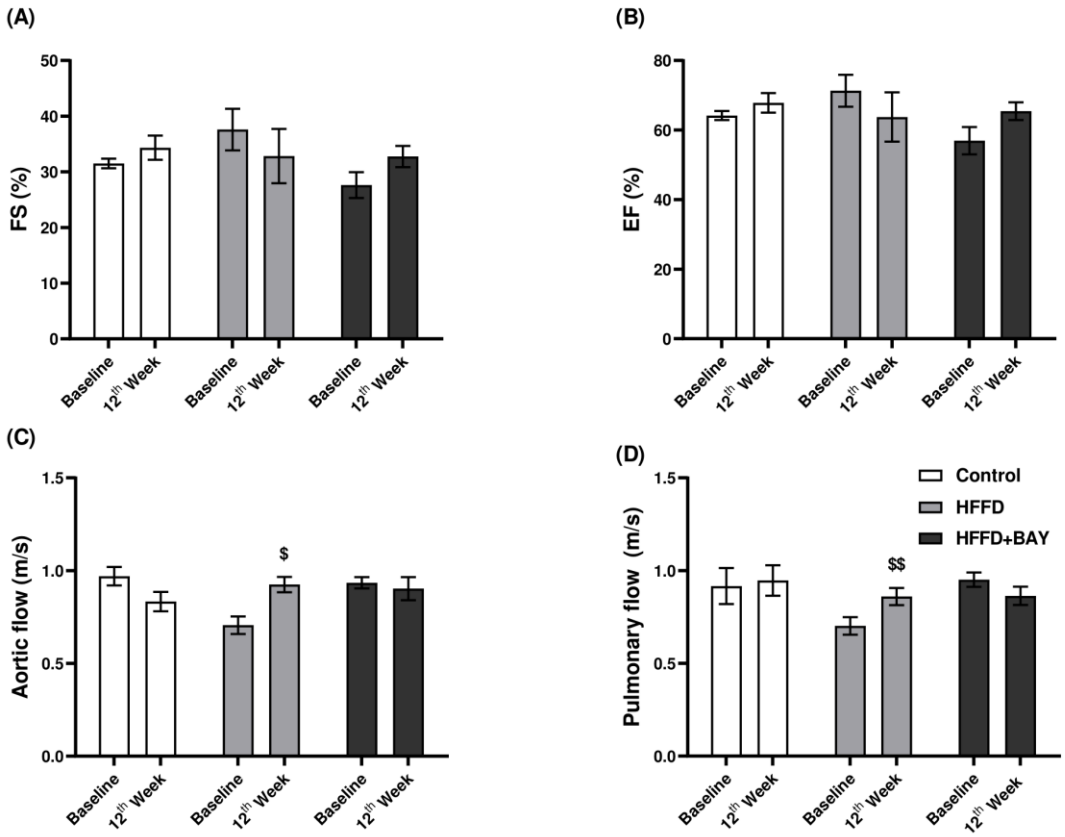

Figure 3: Effect of HFFD and treatment with BAY 41-2272 on LV systolic function, blood flow and LV dilation. Fractional shortening (A), ejection fraction (B), aortic flow (C), pulmonary flow (D). Values are expressed as mean ± SEM. a two-way Anova test was used for statistical analysis. n=3 for Control, n=6 for HFFD and n=9 for HFFD+BAY $p<0.05, $$p<0.01 12th week vs. Baseline.

To evaluate the effect of HFFD-feeding and long-term treatment with BAY 41-2272 on cardiac contractility, we performed echocardiography **(Figure 3)**. Data indicated no modification in LVFS and LVEF nor in end-systolic and end-diastolic diameters (data not shown) indicating no change in LV systolic function nor in LV dilation. Conversely, the aortic and pulmonary flow velocities were both significantly increased in the HFFD group (12th week vs. Baseline, p= 0.0117 and p= 0.0058, respectively) but remained unchanged in the control and BAY 41-2272 group.

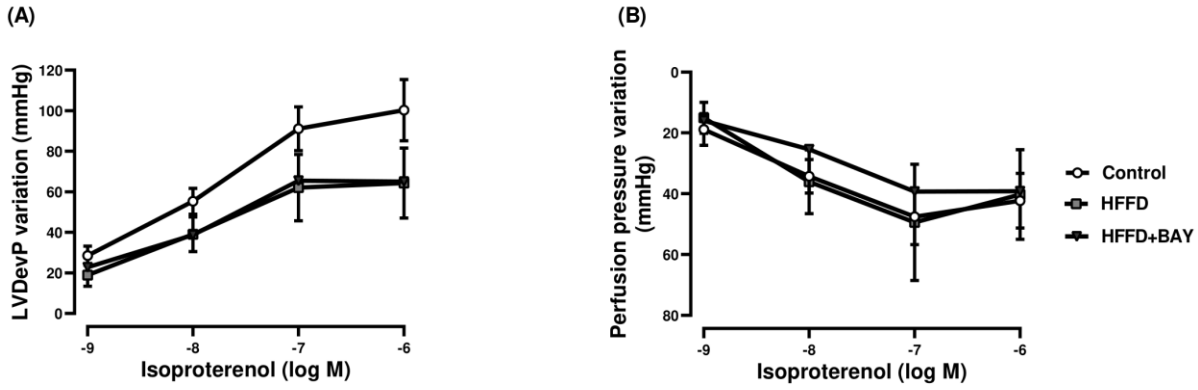

Figure 4: Effects of ß-adrenoceptor stimulation on cardiac contractility and coronary vasodilation Cardiac parameters were assessed after ß-adrenoceptor stimulation by building non-cumulative concentration response-curves to isoproterenol (10^{-9} to 10^{-6}). The LVDevP (A) and perfusion pressure (B), reflecting cardiac inotropy and coronary vasodilation, respectively, were evaluated. Data are represented as mean ± SEM and determined using LME.

To determine the effects of ß-adrenoceptor stimulation on cardiac contractility and coronary vasodilation, non-cumulative concentration response-curves to isoproterenol, were constructed and different parameters were evaluated **(Figure 4)**. The LVDevP was decreased in both the HFFD and HFFD+BAY groups compared to the control group; however, this decrease was not statistically significant. In terms of coronary vasodilation, no change was observed.

To assess the vascular reactivity, whether vasoconstriction or vasorelaxation, cumulative concentration–response curves (CCRCs), were built **(Figure 5)**. Even though there was no change

in the Phe-induced maximal contractile response (E_{max}); the curve significantly shifted to the left (significantly higher pD_2, p=0.0019) in the HFFD compared to the control group. Indicating a higher α_1-AR sensitivity. Meanwhile treatment with mirabegron prevented this shift. The pD2 was significantly lower in the HFFD+BAY group compared the HFFD group (p<0.0001). On the other hand, we observed no difference neither in the maximal response nor in pD_2 values, corresponding to endothelium-dependent Ach-induced relaxation and to endothelium-independent relaxation response to sodium nitroprusside (10^{-10} to 3.10^{-5} M) (data not shown). Meanwhile, the HFFD group showed a significantly lower Ins-induced vasorelaxation (p=0.001 vs. control). When compared to the HFFD group, BAY-treated group did not shown any difference in terms of Ins-mediated vasodilation.

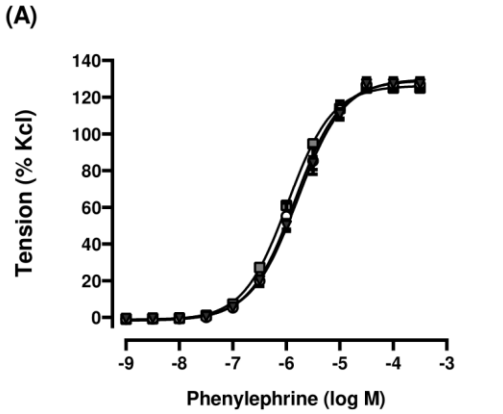

	Control	HFFD	HFFD+MIR
E_{max}	128.93 ± 3.94	126.02 ± 1.40	132.57 ± 2.86
pD_2	5.81 ± 0.07 *	5.96 ± 0.03	-5.75 ± 0.04 $$$$

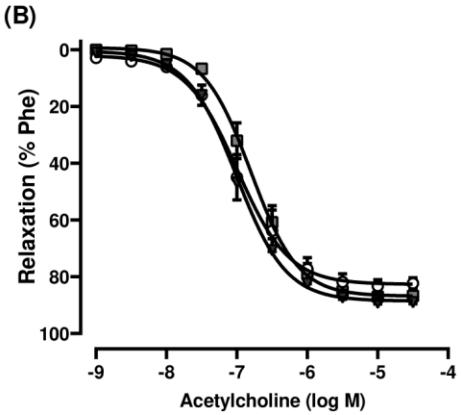

	Control	HFFD	HFFD+MIR
E_{max}	81.90 ± 1.99	86.12 ± 2.45	88.81 ± 2.46
pD_2	6.97 ± 0.14	6.78 ± 0.08	7.00 ± 0.06

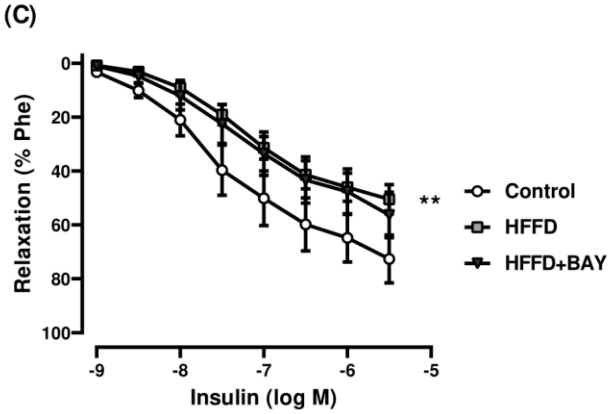

Figure 5: Effect of HFFD feeding and treatment with BAY 41-2272 on carotid vasoreactivity. To assess the vascular reactivity of the carotid artery, cumulative concentration–response curves (CCRCs) were built. Carotid contractile response was evaluated using phenylephrine (Phe, 10^{-10} to 3.10^{-5}) (A). Meanwhile, relaxation responses were assessed by constructing cumulative concentration–relaxation curves to acetylcholine (Ach, 10^{-9} to 3.10^{-5} M) (B) and insulin (Ins, 10^{-9} to 3.10^{-6} M) (C) on phenylephrine-pre-contracted carotid rings. The calculated contraction and relaxation percentages are relative to the maximal changes from the pre-contraction produced by KCL and phenylephrine, respectively. Data are expressed as mean ± SEM and determined using NLME for Phe and Ach and LME for Ins. n=9 for Control, n=12 for HFFD and n=9 for HFFD+BAY. *p<0.05, **< 0.01 Control vs. HFFD; $$$$ p<0.0001 HFFD+BAY vs. HFFD

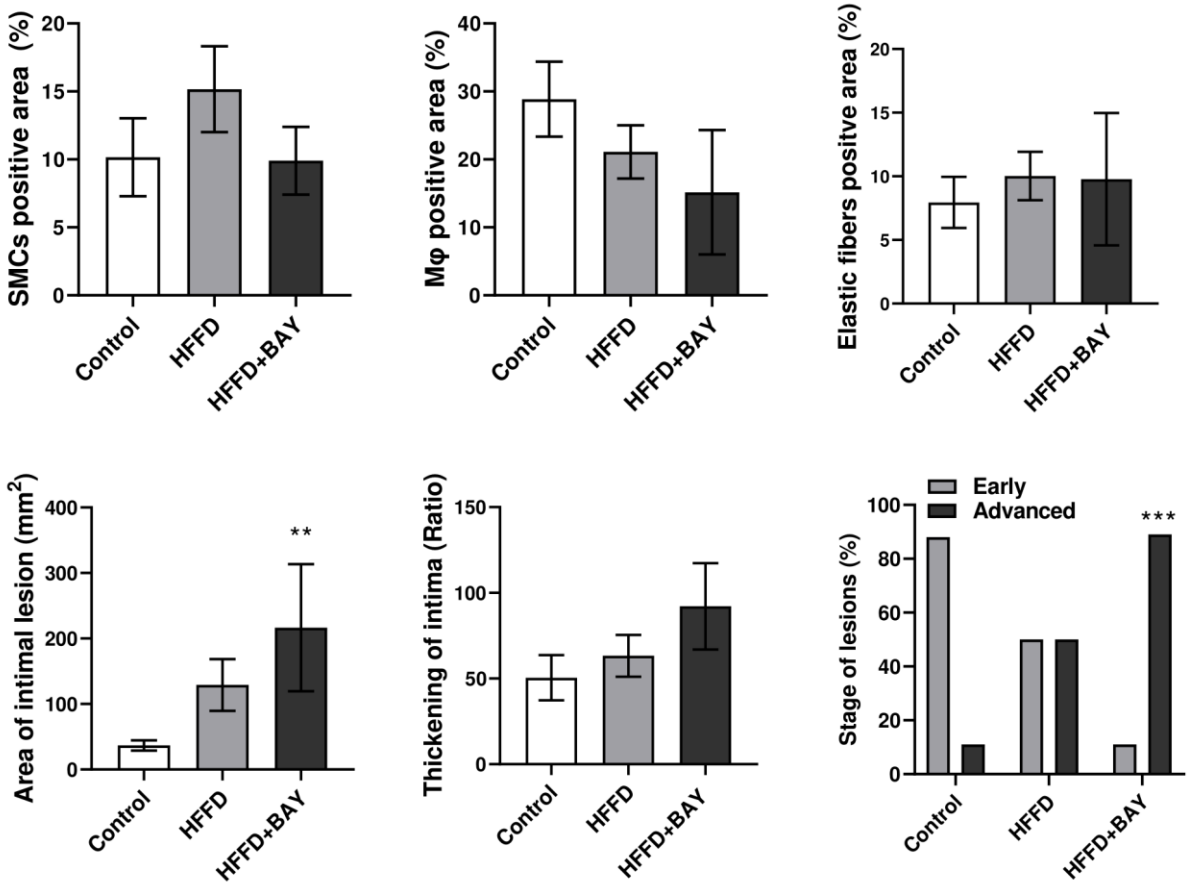

Figure 6: Quantification of aortic atherosclerosis, 12 weeks after HFFD feeding and treatment with mirabegron. Positively immuno-stained area of SMCs, macrophages (Mφ) and elastic fibers were quantified using an image analysis system as described in the Methods. The same image analysis system was used to determine the intimal lesion area whereas the thickening of intima was determined by dividing the area of intimal lesion by the length of media. Plaques were classified into early (type II and III plaques) and advanced (type IV and V plaques) stage lesions. Data in all graphs are represented as the mean ± SEM except for the stage of lesions, which was

expressed in percentages. Statistical analysis was performed using one-way Anova for all parameters except for stage of lesions, for which a Chi square test was used. n=9 for Control, n=12 for HFFD and n=9 for HFFD+BAY. *p<0.05, **p<0.01 HFFD+BAY vs. Control.

No difference, between groups, was observed regarding the average thickening of the intima (Area of intimal lesion/length of media). The area of intimal lesion increased in both the HFFD and the HFFD+BAY groups compared to the control group. However, the increase was only significant in the HFFD+BAY (p=0.0045 vs. Control). SMCs (evaluated using an anti-HHF35 antibody), Mφ (evaluated using an anti-RAM11 antibody) and elastic fibers (evaluated using the Orceine stain) were not significantly different neither when comparing the HFFD to the control group nor when comparing the HFFD+BAY to the HFFD group. When comparing early versus advanced lesions, the difference was only significant in the HFFD+BAY (p=0.0013 vs. Control). Nevertheless we also observed a clear trend towards advanced lesions in the HFFD (p=0.0679 vs. Control) **(Figure 6)**.

Table 2: Classification of atheroma plaques. The presence of extracellular lipid, fibrous cap, mineralization, lipid core and collagen's deposition (using green Masson's trichrome stain) were graded using a semi-quantitative scale from 0 to 4. Type of plaques were classified according to the guidelines of the American Heart Association. The results were expressed as frequency and percentage. Statistical analysis was performed using a Chi-square test.

Histologic parameter evaluated	**Classifica-tion**	**Control (n=9)**	**HFFD (n=12)**	**HFFD+BAY (n=9)**	**p value Control vs. HFFD**	**p value HFFD+BAY vs. HFFD**
Extracellular lipids	Absence	3 (33.3%)	4 (33.3%)	0	0.0567	0.2349
	Grade 1	5 (55.6%)	1 (8.3%)	1 (11.1%)		
	Grade 2	1 (11.1%)	3 (25.0%)	2 (22.2%)		
	Grade 3	0	4 (33.3%)	6 (66.7%)		
	Grade 4	0	0	0		
Fibrous cap	Absence	7 (77.8%)	6 (50.0%)	0	0.0502	0.0198 *
	Grade 1	2 (22.2%)	0	3 (33.3%)		
	Grade 2	0	5 (41.7%)	6 (66.7%)		
	Grade 3	0	1 (8.3%)	0		

	Grade 4	0	0	0		
Mineralization	Absence	8 (88.9%)	9 (75.0%)	1 (11.1%)	0.43	0.0126 *
	Grade 1	1 (11.1%)	3 (25.0%)	7 (77.8%)		
	Grade 2	0	0	1 (11.1%)		
	Grade 3	0	0	0		
	Grade 4	0	0	0		
Lipid core	Absence	6 (66.7%)	5 (41.7%)	0	0.2753	0.1632
	Grade 1	2 (22.2%)	1 (8.3%)	2 (22.2%)		
	Grade 2	1 (11.1%)	4 (33.3%)	5 (55.6%)		
	Grade 3	0	2 (16.7%)	2 (22.2%)		
	Grade 4	0	0	0		
Collagen deposition	Absence	1 (11.1%)	0	0	0.1888	0.2531
	Grade 1	1 (11.1%)	0	0		
	Grade 2	4 (44.4%)	2 (16.7%)	3 (33.3%)		
	Grade 3	2 (22.2%)	7 (58.3%)	2 (22.2%)		
	Grade 4	1 (11.1%)	3 (25.0%)	4 (44.4%)		
Type of plaque	No plaque	1 (11.1%)	0	0	0.09	0.1656
	Type II	4 (44.4%)	4 (33.3%)	0		
	Type III	3 (33.3%)	2 (16.7%)	1 (11.1%)		
	Type IV	1 (11.1%)	0	1 (11.1%)		
	Type V	0	6 (50.0%)	7 (77.8%)		

Extracellular lipid deposition and Fibrous cap presence were almost significantly increased (p=0.0567 and p=0.0502, respectively) in the HFFD group compared to the control group. The extent of mineralization was not significantly different between the HFFD group and the control group. There was no statistically significant difference between the two groups in terms of lipid core severity. However, more advanced grades were clearly observed in the HFFD group. Collagen deposition was not significantly different between the two groups. Nevertheless, marked and severe collagen deposition were frequently observed in the HFFD group and rarely in the control group. Regarding the type of plaques, most of the present plaques in the control group were either

type II (4/9) or type III (3/9) and no type V plaques were observed in contrast with the HFFD group in which 50% of the plaques (6/12) were type V plaques. In the current study, only type II, III, IV and V lesions were observed. There was significant difference between the HFFD group and the group that received the BAY 41-2272 treatment in regards to fibrous cap presence and extent of mineralization (p=0.0198 and p=0.0126, respectively) but not in terms of lipid core presence and severity, collagen deposition and plaque types **(Table2)**.

Table 3: cGMP levels determination in thoracic aorta, heart and adipose tissue

	Groups		
cGMP	Control (n=9)	HFFD (n=12)	HFFD+BAY (n=9)
Thoracic aorta (pmol/mg of protein)	3.27 ± 1.07	5.69 ± 1.58	2.43 ± 0.83
Heart tissue (pmol/mg of protein)	1.34 ± 0.30	1.79 ± 0.35	2.14 ± 0.62
Adipose tissue (fmol/mg of protein)	0.0506 ± 0.0050	0.0465 ± 0.0089	0.0681 ± 0.0089

Data are expressed as mean ± SEM. One-way ANOVA test was used for statistical analysis.

cGMP intracellular concentrations were determined in thoracic aorta, heart and adipose tissue samples. No difference between the groups was observed in any of the tissues **(Table 3)**.

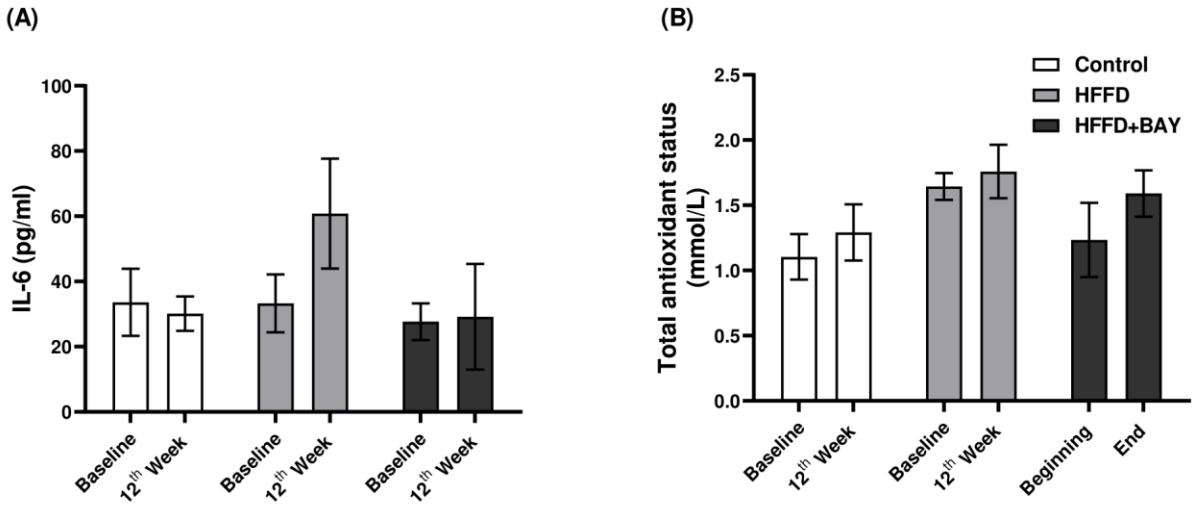

Figure 7: Interleukin-6 (A) and total antioxidant status (B) measurements. Data are expressed as mean ± SEM. A two-way Anova test was used for statistical analysis. n=9 for Control, n=12 for HFFD and n=9 for HFFD+MIR.

We assessed the levels of two main inflammatory cytokines, tumor necrosis factor-alpha (TNF-α) and interleukin-6 (IL-6). We also measured the total antioxidant status (TAS) **(Figure 7)**. We were not able to detect TNF-α concentrations. We observed a strong tendency of increase in the Il-6 concentrations of the HFFD-fed group compared to the control group at the end of the protocol (at the12th week, p= 0.069). Meanwhile, no change was observed in the TAS levels.

Discussion

In the current study, we investigated whether chronic treatment with the BAY 41-2272 would counteract or prevent the establishment of metabolic and cardiovascular disturbances that are associated with the combination, of two main components of the MetS, dyslipidemia-IR. We were able to produce this combination by feeding a HFFD (to induce IR), to a spontaneously dyslipidaemic rabbit model. Our purpose was to induce insulin resistance rather than obesity, which might be a confounding factor. Thus we used a HFFD that, compared to the standard chow, is rich in sugar and fat but contains less protein and fibers [24].

We were able to show that after 12 weeks of HFFD feeding, these rabbits exhibited increased fasting insulin, HOMA-IR, TG and cholesterol (TC and LDL-C) levels as well as impaired glucose tolerance, compared to their counterparts in the control group. We also showed that long-term

treatment (12 weeks) with BAY 41-2272 exhibited global improvement of the metabolic status. It prevented weight gain and increased TG levels, improved insulin sensitivity and endothelial function.

Even though both the weight and abdominal circumference parameters significantly increased in both HFFD and control, groups (12^{th} week vs. Baseline); at the end of the protocol the increase was not higher in the HFFD compared to the control group. Therefore, this increase was not attributed to the HFFD-feeding. As mentioned earlier, the HFFD that we used is rich in fat and sugar but with less protein and fibers. This might explain the absence of excessive weight gain. Whereas, after 12 weeks of treatment with BAY 41-2272 along with HFFD-feeding, we did not observe any increase in weight nor in abdominal circumference as seen in both the control and HFFD groups. This suggests that BAY 41-2272 stabilized and prevented the increase in both the weight and abdominal circumference. This is in consistence with the findings of Hoffman et al. who demonstrated that BAY 41-8543 (in mice), a stimulator of sGC protects against diet-induced weight gain, induces weight loss in established obesity, and also improves the diabetic phenotype through mechanisms that involved enhancement of lipid uptake into BAT and an increase in whole-body EE [31]. In addition, several studies have demonstrated that increased cGMP promotes healthy expansion and browning of WAT [14]–[16]. The browning of WAT has been reported to promote EE and counterbalance the positive energy balance associated with over-nutrition thereby leading to reduced obesity [13],[32]. Moreover, treatment with sildenafil citrate, an indirect activator of the cGMP pathway [33] was reported to reduce body weight in humans [9] and rodents [7],[11]. We determined the cGMP levels in the adipose tissue; however, we found no difference between groups. Therefore, this improvement might not be related to the NO-cGMP pathway. Accordingly, further investigation is needed to determine the possible mechanisms behind weight stabilization.

In addition, individuals that were subjected to the HFFD exhibited hyperinsulinemia, increased HOMA-IR, decreased glucose tolerance (AUC_{Glu}) but no change in fasting glycaemia, compared to both their baseline levels and their counterparts in the control group. Whereas those that were additionally treated with BAY 41-2272 showed no increase in their fasting insulin nor in their HOMA-IR levels. This indicates that BAY 41-2272 was able to counteract the decreased insulin sensitivity induced by HFFD feeding. Treatment with sildenafil, a drug that, similarly to BAY 41-

2272, increases the bioavailability of cGMP [33] has proven to improve insulin action in a mouse model of diet-induced obesity and insulin resistance [7]. During IR, endothelial-mediated vasodilation is compromised leading to decreased delivery of glucose and insulin to their target organs as reviewed by Barett et al. [34]. Therefore, the improved insulin sensitivity found in our study could be related to sGC-cGMP-stimulated vasodilation that lead to enhanced blood flow and thereby to improved glucose and insulin delivery to insulin sensitive tissues [35]. Moreover, cGMP has proven to increase insulin sensitivity in skeletal muscle by promoting the translocation of glucose transporter 4 to the cell membrane [36]. In the current study we found no improvement in the glucose tolerance. This discordance may have been because the amelioration of insulin sensitivity precedes that of glucose tolerance and that a longer treatment duration would have been needed. Moreover, insulin's action involves glucose uptake and suppression of glucose production; thus, it might be argued that even if one or both these actions increased with improved insulin sensitivity, the concomitant exposure to the HFFD, still impaired the glucose tolerance.

It has been well established that low-grade inflammation plays an important role in mediating insulin resistance during MetS. Therefore, we measured two main inflammatory cytokines, TNF-alpha and IL-6 levels, that were proven to decrease insulin sensitivity [37],[38]. We found no difference between groups in terms of IL-6 levels (TNF-alpha levels were undetectable) indicating that IR in WHHL rabbits involve likely cytokines-independent-component.

Our results showed that TG levels were significantly increased amongst HFFD-group individuals but not in the control nor in the HFFD+BAY groups. This indicates that treatment with BAY 41-2272 prevented the increase of TG levels. Several studies have demonstrated that activation of the NO-cGMP pathway promotes lipolysis and stimulate thermogenic pathways, leading to decreased WAT-mediated fat storage and to increased BAT-mediated energy expenditure, respectively [12],[13]. Moreover, it has been proposed that a lower TG level could result from chronic stimulation of BAT that leads to increased triglyceride-rich lipoproteins consumption [39],[40]. In fact, it has been well established that BAT uptakes and combusts high amounts of fatty acids, leading to decreased plasma triglyceride levels and thereby improves obesity [41]. Which also explains the stabilized weight observed in our study.

Our results are in consistence with the findings of El-Mahmoudy et al. who found that treatment with sildenafil significantly decreased the serum TGs. In their study, they also found a decrease in cholesterol, HDL-C and LDL-C concentrations of rats fed a fat-enriched diet, in response to sildenafil treatment [42]. Those results are not in agreement with our findings since we found no improvement in TC nor in LDL-C levels and no change in HDL-C levels, in response to BAY 41-2272 treatment. Even though, BAT activation has been documented to stimulate carbohydrates and cholesterol uptake, and thereby to reduce hypercholesterolemia and protect from atherosclerosis development [41],[43]. In addition, besides being associated with decreased NO bioavailability, atherosclerosis has also been described to be connected to alterations in signal-transduction components downstream of NO, such as sGC and cGMP. Therefore, sGC has been proposed as an attractive, novel pharmacological target in the treatment of atherosclerosis [44]. However, in the current study, treatment with BAY 41-2272 did not counteract the increase in both TC and LDL-C that resulted from HFFD feeding nor improved atherosclerosis. Moreover, our results showed that BAY 41-2272-treated rabbits displayed larger plaques and more advanced lesions when compared to the control group but showed almost similar lesions as the HFFD-fed group. This result is in contrast with the findings of Balarini et al. who demonstrated that chronic treatment with sildenafil reduced the progression of atherosclerosis in large vessels of western diet fed-*ApoE*$^{-/-}$mice, models that, like Watanabe rabbit, develop spontaneous hypercholesterolemia. In their study Balarini et al. were able to prove that this improvement is related to enhanced activation of the NO pathway [33]. It might be that a longer duration of treatment might have been needed in order to be able to witness an improvement in atherosclerosis.

In the current study, PWV values, reflecting the arterial stiffness, significantly increased in both the HFFD and HFFD+BAY groups, however we could not consider these results given that the PWV almost did not change amongst individuals of both the HFFD and HFFD+BAY group (no difference between the baseline and the 12th week values). Moreover, atherosclerosis has been described to lead to increased arterial stiffness through thickening and stiffening of the arterial wall [45],[46]. Discrepancies between atheroma plaques evaluation and PWV results might be related to the early stage of disease progression; as reported by katsuda et al., the protocol in our study only lasted for 12 weeks and the rabbits were young (less than 12 months of age) [47]. Thus,

it is highly possible that the evolution of increased arterial stiffness needs a long period of time before it becomes detectable through PWV measurements.

It has been proposed that the hyperinsulinemia encountered during IR and dyslipidemia leads to sympathetic nervous system (SNS) up-regulation [48],[49]; and that SNS overactivation in turn might lead to decreased contractile responsiveness to β-stimulation [50]. We evaluated the effects of *ex vivo* β-AR stimulation on cardiac inotropy and coronary vasodilation. Our results showed a decrease in positive inotropy in both the HFFD and HFFD+BAY groups with no change in coronary vasodilation. This suggests that the HFFD-induced IR was responsible for a decreased β_1-AR reactivity (i.e., modification in β-AR expression and/or β-ARs-linked mechanisms) that was not improved in response to treatment with BAY 41-2272.

Our echocardiographic data showed no difference in LVFS, LVEF, end-systolic and end-diastolic diameters indicating no change in LV systolic function nor in LV dilation, in consistence with our *ex vivo* results. However, an increase in both the aortic and pulmonary flow velocities was seen in the HFFD group. This increase is reported to be either related to increase flow through the valves or to decreased compliance of the pulmonary and aortic arteries in the HFFD group [51],[52]. The former is less likely to be accurate since the LVFS and LVEF were not changed. The latter cannot be confirmed either due to our results regarding the unchanged PWV.

Both IR and dyslipidemia has been associated to endothelial dysfunction (ED) [49],[53],[54]. ED is not only associated with impaired vasodilation but might as well be related to increased vasoconstriction due to enhanced vascular sensitivity or production of endothelial-dependent vasoconstricting factors [55]. Thus, we evaluated the vascular reactivity (vasoconstriction and vasorelaxation) of the carotid artery. HFFD-feeding enhanced the vascular reactivity to Phe in terms of pD_2, indicating an increase of α_1-AR sensitivity in the HFFD group. HFFD-induced IR enhanced the vascular reactivity to Phe in terms of pD_2, indicating heightened α_1-AR sensitivity. There is evidence in support of hyperinsulinemia/IR promoting sympathetic nerve activity [48]. Therefore, HFFD-induced IR appears to evoke an exaggerated α_1-AR sensitivity in the HFFD-fed Watanabe rabbits, due to SNS overactivation. Hyperlipidemia has been reported to decrease the NO production [56],[57]. Thus the heightened α_1-AR sensitivity might also be due to reduced NO bioavailability and/or increased oxidative stress causing an enhanced vascular adrenergic

responsiveness [58]. In support of this hypothesis, we evaluated the TAS levels in all groups but found no difference between groups. This increase was counteracted in response to treatment with BAY 41-2272, since the pD_2 was significantly decreased compared to the HFFD group. This suggests that treatment with BAY 41-2272 prevented the phenylephrine hypersensitivity induced by the HFFD probably by modulating the aortic reactivity *via* a change in NO-cGMP intracellular level, that diminishes the sensitivity of the α_1-AR -linked mechanisms [59],[60]. In this regard, we determined the tissular aortic cGMP levels, but found no significant difference between groups, the cGMP level neither decreased in the HFFD group nor increased in response to BAY 41-2272 treatment. Therefore, further investigation is needed in support of our hypothesis.

In contrast, the HFFD did not affect relaxation to SNP nor to Ach, meaning that neither endothelium-independent nor endothelium-dependent vasorelaxation were affected. However, we found that HFFD impaired insulin-induced vasorelaxation. This is most probably due to the IR state that compromised the vasodilatory effect of insulin as found by others [61],[62]. In fact, during IR there is selective insulin resistance in PI3K-Akt-NO signaling with intact or heightened MAPK-ET1 signaling, that results in impaired NO-mediated vasodilation and augmented ET-1-mediated vasoconstriction in response to insulin [35],[63]. This result is in accordance with the findings of a study done by kim et al., who found that diet-induced IR impaired Ins-mediated vasorelaxation [64]. In the current study, we found no improvement in Ins-induced vasorelaxation in response to BAY 41-2272 treatment. Nevertheless, this treatment improved endothelial function by counteracting the HFFD-induced Phe-hypersensitivity.

Conclusion

In the current study, we found that BAY 41-2272 decreased weight gain, improved insulin sensitivity and stabilized TG levels and prevented hypersensitivity to α_1-AR-mediated vasoconstriction. We demonstrated that long-term treatment with BAY 41-2272 shows a promising improvement in the metabolic status and endothelial function of HFFD-fed WHHL rabbits. Accordingly, our results support the investigation of BAY 41-2272 as a pharmacological mean for the management of MetS.

References

[1] Y. Rochlani, N. V. Pothineni, S. Kovelamudi, and J. L. Mehta, "Metabolic syndrome: pathophysiology, management, and modulation by natural compounds," *Ther. Adv. Cardiovasc. Dis. Rev.*, vol. 11, no. 8, pp. 215–225, 2017, doi: 10.1177/1753944717711379.

[2] P. W. F. Wilson, R. B. D'Agostino, H. Parise, L. Sullivan, and J. B. Meigs, "Metabolic syndrome as a precursor of cardiovascular disease and type 2 diabetes mellitus," *Circulation*, vol. 112, no. 20, pp. 3066–3072, Nov. 2005, doi: 10.1161/CIRCULATIONAHA.105.539528.

[3] K. Obunai, S. Jani, and G. D. Dangas, "Cardiovascular Morbidity and Mortality of the Metabolic Syndrome," *Med. Clin. North Am.*, vol. 91, no. 6, pp. 1169–1184, Nov. 2007, doi: 10.1016/J.MCNA.2007.06.003.

[4] A. Alkerwi, A. Albert, and M. Guillaume, "Cardiometabolic Syndrome," in *Cardiovascular Risk Factors*, 2012, pp. 161–189.

[5] M. D. Jensen, D. H. Ryan, C. M. Apovian, J. D. Ard, A. G. Comuzzie, *et al.*, "2013 AHA/ACC/TOS guideline for the management of overweight and obesity in adults: A report of the American College of cardiology/American Heart Association task force on practice guidelines and the obesity society," *Circulation*, vol. 129, no. 25 SUPPL. 1. Lippincott Williams and Wilkins, pp. S102–S138, Jun. 24, 2014, doi: 10.1161/01.cir.0000437739.71477.ee.

[6] J. Rask Larsen, L. Dima, C. U. Correll, and P. Manu, "The pharmacological management of metabolic syndrome," *Expert Rev. Clin. Pharmacol.*, vol. 11, no. 4, pp. 397–410, 2018, doi: 10.1080/17512433.2018.1429910.

[7] J. E. Ayala, D. P. Bracy, B. M. Julien, J. N. Rottman, P. T. Fueger, *et al.*, "Chronic treatment with sildenafil improves energy balance and insulin action in high fat-fed conscious mice," *Diabetes*, vol. 56, no. 4, pp. 1025–1033, Apr. 2007, doi: 10.2337/db06-0883.

[8] D. Behr-Roussel, A. Oudot, S. Caisey, O. L. E. Coz, D. Gorny, *et al.*, "Daily Treatment with Sildenafil Reverses Endothelial Dysfunction and Oxidative Stress in an Animal Model of Insulin Resistance," *Eur. Urol.*, vol. 53, no. 6, pp. 1272–1281, Jun. 2008, doi: 10.1016/j.eururo.2007.11.018.

[9] A. Salih Sahib, H. Abdulhafith Al-biati, S. Hussein Ismail, F. Abdul Kareem Kazaal, and S. Al-Rubaie, "Effects of sildenafil on lipid profile and glycemic control in patients with type 2 diabetes mellitus and metabolic syndrome. IJBCP International Journal of Basic & Clinical Pharmacology Effects of sildenafil on lipid profile and glycemic control in patie," *Int. J. Basic Clin. Pharmacol.*, vol. 6, pp. 1048–1051, 2014, doi: 10.5455/2319-2003.ijbcp20141217.

[10] C. E. Ramirez, H. Nian, C. Yu, J. L. Gamboa, J. M. Luther, *et al.*, "Treatment with Sildenafil Improves Insulin Sensitivity in Prediabetes: A Randomized, Controlled Trial," *J. Clin. Endocrinol. Metab.*, vol. 100, no. 12, pp. 4533–4540, Dec. 2015, doi: 10.1210/jc.2015-3415.

[11] Y. Doghri, F. Chetaneau, M. Rhimi, A. Kriaa, V. Lalanne, *et al.*, "Sildenafil citrate long-term treatment effects on cardiovascular reactivity in a SHR experimental model of metabolic syndrome," *PLoS One*, vol. 14, no. 11, Nov. 2019, doi: 10.1371/journal.pone.0223914.

[12] A. M. Cypess and C. R. Kahn, "Brown fat as a therapy for obesity and diabetes," *Curr. Opin. Endocrinol. Diabetes Obes.*, vol. 17, no. 2, pp. 143–149, Apr. 2010, doi: 10.1097/MED.0b013e328337a81f.

[13] G. W. Kim, J. E. Lin, E. S. Blomain, and S. A. Waldman, "Antiobesity pharmacotherapy: New drugs and emerging targets," *Clin. Pharmacol. Ther.*, vol. 95, no. 1, pp. 53–66, Jan. 2014, doi: 10.1038/clpt.2013.204.

[14] M. M. Mitschke, L. S. Hoffmann, T. Gnad, D. Scholz, K. Kruithoff, *et al.*, "Increased cGMP promotes healthy expansion and browning of white adipose tissue," *FASEB J.*, vol. 27, no. 4, pp. 1621–1630, Apr. 2013, doi: 10.1096/fj.12-221580.

[15] B. Cannon and J. Nedergaard, "Brown Adipose Tissue: Function and Physiological Significance," 2004, doi: 10.1152/physrev.00015.2003.-The.

[16] A. Pfeifer, A. Kilić, and L. S. Hoffmann, "Regulation of metabolism by cGMP," *Pharmacology and Therapeutics*, vol. 140, no. 1. Elsevier Inc., pp. 81–91, Oct. 01, 2013, doi: 10.1016/j.pharmthera.2013.06.001.

[17] O. V. Evgenov, P. Pacher, P. M. Schmidt, G. Haskó, H. H. H. W. Schmidt, *et al.*, "NO-independent stimulators and activators of soluble guanylate cyclase: Discovery and therapeutic potential," *Nature Reviews Drug Discovery*, vol. 5, no. 9. NIH Public Access, pp. 755–768, Sep. 2006, doi: 10.1038/nrd2038.

[18] G. Boerrigter and J. C. Burnett, "Nitric Oxide-Independent Stimulation of Soluble Guanylate Cyclase with BAY 41-2272 in Cardiovascular Disease," *Cardiovasc. Drug Rev.*, vol. 25, no. 1, pp. 30–45, Apr. 2007, doi: 10.1111/j.1527-3466.2007.00003.x.

[19] N. O. Rizzo, E. Maloney, M. Pham, I. Luttrell, H. Wessell, *et al.*, "Reduced Nitric Oxide/cGMP Signaling Contributes to Vascular Inflammation and Insulin Resistance Induced by High Fat Feeding," *Arter. Thromb Vasc Biol*, vol. 30, no. 4, pp. 758–765, 2010, doi: 10.1161/ATVBAHA.109.199893.

[20] K. Johann, M. C. Reis, L. Harder, B. Herrmann, S. Gachkar, *et al.*, "Effects of sildenafil treatment on thermogenesis and glucose homeostasis in diet-induced obese mice," *Nutr. Diabetes*, vol. 8, no. 1, p. 9, Dec. 2018, doi: 10.1038/s41387-018-0026-0.

[21] C. Belge, J. Hammond, E. Dubois-Deruy, B. Manoury, J. Hamelet, *et al.*, "Enhanced expression of β3-adrenoceptors in cardiac myocytes attenuates neurohormone-induced hypertrophic remodeling through nitric oxide synthase," *Circulation*, vol. 129, no. 4, pp. 451–462, Jan. 2014, doi: 10.1161/CIRCULATIONAHA.113.004940.

[22] M. Park, P. Sandner, and T. Krieg, "cGMP at the centre of attention: emerging strategies for activating the cardioprotective PKG pathway," *Basic Research in Cardiology*, vol. 113, no. 4. Dr. Dietrich Steinkopff Verlag GmbH and Co. KG, Jul. 01, 2018, doi:

10.1007/s00395-018-0679-9.

[23] E. J. Tsai and D. A. Kass, “Cyclic GMP signaling in cardiovascular pathophysiology and therapeutics,” *Pharmacology and Therapeutics*, vol. 122, no. 3. pp. 216–238, Jun. 2009, doi: 10.1016/j.pharmthera.2009.02.009.

[24] B. Ning, X. Wang, Y. Yu, A. B. Waqar, Q. Yu, *et al.*, “High-fructose and high-fat diet-induced insulin resistance enhances atherosclerosis in Watanabe heritable hyperlipidemic rabbits,” *Nutr. Metab.*, vol. 12, no. 1, p. 30, Dec. 2015, doi: 10.1186/s12986-015-0024-3.

[25] M. Ibrahim, I. A. Ahmed, M. A. Mikail, A. A. Ishola, S. Draman, *et al.*, “Baccaurea angulata fruit juice reduces atherosclerotic lesions in diet-induced Hypercholesterolemic rabbits,” *Lipids Health Dis.*, vol. 16, no. 1, p. 134, Jul. 2017, doi: 10.1186/s12944-017-0526-2.

[26] O. J. Arias-Mutis, V. G. Marrachelli, A. Ruiz-Saurí, A. Alberola, J. M. Morales, *et al.*, “Development and characterization of an experimental model of diet-induced metabolic syndrome in rabbit,” pp. 1–18, 2017, doi: 10.1371/journal.pone.0178315.

[27] T. Helfenstein, F. A. Fonseca, S. S. Ihara, J. M. Bottós, F. T. Moreira, *et al.*, “Impaired glucose tolerance plus hyperlipidaemia induced by diet promotes retina microaneurysms in New Zealand rabbits,” *Int. J. Exp. Pathol.*, vol. 92, no. 1, pp. 40–49, Feb. 2011, doi: 10.1111/j.1365-2613.2010.00753.x.

[28] F. Tissier, Y. Mallem, C. Goanvec, R. Didier, T. Aubry, *et al.*, “A non-hypocholesterolemic atorvastatin treatment improves vessel elasticity by acting on elastin composition in WHHL rabbits,” *Atherosclerosis*, vol. 251, pp. 70–77, Aug. 2016, doi: 10.1016/j.atherosclerosis.2016.05.039.

[29] H. C. Stary, A. B. Chandler, R. E. Dinsmore, V. Fuster, S. Glagov, *et al.*, “A Definition of Advanced Types of Atherosclerotic Lesions and a Histological Classification of Atherosclerosis,” *Circulation*, vol. 92, no. 5, pp. 1355–1374, Sep. 1995, doi: 10.1161/01.CIR.92.5.1355.

[30] C. Thorin, M. Y. Mallem, J. Noireaud, M. Gogny, and J.-C. Desfontis, “Nonlinear mixed effects models applied to cumulative concentration-response curves,” *J. Pharm. Pharmacol.*, vol. 62, no. 3, pp. 339–345, Mar. 2010, doi: 10.1211/jpp.62.03.0008.

[31] L. S. Hoffmann, J. Etzrodt, L. Willkomm, A. Sanyal, L. Scheja, *et al.*, “Stimulation of soluble guanylyl cyclase protects against obesity by recruiting brown adipose tissue,” *Nat. Commun.*, vol. 6, no. 1, pp. 1–9, May 2015, doi: 10.1038/ncomms8235.

[32] L. P. Kozak and R. A. Koza, “The genetics of brown adipose tissue.,” *Progress in molecular biology and translational science*, vol. 94. Academic Press, pp. 75–123, Jan. 01, 2010, doi: 10.1016/b978-0-12-375003-7.00004-2.

[33] C. M. Balarini, M. A. Leal, I. B. S. Gomes, T. M. C. Pereira, A. L. Gava, *et al.*, “Sildenafil restores endothelial function in the apolipoprotein E knockout mouse,” *J. Transl. Med.*, vol. 11, no. 1, p. 3, Jan. 2013, doi: 10.1186/1479-5876-11-3.

[34] E. J. Barrett, H. Wang, C. T. Upchurch, and Z. Liu, “Insulin regulates its own delivery to skeletal muscle by feed-forward actions on the vasculature,” *American Journal of*

Physiology - Endocrinology and Metabolism, vol. 301, no. 2. American Physiological Society, p. E252, Aug. 2011, doi: 10.1152/ajpendo.00186.2011.

[35] A. A. Arce-Esquivel, K. A. Bunker, R. C. Mikus, and M. H. Laughlin, "Insulin Resistance and Endothelial Dysfunction: Macro and Microangiopathy," in *Type 2 Diabetes*, InTech, 2013.

[36] D. Roy, M. Perreault, and A. Marette, "Insulin stimulation of glucose uptake in skeletal muscles and adipose tissues in vivo is NO dependent," *Am. J. Physiol. - Endocrinol. Metab.*, vol. 274, no. 4 37-4, 1998, doi: 10.1152/ajpendo.1998.274.4.e692.

[37] M. Rydén and P. Arner, "Tumour necrosis factor-α in human adipose tissue - From signalling mechanisms to clinical implications," in *Journal of Internal Medicine*, Oct. 2007, vol. 262, no. 4, pp. 431–438, doi: 10.1111/j.1365-2796.2007.01854.x.

[38] P. Pazos, L. Lima, F. F. Casanueva, C. Diéguez, and M. C. García, "Interleukin 6 Deficiency Modulates the Hypothalamic Expression of Energy Balance Regulating Peptides during Pregnancy in Mice," *PLoS One*, vol. 8, no. 8, p. 72339, Aug. 2013, doi: 10.1371/journal.pone.0072339.

[39] A. Bartelt, O. T. Bruns, R. Reimer, H. Hohenberg, H. Ittrich, *et al.*, "Brown adipose tissue activity controls triglyceride clearance," *Nat. Med.*, vol. 17, no. 2, pp. 200–206, Feb. 2011, doi: 10.1038/nm.2297.

[40] G. Hoeke, S. Kooijman, M. R. Boon, P. C. N. Rensen, and J. F. P. Berbeé, "Role of Brown Fat in Lipoprotein Metabolism and Atherosclerosis," *Circulation Research*, vol. 118, no. 1. Lippincott Williams and Wilkins, pp. 173–182, Jan. 08, 2016, doi: 10.1161/CIRCRESAHA.115.306647.

[41] J. F. P. Berbeé, M. R. Boon, P. P. S. J. Khedoe, A. Bartelt, C. Schlein, *et al.*, "Brown fat activation reduces hypercholesterolaemia and protects from atherosclerosis development," *Nat. Commun.*, vol. 6, no. 1, pp. 1–11, Mar. 2015, doi: 10.1038/ncomms7356.

[42] A. El-Mahmoudy, S. Shousha, H. Abdel-Maksoud, and O. A. Zaid, "Effect of long-term administration of sildenafil on lipid profile and organ functions in hyperlipidemic rats," *Acta Biomed.*, vol. 84, no. 1, pp. 12–22, 2013.

[43] A. Worthmann, C. John, M. C. Rühlemann, M. Baguhl, F. A. Heinsen, *et al.*, "Cold-induced conversion of cholesterol to bile acids in mice shapes the gut microbiome and promotes adaptive thermogenesis," *Nat. Med.*, vol. 23, no. 7, pp. 839–849, Jul. 2017, doi: 10.1038/nm.4357.

[44] V. O. Melichar, D. Behr-Roussel, U. Zabel, L. O. Uttenthal, J. Rodrigo, *et al.*, "Reduced cGMP signaling associated with neointimal proliferation and vascular dysfunction in late-stage atherosclerosis," *Proc. Natl. Acad. Sci.*, vol. 101, no. 47, pp. 16671–16676, Nov. 2004, doi: 10.1073/pnas.0405509101.

[45] Y. Güneş, M. Tuncer, M. Yildirim, Ü. Güntekin, H. A. Gümrükçüoğlu, *et al.*, "A novel echocardiographic method for the prediction of coronary artery disease," *Med. Sci. Monit.*, vol. 14, no. 9, pp. 42–46, 2008.

[46] F. Tissier, Y. Mallem, C. Goanvec, R. Didier, T. Aubry, *et al.*, "A non-hypocholesterolemic atorvastatin treatment improves vessel elasticity by acting on elastin composition in WHHL rabbits," *Atherosclerosis*, vol. 251, pp. 70–77, Aug. 2016, doi: 10.1016/j.atherosclerosis.2016.05.039.

[47] S. I. Katsuda, N. Machida, M. Hasegawa, H. Miyashita, M. Kusanagi, *et al.*, "Change in the static rheological properties of the aorta in Kurosawa and Kusanagi-Hypercholesterolemic (KHC) rabbits with progress of atherosclerosis," *Physiol. Meas.*, vol. 25, no. 2, pp. 505–522, Apr. 2004, doi: 10.1088/0967-3334/25/2/009.

[48] A. A. Thorp, M. P. Schlaich, and J. H. Southerland, "Relevance of Sympathetic Nervous System Activation in Obesity and Metabolic Syndrome," 2015, doi: 10.1155/2015/341583.

[49] E. Lambert, N. Straznicky, C. I. Sari, N. Eikelis, D. Hering, *et al.*, "Dyslipidemia is associated with sympathetic nervous activation and impaired endothelial function in young females," *Am. J. Hypertens.*, vol. 26, no. 2, pp. 250–256, Feb. 2013, doi: 10.1093/ajh/hps016.

[50] A. Lymperopoulos, G. Rengo, and W. J. Koch, "Adrenergic nervous system in heart failure: Pathophysiology and therapy," *Circ. Res.*, vol. 113, no. 6, pp. 739–753, 2013, doi: 10.1161/CIRCRESAHA.113.300308.

[51] P. M. Ridker, N. Rifai, M. J. Stampfer, and C. H. Hennekens, "Plasma Concentration of Interleukin-6 and the Risk of Future Myocardial Infarction Among Apparently Healthy Men," *Circulation*, vol. 101, no. 15, pp. 1767–1772, Apr. 2000, doi: 10.1161/01.CIR.101.15.1767.

[52] S. J. Goldberg, N. Wilson, and D. F. Dickinson, "Increased blood velocities in the heart and great vessels of patients with congenital heart disease. An assessment of their significance in the absence of valvular stenosis," *Br. Heart J.*, vol. 53, no. 6, pp. 640–644, 1985, doi: 10.1136/hrt.53.6.640.

[53] J. A. Kim, M. Montagnani, K. K. Kwang, and M. J. Quon, "Reciprocal relationships between insulin resistance and endothelial dysfunction: Molecular and pathophysiological mechanisms," *Circulation*, vol. 113, no. 15. Circulation, pp. 1888–1904, Apr. 2006, doi: 10.1161/CIRCULATIONAHA.105.563213.

[54] J. A. Kim, M. Montagnani, S. Chandrasekran, and M. J. Quon, "Role of Lipotoxicity in Endothelial Dysfunction," *Heart Failure Clinics*, vol. 8, no. 4. NIH Public Access, pp. 589–607, Oct. 2012, doi: 10.1016/j.hfc.2012.06.012.

[55] J. D. Tune, A. G. Goodwill, D. J. Sassoon, and K. J. Mather, "Cardiovascular consequences of metabolic syndrome," *Translational Research*, vol. 183. Mosby Inc., pp. 57–70, May 01, 2017, doi: 10.1016/j.trsl.2017.01.001.

[56] A. A. Thorp, M. P. Schlaich, and J. H. Southerland, "Relevance of Sympathetic Nervous System Activation in Obesity and Metabolic Syndrome," 2015, doi: 10.1155/2015/341583.

[57] O. Pechánová, Z. V Varga, M. Cebová, Z. Giricz, P. Pacher, *et al.*, "Cardiac NO signalling in the metabolic syndrome Correspondence LINKED ARTICLES," *www.brjpharmacol.org*

Br. J. Pharmacol., vol. 172, p. 1415, 2015, doi: 10.1111/bph.2015.172.issue-6.

[58] O. Feron, C. Dessy, S. Moniotte, J. P. Desager, and J. L. Balligand, "Hypercholesterolemia decreases nitric oxide production by promoting the interaction of caveolin and endothelial nitric oxide synthase," *J. Clin. Invest.*, vol. 103, no. 6, pp. 897–905, 1999, doi: 10.1172/JCI4829.

[59] V. Conti, G. Russomanno, G. Corbi, V. Izzo, C. Vecchione, *et al.*, "Adrenoreceptors and nitric oxide in the cardiovascular system," *Frontiers in Physiology*, vol. 4 NOV. 2013, doi: 10.3389/fphys.2013.00321.

[60] J. N. Trochu, V. Leblais, Y. Rautureau, F. Bévérelli, H. Le Marec, *et al.*, "Beta 3-adrenoceptor stimulation induces vasorelaxation mediated essentially by endothelium-derived nitric oxide in rat thoracic aorta," *Br. J. Pharmacol.*, vol. 128, no. 1, pp. 69–76, 1999, doi: 10.1038/sj.bjp.0702797.

[61] T. S. Cunha, M. J. C. S. Moura, C. F. Bernardes, A. P. Tanno, and F. K. Marcondes, "Vascular sensitivity to phenylephrine in rats submitted to anaerobic training and nandrolone treatment.," *Hypertension*, vol. 46, no. 4, pp. 1010–1015, Oct. 2005, doi: 10.1161/01.HYP.0000174600.51515.e7.

[62] H. O. Steinberg, H. Chaker, R. Leaming, A. Johnson, G. Brechtel, *et al.*, "Obesity/insulin resistance is associated with endothelial dysfunction: Implications for the syndrome of insulin resistance," *J. Clin. Invest.*, vol. 97, no. 11, pp. 2601–2610, Jun. 1996, doi: 10.1172/JCI118709.

[63] M. A. Vincent, M. Montagnani, and M. J. Quon, "Molecular and physiologic actions of insulin related to production of nitric oxide in vascular endothelium," *Current Diabetes Reports*, vol. 3, no. 4. Current Science Ltd, pp. 279–288, 2003, doi: 10.1007/s11892-003-0018-9.

[64] R. Muniyappa and J. R. Sowers, "Role of insulin resistance in endothelial dysfunction," *Rev. Endocr. Metab. Disord.*, vol. 14, no. 1, pp. 5–12, 2013, doi: 10.1007/s11154-012-9229-1.

[65] J. A. Kim, H. J. Jang, and D. H. Hwang, "Toll-like receptor 4-induced endoplasmic reticulum stress contributes to impairment of vasodilator action of insulin," *Am. J. Physiol. - Endocrinol. Metab.*, vol. 309, no. 9, pp. E767–E776, 2015, doi: 10.1152/ajpendo.00369.2015.

IV. Discussion & Conclusion

7. Discussion

It has been well established that both abdominal obesity and IR represent the major and central pathophysiological features of the MetS (Cornier et al. 2008; Gallagher et al. 2010). However, the pathogenesis of the latter is not fully understood due to its complexity and to the interconnection between its components (Cornier et al. 2008). What is evident is that in obesity, the adipose tissue undergoes hypertrophy and hyperplasia, in response to increased energy (Sun et al. 2011; Chan and Hsieh 2017; Longo et al. 2019). This leads to overproduction of adipocytokines, a state that underlies the development of insulin resistance, particularly due to increased release of FFA and inflammatory cytokine levels (S. E. Kahn et al. 2006; Chan and Hsieh 2017). Moreover, most of the pathophysiological processes that lead to the other components of the MetS i.e. hypertension and dyslipidemia, also seem to originate from obesity and/or IR (Ferrannini et al. 1997; Yanai et al. 2008; Giannini et al. 2011; Hwang et al. 2016). However, not all kinds of obesity seem to be incriminated in these processes. In fact, the increased buildup of abdominal/visceral adiposity was found to have much more harmful metabolic consequences than peripheral and subcutaneous adiposity (Castro et al. 2014), due to higher rates of IR and lipolysis in visceral rather than in peripheral fat (Jensen 1997; Cnop et al. 2002). Thus, fat distribution has been revealed as an important player in the metabolic outcome of obesity and the MetS. Accordingly, the concept of healthy obesity has recently become common in the research field. It is not uncommon to find "metabolically healthy" individuals among a group of obese subjects who have increased subcutaneous rather than abdominal/visceral adiposity (Brandão et al. 2020). It is not unusual either, to find "metabolically unhealthy" individuals in a group of non-obese (normal weight) subjects (Ruderman et al. 1998). In fact, the hypothesized role of insulin resistance independent of BMI has recently given rise to the concept of a "metabolically healthy" obese and "metabolically unhealthy" non-obese individuals. For instance, obese individuals without other components of the MetS have lower cardiovascular risks compared to non-obese individuals with MetS (Karelis et al. 2005). Thus, one of the common slips made in the research field is that most of the established studies focus, on obesity, as the core of the MetS; and little is known on the relationship/connection between the other components of the latter, independently from the obesity factor.

Accordingly, in the current study we chose to shed the light on a category of people that is undoubtedly present among MetS patients, that involves "metabolically obese normal-weight[28]" patients. We also expected that by avoiding excessive weight gain in our animal models we would be eluding the obesity-related confounding factors (e.g. mechanical and inflammatory components).

In general, rabbits represent the best candidates in terms of animal models for the study of lipid/lipoprotein metabolism and atherosclerosis (Fan et al. 2015a). In fact, unlike rodents, rabbits have a humanoid (human-like) lipoprotein metabolism, they display a high expression CETP, a regulator of reverse cholesterol transport (Trajkovska and Topuzovska 2017). The CETP transfers cholesteryl esters from HDL to LDL in exchange for TGs, leading to increased atherogenicity (Barter and Rye 1994; Kleber et al. 2010). Meanwhile, mice and rats do not only have apoB-48 in their exogenous but in their endogenous lipoproteins as well. This results in a rapid disappearance of apoB-48 enriched VLDL and LDL from the circulation and thereby to a decrease in LDL levels in these species (Kobayashi et al. 2011; Fan et al. 2015). Therefore, murine models have limitations in terms of lipid/lipoprotein metabolism in translational studies (Y. T. Lee et al. 2017) and thus might not be the most suitable animal models for studying MetS (Karimi 2012), particularly when the latter includes dyslipidemia. Moreover, CETP has also been reported to be absent or expressed in low concentrations in other animal models e.g. dogs and pigs, making them unsuitable for studying lipid metabolism in translational research and protecting them against atherogenecity (Yin et al. 2012; T. Chen et al. 2017; Kaabia et al. 2018).

Moreover, the WHHL rabbit, in particular, is an animal model of human familial hypercholesterolemia (FH) due to a genetic defect in its LDL receptor. As in FH, the deficiency in the low-density lipoprotein receptor (LDLr) activity leads to a delayed clearance of LDL particles from the circulation and consequently to their accumulation in the plasma; which subsequently, leads to hyperlipidemia and spontaneous atherosclerosis (Kobayashi et al. 2011; Shiomi and Ito 2009).

[28] metabolically obese normal-weight are individuals who are not obese on the basis of height and weight, but who, like people with overt obesity, are hyperinsulinemic, insulin-resistant, and predisposed to type 2 diabetes, hypertriglyceridemia, and premature coronary heart disease.

Diets rich in sugar (sucrose or fructose) or fat have been widely used to induce the MetS in experimental animal models (Wong et al. 2016; Lozano et al. 2019). Several studies demonstrated that high sugar diets lead to the establishment of obesity, hyperglycemia, hypertension and dyslipidemia in animals. For instance, Mahmoud et al. demonstrated that adding 10% of fructose for 12 weeks Wistar rats leads to the development of the four components of the MetS (Mahmoud and Elshazly 2014). In another study, Mansour et al. showed that when fed a high fructose diet for 16 weeks, albino Wistar rats exhibited three components of the MetS, obesity, hyperglycemia and dyslipidemia (Mansour et al. 2013). Moreover, after 12 week of high sucrose (40%) feeding, rabbits exhibited hyperglycemia, hypercholesterolemia, and a marked increase in total cholesterol, triglycerides, and LDL (Helfenstein et al. 2011b). On the other hand, studies indicated that high-fat diet studies over 12 weeks showed a significant increase in visceral adipose tissue, fasting glycemia, cholesterol, triglycerides, mean arterial pressure, and a marked decrease in glucose intolerance and HDL in rodents and rabbits. Carol et al. demonstrated that 15 % (10% corn oil and 5% lard) high fat feeding induces all the components of the MetS in New Zealand white rabbits (Joan F. Carroll et al. 1996). High fat feeding to mice have proven to induce obesity, hyperglycemia and dyslipidemia (Y. Li et al. 2015). Moreover, Suman et al. showed that 10 weeks of high-fat feeding also leads the development of four components of the MetS in Wistar rats (Suman et al. 2016).

When combined high-fructose and high-fat diets also showed to be effective in inducing the MetS in animal models. For example, 8 weeks of high-fat high fructose feeding leads to obesity, hyperglycemia and dyslipidemia in Wistar rats (Gancheva et al. 2015). In addition, in a study on WHHL rabbits fed a 30% fructose and 10% coconut oil diet for 8 weeks, animals exhibited dyslipidemia and IR (Ning et al. 2015). Interestingly, it has also been demonstrated that consuming a normal number of calories, whether of a high fructose diet or of a high fructose-fat diet or even a combination of both induces insulin resistance and other components of the MetS without obesity in rabbit models (Ning et al. 2015)(Waqar et al. 2010).

Both fructose and fat provide excess lipids from different sources; fructose increases the availability of endogenous lipids, whereas fat increases the availability of exogenous lipids (Namekawa et al. 2017). Fructose is very well known as a highly lipogenic nutrient. Its catabolism produces glucose, glycogen, lactate and pyruvate and eventually provides both glycerol and acyl

portions of TG molecules. Thus, the exposure of the liver to high fructose concentrations leads to enhanced rate of de novo lipogenesis and TG synthesis, leading to increased TG production and ultimately to elevated VLDL concentrations (TG is packaged with Apo-B in the liver and secreted as VLDL particles) (Basciano et al. 2005). The excess VLDL secretion then delivers higher levels of Fatty Acids (FAs) and TG to muscle and other tissues, that in turn contributes to reduced insulin sensitivity and to hepatic IR/glucose intolerance (Basciano, Federico, and Adeli 2005), further inducing IR (Choi and Ginsberg 2011). Fat also known as TG is an ester composed of three chains of fatty acids and glycerol. When fat is administrated, high levels of glycerol and fatty acids are absorbed into the bloodstream and mobilized towards the liver where they undergo lipogenesis (TG synthesis) and eventually become substrates for VLDL and LDL particles production. The higher the amount of fat ingested the higher the levels of fatty acids and eventually TG, VLDL and LDL levels. Higher lipogenesis also occurs in fat tissues, where FAs-derived from fat ingestion form TGs and new fat reserve (Lozano et al. 2019).

In the current study, we used a high-fructose high-fat diet consisting of a chow diet, supplemented with 30 % fructose and 10 % coconut oil (91% saturated fatty acids). Since our objective was to avoid excessive weight gain-related confounding factors e.g. mechanical and inflammatory effects of obesity *per se*; the diet that we used was rich in fat and sugar but was reduced in protein and fibers, so that it finally contains the same amount of calories as the control/chow diet.

Data on the association between dyslipidemia and IR in the MetS are scarce, and whether this association is independent of other components of the MetS, has not been reported. We hypothesized that by excluding the obesity factor, we would be able to describe the relationship between IR and dyslipidemia and to investigate the metabolic and cardiovascular disturbances that are associated with the combination dyslipidemia and IR, independently from other components of the MetS, i.e. obesity. In this regard, the first purpose of the study was to develop an animal model that combines two main risk factors of the MetS, dyslipidemia and insulin resistance, independent from obesity.

Finding a suitable molecule for the management of the MetS is of great importance. Drugs with pleiotropic effects have been reported to be the most successful in managing a multifactorial

complex disease i.e. the MetS (Rask Larsen et al. 2018). Modulation of the NO-sGC-cGMP signaling pathway has shown promising results related to the treatment of metabolic and cardiovascular disease (J.-P. Stasch et al. 2002; Mitschke et al. 2013; Nossaman and Kadowitz 2013; Pfeifer et al. 2013; Ramirez et al. 2015; M. Park et al. 2018). We hypothesized that modulating the NO-cGMP signaling by pharmacological tools might represent a promising therapeutic modality for managing the MetS and its related cardiovascular pathologies. Accordingly, we chose to work on two different molecules, BAY 41-2272 and mirabegron, known for their ability to stimulate the NO-cGMP signaling pathway, through direct stimulation of sGC and β_3-AR agonism, respectively.

It is noteworthy that BAY 41-2272 and mirabegron have been approved, by food and drug administration (FDA) and the European medicines agency (EMA), for the treatment of pulmonary arterial hypertension (PAH) and overactive bladder (OAB) syndrome, respectively. In general, a drug development process might take up to 15-20 years before the drug is approved and put on the market. In fact, it usually takes up to 15 years until the drug even reaches the clinical trial phase. Which sometimes turns up to be unsuccessful. Therefore, using repurposing drugs[29] instead of developing new molecules saves a lot of time, energy and resources.

Even though both the weight and abdominal circumference parameters significantly increased in both HFFD and control groups (12^{th} week vs. baseline), at the end of the protocol the increase was not higher in the HFFD compared to the control group. Therefore, it might be argued that this increase was not attributed to the HFFD-feeding. As mentioned earlier, the HFFD that we used is rich in fat and sugar but with less protein and fibers. This might explain the absence of excessive weight gain. Whereas after 12 weeks of treatment with mirabegron and BAY 41-2272 along with HFFD-feeding, we did not observe any increase in weight nor in abdominal circumference as the one seen in both the control and HFFD groups. This suggests that both mirabegron and BAY 41-2272 stabilized and prevented the increase of both weight and abdominal circumference. This is most likely related to the activation of NO-cGMP axis. Even though mirabegron activates the latter pathway upstream of NO and BAY 41-2272 activates it downstream of NO, it is agreed that both molecules lead to the same outcome which is the increase in cGMP levels. However, the difference

[29]Repurposing drugs are drugs that were originally developed for treating a certain disease and were found to have promising beneficial effects in the treatment of another disease

between both molecules is that one depends on NO (mirabegron) whereas the other increases the cGMP levels independently of NO (BAY 41-2272). Whether through β_3-AR agonism (e.g. mirabegron and CL316,243) or direct sGC stimulation (e.g. BAY 41-8543) or even PDE5 inhibition (e.g. sildenafil citrate), increasing cGMP levels has proven to be effective in preventing weight gain or even decreasing the weight/BMI (Ayala et al. 2007; Salih Sahib et al. 2014; Berbeé et al. 2015; Hoffmann et al. 2015b). Reduced obesity/weight gain has been attributed to the enhancement of lipid uptake into BAT, to an increase in whole-body EE (Cannon and Nedergaard 2004; Mitschke et al. 2013; Pfeifer et al. 2013); and to the browning of WAT that in turn promotes EE and to a counterbalance of the positive energy balance associated with over-nutrition (Kozak and Koza 2010; G. W. Kim et al. 2014). In a randomized, prospective clinical trial, 3 months treatment with sildenafil citrate, significantly decreased the BMI of diabetic patients with MetS (Salih Sahib et al. 2014). Another study demonstrated that long-term treatment with sildenafil citrate leads to weight reduction through increased EE in obese, insulin resistant mice (Ayala et al. 2007). BAY 41-8543, a stimulator of sGC, was proven to protect against diet-induced weight gain and to induce weight loss in established obesity (Hoffmann et al. 2015b). Mirabegron has been described to reduce weight gain through another mechanism that is related to the β_3-AR stimulation itself; β_3-AR agonists are thought to pharmacologically mimic the cold-stimulated activation of mitochondrial UCP1 of brown adipocytes; which induces lipolysis, thermogenesis thereby leading to increased EE (Berbeé et al. 2015).

WHHL rabbits that were subjected to the HFFD exhibited hyperinsulinemia and increased HOMA-IR compared to both their baseline levels and their counterparts in the control group. This indicates that 12 weeks of HFFD-feeding leads to an IR state. These results along with the absence of significant increase in weight and abdominal circumference is in consistence with several studies, that have demonstrated that consuming a normal number of calories, whether of a high fructose diet or of a high fructose-fat diet, induces IR without obesity in rabbit models (Ning et al. 2015; Waqar et al. 2010). Whereas those that were additionally treated with mirabegron and BAY 41-2272 showed no increase in their fasting insulin nor in their HOMA-IR levels, indicating that both molecules were able to offset the decreased insulin sensitivity induced by HFFD feeding. This result is in agreement with the findings of a study, done by Hao et al., who found that treatment with mirabegron was accompanied with improved insulin sensitivity and prevention

from high-fat diet-induced obesity, in mice (Hao et al. 2019). Moreover, treatment with sildenafil citrate has proven to improve insulin action in a mouse model of diet-induced obesity and IR (Ayala et al. 2007).

As reviewed by Barrett et al., during IR, endothelial-mediated vasodilation is compromised leading to decreased delivery of glucose and insulin to their target organs (Barrett et al. 2011a). Therefore, the potential mechanisms behind improved insulin sensitivity by both molecules found in our study, could be related to cGMP-stimulated vasodilation that leads to enhanced blood flow and thereby to improved glucose and insulin delivery to insulin sensitive tissues (Arce-Esquivel et al. 2013). Another possible mechanism is a cGMP-stimulated translocation of glucose transporter 4 to cell membrane, that stimulates glucose uptake and thereby increases insulin sensitivity (Roy, Perreault, and Marette 1998).

In our study, AUC_{Glu} decreased in the HFFD-fed rabbits but was not improve in response to treatment with either of the two molecules. This discordance with the improvement of IR in both treated groups may have been because the amelioration of insulin sensitivity precedes that of glucose tolerance and that a longer treatment duration would have been needed. In fact, insulin's action involves glucose uptake and suppression of glucose production; thus, it might be argued that even if one or both these actions increased with improved insulin sensitivity, the concomitant exposure to the HFFD still impaired the glucose tolerance.

As mentioned earlier, a high-fructose high-fat diet stimulates endogenous and exogenous lipogenesis, respectively (Namekawa et al. 2017). When exposed to high fructose, the liver increases its *de novo* lipogenesis and TG synthesis, leading to elevated VLDL levels (Basciano, Federico, and Adeli 2005). This explains our results regarding the increased TG levels found in response to HFFD-feeding, in agreement with the findings of other studies (Toklu et al. 2016). The excess of VLDL production then delivers higher levels of FAs and TG to skeletal muscle and adipose tissue, further inducing IR (Choi and Ginsberg 2011), which in turn explains our results, concerning, the decrease in insulin sensitivity in the HFFD group (increased insulinemia and HOMA-IR). Besides being related to the HFFD diet itself, increased TG levels might result from the IR state which has been reported to lead to increased hepatic VLDL production and thereby to increased TG levels (Kaur 2014). TG levels were significantly increased amongst HFFD-group

individuals but not in the HFFD+MIR group nor in the HFFD+BAY group. Even if there were no decrease in TG levels, we still found that treatment with mirabegron and BAY 41-2272 prevented the increase of TG levels. Given that mirabegron- and BAY 41-2272-treated rabbits simultaneously received the HFFD; assuming that mirabegron and BAY 41-2272 had no effect on the TG levels, we would have witnessed the same increase, as in the HFFD group. Several studies have demonstrated that activation of the NO-cGMP pathway promotes lipolysis and stimulates thermogenic pathways, leading to decreased WAT-mediated fat storage and to increased BAT-mediated energy expenditure, respectively (Cypess and Kahn 2010; G. W. Kim et al. 2014). Moreover, it has been proposed that a lower TG level could result from chronic stimulation of BAT that leads to increased TG-rich lipoproteins consumption (Bartelt et al. 2011; Hoeke et al. 2016). In fact it has been well established that BAT uptakes and combusts high amounts of FAs, leading to decreased plasma TG levels and thereby decreases obesity (Berbeé et al. 2015). Which also explains the stabilized weight observed in our study.

It has been well established that low-grade inflammation plays an important role in mediating IR during the MetS. Therefore, we measured two main inflammatory cytokines, TNF-α and IL-6 levels, that were proven to decrease insulin sensitivity (Rydén and Arner 2007; Pazos et al. 2013). Our results revealed that mirabegron exhibited a tendency to decrease the inflammatory cytokine IL-6, which might explain the improved insulin sensitivity. However, after 12 weeks of treatment with BAY 41-2272 insulin sensitivity improved without any change in IL-6 levels.

It has been described, that in states of obesity, fasting leads to mobilization of energy stores (TG) in adipose tissue via lipolysis, resulting in increased FFA levels (McCracken, Monaghan, and Sreenivasan 2018), and that abdominal subcutaneous adipose tissue is the only significant site of FFA liberation, meanwhile only a small, insignificant proportion arises from visceral adipose tissue (Jensen 2002). Therefore, the stable unchanged FFA levels in the HFFD-fed rabbits might be explained by the absence of both excessive weight gain and increased abdominal circumference. We also observed no change in the FFA levels in mirabegron- and BAY 41-2272-treated groups. The lack of increased FFA does not rule out our hypothesis regarding increased lipolysis in response to both treatments, since the increased plasma FFA levels may only be transient. For instance, Olsen et al. has already documented that increased plasma FFA levels are only transient

following β_3-AR-stimulated WAT lipolysis due to increased energy cost during BAT-induced thermogenesis (Olsen et al. 2019).

WHHL rabbits spontaneously develop hypercholesterolemia due a mutation in their LDLr. However, our results still showed extensive hypercholesterolemia (significantly increased TC and LDL-C levels) in response to the HFFD-feeding, when compared to the control group. The HFFD probably increases the production of TG-enriched VLDL particles (as described above) which then undergo lipolysis leading to higher levels of cholesterol-enriched LDL particles in the circulation. In WHHL rabbits, the reduced clearance of lipoproteins (mutated LDLr) probably further increases blood cholesterol levels. While on the other hand, the CETP-stimulated TG-enriched LDL particles production, leads to smaller dense LDL particles, with higher atherogenic properties (Miccoli et al. 2017) which explains the enhancement of atherosclerosis in the treated groups (discussed later).

Even though several studies found that mirabegron and sildenafil treatment reduce hypercholesterolemia and protect from atherosclerosis through BAT activation, in the current study neither mirabegron nor BAY 41-2272 counteracted the increase in cholesterol levels (Hoeke et al. 2016; Worthmann et al. 2017; El-Mahmoudy et al. 2013). It has been reported that BAT stimulation increases the uptake of lipoprotein-derived TGs, carbohydrates and cholesterol into the BAT itself (Worthmann et al. 2017). Moreover, It was mechanistically demonstrated that when BAT is activated, it enhances the selective uptake of FAs from TG-rich lipoproteins, leaving behind cholesterol-rich remnants which are then cleared by the liver (Berbeé et al. 2015). However, the hepatic clearance of these particles depends on the ApoE-LDLr axis. Therefore, in animals with a defect in the LDL receptor, i.e. the WHHL rabbit, these particles are more likely to accumulate in the circulation leading to increased levels of cholesterol. This might explain why both mirabegron and BAY 41-2272 improved TG levels but not TC and LDL-C nor atherosclerosis. Our results agree with the findings of several studies that also worked on animal models with a defective ApoE-LDLr axis i.e. *Apoe*$^{-/-}$ and *Ldlr*$^{-/-}$ mice (Berbeé et al. 2015; Sui et al. 2019).

As reviewed by Ormawabal et al., IR can alter systemic lipid metabolism leading to the development of dyslipidemia and the well-known lipid triad: first, by increasing plasma

triglyceride levels; second, by decreasing HDL levels and third, through stimulating small dense low-density lipoproteins formation (Ormazabal et al. 2018). Thus, it is highly possible that the exacerbation of dyslipidemia in the HFFD group, in our study, is related to the HFFD-induced IR; and that the stabilized TG levels in response to mirabegron and BAY 41-2272 treatments is connected to the improved insulin sensitivity *per se*.

So many conflicting data in the literature exist regarding the effects of the treatments identical or similar to the ones used in our study on the HDL concentrations. Treatments with BRL37344, a preferential β_3-AR agonist and mirabegron were shown to increase HDL-C levels in rats and humans, respectively (Negres et al. 2017; O'Mara et al. 2020). Whereas, long-term administration of sildenafil was found to decrease HDL-C concentrations of rats fed on fat-enriched diet (El-Mahmoudy et al. 2013). However, those studies were not performed on models with an ApoE-LDLr defective axis. For instance, In agreement with our results, in their study, performed on *Apoe*$^{-/-}$ and *Ldlr*$^{-/-}$ mice, Sui et al. did not find any significant difference in HDL levels between mirabegron-treated and control groups (Sui et al. 2019).

Moreover, our results showed that mirabegron and BAY 41-2272-treated rabbits displayed larger plaques and more advanced lesions when compared to the control group but showed almost similar lesions as the HFFD-fed group. This result is in contrast with the findings of Balarini et al. who demonstrated that long-term treatment with sildenafil citrate reduced the progression of atherosclerosis in large vessels of western diet fed-*ApoE*$^{-/-}$mice, models that, like Watanabe rabbit, develop spontaneous hypercholesterolemia. In their study, Balarini et al. were able to prove that this improvement is related to enhanced activation of the NO pathway (Balarini et al. 2013). Therefore, sGC has been proposed as an attractive, novel pharmacological target in the treatment of atherosclerosis (Melichar et al. 2004). In the present study, the absence of improvement in atherosclerotic lesions might be due to the concomitant exposure to HFFD in treated rabbits or even to the fact that the animal model (Watanabe rabbit) used in our study has a mutation in its LDLr. For instance, Sui et al. found that treatment with mirabegron not only does not improve atherosclerosis but also excarebates atherosclerotic plaque development particularly in animals with defective ApoE-LDLr axis. In their study, they attributed this effect to the activation of brown fat-mediated lipolysis that leads to an increase in plasma levels of both LDL-C and VLDL-C remnants and thereby to an acceleration of plaque growth and instability (Sui et al. 2019).

Moreover, Berbeé et al. demonstrated that activation of BAT using a β_3-agonist, in *Apoe*$^{-/-}$ and *Ldlr*$^{-/-}$ mice does not attenuate hypercholesterolemia and atherosclerosis (Berbeé et al. 2015).

According to the American Heart Association, an individual is diagnosed with MetS when presenting three out of five risk factors: increased waist circumference (central or abdominal obesity), elevated triglyceride levels, reduced high-density lipoprotein cholesterol (HDL-C), high blood pressure and elevated fasting glycaemia (Alberti et al. 2009). We found impaired glucose tolerance (increased AUC_{Glu} and 2h glycaemia), hyperinsulinemia and increased HOMA-IR, all indicators of IR. WHHL rabbits also exhibited increased TG levels and low HDL-C. Taken all together, these findings confirm that after 12 weeks of HFFD feeding, Watanabe rabbits developed MetS with two main features, dyslipidemia and IR.

Increased arterial stiffness was proven to be correlated to the MetS in humans and experimental animal models (Lopes-Vicente et al. 2017), and to be associated with IR independent of glucose tolerance status (Sengstock, Vaitkevicius, and Supiano 2005). Moreover, Bhatta et al. found that PWV increases in an animal model of diet-induced metabolic syndrome (Bhatta et al. 2017). However, in our study we found no change in the PWV values. Even though PWV values significantly increased in the HFFD, HFFD+MIR and HFFD+BAY groups compared to the control group, we could not consider these results, given that the PWV almost did not change amongst individuals of both the HFFD, HFFD+MIR and HFFD+BAY groups. In their study, Tissier et al. found that PWV in Watanabe rabbits augmented with age (Tissier et al. 2016a). Therefore, it might be possible that the PWV did not change because the rabbits in our study were young and the protocol only lasted for 12 weeks. Moreover, the PWV measurement reflects the overall arterial stiffness rather than the localized one. Thus, the absence of increased PWV does not necessarily mean an absence of arterial stiffness, since the latter might be localized rather than generalized.

It has been proposed that the hyperinsulinemia encountered during IR and dyslipidemia leads to sympathetic nervous system (SNS) up-regulation (Thorp et al. 2015; E. Lambert et al. 2013); and that SNS overactivation in turn might lead to decreased contractile responsiveness to β-stimulation (Lymperopoulos, Rengo, and Koch 2013). We evaluated the effects of *ex vivo* β-AR

stimulation on cardiac inotropy and coronary vasodilation. Our *ex vivo* results showed a decrease in positive inotropy in the HFFD and HFFD+BAY groups with increased positive inotropy and lusitropy in HFFD+MIR group. Whereas no change was observed in terms of coronary vasodilation (data only shown for BAY 41-2272). This suggests that the HFFD-feeding was responsible for a decreased β_1-AR (but not β_2-AR) reactivity that was only improved in response to treatment with mirabegron. This is possibly related to a cross-talk between β_1-ARs and β_3-ARs that occurred during the 12 weeks of treatment of mirabegron. Several studies reported a cross-regulation between β_1-ARs and β_3-ARs involving intracellular mechanisms in cardiomyocytes (Montaudon et al. 2015; Ufer and Germack 2009). However, many conflicting findings have been described in the literature regarding the enhanced cardiac contractility and relaxation in response to β_3-agonism. In their study Skeberdis et al. found that β_3-ARs are positively coupled to L-type Ca^{2+} channels and contractility in human atrial tissues through a cAMP-dependent pathway (Skeberdis et al. 2008). However, this study was performed on human atrial and not ventricular cells. Another study, attributed the increased cardiac inotropy and lusitropy to the coupling of β_3-ARs to adenylyl cyclase stimulatory (Gαs) proteins, which then induces the activation of cAMP-PKA signaling pathway (Cannavo and Koch 2016). Whereas, others considered that the mirabegron's cardiostimulant effect is unrelated to β_3-AR activation and discredited a direct interaction with β_1-ARs, given mirabegron's structure. Mirabegron was investigated by Mo et al. for having an indirect sympathomimetic effect, causing cardiostimulation by being taken up into the sympathetic nerves, thereby leading to noradrenaline release (Mo et al. 2017).

Our echocardiographic data showed no difference in LVFS, LVEF, end-systolic and end-diastolic diameters indicating no change in LV systolic function nor in LV dilation, in any of the groups. Even though mirabegron was found to significantly increased the LVEF compared to patients given placebo, it was only found to be beneficial in patients with reduced LVEF (Bundgaard et al. 2017). An increase in both the aortic and pulmonary flow velocities was seen in the HFFD group but not in treated groups, indicating that both treatments prevented the increase in the aortic and pulmonary flow velocities. This increase is reported to be either related to increase flow through the valves or to a decreased in pulmonary and aortic arteries' compliance (Ridker et al. 2000; Goldberg, Wilson, and Dickinson 1985). This result could not be ascribed to increased LV systolic function since both the LVFS and LVEF were not increased. Thus, the increase is

possibly linked to an increased stiffness in the pulmonary and aortic arteries. The discrepancies between this result and the unchanged PWV might be related to the fact the PWV measurement is more generalized and reflects overall arterial stiffness rather than localized arterial stiffness. Treatment with mirabegron and BAY 41-272 prevented this increase probably through the activation of NO-signaling pathway in endothelial cells. Indeed, treatments that lead to vasodilation have been reported to reduce arterial stiffness (I. B. Wilkinson et al. 2004).

Both IR and dyslipidemia has been associated to ED (J.-A. Kim et al. 2006; J. A. Kim et al. 2012; E. Lambert et al. 2013). ED is not only associated with impaired vasodilation but might as well be related to increased vasoconstriction due to enhanced vascular sensitivity or production of endothelial-dependent vasoconstricting factors (Tune et al. 2017). Thus, we evaluated the vascular reactivity (vasoconstriction and vasorelaxation) of the carotid artery. HFFD-induced IR enhanced the vascular reactivity to Phe in terms of pD_2, indicating an increase of α_1-AR sensitivity in the HFFD group. There is evidence in support of hyperinsulinemia/IR promoting sympathetic nerve activity (Thorp and Schlaich 2015). Therefore, HFFD-induced IR appears to evoke an increased of α_1-AR sensitivity in the HFFD-fed Watanabe rabbits, due to SNS overactivation. Heightened α_1-AR sensitivity might also be due to reduced NO bioavailability and/or increased oxidative stress causing an enhanced vascular adrenergic responsiveness (Conti et al. 2013). This increase was counteracted in response to treatment with mirabegron and BAY 41-2272, since the pD_2 was significantly decreased in both treated groups compared to the HFFD group. This suggests that treatment with mirabegron and BAY 41-2272 prevented Phe hypersensitivity, induced by the HFFD-induced IR. This probably occurs by modulating the aortic reactivity *via* a change in NO-cGMP intracellular level, that likely diminishes the sensitivity of the α_1-AR-linked mechanisms (Trochu et al. 1999; Cunha et al. 2005). In this regard, we determined the tissular aortic cGMP levels, but we failed to find any significant difference between groups, the cGMP level neither decreased in the HFFD group nor increased in response to mirabegron and BAY 41-2272 treatment.

In contrast, the HFFD did not affect relaxation to SNP nor to Ach, meaning that neither endothelium-independent nor endothelium-dependent vasorelaxation were affected. However, we found that HFFD impaired insulin-induced vasorelaxation. This is most probably due to the IR state that compromised the vasodilatory effect of insulin as found by others (Steinberg et al. 1996;

Vincent, Montagnani, and Quon 2003). In fact, during IR there is selective IR in PI3K-Akt-NO signaling with intact or heightened MAPK-ET1 signaling, that results in impaired NO-mediated vasodilation and augmented ET-1-mediated vasoconstriction in response to insulin (Arce-Esquivel et al. 2013; Muniyappa and Sowers 2013). This result is in accordance with the findings of a study done by kim et al., who found that diet-induced IR impaired Ins-mediated vasorelaxation (J. A. Kim, Jang, and Hwang 2015). In the current study, we found an improvement in Ins-induced vasorelaxation only in mirabegron-treated rabbits. This improvement likely occurs through increased NOS signaling and thereby to an increase in NO bioavailability that occurred during 12 weeks of treatment with mirabegron. However, this hypothesis is less likely to be accurate since we did not witness the same improvement in response to BAY 41-2272 treatment. Both treatments improved the endothelial function, both by counteracting the HFFD-induced Phe-hypersensitivity and mirabegron by also improving insulin-mediated vasorelaxation.

Both enhanced α_1-AR responsiveness and decreased insulin-mediated vasorelaxation encountered in the HFFD group might be due to an imbalance between oxidative stress and NO bioavailability (Duncan et al. 2008) (Conti et al. 2013). Accordingly, we evaluated the TAS levels, which did not change in the HFFD group but was significantly increased in response to treatment with mirabegron. β_3-AR signaling (ancillary property) was previously suggested to preserve the endothelium of the microvasculature from oxidative activation (Michel and Balligand 2017). In addition, in their study Galougahi et al., demonstrated that β_3-AR stimulation, exerts antioxidant and vasoprotective effects in a rabbit model of hyperglycemia (Galougahi et al. 2016). Moreover, Sichrovska et al. have previously demonstrated the antioxidant activity of mirabegron in an *in vitro* experiment (Sichrovska et al. 2013). Collectively these findings are prominent with the anti-oxidant effect of β_3-AR agonists.

Results summary

To avoid obesity and hyperglycemia-related confounding factors, the HFFD that we used in our study was rich in sugar and fat but with less protein and fibers; it contained the same amount of calories as the chow diet fed to the control group. After 12 weeks of HFFD-feeding, WHHL rabbits exhibited an impaired glucose tolerance (increased AUCGlu and 2h glycaemia), hyperinsulinemia, increased HOMA-IR (all indicators of IR) increased TG levels in addition to

their naturally low HDL-C. Long-term HFFD-feeding also decreased cardiac inotropy, induced hypersensitivity to α1-AR-mediated vasoconstriction and impaired insulin-induced vasorelaxation.

WHHL rabbits that were simultaneously (with HFFD) treated with mirabegron, displayed decreased weight gain, improved insulin sensitivity and stabilized TG levels. Mirabegron also improved cardiac function by increasing cardiac inotropy and ameliorated endothelial function by counteracting the hypersensitivity to α1-AR-mediated vasoconstriction and enhancing insulin-induced vasorelaxation.

After 12 weeks of concomitant (with HFFD) treatment with BAY 41-2272, WHHL rabbits presented a decrease in weight gain, an improvement of insulin sensitivity, stabilization of TG levels and a counteraction of hypersensitivity to α1-AR-mediated vasoconstriction.

Limitations of the study

We are aware that certain measurements or tests could have been performed in support of some of our hypotheses and to rule out confusion and speculations regarding some of our results, these may include:

- The calculation of the BMI at the beginning and end of the protocol would have supported our hypothesis regarding the absence of obesity.
- Measurement of the resting metabolic rate at the beginning and the end of the protocol would have been useful for determining the presence/absence of increased energy expenditure in response to the current used treatment protocol.
- The thorough inspection of abdominal cavity after animal sacrifice would have been beneficial to detect the presence/absence of visceral adiposity, which would have been useful for our interpretation regarding the link between IR and visceral adiposity.
- The distribution/quantification of lipids in lipoproteins by fast protein liquid chromatography (FPLC) would have provided detailed information of the TG and cholesterol composition of each lipoprotein particle.
- Histologic, histomorphometric and immunohistological (i.e. UCP1) examination of WAT and BAT for quantification of visceral and/or peripheral fat (number and size).
- Quantification of eNOS and β-AR in the thoracic aorta and the left ventricle, respectively, using western blot analysis or other molecular biology techniques.
- Ideally, one group of rabbits should have received the treatments (mirabegron and BAY 41-272) without concomitant exposure to the HFFD. This would have allowed better interpretation of the results.

- Exposing rabbits to the HFFD for 12 weeks; then, administrating the treatments (mirabegron and BAY 41-272) for another 12 weeks, would have excluded the possible interference of the simultaneous exposure to the HFFD, with the result interpretation.

8. Conclusion & perspectives

Even though animal models provide important information regarding the pathogenesis and the treatment of the MetS, these models do not necessarily reflect the diet-induced metabolic syndrome in humans or simply sometimes do not reflect the reality. Therefore, developing appropriate animal models that mimic the human metabolic syndrome and its related CVD is essential; first, to be able to properly investigate the causes and progression of this disease; second, to find potential suitable pharmacological interventions for the treatment of this syndrome.

Improving the therapeutic and preventive measures for best management of the MetS is crucial. Lifestyle interventions have been widely used and remain the primary tools for good management of the MetS. These interventions are aimed at normalizing body weight and maintaining cardio-metabolic parameters, including lipid levels, blood glucose, and ABP. Even though, adopting a healthy lifestyle pattern remains one of the most effective strategies, it necessitates long-term behavioral changes. The latter include, decreasing caloric intake, increasing physical activity levels, and optimizing the diet composition. Therefore, lifestyle changes are not always successful especially on a long-term basis. A complementary suitable pharmacological approach should then be implemented for best results in the management of this syndrome. Currently most of the treatments used in the management of this syndrome are directed towards each risk factor alone (e.g. anti-obesity, anti-hypertensive, anti-hyperlipidemic drugs, etc.). Therefore, molecules with pleiotropic effects are expected to be less complicated and much more successful in managing this multifactorial syndrome.

The current thesis was devoted to, first develop and characterize an animal model that mimics the human metabolic syndrome and its related CVD, occurring in a category of individuals called “metabolically obese normal weight”; then explore the NO-sGC-cGMP signaling modulation, as a potential strategy for the management of the MetS, combining two main factors, dyslipidemia and IR.

By subjecting WHHL rabbits, representing a spontaneous dyslipidemia, to long-term HFFD-feeding we were able to induce IR and thereby were able to set up an experimentally-induced MetS model that combines mainly dyslipidemia and IR. After 12 weeks of HFFD-feeding, WHHL rabbits exhibited three main factors of MetS: high TG levels, low HDL-C levels and IR.

Long-term activation of the NO-sGG-cGMP signaling, using mirabegron (upstream of NO through NOS activation) and BAY 41-2272 (downstream of NO through sGC activation), showed to be promising in improving MetS-related metabolic and cardiovascular disturbances.

Our study makes a significant contribution to the current body of metabolic and cardiovascular research. Firstly, most of experimental studies are performed on smaller animal models, mainly rodents (mice and rats) in contrast to our study that was performed on an intermediate-sized animal model (rabbit). Secondly, the use of the WHHL rabbit, an animal model that is not commonly used in research studies. Thirdly, the development of an interesting animal model that combines dyslipidemia and IR without obesity and hyperglycemia as confounding factors. Fourthly, this is one of the first studies, to be performed in purpose of exploring the potential of mirabegron and BAY 41-2272 as treatments in the context of MetS. Fifthly, our study supports the concept of using **repurposing** drugs which can be very beneficial in terms of saving time, energy and resources.

In the future, our work could be completed through: using more WHHL rabbits to increase the power of statistical analyses; implementing experimental protocols to explore the distribution of fat and study the link between visceral adiposity and IR/dyslipidemia; implementing experimental protocols to study the reactivity of the abdominal aorta, mesenteric arteries and coronary arteries; exploreing the effects of sGMP pathway modulators over a longer period of time (e.g. 6 months).

References

Abel, E. Dale, Sheldon E. Litwin, and Gary Sweeney. 2008. "Cardiac Remodeling in Obesity." *Physiological Reviews*. American Physiological Society. https://doi.org/10.1152/physrev.00017.2007.

Abu-Soud, Husam M., and Dennis J. Stuehr. 1993. "Nitric Oxide Synthases Reveal a Role for Calmodulin in Controlling Electron Transfer." *Proceedings of the National Academy of Sciences of the United States of America* 90 (22): 10769–72. https://doi.org/10.1073/pnas.90.22.10769.

Aguila, Luis F. Del, Kevin P. Claffey, and John P. Kirwan. 1999. "TNF-α Impairs Insulin Signaling and Insulin Stimulation of Glucose Uptake in C2C12 Muscle Cells." *American Journal of Physiology - Endocrinology and Metabolism* 276 (5 39-5). https://doi.org/10.1152/ajpendo.1999.276.5.e849.

Alberti, K. G.M.M., Robert H. Eckel, Scott M. Grundy, Paul Z. Zimmet, James I. Cleeman, Karen A. Donato, Jean Charles Fruchart, W. Philip T. James, Catherine M. Loria, and Sidney C. Smith. 2009. "Harmonizing the Metabolic Syndrome: A Joint Interim Statement of the International Diabetes Federation Task Force on Epidemiology and Prevention; National Heart, Lung, and Blood Institute; American Heart Association; World Heart Federation." *Circulation* 120 (16): 1640–45. https://doi.org/10.1161/CIRCULATIONAHA.109.192644.

Alberti, K.G.M.M., and P.Z. Zimmet. 1998. "Definition, Diagnosis and Classification of Diabetes Mellitus and Its Complications. Part 1: Diagnosis and Classification of Diabetes Mellitus. Provisional Report of a WHO Consultation." *Diabetic Medicine* 15 (7): 539–53. https://doi.org/10.1002/(SICI)1096-9136(199807)15:7<539::AID-DIA668>3.0.CO;2-S.

Alcalá, Martín, María Calderon-Dominguez, Dolors Serra, Laura Herrero, and Marta Viana. 2019. "Mechanisms of Impaired Brown Adipose Tissue Recruitment in Obesity." *Frontiers in Physiology*. Frontiers Media S.A. https://doi.org/10.3389/fphys.2019.00094.

Alessi, M. C., and I. Juhan-Vague. 2004. "Contribution of PAI-1 in Cardiovascular Pathology." *Archives Des Maladies Du Coeur et Des Vaisseaux*. https://europepmc.org/article/med/15283042.

Alessi, Marie Christine, and Irène Juhan-Vague. 2006. "PAI-1 and the Metabolic Syndrome: Links, Causes, and Consequences." *Arteriosclerosis, Thrombosis, and Vascular Biology*. Arterioscler Thromb Vasc Biol. https://doi.org/10.1161/01.ATV.0000242905.41404.68.

Alkerwi, Ala'a, Adelin Albert, and Michèle Guillaume. 2012. "Cardiometabolic Syndrome." In *Cardiovascular Risk Factors*, 161–89. https://doi.org/10.1007/978-88-470-1463-3.

Anderssen, S. A., S. Carroll, P. Urdal, and I. Holme. 2007. "Combined Diet and Exercise Intervention Reverses the Metabolic Syndrome in Middle-Aged Males: Results from the Oslo Diet and Exercise Study." *Scandinavian Journal of Medicine and Science in Sports* 17 (6): 687–95. https://doi.org/10.1111/j.1600-0838.2006.00631.x.

Antunes, Luciana C., Jessica L. Elkfury, Manoela N. Jornada, Kelly C. Foletto, and Marcello C. Bertoluci. 2016. "Validation of HOMA-IR in a Model of Insulin-Resistance Induced by a

High-Fat Diet in Wistar Rats." *Archives of Endocrinology and Metabolism* 60 (2): 138–42. https://doi.org/10.1590/2359-3997000000169.

Aoqui, Cristiane, Stefan Chmielewski, Elias Scherer, Ruth Eißler, Daniel Sollinger, Irina Heid, Rickmer Braren, et al. 2014. "Microvascular Dysfunction in the Course of Metabolic Syndrome Induced by High-Fat Diet." *Cardiovascular Diabetology* 13 (1): 31. https://doi.org/10.1186/1475-2840-13-31.

Arce-Esquivel, A. Arturo, K. Aaron Bunker, R. Catherine Mikus, and M. Harold Laughlin. 2013. "Insulin Resistance and Endothelial Dysfunction: Macro and Microangiopathy." In *Type 2 Diabetes*. InTech. https://doi.org/10.5772/56475.

Ard, J., A. Cannon, C. E. Lewis, H. Lofton, T. Vang Skjøth, B. Stevenin, and X. Pi-Sunyer. 2016. "Efficacy and Safety of Liraglutide 3.0 Mg for Weight Management Are Similar across Races: Subgroup Analysis across the SCALE and Phase II Randomized Trials." *Diabetes, Obesity and Metabolism* 18 (4): 430–35. https://doi.org/10.1111/dom.12632.

Arias-Mutis, Oscar Julián, Vannina G Marrachelli, Amparo Ruiz-Saurí, Antonio Alberola, Jose Manuel Morales, Luis Such-Miquel, Daniel Monleon, Francisco J Chorro, Luis Such, and Manuel Zarzoso. 2017. "Development and Characterization of an Experimental Model of Diet-Induced Metabolic Syndrome in Rabbit," 1–18. https://doi.org/10.1371/journal.pone.0178315.

Auger, Cyril, and Valérie B. Schini-Kerth. 2014. "Potentiel Des Polyphénols à Améliorer La Protection Vasculaire En Stimulant La Fonction Endothéliale." *Cahiers de Nutrition et de Dietetique* 49 (4): 160–72. https://doi.org/10.1016/j.cnd.2014.03.005.

Ayala, Julio E., Deanna P. Bracy, Brianna M. Julien, Jeffrey N. Rottman, Patrick T. Fueger, and David H. Wasserman. 2007. "Chronic Treatment with Sildenafil Improves Energy Balance and Insulin Action in High Fat-Fed Conscious Mice." *Diabetes* 56 (4): 1025–33. https://doi.org/10.2337/db06-0883.

Babio, Nancy, Estefanía Toledo, Ramón Estruch, Emilio Ros, Miguel A. Martínez-González, Olga Castañer, Mònica Bulló, et al. 2014. "Mediterranean Diets and Metabolic Syndrome Status in the PREDIMED Randomized Trial." *CMAJ* 186 (17): E649–57. https://doi.org/10.1503/cmaj.140764.

Baena, Miguel, Gemma Sangüesa, Alberto Dávalos, María Jesús Latasa, Aleix Sala-Vila, Rosa María Sánchez, Núria Roglans, Juan Carlos Laguna, and Marta Alegret. 2016. "Fructose, but Not Glucose, Impairs Insulin Signaling in the Three Major Insulin-Sensitive Tissues." *Scientific Reports* 6 (1): 1–15. https://doi.org/10.1038/srep26149.

Bagi, Zsolt, Akos Koller, and Gabor Kaley. 2003. "Superoxide-NO Interaction Decreases Flow- and Agonist-Induced Dilations of Coronary Arterioles in Type 2 Diabetes Mellitus." *American Journal of Physiology - Heart and Circulatory Physiology* 285 (4 54-4). https://doi.org/10.1152/ajpheart.00235.2003.

Balarini, Camille M., Marcos A. Leal, Isabele B.S. Gomes, Thiago M.C. Pereira, Agata L. Gava, Silvana S. Meyrelles, and Elisardo C. Vasquez. 2013. "Sildenafil Restores Endothelial Function in the Apolipoprotein E Knockout Mouse." *Journal of Translational Medicine* 11

(1): 3. https://doi.org/10.1186/1479-5876-11-3.

Balkau, B., and M. A. Charles. 1999. “Comment on the Provisional Report from the WHO Consultation.” *Diabetic Medicine* 16 (5): 442–43. https://doi.org/10.1046/j.1464-5491.1999.00059.x.

Balligand, Jean-Luc. 2016. “Cardiac Salvage by Tweaking with Beta-3-Adrenergic Receptors.” *Cardiovascular Research* 111 (2): 128–33. https://doi.org/10.1093/cvr/cvw056.

Baron, A. D. 1994. “Hemodynamic Actions of Insulin.” *American Journal of Physiology - Endocrinology and Metabolism*. Am J Physiol. https://doi.org/10.1152/ajpendo.1994.267.2.e187.

Barrett, Eugene J., Hong Wang, Charles T. Upchurch, and Zhenqi Liu. 2011a. “Insulin Regulates Its Own Delivery to Skeletal Muscle by Feed-Forward Actions on the Vasculature.” *American Journal of Physiology - Endocrinology and Metabolism*. American Physiological Society. https://doi.org/10.1152/ajpendo.00186.2011.

Barrett, Eugene J, Hong Wang, Charles T Upchurch, and Zhenqi Liu. 2011b. “Insulin Regulates Its Own Delivery to Skeletal Muscle by Feed-Forward Actions on the Vasculature.” *American Journal of Physiology. Endocrinology and Metabolism* 301 (2): E252-63. https://doi.org/10.1152/ajpendo.00186.2011.

Barseghian, Ailin, Teresa Padro, Jürgen Bernhagen, Sang-Hyun Kim, and Hack-Lyoung Kim. 2019. “Pulse Wave Velocity in Atherosclerosis.” *Frontiers in Cardiovascular Medicine | Www.Frontiersin.Org* 1: 41. https://doi.org/10.3389/fcvm.2019.00041.

Bartelt, Alexander, Oliver T. Bruns, Rudolph Reimer, Heinz Hohenberg, Harald Ittrich, Kersten Peldschus, Michael G. Kaul, et al. 2011. “Brown Adipose Tissue Activity Controls Triglyceride Clearance.” *Nature Medicine* 17 (2): 200–206. https://doi.org/10.1038/nm.2297.

Barter, Philip, and Kerry-Anne -A Rye. 1994. “CHOLESTERYL ESTER TRANSFER PROTEIN: ITS ROLE IN PLASMA LIPID TRANSPORT.” *Clinical and Experimental Pharmacology and Physiology*. Clin Exp Pharmacol Physiol. https://doi.org/10.1111/j.1440-1681.1994.tb02569.x.

Basciano, Heather, Lisa Federico, and Khosrow Adeli. 2005. “Fructose, Insulin Resistance, and Metabolic Dyslipidemia.” *Nutrition and Metabolism* 2 (5): 1–14. https://doi.org/10.1186/1743-7075-2-5.

Behr-Roussel, Delphine, Alexandra Oudot, Stéphanie Caisey, Olivier L.E. Coz, Diane Gorny, Jacques Bernabé, Chris Wayman, Laurent Alexandre, and François A. Giuliano. 2008. “Daily Treatment with Sildenafil Reverses Endothelial Dysfunction and Oxidative Stress in an Animal Model of Insulin Resistance.” *European Urology* 53 (6): 1272–81. https://doi.org/10.1016/j.eururo.2007.11.018.

Beilby, John. 2004. “Definition of Metabolic Syndrome: Report of the National Heart, Lung, and Blood Institute/American Heart Association Conference on Scientific Issues Related to Definition.” *The Clinical Biochemist Reviews* 25 (3): 195. https://www.ncbi.nlm.nih.gov/pmc/articles/PMC1880831/.

Beiroa, Daniel, Monica Imbernon, Rosalía Gallego, Ana Senra, Daniel Herranz, Francesc Villarroya, Manuel Serrano, et al. 2014. "GLP-1 Agonism Stimulates Brown Adipose Tissue Thermogenesis and Browning through Hypothalamic AMPK." *Diabetes* 63 (10): 3346–58. https://doi.org/10.2337/db14-0302.

Belge, Catharina, Joanna Hammond, Emilie Dubois-Deruy, Boris Manoury, Julien Hamelet, Christophe Beauloye, Andreas Markl, et al. 2014. "Enhanced Expression of B3-Adrenoceptors in Cardiac Myocytes Attenuates Neurohormone-Induced Hypertrophic Remodeling through Nitric Oxide Synthase." *Circulation* 129 (4): 451–62. https://doi.org/10.1161/CIRCULATIONAHA.113.004940.

Belin de Chantemele, Eric J., and David W. Stepp. 2012. "Influence of Obesity and Metabolic Dysfunction on the Endothelial Control in the Coronary Circulation." *Journal of Molecular and Cellular Cardiology*. Academic Press. https://doi.org/10.1016/j.yjmcc.2011.08.018.

Bell, David S.H., G. L. Bakris, and J. B. McGill. 2009. "Comparison of Carvedilol and Metoprolol on Serum Lipid Concentration in Diabetic Hypertensive Patients." *Diabetes, Obesity and Metabolism* 11 (3): 234–38. https://doi.org/10.1111/j.1463-1326.2008.00927.x.

Benotti, Peter, G. Craig Wood, Deborah A. Winegar, Anthony T. Petrick, Christopher D. Still, George Argyropoulos, and Glenn S. Gerhard. 2014. "Risk Factors Associated with Mortality after Roux-En-Y Gastric Bypass Surgery." *Annals of Surgery* 259 (1): 123–30. https://doi.org/10.1097/SLA.0b013e31828a0ee4.

Berbeé, Jimmy F.P., Mariëtte R. Boon, P. Padmini S.J. Khedoe, Alexander Bartelt, Christian Schlein, Anna Worthmann, Sander Kooijman, et al. 2015. "Brown Fat Activation Reduces Hypercholesterolaemia and Protects from Atherosclerosis Development." *Nature Communications* 6 (1): 1–11. https://doi.org/10.1038/ncomms7356.

Bergman, Richard N., Stella P. Kim, Isabel R. Hsu, Karyn J. Catalano, Jenny D. Chiu, Morvarid Kabir, Joyce M. Richey, and Marilyn Ader. 2007. "Abdominal Obesity: Role in the Pathophysiology of Metabolic Disease and Cardiovascular Risk." *American Journal of Medicine* 120 (2 SUPPL.). https://doi.org/10.1016/j.amjmed.2006.11.012.

Bhatta, Anil, Lin Yao, Zhimin Xu, Haroldo A. Toque, Jijun Chen, Reem T. Atawia, Abdelrahman Y. Fouda, et al. 2017. "Obesity-Induced Vascular Dysfunction and Arterial Stiffening Requires Endothelial Cell Arginase 1." *Cardiovascular Research* 113 (13): 1664–76. https://doi.org/10.1093/cvr/cvx164.

Bilbis, L. S., S. A. Muhammad, Y. Saidu, and Y. Adamu. 2012. "Effect of Vitamins A, C, and e Supplementation in the Treatment of Metabolic Syndrome in Albino Rats." *Biochemistry Research International* 2012. https://doi.org/10.1155/2012/678582.

Bilbis, L.S., S.A. Muhammad, and Y. Saidu. 2014. "The Potentials Of Antioxidant Micronutrients In The Management Of Metabolic Syndrome." *Journal of Antioxidant Activity* 1 (1): 1–21. https://doi.org/10.14302/issn.2471-2140.jaa-14-423.

Binesh Marvasti, T., and Kh Adeli. 2010. "Pharmacological Management of Metabolic Syndrome and Its Lipid Complications." *DARU, Journal of Pharmaceutical Sciences* 18 (3): 146–54. /pmc/articles/PMC3304358/?report=abstract.

Boden, Guenther, Brett Lebed, Melanie Schatz, Carol Homko, and Susan Lemieux. 2001. “Effects of Acute Changes of Plasma Free Fatty Acids on Intramyocellular Fat Content and Insulin Resistance in Healthy Subjects.” *Diabetes* 50 (7): 1612–17. https://doi.org/10.2337/diabetes.50.7.1612.

Boerrigter, Guido, and John C. Burnett. 2007. “Nitric Oxide-Independent Stimulation of Soluble Guanylate Cyclase with BAY 41-2272 in Cardiovascular Disease.” *Cardiovascular Drug Reviews* 25 (1): 30–45. https://doi.org/10.1111/j.1527-3466.2007.00003.x.

Bork, Nadja I., and Viacheslav O. Nikolaev. 2018. “CGMP Signaling in the Cardiovascular System—the Role of Compartmentation and Its Live Cell Imaging.” *International Journal of Molecular Sciences*. MDPI AG. https://doi.org/10.3390/ijms19030801.

Brandão, Inês, Maria João Martins, and Rosário Monteiro. 2020. “Metabolically Healthy Obesity—Heterogeneity in Definitions and Unconventional Factors.” *Metabolites*. MDPI AG. https://doi.org/10.3390/metabo10020048.

Brasier, Allan R., Junyi Li, and Kenneth A. Wimbish. 1996. “Tumor Necrosis Factor Activates Angiotensinogen Gene Expression by the Rel A Transactivator.” *Hypertension* 27 (4): 1009–17. https://doi.org/10.1161/01.HYP.27.4.1009.

Bundgaard, Henning, Anna Axelsson, Jakob Hartvig Thomsen, Mathias Sørgaard, Klaus F. Kofoed, Rasmus Hasselbalch, Natasha A.S. Fry, et al. 2017. “The First-in-Man Randomized Trial of a Beta3 Adrenoceptor Agonist in Chronic Heart Failure: The BEAT-HF Trial.” *European Journal of Heart Failure* 19 (4): 566–75. https://doi.org/10.1002/ejhf.714.

Cai, Hua. 2005. “NAD(P)H Oxidase-Dependent Self-Propagation of Hydrogen Peroxide and Vascular Disease.” *Circulation Research*. Circ Res. https://doi.org/10.1161/01.RES.0000163631.07205.fb.

Cai, Hua, and David G. Harrison. 2000. “Endothelial Dysfunction in Cardiovascular Diseases: The Role of Oxidant Stress.” *Circulation Research* 87 (10): 840–44. https://doi.org/10.1161/01.RES.87.10.840.

Cannavo, Alessandro, and Walter J Koch. 2016. “Targeting b 3-Adrenergic Receptors in the Heart: Selective Agonism and b-Blockade.” www.jcvp.org.

Cannon, Barbara, and Jan Nedergaard. 2004. “Brown Adipose Tissue: Function and Physiological Significance.” https://doi.org/10.1152/physrev.00015.2003.-The.

Cao, Xiaojing, and Yanfang Li. 2017. “B3-Adrenergic Receptor Regulates Hepatic Apolipoprotein A-I Gene Expression.” *Journal of Clinical Lipidology* 11 (5): 1168–76. https://doi.org/10.1016/j.jacl.2017.07.007.

Carlyle, Megan, Oscar B. Jones, Jay J. Kuo, and John E. Hall. 2002. “Chronic Cardiovascular and Renal Actions of Leptin: Role of Adrenergic Activity.” In *Hypertension*, 39:496–501. Hypertension. https://doi.org/10.1161/hy0202.104398.

Carroll, J. F., C. K. Kyser, and M. M. Martin. 2002. “β-Adrenoceptor Density and Adenylyl Cyclase Activity in Obese Rabbit Hearts.” *International Journal of Obesity* 26 (5): 627–32. https://doi.org/10.1038/sj.ijo.0801957.

Carroll, Joan F., Terry M. Dwyer, Andrew W. Grady, Glenn A. Reinhart, Jean Pierre Montant, Kathy Cockrell, Edward F. Meydrech, and H. Leland Mizelle. 1996. "Hypertension, Cardiac Hypertrophy, and Neurohumoral Activity in a New Animal Model of Obesity." *American Journal of Physiology - Heart and Circulatory Physiology* 271 (1 40-1). https://doi.org/10.1152/ajpheart.1996.271.1.h373.

Carroll, Joan F., Alan E. Jones, Robert L. Hester, Glenn A. Reinhart, Kathy Cockrell, and H. Leland Mizelle. 1997. "Reduced Cardiac Contractile Responsiveness to Isoproterenol in Obese Rabbits." *Hypertension* 30 (6): 1376–81. https://doi.org/10.1161/01.HYP.30.6.1376.

Carroll, Joan F., Richard L. Summers, David J. Dzielak, Kathy Cockrell, Jean Pierre Montani, and H. Leland Mizelle. 1999. "Diastolic Compliance Is Reduced in Obese Rabbits." *Hypertension* 33 (3): 811–15. https://doi.org/10.1161/01.HYP.33.3.811.

Castro, Ana, Valeria, Cathryn M Kolka, Stella P Kim, and Richard N Bergman. 2014. "Obesity, Insulin Resistance and Comorbidities-Mechanisms of Association." *Arq Bras Endocrinol Metabol* 58 (6): 600–609.

Celik, Turgay, Atila Iyisoy, Hurkan Kursaklioglu, Ejder Kardesoglu, Selim Kilic, Hasan Turhan, M. Ilker Yilmaz, et al. 2006. "Comparative Effects of Nebivolol and Metoprolol on Oxidative Stress, Insulin Resistance, Plasma Adiponectin and Soluble P-Selectin Levels in Hypertensive Patients." *Journal of Hypertension* 24 (3): 591–96. https://doi.org/10.1097/01.hjh.0000209993.26057.de.

Cero, Cheryl, Alana O'mara, James W. Johnson, Alison S. Baskin, Joyce D. Linderman, and Aaron Cypess. 2018. "Stimulation of the ß 3 -Adrenergic Receptor via Mirabegron Induces Lipolysis and Thermogenesis in Human Adipocytes." *Diabetes* 67 (Supplement 1): 2049-P. https://doi.org/10.2337/db18-2049-p.

Cersosimo, Eugenio, and Ralph A. DeFronzo. 2006. "Insulin Resistance and Endothelial Dysfunction: The Road Map to Cardiovascular Diseases." *Diabetes/Metabolism Research and Reviews*. https://doi.org/10.1002/dmrr.634.

Chan, Pei-Chi, and Po-Shiuan Hsieh. 2017. "The Role of Adipocyte Hypertrophy and Hypoxia in the Development of Obesity-Associated Adipose Tissue Inflammation and Insulin Resistance." In *Adiposity - Omics and Molecular Understanding*. InTech. https://doi.org/10.5772/65458.

Chapple, Christopher R., Linda Cardozo, Victor W. Nitti, Emad Siddiqui, and Martin C. Michel. 2014. "Mirabegron in Overactive Bladder: A Review of Efficacy, Safety, and Tolerability." *Neurourology and Urodynamics* 33 (1): 17–30. https://doi.org/10.1002/nau.22505.

Chen, Kong Y., Robert J. Brychta, Zahraa Abdul Sater, Thomas M. Cassimatis, Cheryl Cero, Laura A. Fletcher, Nikita S. Israni, et al. 2020. "Opportunities and Challenges in the Therapeutic Activation of Human Energy Expenditure and Thermogenesis to Manage Obesity." *Journal of Biological Chemistry* 295 (7): 1926–42. https://doi.org/10.1074/jbc.REV119.007363.

Chen, Tao, Meng Sun, Jia-Qiang Wang, Jin-Jin Cui, Zhong-Hua Liu, and Bo Yu. 2017. "A Novel Swine Model for Evaluation of Dyslipidemia and Atherosclerosis Induced by Human CETP Overexpression." *Lipids in Health and Disease* 16 (1): 169. https://doi.org/10.1186/s12944-

017-0563-x.

Choi, Sung Hee, and Henry N Ginsberg. 2011. “Increased Very Low Density Lipoprotein (VLDL) Secretion, Hepatic Steatosis, and Insulin Resistance.” *Trends in Endocrinology and Metabolism: TEM* 22 (9): 353–63. https://doi.org/10.1016/j.tem.2011.04.007.

Clark, Michael G., Michelle G. Wallis, Eugene J. Barrett, Michelle A. Vincent, Stephen M. Richards, Lucy H. Clerk, and Stephen Rattigan. 2003. “Blood Flow and Muscle Metabolism: A Focus on Insulin Action.” *American Journal of Physiology - Endocrinology and Metabolism* 284 (2 47-2). https://doi.org/10.1152/ajpendo.00408.2002.

Clearfield, Michael B. 2005. “C-Reactive Protein: A New Risk Assessment Tool for Cardiovascular Disease.” *Journal of the American Osteopathic Association*. American Osteopathic Association. https://doi.org/10.7556/jaoa.2005.105.9.409.

Clookey, Stephanie L., Rebecca J. Welly, Dusti Shay, Makenzie L. Woodford, Kevin L. Fritsche, R. Scott Rector, Jaume Padilla, Dennis B. Lubahn, and Victoria J. Vieira-Potter. 2019. “Beta 3 Adrenergic Receptor Activation Rescues Metabolic Dysfunction in Female Estrogen Receptor Alpha-Null Mice.” *Frontiers in Physiology* 10 (FEB). https://doi.org/10.3389/fphys.2019.00009.

Cnop, Miriam, Melinda J. Landchild, Josep Vidal, Peter J. Havel, Negar G. Knowles, Darcy R. Carr, Feng Wang, et al. 2002. “The Concurrent Accumulation of Intra-Abdominal and Subcutaneous Fat Explains the Association between Insulin Resistance and Plasma Leptin Concentrations: Distinct Metabolic Effects of Two Fat Compartments.” *Diabetes* 51 (4): 1005–15. https://doi.org/10.2337/diabetes.51.4.1005.

Collins, Sheila. 2012. “β-Adrenoceptor Signaling Networks in Adipocytes for Recruiting Stored Fat and Energy Expenditure.” *Frontiers in Endocrinology*. Frontiers Media SA. https://doi.org/10.3389/fendo.2011.00102.

Conceição, Miguel Soares, Valéria Bonganha, Felipe Cassaro Vechin, Ricardo Paes de Barros Berton, Manoel Emílio Lixandrão, Felipe Romano Damas Nogueira, Giovana Vergínia de Souza, Mara Patricia Traina Chacon-Mikahil, and Cleiton Augusto Libardi. 2013. “Sixteen Weeks of Resistance Training Can Decrease the Risk of Metabolic Syndrome in Healthy Postmenopausal Women.” *Clinical Interventions in Aging* 8 (September): 1221–28. https://doi.org/10.2147/CIA.S44245.

Conti, Valeria, Giusy Russomanno, Graziamaria Corbi, Viviana Izzo, Carmine Vecchione, and Amelia Filippelli. 2013. “Adrenoreceptors and Nitric Oxide in the Cardiovascular System.” *Frontiers in Physiology*. https://doi.org/10.3389/fphys.2013.00321.

Cooke, John P. 2000. “Does ADMA Cause Endothelial Dysfunction?” *Arteriosclerosis, Thrombosis, and Vascular Biology* 20 (9): 2032–37. https://doi.org/10.1161/01.ATV.20.9.2032.

Copps, K D, and M F White. 2012. “Regulation of Insulin Sensitivity by Serine/Threonine Phosphorylation of Insulin Receptor Substrate Proteins IRS1 and IRS2.” *Diabetologia* 55 (10): 2565–82. https://doi.org/10.1007/s00125-012-2644-8.

Cornier, Marc Andre, Dana Dabelea, Teri L. Hernandez, Rachel C. Lindstrom, Amy J. Steig, Nicole R. Stob, Rachael E. Van Pelt, Hong Wang, and Robert H. Eckel. 2008. "The Metabolic Syndrome." *Endocrine Reviews* 29 (7): 777–822. https://doi.org/10.1210/er.2008-0024.

Cros, G. 1985. "Mécanismes de La Désensibilisation Des Récepteurs Bêta-Adrénergiques." *Bull Eur Physiopathol Respir. ;():.* 21 (5): 35–43. https://pubmed.ncbi.nlm.nih.gov/2865991/.

Cunha, Tatiana Sousa, Maria José Costa Sampaio Moura, Celene Fernandes Bernardes, Ana Paula Tanno, and Fernanda Klein Marcondes. 2005. "Vascular Sensitivity to Phenylephrine in Rats Submitted to Anaerobic Training and Nandrolone Treatment." *Hypertension* 46 (4): 1010–15. https://doi.org/10.1161/01.HYP.0000174600.51515.e7.

Cuspidi, Cesare, Stefano Meani, Veronica Fusi, Barbara Severgnini, Cristiana Valerio, Eleonora Catini, Gastone Leonetti, Fabio Magrini, and Alberto Zanchetti. 2004. "Metabolic Syndrome and Target Organ Damage in Untreated Essential Hypertensives." *Journal of Hypertension* 22 (10): 1991–98. https://doi.org/10.1097/00004872-200410000-00023.

Cypess, Aaron M., Lauren S. Weiner, Carla Roberts-Toler, Elisa Franquet Elía, Skyler H. Kessler, Peter A. Kahn, Jeffrey English, et al. 2015. "Activation of Human Brown Adipose Tissue by a B3-Adrenergic Receptor Agonist." *Cell Metabolism* 21 (1): 33–38. https://doi.org/10.1016/j.cmet.2014.12.009.

Cypess, Aaron M, and C Ronald Kahn. 2010. "Brown Fat as a Therapy for Obesity and Diabetes." *Current Opinion in Endocrinology, Diabetes and Obesity* 17 (2): 143–49. https://doi.org/10.1097/MED.0b013e328337a81f.

Czech, Michael P. 2017. "Insulin Action and Resistance in Obesity and Type 2 Diabetes." *Nature Medicine* 23 (7): 804–14. https://doi.org/10.1038/nm.4350.

Deanfield, John E., Julian P. Halcox, and Ton J. Rabelink. 2007. "Endothelial Function and Dysfunction." *Circulation* 115 (10): 1285–95. https://doi.org/10.1161/CIRCULATIONAHA.106.652859.

DeBoer, Michiel P., Rick I. Meijet, Nienke J. Wijnstok, Amy M. Jonk, Alphons J. Houben, Coen D. Stehouwer, Yvo M. Smulders, Etto C. Eringa, and Erik H. Serne. 2012. "Microvascular Dysfunction: A Potential Mechanism in the Pathogenesis of Obesity-Associated Insulin Resistance and Hypertension." *Microcirculation* 19 (1): 5–18. https://doi.org/10.1111/j.1549-8719.2011.00130.x.

Dehvari, Nodi, Edilson Dantas da Silva Junior, Tore Bengtsson, and Dana Sabine Hutchinson. 2018. "Mirabegron: Potential off Target Effects and Uses beyond the Bladder." *British Journal of Pharmacology* 175 (21): 4072–82. https://doi.org/10.1111/bph.14121.

Dekker, Mark J., Qiaozhu Su, Chris Baker, Angela C. Rutledge, and Khosrow Adeli. 2010. "Fructose: A Highly Lipogenic Nutrient Implicated in Insulin Resistance, Hepatic Steatosis, and the Metabolic Syndrome." *American Journal of Physiology - Endocrinology and Metabolism* 299 (5): 685–94. https://doi.org/10.1152/ajpendo.00283.2010.

Demarco, Vincent G, Annayya R Aroor, and James R Sowers. 2014. "The Pathophysiology of Hypertension in Patients with Obesity." https://doi.org/10.1038/nrendo.2014.44.

Devaraj, Sridevi, David Siegel, and Ishwarlal Jialal. 2011. “Statin Therapy in Metabolic Syndrome and Hypertension Post-JUPITER: What Is the Value of CRP?” *Current Atherosclerosis Reports* 13 (1): 31–42. https://doi.org/10.1007/s11883-010-0143-2.

Dhein, Stefan. 2005. *Practical Methods in Cardiovascular Research*. https://doi.org/10.1007/b137833.

Diaz, Mauricio Berriel, Stephan Herzig, and Alexandros Vegiopoulos. 2014. “Thermogenic Adipocytes: From Cells to Physiology and Medicine.” *Metabolism: Clinical and Experimental*. W.B. Saunders. https://doi.org/10.1016/j.metabol.2014.07.002.

Didion, Sean P., Michael J. Ryan, Lisa A. Didion, Pamela E. Fegan, Curt D. Sigmund, and Frank M. Faraci. 2002. “Increased Superoxide and Vascular Dysfunction in CuZnSOD-Deficient Mice.” *Circulation Research* 91 (10): 938–44. https://doi.org/10.1161/01.RES.0000043280.65241.04.

Dimitrova, S S, I Penchev Georgiev, I N Kanelov, Y I Iliev, S I Tanev, T Mircheva Georgieva, Animal Physiology, Physiological Chemis-, Stara Zagora, and Computer Engineering. 2008. “Intravenous Glucose Tolerance Test and Glucose Kinetic Parameters in Rabbits,” 161–69.

Dincer, U. Deniz. 2011. “Cardiac ß-Adrenoceptor Expression Is Markedly Depressed in Ossabaw Swine Model of Cardiometabolic Risk.” *International Journal of General Medicine*, 493. https://doi.org/10.2147/ijgm.s18175.

Dipla, Konstantina, Andreas Zafeiridis, and Karen M. Tordjman. 2020. “Metabolic Syndrome, Hormones, and Exercise.” In *Contemporary Endocrinology*, 519–34. Humana Press Inc. https://doi.org/10.1007/978-3-030-33376-8_29.

Doghri, Yosra, Fabien Chetaneau, Moez Rhimi, Aicha Kriaa, Valérie Lalanne, Chantal Thorin, Emmanuelle Maguin, M. Yassine Mallem, and Jean Claude Desfontis. 2019. “Sildenafil Citrate Long-Term Treatment Effects on Cardiovascular Reactivity in a SHR Experimental Model of Metabolic Syndrome.” *PLoS ONE* 14 (11). https://doi.org/10.1371/journal.pone.0223914.

Döring, H. J. 1990. “The Isolated Perfused Heart According to Langendorff Technique--Function--Application.” *Physiologia Bohemoslovaca*.

Döring, Hans J., and Heinz. Dehnert. 1988. “The Isolated Perfused Warm-Blooded Heart According to Langendorff.”

Drake, Isabel, Emily Sonestedt, Ulrika Ericson, Peter Wallström, and Marju Orho-Melander. 2018. “A Western Dietary Pattern Is Prospectively Associated with Cardio-Metabolic Traits and Incidence of the Metabolic Syndrome.” *British Journal of Nutrition* 119 (10): 1168–76. https://doi.org/10.1017/S000711451800079X.

Drenowatz, Clemens. 2015. “Reciprocal Compensation to Changes in Dietary Intake and Energy Expenditure within the Concept of Energy Balance.” *Advances in Nutrition* 6 (5): 592–99. https://doi.org/10.3945/an.115.008615.

Dröge, Wulf. 2002. “Free Radicals in the Physiological Control of Cell Function.” *Physiological Reviews*. American Physiological Society. https://doi.org/10.1152/physrev.00018.2001.

Duncan, Edward R., Paul A. Crossey, Simon Walker, Narayana Anilkumar, Lucilla Poston, Gillian Douglas, Vivienne A. Ezzat, Stephen B. Wheatcroft, Ajay M. Shah, and Mark I. Kearney. 2008. "Effect of Endothelium-Specific Insulin Resistance on Endothelial Function in Vivo." *Diabetes* 57 (12): 3307–14. https://doi.org/10.2337/db07-1111.

Eckel, Robert H., Scott M. Grundy, and Paul Z. Zimmet. 2005. "The Metabolic Syndrome." In *Lancet*, 365:1415–28. Elsevier Limited. https://doi.org/10.1016/S0140-6736(05)66378-7.

Egan, Brent M. 2003. "Insulin Resistance and the Sympathetic Nervous System." *Current Hypertension Reports*. Current Science Ltd. https://doi.org/10.1007/s11906-003-0028-7.

Eikelis, Nina, Markus Schlaich, Anuradha Aggarwal, David Kaye, and Murray Esler. 2003. "Interactions between Leptin and the Human Sympathetic Nervous System." *Hypertension* 41 (5): 1072–79. https://doi.org/10.1161/01.HYP.0000066289.17754.49.

El-Bassossy, Hany M., Nora Dsokey, and Ahmed Fahmy. 2014. "Characterization of Vascular Complications in Experimental Model of Fructose-Induced Metabolic Syndrome." *Toxicology Mechanisms and Methods* 24 (8): 536–43. https://doi.org/10.3109/15376516.2014.945109.

El-Mahmoudy, Abubakr, Saad Shousha, Hussein Abdel-Maksoud, and Omayma Abou Zaid. 2013. "Effect of Long-Term Administration of Sildenafil on Lipid Profile and Organ Functions in Hyperlipidemic Rats." *Acta Biomedica* 84 (1): 12–22.

Elam, Marshall B., Henry N. Ginsberg, Laura C. Lovato, Marshall Corson, Joseph Largay, Lawrence A. Leiter, Carlos Lopez, et al. 2017. "Association of Fenofibrate Therapy with Long-Term Cardiovascular Risk in Statin-Treated Patients with Type 2 Diabetes." *JAMA Cardiology* 2 (4): 370–80. https://doi.org/10.1001/jamacardio.2016.4828.

Elam, Marshall, Laura C. Lovato, and Henry Ginsberg. 2011. "Role of Fibrates in Cardiovascular Disease Prevention, the ACCORD-Lipid Perspective." *Current Opinion in Lipidology*. NIH Public Access. https://doi.org/10.1097/MOL.0b013e328341a5a8.

Elliott, Sharon S., Nancy L. Keim, Judith S. Stern, Karen Teff, and Peter J. Havel. 2002. "Fructose, Weight Gain, and the Insulin Resistance Syndrome." *American Journal of Clinical Nutrition* 76 (5): 911–22. https://doi.org/10.1093/ajcn/76.5.911.

Ellulu, Mohammed S., Ismail Patimah, Huzwah Khaza'ai, Asmah Rahmat, and Yehia Abed. 2017. "Obesity & Inflammation: The Linking Mechanism & the Complications." *Archives of Medical Science* 13 (4): 851–63. https://doi.org/10.5114/aoms.2016.58928.

Endemann, Dierk H., and Ernesto L. Schiffrin. 2004. "Endothelial Dysfunction." *Journal of the American Society of Nephrology*. J Am Soc Nephrol. https://doi.org/10.1097/01.ASN.0000132474.50966.DA.

Eringa, Etto C., Coen D.A. Stehouwer, Thomas Merlijn, Nico Westerhof, and Pieter Sipkema. 2002. "Physiological Concentrations of Insulin Induce Endothelin-Mediated Vasoconstriction during Inhibition of NOS or PI3-Kinase in Skeletal Muscle Arterioles." *Cardiovascular Research* 56 (3): 464–71. https://doi.org/10.1016/S0008-6363(02)00593-X.

Eringa, Etto C., Coen D.A. Stehouwer, Marjon H. Roos, Nico Westerhof, and Pieter Sipkema.

2007. “Selective Resistance to Vasoactive Effects of Insulin in Muscle Resistance Arteries of Obese Zucker (Fa/Fa) Rats.” *American Journal of Physiology - Endocrinology and Metabolism* 293 (5). https://doi.org/10.1152/ajpendo.00516.2006.

Estruch, R., E. Ros, J. Salas-Salvadó, M. I. Covas, D. Corella, F. Arós, E. Gómez-Gracia, et al. 2018. “Primary Prevention of Cardiovascular Disease with a Mediterranean Diet Supplemented with Extra-Virgin Olive Oil or Nuts.” *New England Journal of Medicine* 378 (25). https://doi.org/10.1056/NEJMoa1800389.

Evgenov, Oleg V., Pál Pacher, Peter M. Schmidt, György Haskó, Harald H.H.W. Schmidt, and Johannes Peter Stasch. 2006. “NO-Independent Stimulators and Activators of Soluble Guanylate Cyclase: Discovery and Therapeutic Potential.” *Nature Reviews Drug Discovery*. NIH Public Access. https://doi.org/10.1038/nrd2038.

Evgenov, Oleg V, Pál Pacher, Peter M Schmidt, Harald H H W Schmidt, and Johannes-Peter Stasch. 2008. “NO-Independent Stimulators and Activators of Soluble Guanylate Cyclase: Discovery and Therapeutic Potential.” http://www.cyclicgmp.net.

Fan, Jianglin, Shuji Kitajima, Teruo Watanabe, Jie Xu, Jifeng Zhang, Enqi Liu, and Y. Eugene Chen. 2015a. “Rabbit Models for the Study of Human Atherosclerosis: From Pathophysiological Mechanisms to Translational Medicine.” *Pharmacology and Therapeutics*. Elsevier Inc. https://doi.org/10.1016/j.pharmthera.2014.09.009.

———. 2015b. “Rabbit Models for the Study of Human Atherosclerosis: From Pathophysiological Mechanisms to Translational Medicine.” *Pharmacology and Therapeutics* 146: 104–19. https://doi.org/10.1016/j.pharmthera.2014.09.009.

“FDA Requests the Withdrawal of the Weight-Loss Drug Belviq, Belviq XR (Lorcaserin) from the Market | FDA.” 2020. 2020. https://www.fda.gov/drugs/drug-safety-and-availability/fda-requests-withdrawal-weight-loss-drug-belviq-belviq-xr-lorcaserin-market.

Ferdinand, Keith C., William B. White, David A. Calhoun, Eva M. Lonn, Philip T. Sager, Rocco Brunelle, Honghua H. Jiang, Rebecca J. Threlkeld, Kenneth E. Robertson, and Mary Jane Geiger. 2014. “Effects of the Once-Weekly Glucagon-like Peptide-1 Receptor Agonist Dulaglutide on Ambulatory Blood Pressure and Heart Rate in Patients with Type 2 Diabetes Mellitus.” *Hypertension* 64 (4): 731–37. https://doi.org/10.1161/HYPERTENSIONAHA.114.03062.

Fernández-Miranda, Gaudencio, Tatiana Romero-Garcia, Tarín P. Barrera-Lechuga, Martha Mercado-Morales, and Angélica Rueda. 2019. “Impaired Activity of Ryanodine Receptors Contributes to Calcium Mishandling in Cardiomyocytes of Metabolic Syndrome Rats.” *Frontiers in Physiology* 10 (APR). https://doi.org/10.3389/fphys.2019.00520.

Fernández-Real, José Manuel, and Wifredo Ricart. 2003. “Insulin Resistance and Chronic Cardiovascular Inflammatory Syndrome.” *Endocrine Reviews*. Endocrine Society. https://doi.org/10.1210/er.2002-0010.

Feron, Olivier, Chantal Dessy, Stephane Moniotte, Jean Pierre Desager, and Jean Luc Balligand. 1999. “Hypercholesterolemia Decreases Nitric Oxide Production by Promoting the Interaction of Caveolin and Endothelial Nitric Oxide Synthase.” *Journal of Clinical*

Investigation 103 (6): 897–905. https://doi.org/10.1172/JCI4829.

Ferrannini, Ele. 2006. “Is Insulin Resistance the Cause of the Metabolic Syndrome?” *Annals of Medicine*. Taylor & Francis. https://doi.org/10.1080/07853890500415358.

Ferrannini, Ele, Andrea Natali, Bruoella Capaldo, Mikko Lehtovirta, Stefan Jacob, and Hannele Yki-Järvinen. 1997. “Insulin Resistance, Hyperinsulinemia, and Blood Pressure: Role of Age and Obesity.” *Hypertension* 30 (5): 1144–49. https://doi.org/10.1161/01.HYP.30.5.1144.

Ferron, Artur Junio Togneri, Fabiane Valentini Francisqueti, Igor Otávio Minatel, Carol Cristina Vágula de Almeida Silva, Silméia Garcia Zanati Bazan, Koody André Hassemi Kitawara, Jéssica Leite Garcia, Camila Renata Corrêa, Fernando Moreto, and Ana Lucia A. Ferreira. 2018. “Association between Cardiac Remodeling and Metabolic Alteration in an Experimental Model of Obesity Induced by Western Diet.” *Nutrients* 10 (11). https://doi.org/10.3390/nu10111675.

Ferron, Artur Junio Togneri, Bruno Barcellos Jacobsen, Paula Grippa Sant’Ana, Dijon Henrique Salomé De Campos, Loreta Casquel De Tomasi, Renata De Azevedo Mello Luvizotto, Antonio Carlos Cicogna, André Soares Leopoldo, and Ana Paula Lima-Leopoldo. 2015. “Cardiac Dysfunction Induced by Obesity Is Not Related to β-Adrenergic System Impairment at the Receptor-Signalling Pathway.” *PLoS ONE* 10 (9): 1–18. https://doi.org/10.1371/journal.pone.0138605.

Finlin, Brian S., Hasiyet Memetimin, Amy L. Confides, Ildiko Kasza, Beibei Zhu, Hemendra J. Vekaria, Brianna Harfmann, et al. 2018. “Human Adipose Beiging in Response to Cold and Mirabegron.” *JCI Insight* 3 (15). https://doi.org/10.1172/jci.insight.121510.

Finlin, Brian S., Hasiyet Memetimin, Beibei Zhu, Amy L. Confides, Hemendra J. Vekaria, Riham H. El Khouli, Zachary R. Johnson, et al. 2020. “The B3-Adrenergic Receptor Agonist Mirabegron Improves Glucose Homeostasis in Obese Humans.” *Journal of Clinical Investigation* 130 (5): 2319–31. https://doi.org/10.1172/JCI134892.

Flack, John M., Steven A. Atlas, James L. Pool, and William B. White. 2007. “Renin-Angiotensin Aldosterone System and Hypertension: Current Approaches and Future Directions.” *Journal of Managed Care Pharmacy* 13 (8 Supp B): 1–39. https://doi.org/10.18553/jmcp.2007.13.s8-b.1.

Florian, John P., and James A. Pawelczyk. 2010. “Sympathetic and Haemodynamic Responses to Lipids in Healthy Human Ageing.” *Experimental Physiology* 95 (4): 486–97. https://doi.org/10.1113/expphysiol.2009.050997.

Fö Rstermann, Ulrich, and William C Sessa. 2012. “Nitric Oxide Synthases: Regulation and Function.” *European Heart Journal* 33: 829–837. https://doi.org/10.1093/eurheartj/ehr304.

Franken, N. A.P., J. A.J. Camps, F. J.M. Van Ravels, A. Van Der Laarse, E. K.J. Pauwels, and J. Wondergem. 1997. “Comparison of in Vivo Cardiac Function with Ex Vivo Cardiac Performance of the Rat Heart after Thoracic Irradiation.” *British Journal of Radiology* 70 (OCT.): 1004–9. https://doi.org/10.1259/bjr.70.838.9404203.

Friebe, Andreas, Peter Sandner, and Achim Schmidtko. 2020. “CGMP: A Unique 2nd Messenger

Molecule – Recent Developments in CGMP Research and Development." *Naunyn-Schmiedeberg's Archives of Pharmacology*. Springer. https://doi.org/10.1007/s00210-019-01779-z.

Fried, Susan K., Dove A. Bunkin, and Andrew S. Greenberg. 1998. " Omental and Subcutaneous Adipose Tissues of Obese Subjects Release Interleukin-6: Depot Difference and Regulation by Glucocorticoid 1 ." *The Journal of Clinical Endocrinology & Metabolism* 83 (3): 847–50. https://doi.org/10.1210/jcem.83.3.4660.

Frühbeck, Gema. 2015. "Bariatric and Metabolic Surgery: A Shift in Eligibility and Success Criteria." *Nature Reviews Endocrinology*. Nature Publishing Group. https://doi.org/10.1038/nrendo.2015.84.

Fujimoto, Wilfred Y. 2000. "The Importance of Insulin Resistance in the Pathogenesis of Type 2 Diabetes Mellitus." In *American Journal of Medicine*, 108:9–14. Elsevier Inc. https://doi.org/10.1016/s0002-9343(00)00337-5.

Furman, Brian L. 2007. "Orlistat." In *XPharm: The Comprehensive Pharmacology Reference*, 1–3. Elsevier Inc. https://doi.org/10.1016/B978-008055232-3.62333-5.

Gajdova, Jaromira, David Karasek, Dominika Goldmannova, Ondrej Krystynik, Jan Schovanek, Helena Vaverkova, and Josef Zadrazil. 2017. "Pulse Wave Analysis and Diabetes Mellitus. A Systematic Review." *Biomedical Papers*. https://doi.org/10.5507/bp.2017.028.

Gallagher, Emily J., Derek Leroith, and Eddy Karnieli. 2010. "Insulin Resistance in Obesity as the Underlying Cause for the Metabolic Syndrome." *Mount Sinai Journal of Medicine*. John Wiley & Sons, Ltd. https://doi.org/10.1002/msj.20212.

Galougahi, Keyvan Karimi, Chia-Chi Liu, Alvaro Garcia, Carmine Gentile, Natasha A Fry, Elisha J Hamilton, Clare L Hawkins, and Gemma A Figtree. 2016. "B3 Adrenergic Stimulation Restores Nitric Oxide/Redox Balance and Enhances Endothelial Function in Hyperglycemia" 5 (2). https://doi.org/10.1161/JAHA.115.002824.

Gancheva, Silvia, Maria Zhelyazkova-Savova, Bistra Galunska, and Trifon Chervenkov. 2015. "Experimental Models of Metabolic Syndrome in Rats." *Scripta Scientifica Medica* 47 (2): 14. https://doi.org/10.14748/ssm.v47i2.1145.

Gendron, Marie Ève, Nathalie Thorin-Trescases, Louis Villeneuve, and Eric Thorin. 2007. "Aging Associated with Mild Dyslipidemia Reveals That COX-2 Preserves Dilation despite Endothelial Dysfunction." *American Journal of Physiology - Heart and Circulatory Physiology* 292 (1). https://doi.org/10.1152/ajpheart.00551.2006.

Giannini, Cosimo, Nicola Santoro, Sonia Caprio, Grace Kim, Derek Lartaud, Melissa Shaw, Bridget Pierpont, and Ram Weiss. 2011. "The Triglyceride-to-HDL Cholesterol Ratio: Association with Insulin Resistance in Obese Youths of Different Ethnic Backgrounds." *Diabetes Care* 34 (8): 1869–74. https://doi.org/10.2337/dc10-2234.

Ginsberg, Henry N. 2000. "Insulin Resistance and Cardiovascular Disease." *Journal of Clinical Investigation*. The American Society for Clinical Investigation. https://doi.org/10.1172/JCI10762.

Ginsberg, Henry N., Yuan Li Zhang, and Antonio Hernandez-Ono. 2005. “Regulation of Plasma Triglycerides in Insulin Resistance and Diabetes.” *Archives of Medical Research*. Arch Med Res. https://doi.org/10.1016/j.arcmed.2005.01.005.

Gkaliagkousi, E., and S. Douma. 2009. “The Pathogenesis of Arterial Stiffness and Its Prognostic Value in Essential Hypertension and Cardiovascular Diseases.” *Hippokratia*. Hippokratio General Hospital of Thessaloniki.

Golbidi, Saeid, Azam Mesdaghinia, and Ismail Laher. 2012. “Exercise in the Metabolic Syndrome.” *Oxidative Medicine and Cellular Longevity*. https://doi.org/10.1155/2012/349710.

Goldberg, S. J., N. Wilson, and D. F. Dickinson. 1985. “Increased Blood Velocities in the Heart and Great Vessels of Patients with Congenital Heart Disease. An Assessment of Their Significance in the Absence of Valvular Stenosis.” *British Heart Journal* 53 (6): 640–44. https://doi.org/10.1136/hrt.53.6.640.

Goldstein, Barry J. 2002. “Insulin Resistance as the Core Defect in Type 2 Diabetes Mellitus.” *American Journal of Cardiology* 90 (5 SUPPL.): 3–10. https://doi.org/10.1016/S0002-9149(02)02553-5.

Goldstein, Barry J., and Rosario Scalia. 2004. “Adiponectin: A Novel Adipokine Linking Adipocytes and Vascular Function.” *The Journal of Clinical Endocrinology & Metabolism* 89 (6): 2563–68. https://doi.org/10.1210/jc.2004-0518.

Gonzalez-Baró, Maria R., Tal M. Lewin, and Rosalind A. Coleman. 2007. “Regulation of Triglyceride Metabolism II. Function of Mitochondrial GPAT1 in the Regulation of Triacylglycerol Biosynthesis and Insulin Action.” *American Journal of Physiology - Gastrointestinal and Liver Physiology* 292 (5). https://doi.org/10.1152/ajpgi.00553.2006.

Grassi, G., R. Dell’Oro, F. Quarti-Trevano, F. Scopelliti, G. Seravalle, F. Paleari, P. L. Gamba, and G. Mancia. 2005. “Neuroadrenergic and Reflex Abnormalities in Patients with Metabolic Syndrome.” *Diabetologia* 48 (7): 1359–65. https://doi.org/10.1007/s00125-005-1798-z.

Gratl, Victoria, Raphael C. Cheung, Biao Chen, Changiz Taghibiglou, Stephen C. Van Iderstine, and Khosrow Adeli. 2002. “Simvastatin, an HMG-CoA Reductase Inhibitor, Induces the Synthesis and Secretion of Apolipoprotein AI in HepG2 Cells and Primary Hamster Hepatocytes.” *Atherosclerosis* 163 (1): 59–68. https://doi.org/10.1016/S0021-9150(01)00754-7.

Greenberg, S., J. Xie, Y. Wang, B. Cai, J. Kolls, S. Nelson, A. Hyman, W. R. Summer, and H. Lippton. 1993. “Tumor Necrosis Factor-Alpha Inhibits Endothelium-Dependent Relaxation.” *Journal of Applied Physiology* 74 (5): 2394–2403. https://doi.org/10.1152/jappl.1993.74.5.2394.

Greenwald, S E. 2002. “QJM Pulse Pressure and Arterial Elasticity.” *Q J Med* 95: 107–12. https://academic.oup.com/qjmed/article-abstract/95/2/107/1528642.

Greenway, Frank L., Ken Fujioka, Raymond A. Plodkowski, Sunder Mudaliar, Maria Guttadauria, Janelle Erickson, Dennis D. Kim, and Eduardo Dunayevich. 2010. “Effect of Naltrexone plus

Bupropion on Weight Loss in Overweight and Obese Adults (COR-I): A Multicentre, Randomised, Double-Blind, Placebo-Controlled, Phase 3 Trial." *The Lancet* 376 (9741): 595–605. https://doi.org/10.1016/S0140-6736(10)60888-4.

Griendling, Kathy K., Dan Sorescu, and Masuko Ushio-Fukai. 2000. "NAD(P)H Oxidase: Role in Cardiovascular Biology and Disease." *Circulation Research*. Lippincott Williams and Wilkins. https://doi.org/10.1161/01.RES.86.5.494.

Grossman, E. 2009. "Metabolic Syndrome and Biventricular Hypertrophy in Essential Hypertension." *Journal of Human Hypertension* 23 (3): 211–12. https://doi.org/10.1038/jhh.2008.145.

Grujic, Danica, Vedrana S. Susulic, Mary Ellen Harper, Jean Himms-Hagen, Barbara A. Cunningham, Barbara E. Corkey, and Bradford B. Lowell. 1997. "B3-Adrenergic Receptors on White and Brown Adipocytes Mediate B3- Selective Agonist-Induced Effects on Energy Expenditure, Insulin Secretion, and Food Intake: A Study Using Transgenic and Gene Knockout Mice." *Journal of Biological Chemistry* 272 (28): 17686–93. https://doi.org/10.1074/jbc.272.28.17686.

Grundy, Scott M. 2006. "Atherogenic Dyslipidemia Associated with Metabolic Syndrome and Insulin Resistance." *Clinical Cornerstone* 8 (SUPPL. 1). https://doi.org/10.1016/S1098-3597(06)80005-0.

Grundy, Scott M., James I. Cleeman, Stephen R. Daniels, Karen A. Donato, Robert H. Eckel, Barry A. Franklin, David J. Gordon, et al. 2005. "Diagnosis and Management of the Metabolic Syndrome: An American Heart Association/National Heart, Lung, and Blood Institute Scientific Statement." *Circulation*. Lippincott Williams & Wilkins. https://doi.org/10.1161/CIRCULATIONAHA.105.169404.

Guebre-Egziabher, Fitsum, Pascaline M. Alix, Laetitia Koppe, Caroline C. Pelletier, Emilie Kalbacher, Denis Fouque, and Christophe O. Soulage. 2013. "Ectopic Lipid Accumulation: A Potential Cause for Metabolic Disturbances and a Contributor to the Alteration of Kidney Function." *Biochimie* 95 (11): 1971–79. https://doi.org/10.1016/j.biochi.2013.07.017.

Guenther, Mitchell, Roland James, Jacqueline Marks, Shi Zhao, Aniko Szabo, and Srividya Kidambi. 2014. "Adiposity Distribution Influences Circulating Adiponectin Levels." *Translational Research* 164 (4): 270–77. https://doi.org/10.1016/j.trsl.2014.04.008.

Güneş, Yilmaz, Mustafa Tuncer, Mustafa Yildirim, Ünal Güntekin, Hasan Ali Gümrükçüoğlu, and Musa Şahin. 2008. "A Novel Echocardiographic Method for the Prediction of Coronary Artery Disease." *Medical Science Monitor* 14 (9): 42–46.

Halberg, Nils, Ingrid Wernstedt-Asterholm, and Philipp E. Scherer. 2008. "The Adipocyte as an Endocrine Cell." *Endocrinology and Metabolism Clinics of North America*. NIH Public Access. https://doi.org/10.1016/j.ecl.2008.07.002.

Hao, Lei, Sheyenne Scott, Mehrnaz Abbasi, Yujiao Zu, Md Shahjalal Hossain Khan, Yang Yang, Dayong Wu, Ling Zhao, and Shu Wang. 2019. "Beneficial Metabolic Effects of Mirabegron in Vitro and in High-Fat Diet-Induced Obese Mice." *Journal of Pharmacology and Experimental Therapeutics* 369 (3): 419–27. https://doi.org/10.1124/jpet.118.255778.

Hasegawa, Yukiko, Tomoko Nakagami, Junko Oya, Kanako Takahashi, Chisato Isago, Moritoshi Kurita, Yuki Tanaka, Arata Ito, Tadasu Kasahara, and Yasuko Uchigata. 2019. "Body Weight Reduction of 5% Improved Blood Pressure and Lipid Profiles in Obese Men and Blood Glucose in Obese Women: A Four-Year Follow-up Observational Study." *Metabolic Syndrome and Related Disorders* 17 (5): 250–58. https://doi.org/10.1089/met.2018.0115.

He, Dan, Bo Xi, Jian Xue, Pengcheng Huai, Min Zhang, and Jun Li. 2014. "Association between Leisure Time Physical Activity and Metabolic Syndrome: A Meta-Analysis of Prospective Cohort Studies." *Endocrine* 46 (2): 231–40. https://doi.org/10.1007/s12020-013-0110-0.

Heitzer, T., K. Krohn, S. Albers, and T. Meinertz. 2000. "Tetrahydrobiopterin Improves Endothelium-Dependent Vasodilation by Increasing Nitric Oxide Activity in Patients with Type II Diabetes Mellitus." *Diabetologia* 43 (11): 1435–38. https://doi.org/10.1007/s001250051551.

Helfenstein, Tatiana, Francisco A. Fonseca, Sílvia S. Ihara, Juliana M. Bottós, Flávio T. Moreira, Henrique Pott, Michel E. Farah, Maria C. Martins, and Maria C. Izar. 2011a. "Impaired Glucose Tolerance plus Hyperlipidaemia Induced by Diet Promotes Retina Microaneurysms in New Zealand Rabbits." *International Journal of Experimental Pathology* 92 (1): 40–49. https://doi.org/10.1111/j.1365-2613.2010.00753.x.

———. 2011b. "Impaired Glucose Tolerance plus Hyperlipidaemia Induced by Diet Promotes Retina Microaneurysms in New Zealand Rabbits." *International Journal of Experimental Pathology* 92 (1): 40–49. https://doi.org/10.1111/j.1365-2613.2010.00753.x.

Henriksen, Erik J., and Mujalin Prasannarong. 2013. "The Role of the Renin-Angiotensin System in the Development of Insulin Resistance in Skeletal Muscle." *Molecular and Cellular Endocrinology*. Elsevier. https://doi.org/10.1016/j.mce.2012.04.011.

Hill, James O., Holly R. Wyatt, and John C. Peters. 2012. "Energy Balance and Obesity." *Circulation* 126 (1): 126–32. https://doi.org/10.1161/CIRCULATIONAHA.111.087213.

Himms-Hagen, J., J. Cui, E. Danforth, D. J. Taatjes, S. S. Lang, B. L. Waters, and T. H. Claus. 1994. "Effect of CL-316,243, a Thermogenic B3-Agonist, on Energy Balance and Brown and White Adipose Tissues in Rats." *American Journal of Physiology - Regulatory Integrative and Comparative Physiology* 266 (4 35-4). https://doi.org/10.1152/ajpregu.1994.266.4.r1371.

Hoeke, Geerte, Sander Kooijman, Mariëtte R. Boon, Patrick C.N. Rensen, and Jimmy F.P. Berbeé. 2016. "Role of Brown Fat in Lipoprotein Metabolism and Atherosclerosis." *Circulation Research*. Lippincott Williams and Wilkins. https://doi.org/10.1161/CIRCRESAHA.115.306647.

Hoffmann, Linda S., Jennifer Etzrodt, Lena Willkomm, Abhishek Sanyal, Ludger Scheja, Alexander W.C. Fischer, Johannes Peter Stasch, et al. 2015a. "Stimulation of Soluble Guanylyl Cyclase Protects against Obesity by Recruiting Brown Adipose Tissue." *Nature Communications* 6 (May). https://doi.org/10.1038/ncomms8235.

———. 2015b. "Stimulation of Soluble Guanylyl Cyclase Protects against Obesity by Recruiting Brown Adipose Tissue." *Nature Communications* 6 (1): 1–9.

https://doi.org/10.1038/ncomms8235.

Hollander, Priscilla, Alok K. Gupta, Raymond Plodkowski, Frank Greenway, Harold Bays, Colleen Burns, Preston Klassen, and Ken Fujioka. 2013. “Effects of Naltrexone Sustained-Release/Bupropion Sustained-Release Combination Therapy on Body Weight and Glycemic Parameters in Overweight and Obese Patients with Type2 Diabetes.” *Diabetes Care* 36 (12): 4022–29. https://doi.org/10.2337/dc13-0234.

Hong, Guo Bao, Pei Chun Gao, Yun Yin Chen, Yue Xia, Xiao Su Ke, Xiao Fei Shao, Chong Xiang Xiong, et al. 2020. “High-Sensitivity c-Reactive Protein Leads to Increased Incident Metabolic Syndrome in Women but Not in Men: A Five-Year Follow-up Study in a Chinese Population.” *Diabetes, Metabolic Syndrome and Obesity: Targets and Therapy* 13: 581–90. https://doi.org/10.2147/DMSO.S241774.

Hotamisligil, Gökhan S., Pascal Peraldi, Adriane Budavari, Ramsey Ellis, Morris F. White, and Bruce M. Spiegelman. 1996. “IRS-1-Mediated Inhibition of Insulin Receptor Tyrosine Kinase Activity in TNF-α- and Obesity-Induced Insulin Resistance.” *Science* 271 (5249): 665–68. https://doi.org/10.1126/science.271.5249.665.

Hotamisligil, Gökhan S., Narinder S. Shargill, and Bruce M. Spiegelman. 1993. “Adipose Expression of Tumor Necrosis Factor-α: Direct Role in Obesity-Linked Insulin Resistance.” *Science* 259 (5091): 87–91. https://doi.org/10.1126/science.7678183.

How, Ole Jakob, Ellen Aasum, Stanley Kunnathu, David L. Severson, Eivind S.P. Myhre, and Terje S. Larsen. 2005. “Influence of Substrate Supply on Cardiac Efficiency, as Measured by Pressure-Volume Analysis in Ex Vivo Mouse Hearts.” *American Journal of Physiology - Heart and Circulatory Physiology* 288 (6 57-6). https://doi.org/10.1152/ajpheart.00084.2005.

Hu, Miao, and Brian Tomlinson. 2013. “Current Perspectives on Rosuvastatin.” *Integrated Blood Pressure Control*. Dove Press. https://doi.org/10.2147/IBPC.S34814.

Huang, Paul L. 2009. “A Comprehensive Definition for Metabolic Syndrome.” *DMM Disease Models and Mechanisms*. https://doi.org/10.1242/dmm.001180.

Hulthe, Johannes, Lena Bokemark, John Wikstrand, and Björn Fagerberg. 2000. “The Metabolic Syndrome, LDL Particle Size, and Atherosclerosis.” *Arteriosclerosis, Thrombosis, and Vascular Biology* 20 (9): 2140–47. https://doi.org/10.1161/01.ATV.20.9.2140.

Hutley, Louise, and Johannes B. Prins. 2005. “Fat as an Endocrine Organ: Relationship to the Metabolic Syndrome.” In *American Journal of the Medical Sciences*, 330:280–89. Lippincott Williams and Wilkins. https://doi.org/10.1097/00000441-200512000-00005.

Hwang, You Cheol, Wilfred Y. Fujimoto, Tomoshige Hayashi, Steven E. Kahn, Donna L. Leonetti, and Edward J. Boyko. 2016. “Increased Visceral Adipose Tissue Is an Independent Predictor for Future Development of Atherogenic Dyslipidemia.” *Journal of Clinical Endocrinology and Metabolism* 101 (2): 678–85. https://doi.org/10.1210/jc.2015-3246.

Ibrahim, Muhammad, Idris Adewale Ahmed, Maryam Abimbola Mikail, Afeez Adekunle Ishola, Samsul Draman, Muhammad Lokman Md Isa, and Afzan Mat Yusof. 2017. “Baccaurea Angulata Fruit Juice Reduces Atherosclerotic Lesions in Diet-Induced Hypercholesterolemic

Rabbits." *Lipids in Health and Disease* 16 (1): 2–8. https://doi.org/10.1186/s12944-017-0526-2.

Ilanne-Parikka, Pirjo, David E. Laaksonen, Johan G. Eriksson, Timo A. Lakka, Jaana Lindström, Markku Peltonen, Sirkka Aunola, Sirkka Keinänen-Kiukaanniemi, Matti Uusitupa, and Jaakko Tuomilehto. 2010. "Leisure-Time Physical Activity and the Metabolic Syndrome in the Finnish Diabetes Prevention Study." *Diabetes Care* 33 (7): 1610–17. https://doi.org/10.2337/dc09-2155.

Imbrogno, S., A. Gattuso, R. Mazza, T. Angelone, and M. C. Cerra. 2015. "B<inf>3</Inf>-AR and the Vertebrate Heart: A Comparative View." *Acta Physiologica*. https://doi.org/10.1111/apha.12493.

Israili, Zafar H., Badiĝa Lyoussi, Rafael Hernández-Hernández, and Manuel Velasco. 2007. "Metabolic Syndrome: Treatment of Hypertensive Patients." *American Journal of Therapeutics*. Am J Ther. https://doi.org/10.1097/01.pap.0000249936.05650.0c.

Itani, Samar I., Neil B. Ruderman, Frank Schmieder, and Guenther Boden. 2002. "Lipid-Induced Insulin Resistance in Human Muscle Is Associated with Changes in Diacylglycerol, Protein Kinase C, and IκB-α." *Diabetes* 51 (7): 2005–11. https://doi.org/10.2337/diabetes.51.7.2005.

Ito, Akira, Philip S. Tsao, Shanthi Adimoolam, Masumi Kimoto, Tadashi Ogawa, and John P. Cooke. 1999. "Novel Mechanism for Endothelial Dysfunction: Dysregulation of Dimethylarginine Dimethylaminohydrolase." *Circulation* 99 (24): 3092–95. https://doi.org/10.1161/01.CIR.99.24.3092.

Janus, A, E Szahidewicz-Krupska, G Mazur, and A Doroszko. 2016. "Insulin Resistance and Endothelial Dysfunction Constitute a Common Therapeutic Target in Cardiometabolic Disorders." https://doi.org/10.1155/2016/3634948.

Jensen, Michael D. 1997. "Lipolysis: Contribution from Regional Fat." *Annual Review of Nutrition*. Annu Rev Nutr. https://doi.org/10.1146/annurev.nutr.17.1.127.

———. 2002. "Adipose Tissue and Fatty Acid Metabolism in Humans." *Journal of the Royal Society of Medicine, Supplement* 95 (42): 3–7. https://doi.org/12216324.

Jensen, Michael D., Donna H. Ryan, Caroline M. Apovian, Jamy D. Ard, Anthony G. Comuzzie, Karen A. Donato, Frank B. Hu, et al. 2014. "2013 AHA/ACC/TOS Guideline for the Management of Overweight and Obesity in Adults: A Report of the American College of Cardiology/American Heart Association Task Force on Practice Guidelines and the Obesity Society." *Circulation*. Lippincott Williams and Wilkins. https://doi.org/10.1161/01.cir.0000437739.71477.ee.

Jiang, Fan, Han K. Lim, Margaret J. Morris, Larissa Prior, Elena Velkoska, Xiao Wu, and Gregory J. Dusting. 2011. "Systemic Upregulation of NADPH Oxidase in Diet-Induced Obesity in Rats." *Redox Report* 16 (6): 223–29. https://doi.org/10.1179/174329211X13049558293713.

Johann, Kornelia, Marlen Colleen Reis, Lisbeth Harder, Beate Herrmann, Sogol Gachkar, Jens Mittag, and Rebecca Oelkrug. 2018. "Effects of Sildenafil Treatment on Thermogenesis and Glucose Homeostasis in Diet-Induced Obese Mice." *Nutrition and Diabetes* 8 (1): 9.

https://doi.org/10.1038/s41387-018-0026-0.

Jones, Ben J., and Stephen R. Bloom. 2015. “The New Era of Drug Therapy for Obesity: The Evidence and the Expectations.” *Drugs* 75 (9): 935–45. https://doi.org/10.1007/s40265-015-0410-1.

Jonk, Amy M., Alfons J.H.M. Houben, Renate T. De Jongh, Erik H. Serné, Nicoloaas C. Schaper, and Coen D.A. Stehouwer. 2007. “Microvascular Dysfunction in Obesity: A Potential Mechanism in the Pathogenesis of Obesity-Associated Insulin Resistance and Hypertension.” *Physiology*. Physiology (Bethesda). https://doi.org/10.1152/physiol.00012.2007.

Jordan, Jens, Arne Astrup, Stefan Engeli, Krzysztof Narkiewicz, Wesley W. Day, and Nick Finer. 2014. “Cardiovascular Effects of Phentermine and Topiramate: A New Drug Combination for the Treatment of Obesity.” *Journal of Hypertension*. Lippincott Williams and Wilkins. https://doi.org/10.1097/HJH.0000000000000145.

Kaabia, Zied, Julie Poirier, Michelle Moughaizel, Audrey Aguesse, Stéphanie Billon-Crossouard, Fanta Fall, Manon Durand, Elie Dagher, Michel Krempf, and Mikaël Croyal. 2018. “Plasma Lipidomic Analysis Reveals Strong Similarities between Lipid Fingerprints in Human, Hamster and Mouse Compared to Other Animal Species.” *Scientific Reports* 8 (1): 1–9. https://doi.org/10.1038/s41598-018-34329-3.

Kadowitz, Philip J, and Bobby D Nossaman. 2013. “Stimulators of Soluble Guanylyl Cyclase: Future Clinical Indications Nitric Oxide Mechanisms View Project Modulation of Soluble Guanylate Cyclase for the Treatment of Erectile Dysfunction View Project Bobby D Nossaman Ochsner Stimulators of Soluble Guanyl.” *Ochsner Journal* 13: 147–56. https://www.researchgate.net/publication/236083742.

Kahaleh, M B, and P S Fan. 1997. “Effect of Cytokines on the Production of Endothelin by Endothelial Cells.” *Clinical and Experimental Rheumatology* 15 (2): 163–67. http://www.ncbi.nlm.nih.gov/pubmed/9196868.

Kahn, Barbara B., and Jeffrey S. Flier. 2000. “Obesity and Insulin Resistance.” *Journal of Clinical Investigation*. The American Society for Clinical Investigation. https://doi.org/10.1172/JCI10842.

Kahn, Steven E., Rebecca L. Hull, and Kristina M. Utzschneider. 2006. “Mechanisms Linking Obesity to Insulin Resistance and Type 2 Diabetes.” *Nature*. Nature Publishing Group. https://doi.org/10.1038/nature05482.

Kamisaki, Yoshinori, Shuichi Saheki, Masaki Nakane, James A Palmieri, Takayoshi Kuno, Bing Y Chang, Scott A Waldman, and Ferid Murads. 1986. “Soluble Guanylate Cyclase from Rat Lung Exists as a Heterodimer".” *THE JOURNAL OF BIOLOGICAL CHEMISTRY*. Vol. 261.

Kanety, H., R. Feinstein, M. Z. Papa, R. Hemi, and A. Karasik. 1995. “Tumor Necrosis Factor α-Induced Phosphorylation of Insulin Receptor Substrate-1 (IRS-1). Possible Mechanism for Suppression of Insulin-Stimulated Tyrosine Phosphorylation of IRS-1.” *Journal of Biological Chemistry* 270 (40): 23780–84. https://doi.org/10.1074/jbc.270.40.23780.

Karelis, Antony D., May Faraj, Jean Philippe Bastard, David H. St-Pierre, Martin Brochu, Denis

Prud'homme, and Remi Rabasa-Lhoret. 2005. "The Metabolically Healthy but Obese Individual Presents a Favorable Inflammation Profile." *Journal of Clinical Endocrinology and Metabolism* 90 (7): 4145–50. https://doi.org/10.1210/jc.2005-0482.

Karimi, Isaac. 2012. "Animal Models as Tools for Translational Research: Focus on Atherosclerosis, Metabolic Syndrome and Type-II Diabetes Mellitus." In *Lipoproteins - Role in Health and Diseases*. InTech. https://doi.org/10.5772/47769.

Katagiri, Hideki, Tetsuya Yamada, and Yoshitomo Oka. 2007. "Adiposity and Cardiovascular Disorders: Disturbance of the Regulatory System Consisting of Humoral and Neuronal Signals." *Circulation Research*. Circ Res. https://doi.org/10.1161/CIRCRESAHA.107.151621.

Katsimardou, Alexandra, Konstantinos Imprialos, Konstantinos Stavropoulos, Alexandros Sachinidis, Michalis Doumas, and Vasilios Athyros. 2019. "Hypertension in Metabolic Syndrome: Novel Insights." *Current Hypertension Reviews* 16 (1): 12–18. https://doi.org/10.2174/1573402115666190415161813.

Katsuda, Shin Ichiro, Noboru Machida, Masamitsu Hasegawa, Hiroshi Miyashita, Masahiko Kusanagi, Hirokazu Tsubone, and Akihiro Hazama. 2004. "Change in the Static Rheological Properties of the Aorta in Kurosawa and Kusanagi-Hypercholesterolemic (KHC) Rabbits with Progress of Atherosclerosis." *Physiological Measurement* 25 (2): 505–22. https://doi.org/10.1088/0967-3334/25/2/009.

Kaur, Jaspinder. 2014. "A Comprehensive Review on Metabolic Syndrome." *Cardiology Research and Practice* 2014: 1–21. https://doi.org/10.1155/2014/943162.

Kelly, E., C. P. Bailey, and G. Henderson. 2008. "Agonist-Selective Mechanisms of GPCR Desensitization." In *British Journal of Pharmacology*, 153:S379. Wiley-Blackwell. https://doi.org/10.1038/sj.bjp.0707604.

Kershaw, Erin E., and Jeffrey S. Flier. 2004. "Adipose Tissue as an Endocrine Organ." *The Journal of Clinical Endocrinology & Metabolism* 89 (6): 2548–56. https://doi.org/10.1210/jc.2004-0395.

Kim, Francis, Byron Gallis, and Marshall A. Corson. 2001. "TNF-α Inhibits Flow and Insulin Signaling Leading to NO Production in Aortic Endothelial Cells." *American Journal of Physiology - Cell Physiology* 280 (5 49-5). https://doi.org/10.1152/ajpcell.2001.280.5.c1057.

Kim, G. W., J. E. Lin, E. S. Blomain, and S. A. Waldman. 2014. "Antiobesity Pharmacotherapy: New Drugs and Emerging Targets." *Clinical Pharmacology and Therapeutics* 95 (1): 53–66. https://doi.org/10.1038/clpt.2013.204.

Kim, Jeong-A, Monica Montagnani, ; Kwang, Kon Koh, and Michael J Quon. 2006. "Reciprocal Relationships Between Insulin Resistance and Endothelial Dysfunction Molecular and Pathophysiological Mechanisms Basic Science for Clinicians." *Circulation Journal* 113 (15): 1888–1904. https://doi.org/10.1161/CIRCULATIONAHA.105.563213.

Kim, Jeong A., Hyun Ju Jang, and Daniel H. Hwang. 2015. "Toll-like Receptor 4-Induced Endoplasmic Reticulum Stress Contributes to Impairment of Vasodilator Action of Insulin."

American Journal of Physiology - Endocrinology and Metabolism 309 (9): E767–76. https://doi.org/10.1152/ajpendo.00369.2015.

Kim, Jeong A., Monica Montagnani, Sruti Chandrasekran, and Michael J. Quon. 2012. "Role of Lipotoxicity in Endothelial Dysfunction." *Heart Failure Clinics*. NIH Public Access. https://doi.org/10.1016/j.hfc.2012.06.012.

Kim, Jeong A., Monica Montagnani, Kon Koh Kwang, and Michael J. Quon. 2006a. "Reciprocal Relationships between Insulin Resistance and Endothelial Dysfunction: Molecular and Pathophysiological Mechanisms." *Circulation* 113 (15): 1888–1904. https://doi.org/10.1161/CIRCULATIONAHA.105.563213.

———. 2006b. "Reciprocal Relationships between Insulin Resistance and Endothelial Dysfunction: Molecular and Pathophysiological Mechanisms." *Circulation* 113 (15): 1888–1904. https://doi.org/10.1161/CIRCULATIONAHA.105.563213.

Kim, Nam Hoon, Ki Hoon Han, Jimi Choi, Juneyoung Lee, and Sin Gon Kim. 2019. "Use of Fenofibrate on Cardiovascular Outcomes in Statin Users with Metabolic Syndrome: Propensity Matched Cohort Study." *The BMJ* 366 (September). https://doi.org/10.1136/bmj.l5125.

Kim, Nam Hoon, and Sin Gon Kim. 2020. "Fibrates Revisited: Potential Role in Cardiovascular Risk Reduction." *Diabetes & Metabolism Journal*. NLM (Medline). https://doi.org/10.4093/dmj.2020.0001.

Kintscher, Ulrich, Peter Bramlage, W. Dieter Paar, Martin Thoenes, and Thomas Unger. 2007. "Irbesartan for the Treatment of Hypertension in Patients with the Metabolic Syndrome: A Sub Analysis of the Treat to Target Post Authorization Survey. Prospective Observational, Two Armed Study in 14,200 Patients." *Cardiovascular Diabetology* 6 (April). https://doi.org/10.1186/1475-2840-6-12.

Kiranmayi, VS, and KM Bhargav. 2019. "Brown Adipose Tissue in Adult Humans: A Mini Review." *Journal of Clinical and Scientific Research* 8 (1): 24. https://doi.org/10.4103/jcsr.jcsr_35_19.

Kirk, Erik P., and Samuel Klein. 2009. "Pathogenesis and Pathophysiology of the Cardiometabolic Syndrome." *The Journal of Clinical Hypertension* 11 (12): 761–65. https://doi.org/10.1111/j.1559-4572.2009.00054.x.

Kleber, ME, TB Grammer, and W März. 2010. "High-Density Lipoprotein (HDL) and Cholesteryl Ester Transfer Protein (CETP): Role in Lipid Metabolism and Clinical Meaning]." *MMW Fortschr Med.* 152: 47–55. https://pubmed.ncbi.nlm.nih.gov/21591319/.

Kobayashi, Tsutomu, Takashi Ito, and Masashi Shiomi. 2011. "Roles of the WHHL Rabbit in Translational Research on Hypercholesterolemia and Cardiovascular Diseases." *Journal of Biomedicine & Biotechnology* 2011 (April): 1–10. https://doi.org/10.1155/2011/406473.

Kobayasi, Renata, Eliana H. Akamine, Ana P. Davel, Maria A.M. Rodrigues, Carla R.O. Carvalho, and Luciana V. Rossoni. 2010. "Oxidative Stress and Inflammatory Mediators Contribute to Endothelial Dysfunction in High-Fat Diet-Induced Obesity in Mice." *Journal of*

Hypertension 28 (10): 2111–19. https://doi.org/10.1097/HJH.0b013e32833ca68c.

Kohler, Hans P., and Peter J. Grant. 2000. "Plasminogen-Activator Inhibitor Type 1 and Coronary Artery Disease." *New England Journal of Medicine*. N Engl J Med. https://doi.org/10.1056/NEJM200006153422406.

Kohout, Trudy A., and Robert J. Lefkowitz. 2003. "Regulation of G Protein-Coupled Receptor Kinases and Arrestins during Receptor Desensitization." *Molecular Pharmacology*. Mol Pharmacol. https://doi.org/10.1124/mol.63.1.9.

Konukoglu, Dildar, and Hafize Uzun. 2016. "Endothelial Dysfunction and Hypertension." In *Advances in Experimental Medicine and Biology*, 956:511–40. Springer New York LLC. https://doi.org/10.1007/5584_2016_90.

Kopp, Wolfgang. 2019. "How Western Diet and Lifestyle Drive the Pandemic of Obesity and Civilization Diseases." *Diabetes, Metabolic Syndrome and Obesity: Targets and Therapy* 12: 2221–36. https://doi.org/10.2147/DMSO.S216791.

Kozak, Leslie P., and Robert A. Koza. 2010. "The Genetics of Brown Adipose Tissue." *Progress in Molecular Biology and Translational Science*. Academic Press. https://doi.org/10.1016/b978-0-12-375003-7.00004-2.

Kubota, Tetsuya, Naoto Kubota, Hiroki Kumagai, Shinichi Yamaguchi, Hideki Kozono, Takehiro Takahashi, Mariko Inoue, et al. 2011. "Impaired Insulin Signaling in Endothelial Cells Reduces Insulin-Induced Glucose Uptake by Skeletal Muscle." *Cell Metabolism* 13 (3): 294–307. https://doi.org/10.1016/j.cmet.2011.01.018.

Kurotani, Kayo, Toshiaki Miyamoto, Takeshi Kochi, Masafumi Eguchi, Teppei Imai, Akiko Nishihara, Kentaro Tomita, et al. 2017. "Metabolic Syndrome Components and Diabetes Incidence According to the Presence or Absence of Impaired Fasting Glucose: The Japan Epidemiology Collaboration on Occupational Health Study." *Journal of Epidemiology* 27 (9): 408–12. https://doi.org/10.1016/j.je.2016.08.015.

Labazi, Hicham, and Aaron J. Trask. 2017. "Coronary Microvascular Disease as an Early Culprit in the Pathophysiology of Diabetes and Metabolic Syndrome." *Pharmacological Research*. Academic Press. https://doi.org/10.1016/j.phrs.2017.07.004.

Lamarche, Benoît, André Tchernof, Pascale Mauriège, Bernard Cantin, Gilles R. Dagenais, Paul J. Lupien, and Jean Pierre Després. 1998. "Fasting Insulin and Apolipoprotein B Levels and Low-Density Lipoprotein Particle Size as Risk Factors for Ischemic Heart Disease." *Journal of the American Medical Association* 279 (24): 1955–61. https://doi.org/10.1001/jama.279.24.1955.

Lamarche, Benoît, Kristine D. Uffelman, André Carpentier, Jeffrey S. Cohn, George Steiner, P. Hugh Barrett, and Gary F. Lewis. 1999. "Triglyceride Enrichment of HDL Enhances in Vivo Metabolic Clearance of HDL Apo A-I in Healthy Men." *Journal of Clinical Investigation* 103 (8): 1191–99. https://doi.org/10.1172/JCI5286.

Lambert, Elisabeth, Nora Straznicky, Carolina Ika Sari, Nina Eikelis, Dagmara Hering, Geoffrey Head, John Dixon, Murray Esler, Markus Schlaich, and Gavin Lambert. 2013. "Dyslipidemia

Is Associated with Sympathetic Nervous Activation and Impaired Endothelial Function in Young Females." *American Journal of Hypertension* 26 (2): 250–56. https://doi.org/10.1093/ajh/hps016.

Lambert, Gavin W., Nora E. Straznicky, Elisabeth A. Lambert, John B. Dixon, and Markus P. Schlaich. 2010. "Sympathetic Nervous Activation in Obesity and the Metabolic Syndrome-Causes, Consequences and Therapeutic Implications." *Pharmacology and Therapeutics*. Pergamon. https://doi.org/10.1016/j.pharmthera.2010.02.002.

Landsberg, Lewis. 2001. "Insulin-Mediated Sympathetic Stimulation: Pathogenesis of Obesity-Related Hypertension Pathogenesis of Obesity-Related Hypertension." *Journal of Hypertension* 19 (3). https://journals.lww.com/jhypertension/Citation/2001/03001/Insulin_mediated_sympathetic_stimulation__role_in.1.aspx.

Lanktree, Matthew B., and Robert A. Hegele. 2017. "Metabolic Syndrome." In *Genomic and Precision Medicine: Primary Care: Third Edition*, 283–99. Elsevier Inc. https://doi.org/10.1016/B978-0-12-800685-6.00015-1.

Laurent, Sťphane, Pierre Boutouyrie, Roland Asmar, Isabelle Gautier, Brigitte Laloux, Louis Guize, Pierre Ducimetiere, and Athanase Benetos. 2001. "Aortic Stiffness Is an Independent Predictor of All-Cause and Cardiovascular Mortality in Hypertensive Patients." *Hypertension* 37 (5): 1236–41. https://doi.org/10.1161/01.HYP.37.5.1236.

Ledoux, Jonathan, Matthias E. Werner, Joseph E. Brayden, and Mark T. Nelson. 2006. "Quintessence of Vascular Ca 2+ and K + Channels" 21: 69–79. http://physiologyonline.physiology.org/.

Lee, Dong I., Susan Vahebi, Carlo Gabriele Tocchetti, Lili A. Barouch, R. John Solaro, Eiki Takimoto, and David A. Kass. 2010. "PDE5A Suppression of Acute β-Adrenergic Activation Requires Modulation of Myocyte Beta-3 Signaling Coupled to PKG-Mediated Troponin i Phosphorylation." *Basic Research in Cardiology* 105 (3): 337–47. https://doi.org/10.1007/s00395-010-0084-5.

Lee, S. H., K. Han, H. K. Yang, H. S. Kim, J. H. Cho, H. S. Kwon, Y. M. Park, B. Y. Cha, and K. H. Yoon. 2015. "A Novel Criterion for Identifying Metabolically Obese but Normal Weight Individuals Using the Product of Triglycerides and Glucose." *Nutrition and Diabetes* 5 (4): 149. https://doi.org/10.1038/nutd.2014.46.

Lee, Yee Ting, Hiu Yu Lin, Yin Wah Fiona Chan, Ka Hou Christien Li, Olivia Tsz Ling To, Bryan P. Yan, Tong Liu, et al. 2017. "Mouse Models of Atherosclerosis: A Historical Perspective and Recent Advances." *Lipids in Health and Disease*. BioMed Central Ltd. https://doi.org/10.1186/s12944-016-0402-5.

Lerman, Amir, and Andreas M. Zeiher. 2005. "Endothelial Function: Cardiac Events." *Circulation*. Circulation. https://doi.org/10.1161/01.CIR.0000153339.27064.14.

Levine, T. Barry., and Arlene B. Levine. 2013. *Metabolic Syndrome and Cardiovascular Disease*. Wiley-Blackwell.

Lewis, Gary F., and George Steiner. 1996. “Acute Effects of Insulin in the Control of VLDL Production in Humans: Implications for the Insulin-Resistant State.” In *Diabetes Care*, 19:390–93. American Diabetes Association Inc. https://doi.org/10.2337/diacare.19.4.390.

Lewis, Gary F., Kristine D. Uffelman, Linda W. Szeto, Barbara Weller, and George Steiner. 1995. “Interaction between Free Fatty Acids and Insulin in the Acute Control of Very Low Density Lipoprotein Production in Humans.” *Journal of Clinical Investigation* 95 (1): 158–66. https://doi.org/10.1172/jci117633.

Li, Qiang, Ji Youn Youn, and Hua Cai. 2015. “Mechanisms and Consequences of Endothelial Nitric Oxide Synthase Dysfunction in Hypertension.” *Journal of Hypertension*. Lippincott Williams and Wilkins. https://doi.org/10.1097/HJH.0000000000000587.

Li, Y., Z. Lu, X. Zhang, H. Yu, K. L. Kirkwood, M. F. Lopes-Virella, and Y. Huang. 2015. “Metabolic Syndrome Exacerbates Inflammation and Bone Loss in Periodontitis.” *Journal of Dental Research* 94 (2): 362–70. https://doi.org/10.1177/0022034514561658.

Liao, R., B. K. Podesser, and C. C. Lim. 2012. “The Continuing Evolution of the Langendorff and Ejecting Murine Heart: New Advances in Cardiac Phenotyping.” *AJP: Heart and Circulatory Physiology* 303 (2): H156–67. https://doi.org/10.1152/ajpheart.00333.2012.

Liese, Angela D., Elizabeth J. Mayer-Davis, and Steven M. Haffner. 1998. “Development of the Multiple Metabolic Syndrome: An Epidemiologic Perspective.” *Epidemiologic Reviews*. John Hopkins University School of Hygiene and Public Health. https://doi.org/10.1093/oxfordjournals.epirev.a017978.

Lima-Leopoldo, Ana Paula, André S. Leopoldo, Danielle C.T. Da Silva, André F. Do Nascimento, Dijon H.S. De Campos, Renata A.M. Luvizotto, Adriana F. De Deus, et al. 2014. “Long-Term Obesity Promotes Alterations in Diastolic Function Induced by Reduction of Phospholamban Phosphorylation at Serine-16 without Affecting Calcium Handling.” *Journal of Applied Physiology* 117 (6): 669–78. https://doi.org/10.1152/japplphysiol.00088.2014.

Lima-Leopoldo, Ana Paula, André S. Leopoldo, Mário M. Sugizaki, Alessandro Bruno, André F. Nascimento, Renata A.M. Luvizotto, Silvio A.Oliveira Junior, Edson Castardeli, Carlos R. Padovani, and Antonio C. Cicogna. 2011. “Myocardial Dysfunction and Abnormalities in Intracellular Calcium Handling in Obese Rats.” *Arquivos Brasileiros de Cardiologia* 97 (3): 232–40. https://doi.org/10.1590/S0066-782X2011005000061.

Lobato, N. S., F. P. Filgueira, E. H. Akamine, R. C. Tostes, M. H.C. Carvalho, and Z. B. Fortes. 2012. “Mechanisms of Endothelial Dysfunction in Obesity-Associated Hypertension.” *Brazilian Journal of Medical and Biological Research*. Braz J Med Biol Res. https://doi.org/10.1590/S0100-879X2012007500058.

Longo, Michele, Federica Zatterale, Jamal Naderi, Luca Parrillo, Pietro Formisano, Gregory Alexander Raciti, Francesco Beguinot, and Claudia Miele. 2019. “Adipose Tissue Dysfunction as Determinant of Obesity-Associated Metabolic Complications.” *International Journal of Molecular Sciences* 20 (9). https://doi.org/10.3390/ijms20092358.

Lonn, Eva, Jackie Bosch, Salim Yusuf, Patrick Sheridan, Janice Pogue, J Malcolm Arnold, Catherine Ross, et al. 2005. “Effects of Long-Term Vitamin E Supplementation on

Cardiovascular Events and Cancer: A Randomized Controlled Trial." *Journal of the American Medical Association* 293 (11): 1338–47. https://doi.org/10.1001/jama.293.11.1338.

Lopaschuk, Gary D. 2016. "Fatty Acid Oxidation and Its Relation with Insulin Resistance and Associated Disorders." *Annals of Nutrition and Metabolism* 68 (3): 15–20. https://doi.org/10.1159/000448357.

Lopaschuk, Gary D., John R. Ussher, Clifford D.L. Folmes, Jagdip S. Jaswal, and William C. Stanley. 2010. "Myocardial Fatty Acid Metabolism in Health and Disease." *Physiological Reviews*. Physiol Rev. https://doi.org/10.1152/physrev.00015.2009.

Lopes-Vicente, Wanda R.P., Sara Rodrigues, Felipe X. Cepeda, Camila Paixão Jordão, Valéria Costa-Hong, Akothirene C.B. Dutra-Marques, Jefferson C. Carvalho, Maria Janieire N.N. Alves, Luiz A. Bortolotto, and Ivani C. Trombetta. 2017. "Arterial Stiffness and Its Association with Clustering of Metabolic Syndrome Risk Factors." *Diabetology and Metabolic Syndrome* 9 (1): 87. https://doi.org/10.1186/s13098-017-0286-1.

Lou, Qing, Wenwen Li, and Igor R. Efimov. 2011. "Multiparametric Optical Mapping of the Langendorff-Perfused Rabbit Heart." *Journal of Visualized Experiments*, no. 55: 1–5. https://doi.org/10.3791/3160.

Lozano, Wilson M., Oscar J. Arias-Mutis, Conrado J. Calvo, Francisco J. Chorro, and Manuel Zarzoso. 2019. "Diet-Induced Rabbit Models for the Study of Metabolic Syndrome." *Animals* 9 (7): 463. https://doi.org/10.3390/ani9070463.

Ludwig, David S. 2000. "Dietary Glycemic Index and Obesity." *Journal of Nutrition* 130 (2 SUPPL.): 280–83. https://doi.org/10.1093/jn/130.2.280s.

Lundberg, Jon O., Mark T. Gladwin, and Eddie Weitzberg. 2015. "Strategies to Increase Nitric Oxide Signalling in Cardiovascular Disease." *Nature Reviews Drug Discovery*. Nature Publishing Group. https://doi.org/10.1038/nrd4623.

Lustig, Robert H. 2015. "Metabolic Syndrome and the 'Western Diet': Science and Politics." *Pediatric and Adolescent Medicine* 19: 137–47. https://doi.org/10.1159/000368125.

Lymperopoulos, Anastasios, Giuseppe Rengo, and Walter J. Koch. 2013. "Adrenergic Nervous System in Heart Failure: Pathophysiology and Therapy." *Circulation Research* 113 (6): 739–53. https://doi.org/10.1161/CIRCRESAHA.113.300308.

Magkos, Faidon, Mary Yannakoulia, Jean L. Chan, and Christos S. Mantzoros. 2009. "Management of the Metabolic Syndrome and Type 2 Diabetes through Lifestyle Modification." *Annual Review of Nutrition*. NIH Public Access. https://doi.org/10.1146/annurev-nutr-080508-141200.

Mahmoud, Amr A. A., and Shimaa M. Elshazly. 2014. "Ursodeoxycholic Acid Ameliorates Fructose-Induced Metabolic Syndrome in Rats." Edited by Anna Alisi. *PLoS ONE* 9 (9): e106993. https://doi.org/10.1371/journal.pone.0106993.

Makki, Kassem, Philippe Froguel, and Isabelle Wolowczuk. 2013. "Adipose Tissue in Obesity-Related Inflammation and Insulin Resistance: Cells, Cytokines, and Chemokines" 2013: 12.

https://doi.org/10.1155/2013/139239.

Malhotra, Ashwani, Barinder P.S. Kang, Simon Cheung, David Opawumi, and Leonard G. Meggs. 2001. “Angiotensin II Promotes Glucose-Induced Activation of Cardiac Protein Kinase C Isozymes and Phosphorylation of Troponin I.” *Diabetes* 50 (8): 1918–26. https://doi.org/10.2337/diabetes.50.8.1918.

Mallare, Johanna T., Ana H. Karabell, Pedro Velasquez-Mieyer, Sarah R.S. Stander, and Michael L. Christensen. 2005. “Current and Future Treatment of Metabolic Syndrome and Type 2 Diabetes in Children and Adolescents.” *Diabetes Spectrum*. American Diabetes Association. https://doi.org/10.2337/diaspect.18.4.220.

Mancia, Giuseppe, Guido Grassi, and Alberto Zanchetti. 2006. “New-Onset Diabetes and Antihypertensive Drugs.” *Journal of Hypertension* 24 (1): 3–10. https://doi.org/10.1097/01.hjh.0000194119.42722.21.

Mansour, Suzan M., Hala F. Zaki, and Ezz-El-Din S. El-Denshary. 2013. “Beneficial Effects of Co-Enzyme Q10 and Rosiglitazone in Fructose-Induced Metabolic Syndrome in Rats.” *Bulletin of Faculty of Pharmacy, Cairo University* 51 (1): 13–21. https://doi.org/10.1016/j.bfopcu.2012.10.001.

Mark, Allyn L., Marcelo L. G. Correia, Kamal Rahmouni, and William G. Haynes. 2002. “Selective Leptin Resistance: A New Concept in Leptin Physiology with Cardiovascular Implications.” *Journal of Hypertension* 20 (7): 1245–50. https://doi.org/10.1097/00004872-200207000-00001.

Martin, R. De, M. Hoeth, R. Hofer-Warbinek, and J. A. Schmid. 2000. “The Transcription Factor NF-Kappa B and the Regulation of Vascular Cell Function.” *Arteriosclerosis, Thrombosis, and Vascular Biology*. Arterioscler Thromb Vasc Biol. https://doi.org/10.1161/01.ATV.20.11.e83.

Martinez-Martin, F. J., H. Rodriguez-Rosas, I. Peiro-Martinez, P. Soriano-Perera, P. Pedrianes-Martin, and C. Comi-Diaz. 2011. “Olmesartan/Amlodipine vs Olmesartan/Hydrochlorothiazide in Hypertensive Patients with Metabolic Syndrome: The OLAS Study.” *Journal of Human Hypertension* 25 (6): 346–53. https://doi.org/10.1038/jhh.2010.104.

Martins Gregório, Bianca, Diogo Benchimol De Souza, Fernanda Amorim de Morais Nascimento, Leonardo Matta, and Caroline Fernandes-Santos. 2016. “The Potential Role of Antioxidants in Metabolic Syndrome.” *Current Pharmaceutical Design* 22 (7): 859–69. https://doi.org/10.2174/1381612822666151209152352.

Matsumoto, Takayuki, Atsushi Sato, Hiroshi Suenaga, Tsuneo Kobayashi, and Katsuo Kamata. 2004. “Modulations of Shear Stress-Induced Contractile Responses and Agonist-Induced Vasodilation in Hypercholesterolemic Rats.” *Atherosclerosis* 175 (1): 31–38. https://doi.org/10.1016/j.atherosclerosis.2004.02.017.

Matsuzawa, Yuji, Tohru Funahashi, Shinji Kihara, and Iichiro Shimomura. 2004. “Adiponectin and Metabolic Syndrome.” *Arteriosclerosis, Thrombosis, and Vascular Biology*. Lippincott Williams & Wilkins. https://doi.org/10.1161/01.ATV.0000099786.99623.EF.

Matthews, D R, J R Hosker, A S Rudenski, B A Naylor, D F Treacher, R C Turner, and Radcliffe Infirmary. 1985. “Homeostasis Model Assessment: Insulin Resistance and B-Cell Function from Fasting Plasma Glucose and Insulin Concentrations in Man,” 412–19.

Mazumder, Pradip K., Brian T. O’Neill, Matthew W. Roberts, Jonathan Buchanan, Ui Jeong Yun, Robert C. Cooksey, Sihem Boudina, and E. Dale Abel. 2004. “Impaired Cardiac Efficiency and Increased Fatty Acid Oxidation in Insulin-Resistant Ob/Ob Mouse Hearts.” *Diabetes* 53 (9): 2366–74. https://doi.org/10.2337/diabetes.53.9.2366.

McCracken, Emma, Monica Monaghan, and Shiva Sreenivasan. 2018. “Pathophysiology of the Metabolic Syndrome.” *Clinics in Dermatology* 36 (1): 14–20. https://doi.org/10.1016/j.clindermatol.2017.09.004.

McLaughlin, Tracey, Fahim Abbasi, Cindy Lamendola, Lynn Liang, Gerald Reaven, Patricia Schaaf, and Peter Reaven. 2002. “Differentiation between Obesity and Insulin Resistance in the Association with C-Reactive Protein.” *Circulation* 106 (23): 2908–12. https://doi.org/10.1161/01.CIR.0000041046.32962.86.

Melichar, V. O., D. Behr-Roussel, U. Zabel, L. O. Uttenthal, J. Rodrigo, A. Rupin, T. J. Verbeuren, A. Kumar H. S., and H. H. H. W. Schmidt. 2004. “Reduced CGMP Signaling Associated with Neointimal Proliferation and Vascular Dysfunction in Late-Stage Atherosclerosis.” *Proceedings of the National Academy of Sciences* 101 (47): 16671–76. https://doi.org/10.1073/pnas.0405509101.

Mendizábal, Yolanda, Silvia Llorens, and Eduardo Nava. 2013. “Hypertension in Metabolic Syndrome: Vascular Pathophysiology.” *International Journal of Hypertension* 2013. https://doi.org/10.1155/2013/230868.

“METABOLIC SYNDROME.” n.d.

Miccoli, Roberto, Dieuwke De Keyzer, David Giuseppe Penno, David Stefano, and Del Prato. 2017. “Future Lipidology Insulin Resistance and Lipid Disorders.” https://doi.org/10.2217/17460875.3.6.651.

Michel, Lauriane Y.M., and Jean Luc Balligand. 2017. “New and Emerging Therapies and Targets: Beta-3 Agonists.” In *Handbook of Experimental Pharmacology*, 243:205–23. Springer New York LLC. https://doi.org/10.1007/164_2016_88.

Mirhoseini, Mahmood, Hamid Daemi, Mahshid Masoom Babaiee, Majid Asadi-Samani, Leilaassadat Mirhoseini, and Morteza Sedehi. 2018. “Serum Concentration of Hs-CRP in Obese Individuals with and without Metabolic Syndrome and Its Association with Parameters of Metabolic Syndrome.” *Journal of Renal Injury Prevention* 7 (4): 297–300. https://doi.org/10.15171/jrip.2018.65.

Misra, Anoop, Narendra K. Alappan, Naval K. Vikram, Kashish Goel, Nidhi Gupta, Kanchan Mittal, Suryaprakash Bhatt, and Kalpana Luthra. 2008. “Effect of Supervised Progressive Resistance-Exercise Training Protocol on Insulin Sensitivity, Glycemia, Lipids, and Body Composition in Asian Indians with Type 2 Diabetes.” *Diabetes Care* 31 (7): 1282–87. https://doi.org/10.2337/dc07-2316.

Misra, Anoop, Neha Singhal, and Lokesh Khurana. 2010. “Obesity, the Metabolic Syndrome, and Type 2 Diabetes in Developing Countries: Role of Dietary Fats and Oils.” *Journal of the American College of Nutrition* 29 (June): 289S-301S. https://doi.org/10.1080/07315724.2010.10719844.

Mitchell, Gary F. 2009. “Arterial Stiffness and Wave Reflection: Biomarkers of Cardiovascular Risk.” *Artery Research*. NIH Public Access. https://doi.org/10.1016/j.artres.2009.02.002.

Mitschke, Michaela M., Linda S. Hoffmann, Thorsten Gnad, Daniela Scholz, Katja Kruithoff, Peter Mayer, Bodo Haas, Antonia Sassmann, Alexander Pfeifer, and Ana Kilić. 2013. “Increased CGMP Promotes Healthy Expansion and Browning of White Adipose Tissue.” *The FASEB Journal* 27 (4): 1621–30. https://doi.org/10.1096/fj.12-221580.

Mo, Weilan, Martin C. Michel, Xiang Wen Lee, Alberto J. Kaumann, and Peter Molenaar. 2017. “The B3-Adrenoceptor Agonist Mirabegron Increases Human Atrial Force through B1-Adrenoceptors: An Indirect Mechanism?” *British Journal of Pharmacology* 174 (16): 2706–15. https://doi.org/10.1111/bph.13897.

Mollnau, Hanke, Maria Wendt, Katalin Szöcs, Bernard Lassègue, Eberhard Schulz, Mathias Oelze, Huige Li, et al. 2002. “Effects of Angiotensin II Infusion on the Expression and Function of NAD(P)H Oxidase and Components of Nitric Oxide/CGMP Signaling.” *Circulation Research* 90 (4). https://doi.org/10.1161/01.res.0000012569.55432.02.

Moncada, S, and J R Vane. 1978. “Pharmacology and Endogenous Roles of Prostaglandin Endoperoxides, Thromboxane A2, and Prostacyclin.” *Pharmacological Reviews* 30 (3).

Montaudon, E., L. Dubreil, V. Lalanne, M. Vermot Des Roches, G. Toumaniantz, M. Fusellier, J. C. Desfontis, L. Martignat, and M. Y. Mallem. 2015. “Cardiac Effects of Long-Term Active Immunization with the Second Extracellular Loop of Human B1- and/or B3-Adrenoceptors in Lewis Rats.” *Pharmacological Research* 100: 210–19. https://doi.org/10.1016/j.phrs.2015.08.006.

Morton, Gregory J., and Michael W. Schwartz. 2011. “Leptin and the Central Nervous System Control of Glucose Metabolism.” *Physiological Reviews* 91 (2): 389–411. https://doi.org/10.1152/physrev.00007.2010.

Mudau, Mashudu, Amanda Genis, Amanda Lochner, and Hans Strijdom. 2012. “Endothelial Dysfunction: The Early Predictor of Atherosclerosis.” *Cardiovascular Journal of Africa*. Cardiovasc J Afr. https://doi.org/10.5830/CVJA-2011-068.

Müller, Alison L., and Naranjan S. Dhalla. 2013. “Differences in Concentric Cardiac Hypertrophy and Eccentric Hypertrophy.” In *Cardiac Adaptations: Molecular Mechanisms*, 4:147–66. Springer New York. https://doi.org/10.1007/978-1-4614-5203-4_8.

Mundy, Alexa L., Elvira Haas, Indranil Bhattacharya, Corinne C. Widmer, Martin Kretz, Karin Baumann, and Matthias Barton. 2007. “Endothelin Stimulates Vascular Hydroxyl Radical Formation: Effect of Obesity.” *American Journal of Physiology - Regulatory Integrative and Comparative Physiology* 293 (6). https://doi.org/10.1152/ajpregu.00295.2007.

Muniyappa, Ranganath, Micaela Iantorno, and Michael J Quon. 2008. “An Integrated View of

Insulin Resistance and Endothelial Dysfunction." *Endocrinol Metab Clin North Am* 37 (3): 685–x. https://doi.org/10.1016/j.ecl.2008.06.001.

Muniyappa, Ranganath, and James R. Sowers. 2013. "Role of Insulin Resistance in Endothelial Dysfunction." *Reviews in Endocrine and Metabolic Disorders* 14 (1): 5–12. https://doi.org/10.1007/s11154-012-9229-1.

Münzel, Thomas, Robert Feil, Alexander Mülsch, Suzanne M. Lohmann, Franz Hofmann, and Ulrich Walter. 2003. "Physiology and Pathophysiology of Vascular Signaling Controlled by Cyclic Guanosine 3′,5′-Cyclic Monophosphate-Dependent Protein Kinase." *Circulation*. Lippincott Williams & Wilkins. https://doi.org/10.1161/01.CIR.0000094403.78467.C3.

Murphy, Kevin G., and Stephen R. Bloom. 2006. "Gut Hormones and the Regulation of Energy Homeostasis." *Nature*. Nature Publishing Group. https://doi.org/10.1038/nature05484.

Namekawa, Junichi, Yoshiichi Takagi, Kaoru Wakabayashi, Yuki Nakamura, Ayaka Watanabe, Dai Nagakubo, Mitsuyuki Shirai, and Fumitoshi Asai. 2017. "Effects of High-Fat Diet and Fructose-Rich Diet on Obesity, Dyslipidemia and Hyperglycemia in the WBN/Kob-Leprfa Rat, a New Model of Type 2 Diabetes Mellitus." *Journal of Veterinary Medical Science* 79 (6): 988–91. https://doi.org/10.1292/jvms.17-0136.

Naples, Mark, Lisa M. Federico, Elaine Xu, Joanna Nelken, and Khosrow Adeli. 2008. "Effect of Rosuvastatin on Insulin Sensitivity in an Animal Model of Insulin Resistance: Evidence for Statin-Induced Hepatic Insulin Sensitization." *Atherosclerosis* 198 (1): 94–103. https://doi.org/10.1016/j.atherosclerosis.2007.11.003.

Nathan, Carl, and Qiao wen Xie. 1994. "Nitric Oxide Synthases: Roles, Tolls, and Controls." *Cell*. Cell. https://doi.org/10.1016/0092-8674(94)90266-6.

Negres, Simona, Cornel Chirita, Andreea Letitia Arsene, Denisa Margina, Elena Morosan, and Cristina Elena Zbarcea. 2017. "New Potential Beta-3 Adrenergic Agonists with Beta-Phenylethylamine Structure, Synthesized for the Treatment of Dyslipidemia and Obesity." In *Adiposity - Epidemiology and Treatment Modalities*. InTech. https://doi.org/10.5772/65328.

Nematy, Mohsen, Farnaz Ahmadpour, Zahra Behnam Rassouli, Hosein Mohaddes Ardabili, and Mohsen Azimi-Nezhad. 2014. "A Review on Underlying Differences in the Prevalence of Metabolic Syndrome in the Middle East, Europe and North America." https://doi.org/10.4172/1747-0862.S1-019.

Nguyen, Quang, Joann Dominguez, Loida Nguyen, and Nageshwara Gullapalli. 2010. "Hypertension Management: An Update." *American Health and Drug Benefits* 3 (1): 47–55. www.AHDBonline.com.

Ning, Bo, Xiaoyan Wang, Ying Yu, Ahmed Bilal Waqar, Qi Yu, Tomonari Koike, Masashi Shiomi, Enqi Liu, Yifei Wang, and Jianglin Fan. 2015. "High-Fructose and High-Fat Diet-Induced Insulin Resistance Enhances Atherosclerosis in Watanabe Heritable Hyperlipidemic Rabbits." *Nutrition and Metabolism* 12 (30): 1–11. https://doi.org/10.1186/s12986-015-0024-3.

Nossaman, Bobby D, and Philip J Kadowitz. 2013. "Stimulators of Soluble Guanylyl Cyclase:

Future Clinical Indications." *The Ochsner Journal* 13 (1): 147–56. http://www.ncbi.nlm.nih.gov/pubmed/23532174.

O'Mara, Alana E., James W. Johnson, Joyce D. Linderman, Robert J. Brychta, Suzanne McGehee, Laura A. Fletcher, Yael A. Fink, et al. 2020. "Chronic Mirabegron Treatment Increases Human Brown Fat, HDL Cholesterol, and Insulin Sensitivity." *Journal of Clinical Investigation* 130 (5): 2209–19. https://doi.org/10.1172/JCI131126.

O'Neill, S., and L. O'Driscoll. 2015. "Metabolic Syndrome: A Closer Look at the Growing Epidemic and Its Associated Pathologies." *Obesity Reviews* 16 (1): 1–12. https://doi.org/10.1111/obr.12229.

Obunai, Kotaro, Sonal Jani, and George D. Dangas. 2007. "Cardiovascular Morbidity and Mortality of the Metabolic Syndrome." *Medical Clinics of North America* 91 (6): 1169–84. https://doi.org/10.1016/J.MCNA.2007.06.003.

Okatan, Esma N., Aysegul Toy Durak, and Belma Turan. 2016. "Electrophysiological Basis of Metabolic-Syndrome-Induced Cardiac Dysfunction." *Canadian Journal of Physiology and Pharmacology* 94 (10): 1064–73. https://doi.org/10.1139/cjpp-2015-0531.

Okon, Elena B., Tania Szado, Ismail Laher, Bruce McManus, and Cornelis Van Breemena. 2003. "Augmented Contractile Response of Vascular Smooth Muscle in a Diabetic Mouse Model." *Journal of Vascular Research* 40 (6): 520–30. https://doi.org/10.1159/000075238.

Olejnickova, Veronika, Marie Novakova, and Ivo Provaznik. 2015. "Isolated Heart Models: Cardiovascular System Studies and Technological Advances." *Medical and Biological Engineering and Computing* 53 (7): 669–78. https://doi.org/10.1007/s11517-015-1270-2.

Olsen, Jessica M., Alice Åslund, Muhammad Hamza Bokhari, Dana S. Hutchinson, and Tore Bengtsson. 2019. "Acute β-Adrenoceptor Mediated Glucose Clearance in Brown Adipose Tissue; a Distinct Pathway Independent of Functional Insulin Signaling." *Molecular Metabolism* 30 (December): 240–49. https://doi.org/10.1016/j.molmet.2019.10.004.

Ormazabal, Valeska, Soumyalekshmi Nair, Omar Elfeky, Claudio Aguayo, Carlos Salomon, and Felipe A. Zuñiga. 2018. "Association between Insulin Resistance and the Development of Cardiovascular Disease." *Cardiovascular Diabetology*. BioMed Central Ltd. https://doi.org/10.1186/s12933-018-0762-4.

Ouchi, Noriyuki, Shinji Kihara, Yukio Arita, Yoshihisa Okamoto, Kazuhisa Maeda, Hiroshi Kuriyama, Kikuko Hotta, et al. 2000. "Adiponectin, an Adipocyte-Derived Plasma Protein, Inhibits Endothelial NF-KB Signaling through a CAMP-Dependent Pathway." *Circulation* 102 (11): 1296–1301. https://doi.org/10.1161/01.CIR.102.11.1296.

Owei, Ibiye, Nkiru Umekwe, Casey Provo, Jim Wan, and Samuel Dagogo-Jack. 2017. "Insulin-Sensitive and Insulin-Resistant Obese and Non-Obese Phenotypes: Role in Prediction of Incident Pre-Diabetes in a Longitudinal Biracial Cohort." *BMJ Open Diabetes Research and Care* 5 (1): e000415. https://doi.org/10.1136/bmjdrc-2017-000415.

Pallazola, Vincent A., Dorothy M. Davis, Seamus P. Whelton, Rhanderson Cardoso, Jacqueline M. Latina, Erin D. Michos, Sudipa Sarkar, et al. 2019. "A Clinician's Guide to Healthy Eating

for Cardiovascular Disease Prevention." *Mayo Clinic Proceedings: Innovations, Quality & Outcomes* 3 (3): 251–67. https://doi.org/10.1016/j.mayocpiqo.2019.05.001.

Panchal, Sunil K., Hemant Poudyal, Abishek Iyer, Reeza Nazer, Ashraful Alam, Vishal Diwan, Kathleen Kauter, et al. 2011. "High-Carbohydrate High-Fat Diet-Induced Metabolic Syndrome and Cardiovascular Remodeling in Rats." *Journal of Cardiovascular Pharmacology* 57 (1): 51–64. https://doi.org/10.1097/FJC.0b013e3181feb90a.

Papanicolaou, D. A., J. S. Petrides, C. Tsigos, S. Bina, K. T. Kalogeras, R. Wilder, P. W. Gold, P. A. Deuster, and G. P. Chrousos. 1996. "Exercise Stimulates Interleukin-6 Secretion: Inhibition by Glucocorticoids and Correlation with Catecholamines." *American Journal of Physiology - Endocrinology and Metabolism* 271 (3 34-3). https://doi.org/10.1152/ajpendo.1996.271.3.e601.

Park, Jong Seon, Young Jo Kim, Ji Yong Choi, Yoon Nyun Kim, Teck Jong Hong, Dong Soo Kim, Ki Young Kim, et al. 2010. "Comparative Study of Low Doses of Rosuvastatin and Atorvastatin on Lipid and Glycemic Control in Patients with Metabolic Syndrome and Hypercholesterolemia." *Korean Journal of Internal Medicine* 25 (1): 27–35. https://doi.org/10.3904/kjim.2010.25.1.27.

Park, Min, Peter Sandner, and Thomas Krieg. 2018. "CGMP at the Centre of Attention: Emerging Strategies for Activating the Cardioprotective PKG Pathway." *Basic Research in Cardiology*. Dr. Dietrich Steinkopff Verlag GmbH and Co. KG. https://doi.org/10.1007/s00395-018-0679-9.

Park, So Young, You Ree Cho, Hyo Jeong Kim, Takamasa Higashimori, Cheryl Danton, Mi Kyung Lee, Asim Dey, et al. 2005. "Unraveling the Temporal Pattern of Diet-Induced Insulin Resistance in Individual Organs and Cardiac Dysfunction in C57BL/6 Mice." *Diabetes* 54 (12): 3530–40. https://doi.org/10.2337/diabetes.54.12.3530.

Pazos, Patricia, Luis Lima, Felipe F. Casanueva, Carlos Diéguez, and María C. García. 2013. "Interleukin 6 Deficiency Modulates the Hypothalamic Expression of Energy Balance Regulating Peptides during Pregnancy in Mice." *PLoS ONE* 8 (8): 72339. https://doi.org/10.1371/journal.pone.0072339.

Pearson, Thomas A., Margo A. Denke, Patrick E. McBride, Wendy P. Battisti, William E. Brady, and Joanne Palmisano. 2005. "A Community-Based, Randomized Trial of Ezetimibe Added to Statin Therapy to Attain NCEP ATP III Goals for LDL Cholesterol in Hypercholesterolemic Patients: The Ezetimibe Add-on to Statin for Effectiveness (EASE) Trial." *Mayo Clinic Proceedings* 80 (5): 587–95. https://doi.org/10.4065/80.5.587.

Pechánová, O, Z V Varga, M Cebová, Z Giricz, P Pacher, P Ferdinandy, and Olga Pechánová. 2015. "Cardiac NO Signalling in the Metabolic Syndrome Correspondence LINKED ARTICLES." *Www.Brjpharmacol.Org British Journal of Pharmacology* 172: 1415. https://doi.org/10.1111/bph.2015.172.issue-6.

Pedersen, Bente Klarlund, Adam Steensberg, and Peter Schjerling. 2001. "Muscle-Derived Interleukin-6: Possible Biological Effects." *Journal of Physiology*. J Physiol. https://doi.org/10.1111/j.1469-7793.2001.0329c.xd.

Pellegrin, M., L. Mazzolai, A. Berthelot, and P. Laurant. 2009. “Dysfonction Endothéliale et Risque Cardiovasculaire. L’exercice Protège La Fonction Endothéliale et Prévient La Maladie Cardiovasculaire.” *Science and Sports*. https://doi.org/10.1016/j.scispo.2008.10.003.

Pérez-Martínez, Pablo, Dimitri P. Mikhailidis, Vasilios G. Athyros, Mónica Bullo, Patrick Couture, María I. Covas, Lawrence de Koning, et al. 2017. “Lifestyle Recommendations for the Prevention and Management of Metabolic Syndrome: An International Panel Recommendation.” *Nutrition Reviews* 75 (5): 307–26. https://doi.org/10.1093/nutrit/nux014.

Petersen, Kitt Falk, Sylvie Dufour, Douglas Befroy, Rina Garcia, and Gerald I. Shulman. 2004. “Impaired Mitochondrial Activity in the Insulin-Resistant Offspring of Patients with Type 2 Diabetes.” *New England Journal of Medicine* 350 (7): 664–71. https://doi.org/10.1056/NEJMoa031314.

Pfeifer, Alexander, Ana Kilić, and Linda Sarah Hoffmann. 2013. “Regulation of Metabolism by CGMP.” *Pharmacology and Therapeutics*. Elsevier Inc. https://doi.org/10.1016/j.pharmthera.2013.06.001.

Philipson, L. H. 2002. “β-Agonists and Metabolism.” In *Journal of Allergy and Clinical Immunology*, 110:S313–17. Mosby Inc. https://doi.org/10.1067/mai.2002.129702.

Pi-Sunyer, Xavier, Arne Astrup, Ken Fujioka, Frank Greenway, Alfredo Halpern, Michel Krempf, David C.W. Lau, et al. 2015. “A Randomized, Controlled Trial of 3.0 Mg of Liraglutide in Weight Management.” *New England Journal of Medicine* 373 (1): 11–22. https://doi.org/10.1056/NEJMoa1411892.

Picchi, Andrea. 2010. “Coronary Microvascular Dysfunction in Diabetes Mellitus: A Review.” *World Journal of Cardiology* 2 (11): 377. https://doi.org/10.4330/wjc.v2.i11.377.

Pizzino, Gabriele, Natasha Irrera, Mariapaola Cucinotta, Giovanni Pallio, Federica Mannino, Vincenzo Arcoraci, Francesco Squadrito, Domenica Altavilla, and Alessandra Bitto. 2017. “Oxidative Stress: Harms and Benefits for Human Health.” https://doi.org/10.1155/2017/8416763.

Poher, Anne Laure, Jordi Altirriba, Christelle Veyrat-Durebex, and Françoise Rohner-Jeanrenaud. 2015. “Brown Adipose Tissue Activity as a Target for the Treatment of Obesity/Insulin Resistance.” *Frontiers in Physiology*. Frontiers Research Foundation. https://doi.org/10.3389/fphys.2015.00004.

Polovina, Marija M., and Tatjana S. Potpara. 2014. “Endothelial Dysfunction in Metabolic and Vascular Disorders.” *Postgraduate Medicine*. Taylor and Francis Inc. https://doi.org/10.3810/pgm.2014.03.2739.

Pouleur, Anne Catherine, Stefan Anker, Dulce Brito, Oana Brosteanu, Dirk Hasenclever, Barbara Casadei, Frank Edelmann, et al. 2018. “Rationale and Design of a Multicentre, Randomized, Placebo-Controlled Trial of Mirabegron, a Beta3-Adrenergic Receptor Agonist on Left Ventricular Mass and Diastolic Function in Patients with Structural Heart Disease Beta3-Left Ventricular Hypertrophy (Beta3-LVH).” *ESC Heart Failure* 5 (5): 830–41. https://doi.org/10.1002/ehf2.12306.

Pritchard, Kirkwood A, Allan W Ackerman, Eric R Gross, David W Stepp, Yang Shi, Jason T Fontana, John E Baker, and William C Sessa. 2001. “Heat Shock Protein 90 Mediates the Balance of Nitric Oxide and Superoxide Anion from Endothelial Nitric-Oxide Synthase for ENOS-Dependent NO Production and That Inhibition of ATP-Dependent Con-Formational Changes in Hsp90 Uncouples ENOS Activity and Incr.” https://doi.org/10.1074/jbc.C100084200.

Ramirez, Claudia E., Hui Nian, Chang Yu, Jorge L. Gamboa, James M. Luther, Nancy J. Brown, and Cyndya A. Shibao. 2015. “Treatment with Sildenafil Improves Insulin Sensitivity in Prediabetes: A Randomized, Controlled Trial.” *The Journal of Clinical Endocrinology & Metabolism* 100 (12): 4533–40. https://doi.org/10.1210/jc.2015-3415.

Rask Larsen, Julie, Lorena Dima, Christoph U. Correll, and Peter Manu. 2018. “The Pharmacological Management of Metabolic Syndrome.” *Expert Review of Clinical Pharmacology* 11 (4): 397–410. https://doi.org/10.1080/17512433.2018.1429910.

Reaven, G. M. 2000. “Diet and Syndrome X.” *Current Atherosclerosis Reports*. Springer. https://doi.org/10.1007/s11883-000-0050-z.

Reinehr, Thomas, Wieland Kiess, Thomas Kapellen, and Werner Andler. 2004. “Insulin Sensitivity among Obese Children and Adolescents, According to Degree of Weight Loss.” *Pediatrics* 114 (6): 1569–73. https://doi.org/10.1542/peds.2003-0649-F.

Rena, Graham, & D Grahame, and Ewan R Pearson. 2017. “The Mechanisms of Action of Metformin-Carboxamide Ribonucleoside AMPK AMP-Activated Protein Kinase EGP Endogenous Glucose Production FDG Fluorodeoxyglucose G6Pase Glucose-6-Phosphatase GI Gastrointestinal GLP-1 Glucagon-like Peptide-1 MGPD Mitochondrial G.” *Diabetologia* 60 (1577–1585). https://doi.org/10.1007/s00125-017-4342-z.

Rider, O. J., P. Cox, D. Tyler, K. Clarke, and S. Neubauer. 2013. “Myocardial Substrate Metabolism in Obesity.” *International Journal of Obesity*. Int J Obes (Lond). https://doi.org/10.1038/ijo.2012.170.

Ridker, Paul M., Nader Rifai, Meir J. Stampfer, and Charles H. Hennekens. 2000. “Plasma Concentration of Interleukin-6 and the Risk of Future Myocardial Infarction Among Apparently Healthy Men.” *Circulation* 101 (15): 1767–72. https://doi.org/10.1161/01.CIR.101.15.1767.

Rizzo, Nico S., Joan Sabaté, Karen Jaceldo-Siegl, and Gary E. Fraser. 2011. “Vegetarian Dietary Patterns Are Associated with a Lower Risk of Metabolic Syndrome: The Adventist Health Study 2.” *Diabetes Care* 34 (5): 1225–27. https://doi.org/10.2337/dc10-1221.

Rizzo, Norma O, Ezekiel Maloney, Matilda Pham, Ian Luttrell, Hunter Wessell, Sanshiro Tateya, Guenter Daum, Priya Handa, Michael W Schwartz, and Francis Kim. 2010. “Reduced Nitric Oxide/CGMP Signaling Contributes to Vascular Inflammation and Insulin Resistance Induced by High Fat Feeding.” *Arterioscler Thromb Vasc Biol* 30 (4): 758–65. https://doi.org/10.1161/ATVBAHA.109.199893.

Roberts, Christian K., R. James Barnard, Ram K. Sindhu, Michael Jurczak, Ashkan Ehdaie, and Nosratola D. Vaziri. 2005a. “A High-Fat, Refined-Carbohydrate Diet Induces Endothelial

Dysfunction and Oxidant/Antioxidant Imbalance and Depresses NOS Protein Expression." *Journal of Applied Physiology* 98 (1): 203–10. https://doi.org/10.1152/japplphysiol.00463.2004.

———. 2005b. "A High-Fat, Refined-Carbohydrate Diet Induces Endothelial Dysfunction and Oxidant/Antioxidant Imbalance and Depresses NOS Protein Expression." *Journal of Applied Physiology* 98 (1): 203–10. https://doi.org/10.1152/japplphysiol.00463.2004.

Rochlani, Yogita, Naga Venkata Pothineni, Swathi Kovelamudi, and Jawahar L. Mehta. 2017. "Metabolic Syndrome: Pathophysiology, Management, and Modulation by Natural Compounds." *Therapeutic Advances in Cardiovascular Disease Review* 11 (8): 215–25. https://doi.org/10.1177/1753944717711379.

Rojas, Lilian Beatriz Aguayo, and Marilia Brito Gomes. 2013. "Metformin: An Old but Still the Best Treatment for Type 2 Diabetes." *Diabetology and Metabolic Syndrome*. BioMed Central. https://doi.org/10.1186/1758-5996-5-6.

Rosol, Thomas J. 2013. "On-Target Effects of GLP-1 Receptor Agonists on Thyroid C-Cells in Rats and Mice." *Toxicologic Pathology* 41 (2): 303–9. https://doi.org/10.1177/0192623312472402.

Roy, Denis, Mylène Perreault, and André Marette. 1998. "Insulin Stimulation of Glucose Uptake in Skeletal Muscles and Adipose Tissues in Vivo Is NO Dependent." *American Journal of Physiology - Endocrinology and Metabolism* 274 (4 37-4). https://doi.org/10.1152/ajpendo.1998.274.4.e692.

Rozec, Bertrand, and Chantal Gauthier. 2006. "B3-Adrenoceptors in the Cardiovascular System: Putative Roles in Human Pathologies." *Pharmacology and Therapeutics*. Pharmacol Ther. https://doi.org/10.1016/j.pharmthera.2005.12.002.

Ruderman, Neil, D. Chisholm, X. Pi-Sunyer, and S. Schneider. 1998. "The Metabolically Obese, Normal-Weight Individual Revisited." *Diabetes*. Diabetes. https://doi.org/10.2337/diabetes.47.5.699.

Rydén, M., and P. Arner. 2007. "Tumour Necrosis Factor-α in Human Adipose Tissue - From Signalling Mechanisms to Clinical Implications." In *Journal of Internal Medicine*, 262:431–38. J Intern Med. https://doi.org/10.1111/j.1365-2796.2007.01854.x.

Safar, Michel E., and Edward D. Frohlich. 1995. "The Arterial System in Hypertension." In *Hypertension*, 26:10–14. https://doi.org/10.1161/01.hyp.26.1.10.

Saklayen, Mohammad G. 2018. "The Global Epidemic of the Metabolic Syndrome." *Current Hypertension Reports* 20 (2): 1–8. https://doi.org/10.1007/s11906-018-0812-z.

Salih Sahib, Ahmed, Haedar Abdulhafith Al-biati, Sajida Hussein Ismail, Faris Abdul Kareem Kazaal, and Salim Al-Rubaie. 2014. "Effects of Sildenafil on Lipid Profile and Glycemic Control in Patients with Type 2 Diabetes Mellitus and Metabolic Syndrome. IJBCP International Journal of Basic & Clinical Pharmacology Effects of Sildenafil on Lipid Profile and Glycemic Control in Patie." *International Journal of Basic & Clinical Pharmacology* 6: 1048–51. https://doi.org/10.5455/2319-2003.ijbcp20141217.

Salonen, Riitta M., Kristiina Nyyssönen, Jari Kaikkonen, Elina Porkkala-Sarataho, Sari Voutilainen, Tiina H. Rissanen, Tomi Pekka Tuomainen, et al. 2003. “Six-Year Effect of Combined Vitamin C and E Supplementation on Atherosclerotic Progression: The Antioxidant Supplementation in Atherosclerosis Prevention (ASAP) Study.” *Circulation* 107 (7): 947–53. https://doi.org/10.1161/01.CIR.0000050626.25057.51.

Sandner, Peter, Peter Berger, and Christoph Zenzmaier. 2017. “The Potential of SGC Modulators for the Treatment of Age-Related Fibrosis: A Mini-Review.” *Gerontology* 63 (3): 216–27. https://doi.org/10.1159/000450946.

Sandoo, Aamer, Jet J C S Veldhuijzen Van Zanten, George S Metsios, Douglas Carroll, and George D Kitas. 2010. “The Endothelium and Its Role in Regulating Vascular Tone.” *The Open Cardiovascular Medicine Journal*. Vol. 4. https://www.ncbi.nlm.nih.gov/pmc/articles/PMC3040999/pdf/TOCMJ-4-302.pdf.

Saneei, Parvane, Mahin Hashemipour, Roya Kelishadi, Somayeh Rajaei, and Ahmad Esmaillzadeh. 2013. “Effects of Recommendations to Follow the Dietary Approaches to Stop Hypertension (DASH) Diet v. Usual Dietary Advice on Childhood Metabolic Syndrome: A Randomised Cross-over Clinical Trial.” *British Journal of Nutrition* 110 (12): 2250–59. https://doi.org/10.1017/S0007114513001724.

Sanossian, Nerses, Jeffrey L. Saver, Mohamad Navab, and Bruce Ovbiagele. 2007. “High-Density Lipoprotein Cholesterol: An Emerging Target for Stroke Treatment.” *Stroke*. Stroke. https://doi.org/10.1161/01.STR.0000258347.19449.0f.

Santaniemi, Merja, Y. Antero Kesäniemi, and Olavi Ukkola. 2006. “Low Plasma Adiponectin Concentration Is an Indicator of the Metabolic Syndrome.” *European Journal of Endocrinology* 155 (5): 745–50. https://doi.org/10.1530/eje.1.02287.

Santilli, Francesca, Damiano D’Ardes, and Giovanni Davì. 2015. “Oxidative Stress in Chronic Vascular Disease: From Prediction to Prevention.” *Vascular Pharmacology*. Elsevier Inc. https://doi.org/10.1016/j.vph.2015.09.003.

Sarafidis, P. A., and G. L. Bakris. 2007. “Non-Esterified Fatty Acids and Blood Pressure Elevation: A Mechanism for Hypertension in Subjects with Obesity/Insulin Resistance?” *Journal of Human Hypertension*. J Hum Hypertens. https://doi.org/10.1038/sj.jhh.1002103.

Sarafidis, Pantelis A., and George L. Bakris. 2007. “Insulin and Endothelin: An Interplay Contributing to Hypertension Development?” *The Journal of Clinical Endocrinology & Metabolism* 92 (2): 379–85. https://doi.org/10.1210/jc.2006-1819.

Saraswathi, Viswanathan, and Alyssa H. Hasty. 2006. “The Role of Lipolysis in Mediating the Proinflammatory Effects of Very Low Density Lipoproteins in Mouse Peritoneal Macrophages.” *Journal of Lipid Research* 47 (7): 1406–15. https://doi.org/10.1194/jlr.M600159-JLR200.

Scheller, Jürgen, Athena Chalaris, Dirk Schmidt-Arras, and Stefan Rose-John. 2011. “The Pro- and Anti-Inflammatory Properties of the Cytokine Interleukin-6.” *Biochimica et Biophysica Acta - Molecular Cell Research*. Elsevier. https://doi.org/10.1016/j.bbamcr.2011.01.034.

Schiffrin, Ernesto L. 2008. “Oxidative Stress, Nitric Oxide Synthase, and Superoxide Dismutase: A Matter of Imbalance Underlies Endothelial Dysfunction in the Human Coronary Circulation.” *Hypertension*. Lippincott Williams & Wilkins. https://doi.org/10.1161/HYPERTENSIONAHA.107.103226.

Schillaci, Giuseppe, Matteo Pirro, Gaetano Vaudo, Fabio Gemelli, Simona Marchesi, Carlo Porcellati, and Elmo Mannarino. 2004. “Prognostic Value of the Metabolic Syndrome in Essential Hypertension.” *Journal of the American College of Cardiology* 43 (10): 1817–22. https://doi.org/10.1016/j.jacc.2003.12.049.

Schubert, Rudolf. 2005. “2.4 Isolated Vessels.” In , 198–211.

Scuteri, Angelo, Stephane Laurent, Francesco Cucca, John Cockcroft, Pedro Guimaraes Cunha, Leocadio Rodriguez Mañas, Francesco U Mattace Raso, et al. 2015. “THE METABOLIC SYNDROME ACROSS EUROPE-DIFFERENT CLUSTERS OF RISK FACTORS Metabolic Syndrome and Arteries REsearch (MARE) Consortium HHS Public Access.” *European Journal of Preventive Cardiology* 22 (4): 486–91. https://doi.org/10.1177/2047487314525529.

Sengstock, David M., Peter V. Vaitkevicius, and Mark A. Supiano. 2005. “Arterial Stiffness Is Related to Insulin Resistance in Nondiabetic Hypertensive Older Adults.” *The Journal of Clinical Endocrinology & Metabolism* 90 (5): 2823–27. https://doi.org/10.1210/jc.2004-1686.

Senn, Joseph J., Peter J. Klover, Irena A. Nowak, and Robert A. Mooney. 2002. “Interleukin-6 Induces Cellular Insulin Resistance in Hepatocytes.” *Diabetes* 51 (12): 3391–99. https://doi.org/10.2337/diabetes.51.12.3391.

Serpillon, Sabrina, Beverly C. Floyd, Rakhee S. Gupte, Shimran George, Mark Kozicky, Venessa Neito, Fabio Recchia, William Stanley, Michael S. Wolin, and Sachin A. Gupte. 2009. “Superoxide Production by NAD(P)H Oxidase and Mitochondria Is Increased in Genetically Obese and Hyperglycemic Rat Heart and Aorta before the Development of Cardiac Dysfunction. The Role of Glucose-6-Phosphate Dehydrogenase-Derived NADPH.” *American Journal of Physiology - Heart and Circulatory Physiology* 297 (1). https://doi.org/10.1152/ajpheart.01142.2008.

Sesso, Howard D., Julie E. Buring, Nader Rifai, Gavin J. Blake, J. Michael Gaziano, and Paul M. Ridker. 2003. “C-Reactive Protein and the Risk of Developing Hypertension.” *Journal of the American Medical Association* 290 (22): 2945–51. https://doi.org/10.1001/jama.290.22.2945.

Shah, Ravi V., Siddique A. Abbasi, Bobak Heydari, Carsten Rickers, David R. Jacobs, Lu Wang, Raymond Y. Kwong, David A. Bluemke, Joao A.C. Lima, and Michael Jerosch-Herold. 2013. “Insulin Resistance, Subclinical Left Ventricular Remodeling, and the Obesity Paradox: MESA (Multi-Ethnic Study of Atherosclerosis).” *Journal of the American College of Cardiology* 61 (16): 1698–1706. https://doi.org/10.1016/j.jacc.2013.01.053.

Sharma, Arya M., Tobias Pischon, Sandra Hardt, Iris Kunz, and Friedrich C. Luft. 2001. “β-Adrenergic Receptor Blockers and Weight Gain a Systematic Analysis.” *Hypertension*.

Lippincott Williams and Wilkins. https://doi.org/10.1161/01.HYP.37.2.250.

Shi, Yi, Thomas F. Lüscher, and Giovanni G. Camici. 2014. "Dual Role of Endothelial Nitric Oxide Synthase in Oxidized LDL-Induced, P66Shc-Mediated Oxidative Stress in Cultured Human Endothelial Cells." *PLoS ONE* 9 (9). https://doi.org/10.1371/journal.pone.0107787.

Shiomi, Masashi, and Takashi Ito. 2009. "The Watanabe Heritable Hyperlipidemic (WHHL) Rabbit, Its Characteristics and History of Development: A Tribute to the Late Dr. Yoshio Watanabe." *Atherosclerosis* 207 (1): 1–7. https://doi.org/10.1016/j.atherosclerosis.2009.03.024.

Shulman, Gerald I. 2004. "Unraveling the Cellular Mechanism of Insulin Resistance in Humans: New Insights from Magnetic Resonance Spectroscopy." *Physiology*. American Physiological Society. https://doi.org/10.1152/physiol.00007.2004.

Sibal, Latika, Sharad C Agarwal, Philip D Home, and Rainer H Boger. 2010. "The Role of Asymmetric Dimethylarginine (ADMA) in Endothelial Dysfunction and Cardiovascular Disease." *Current Cardiology Reviews* 6 (2): 82–90. https://doi.org/10.2174/157340310791162659.

Sichrovska, Lubica, Ivan Malik, Eva Sedlarova, Jozef Csollei, and Jan Muselik. 2013. "In Vitro Antioxidant Properties of Novel B3-Adrenoceptor Agonists Bearing Benzenesulfonamide Fragment." *Dhaka University Journal of Pharmaceutical Sciences* 12 (1): 23–28. https://doi.org/10.3329/dujps.v12i1.16296.

Simons, Leon A, and David R Sullivan. 2005. "Lipid-modifying Drugs." *Medical Journal of Australia* 182 (6): 286–89. https://doi.org/10.5694/j.1326-5377.2005.tb06703.x.

Sjöström, Lars, Markku Peltonen, Peter Jacobson, C. David Sjöström, Kristjan Karason, Hans Wedel, Sofie Ahlin, et al. 2012. "Bariatric Surgery and Long-Term Cardiovascular Events." *JAMA - Journal of the American Medical Association* 307 (1): 56–65. https://doi.org/10.1001/jama.2011.1914.

Skeberdis, V. Arvydas, Vida Gendviliene, Danguoledot Zablockaite, Rimantas Treinys, Regina Mačianskiene, Andrius Bogdelis, Jonas Jurevičius, and Rodolphe Fischmeister. 2008. "B3-Adrenergic Receptor Activation Increases Human Atrial Tissue Contractility and Stimulates the L-Type Ca2+ Current." *Journal of Clinical Investigation* 118 (9): 3219–27. https://doi.org/10.1172/JCI32519.

Skerrett, Patrick J., and Walter C. Willett. 2010. "Essentials of Healthy Eating: A Guide." *Journal of Midwifery and Women's Health* 55 (6): 492–501. https://doi.org/10.1016/j.jmwh.2010.06.019.

Skrapari, Ioanna, Nicholas Tentolouris, Despoina Perrea, Christos Bakoyiannis, Athanasia Papazafiropoulou, and Nicholas Katsilambros. 2007. "Baroreflex Sensitivity in Obesity: Relationship With Cardiac Autonomic Nervous System Activity*." *Obesity* 15 (7): 1685–93. https://doi.org/10.1038/oby.2007.201.

Skrzypiec-Spring, Monika, Bartosz Grotthus, Adam Szelag, and Richard Schulz. 2007. "Isolated Heart Perfusion According to Langendorff-Still Viable in the New Millennium." *Journal of*

Pharmacological and Toxicological Methods 55 (2): 113–26. https://doi.org/10.1016/j.vascn.2006.05.006.

Sleiman, Dana, Marwa R. Al-Badri, and Sami T. Azar. 2015. "Effect of Mediterranean Diet in Diabetes Control and Cardiovascular Risk Modification: A Systematic Review." *Frontiers in Public Health* 3 (April): 69. https://doi.org/10.3389/fpubh.2015.00069.

Soto González, A., D. Bellido Guerrero, M. Buño Soto, S. Pértega Díaz, M. Martinez-Olmos, and O. Vidal. 2006. "Metabolic Syndrome, Insulin Resistance and the Inflammation Markers C-Reactive Protein and Ferritin." *European Journal of Clinical Nutrition* 60 (6): 802–9. https://doi.org/10.1038/sj.ejcn.1602384.

Sparks, Janet D, Charles E Sparks, and Khosrow Adeli. 2012. "Selective Hepatic Insulin Resistance, VLDL Overproduction, and Hypertriglyceridemia ATVB in Focus New Developments in Hepatic Lipoprotein Production and Clinical Relevance." *Arterioscler Thromb Vasc Biol* 32: 2104–12. https://doi.org/10.1161/ATVBAHA.111.241463.

Staels, Bart, Jean Dallongeville, Johan Auwerx, Kristina Schoonjans, Eran Leitersdorf, and Jean-Charles Fruchart. 1998. "Mechanism of Action of Fibrates on Lipid and Lipoprotein Metabolism." *Circulation* 98 (19): 2088–93. https://doi.org/10.1161/01.CIR.98.19.2088.

Stary, Herbert C., A. Bleakley Chandler, Robert E. Dinsmore, Valentin Fuster, Seymour Glagov, William Insull, Michael E. Rosenfeld, Colin J. Schwartz, William D. Wagner, and Robert W. Wissler. 1995. "A Definition of Advanced Types of Atherosclerotic Lesions and a Histological Classification of Atherosclerosis." *Circulation* 92 (5): 1355–74. https://doi.org/10.1161/01.CIR.92.5.1355.

Stasch, Johannes-Peter, Pál Pacher, and Oleg V Evgenov. 2011. "Soluble Guanylate Cyclase as an Emerging Therapeutic Target in Cardiopulmonary Disease." *Circulation Journal* 123 (20): 2236–73. https://doi.org/10.1161/CIRCULATIONAHA.110.981738.

Stasch, Johannes-Peter, Peter Schmidt, Cristina Alonso-Alija, Heiner Apeler, Klaus Dembowsky, Michael Haerter, Markus Heil, et al. 2002. "NO- and Haem-Independent Activation of Soluble Guanylyl Cyclase: Molecular Basis and Cardiovascular Implications of a New Pharmacological Principle." *British Journal of Pharmacology* 136: 773–83. https://doi.org/10.1038/sj.bjp.0704778.

Stasch, Johannes Peter, Pál Pacher, and Oleg V. Evgenov. 2011. "Soluble Guanylate Cyclase as an Emerging Therapeutic Target in Cardiopulmonary Disease." *Circulation* 123 (20): 2263–73. https://doi.org/10.1161/CIRCULATIONAHA.110.981738.

Steinberg, Helmut O., Haitham Chaker, Rosalind Leaming, Ann Johnson, Ginger Brechtel, and Alain D. Baron. 1996. "Obesity/Insulin Resistance Is Associated with Endothelial Dysfunction: Implications for the Syndrome of Insulin Resistance." *Journal of Clinical Investigation* 97 (11): 2601–10. https://doi.org/10.1172/JCI118709.

Stenlöf, Kaj, Ingrid Wernstedt, Ted Fjällman, Ville Wallenius, Kristina Wallenius, and John Olov Jansson. 2003. "Interleukin-6 Levels in the Central Nervous System Are Negatively Correlated with Fat Mass in Overweight/Obese Subjects." *Journal of Clinical Endocrinology and Metabolism* 88 (9): 4379–83. https://doi.org/10.1210/jc.2002-021733.

Strasser, Barbara. 2013. “Physical Activity in Obesity and Metabolic Syndrome.” *Annals of the New York Academy of Sciences* 1281 (1): 141–59. https://doi.org/10.1111/j.1749-6632.2012.06785.x.

Straznicky, Nora E., Nina Eikelis, Elisabeth A. Lambert, and Murray D. Esler. 2008. “Mediators of Sympathetic Activation in Metabolic Syndrome Obesity.” *Current Hypertension Reports*. Curr Hypertens Rep. https://doi.org/10.1007/s11906-008-0083-1.

Straznicky, Nora E, Gavin W Lambert, Kazuko Masuo, Tye Dawood, Nina Eikelis, Paul J Nestel, Mariee T McGrane, et al. 2009. “Blunted Sympathetic Neural Response to Oral Glucose in Obese Subjects with the Insulin-Resistant Metabolic Syndrome.” *The American Journal of Clinical Nutrition* 89 (1): 27–36. https://doi.org/10.3945/ajcn.2008.26299.

Studyštefan, Studyˇ, Farsk´y Farsk´y, Andrea Strišková, and Marián Borčin. 2017. “Hypertension Treatment in Patients with Metabolic Syndrome and/or Type 2 Diabetes Mellitus: Analysis of the Therapy Effectivity and the Therapeutic Inertia in Outpatient StudyŠtefan.” *Cardiology Research and Practice*. https://doi.org/10.1155/2018/8387613.

Stumvoll, Michael, Barry J. Goldstein, and Timon W. Van Haeften. 2005. “Type 2 Diabetes: Principles of Pathogenesis and Therapy.” In *Lancet*, 365:1333–46. Elsevier Limited. https://doi.org/10.1016/S0140-6736(05)61032-X.

Sui, Wenhai, Hongshi Li, Yunlong Yang, Xu Jing, Fei Xue, Jing Cheng, Mei Dong, et al. 2019. “Bladder Drug Mirabegron Exacerbates Atherosclerosis through Activation of Brown Fat-Mediated Lipolysis.” *Proceedings of the National Academy of Sciences of the United States of America* 166 (22): 10937–42. https://doi.org/10.1073/pnas.1901655116.

Suman, Rajesh Kumar, Ipseeta Ray Mohanty, Manjusha K. Borde, Ujwala Maheshwari, and Y. A. Deshmukh. 2016. “Development of an Experimental Model of Diabetes Co-Existing with Metabolic Syndrome in Rats.” *Advances in Pharmacological Sciences* 2016. https://doi.org/10.1155/2016/9463476.

Sun, Kai, Christine M. Kusminski, and Philipp E. Scherer. 2011. “Adipose Tissue Remodeling and Obesity.” *Journal of Clinical Investigation*. American Society for Clinical Investigation. https://doi.org/10.1172/JCI45887.

Suzuki, Keisuke, Katherine A. Simpson, James S. Minnion, Joyceline C. Shillito, and Stephen R. Bloom. 2010. “The Role of Gut Hormones and the Hypothalamus in Appetite Regulation.” *Endocrine Journal*. Endocr J. https://doi.org/10.1507/endocrj.K10E-077.

Symonds, Michael E., Peter Aldiss, Mark Pope, and Helen Budge. 2018. “Recent Advances in Our Understanding of Brown and Beige Adipose Tissue: The Good Fat That Keeps You Healthy [Version 1; Referees: 2 Approved].” *F1000Research*. F1000 Research Ltd. https://doi.org/10.12688/f1000research.14585.1.

Szentirmai, Eva, and Levente Kapas. 2017a. “The Role of the Brown Adipose Tissue in B3-Adrenergic Receptor Activation-Induced Sleep, Metabolic and Feeding Responses.” *Scientific Reports* 7 (1): 1–14. https://doi.org/10.1038/s41598-017-01047-1.

———. 2017b. “The Role of the Brown Adipose Tissue in B3-Adrenergic Receptor Activation-

Induced Sleep, Metabolic and Feeding Responses." *Scientific Reports* 7 (1): 1–14. https://doi.org/10.1038/s41598-017-01047-1.

Takagi, Hisato, Masao Niwa, Yusuke Mizuno, Shin Nosuke Goto, and Takuya Umemoto. 2013. "Telmisartan as a Metabolic Sartan: The First Meta-Analysis of Randomized Controlled Trials in Metabolic Syndrome." *Journal of the American Society of Hypertension* 7 (3): 229–35. https://doi.org/10.1016/j.jash.2013.02.006.

Takano, M, N Itoh, K Yayama, M Yamano, R Ohtani, and H Okamoto. 1993. "Interleukin-6 as a Mediator Responsible for Inflammation-Induced Increase in Plasma Angiotensinogen." *Biochemical Pharmacology* 45 (1): 201–6.

Takimoto, Eiki. 2012. "Cyclic GMP-Dependent Signaling in Cardiac Myocytes." *Circulation Journal*. https://doi.org/10.1253/circj.CJ-12-0664.

Thorin, Chantal, Mohamed Yassine Mallem, Jacques Noireaud, Marc Gogny, and Jean-Claude Desfontis. 2010. "Nonlinear Mixed Effects Models Applied to Cumulative Concentration-Response Curves." *Journal of Pharmacy and Pharmacology* 62 (3): 339–45. https://doi.org/10.1211/jpp.62.03.0008.

Thorp, Alicia A, and Markus P Schlaich. 2015. "Relevance of Sympathetic Nervous System Activation in Obesity and Metabolic Syndrome." *Journal of Diabetes Research* 2015: 1–11. https://doi.org/10.1155/2015/341583.

Tirziu, Daniela, and Michael Simons. 2008. "Endothelium-Driven Myocardial Growth or Nitric Oxide at the Crossroads." *Trends in Cardiovascular Medicine*. NIH Public Access. https://doi.org/10.1016/j.tcm.2009.01.002.

Tissier, Florine, Yassine Mallem, Christelle Goanvec, Romain Didier, Thierry Aubry, Nathalie Bourgeois, Jean-Claude Desfontis, et al. 2016a. "A Non-Hypocholesterolemic Atorvastatin Treatment Improves Vessel Elasticity by Acting on Elastin Composition in WHHL Rabbits." *Atherosclerosis* 251 (August): 70–77. https://doi.org/10.1016/j.atherosclerosis.2016.05.039.

Tissier, Florine, Yassine Mallem, Christelle Goanvec, Romain Didier, Thierry Aubry, Nathalie Bourgeois, Jean Claude Desfontis, et al. 2016b. "A Non-Hypocholesterolemic Atorvastatin Treatment Improves Vessel Elasticity by Acting on Elastin Composition in WHHL Rabbits." *Atherosclerosis* 251 (August): 70–77. https://doi.org/10.1016/j.atherosclerosis.2016.05.039.

Toklu, Hale Zerrin, J. Muller-Delp, Y. Sakarya, S. Oktay, N. Kirichenko, M. Matheny, C. S. Carter, et al. 2016. "High Dietary Fructose Does Not Exacerbate the Detrimental Consequences of High Fat Diet on Basilar Artery Function." *Journal of Physiology and Pharmacology* 67 (2): 205–16. https://doi.org/27226180.

Toque, Haroldo A., Kenia P. Nunes, Modesto Rojas, Anil Bhatta, Lin Yao, Zhimin Xu, Maritza J. Romero, R. Clinton Webb, Ruth B. Caldwell, and R. William Caldwell. 2013. "Arginase 1 Mediates Increased Blood Pressure and Contributes to Vascular Endothelial Dysfunction in Deoxycorticosterone Acetate-Salt Hypertension." *Frontiers in Immunology* 4 (JUL). https://doi.org/10.3389/fimmu.2013.00219.

Townsend, Kristy, and Yu-Hua Tseng. 2012. "Brown Adipose Tissue." *Adipocyte* 1 (1): 13–24.

https://doi.org/10.4161/adip.18951.

Trajkovska, Katerina Tosheska, and Sonja Topuzovska. 2017. “High-Density Lipoprotein Metabolism and Reverse Cholesterol Transport: Strategies for Raising HDL Cholesterol.” *Anatolian Journal of Cardiology* 18 (2): 149–54. https://doi.org/10.14744/AnatolJCardiol.2017.7608.

Tran, Vivian, T. Michael De Silva, Christopher G. Sobey, Kyungjoon Lim, Grant R. Drummond, Antony Vinh, and Maria Jelinic. 2020. “The Vascular Consequences of Metabolic Syndrome: Rodent Models, Endothelial Dysfunction, and Current Therapies.” *Frontiers in Pharmacology*. Frontiers Media S.A. https://doi.org/10.3389/fphar.2020.00148.

Traupe, Tobias, Matthias Lang, Winfried Goettsch, Klaus Münter, Henning Morawietz, Wilhelm Vetter, and Matthias Barton. 2002. “Obesity Increases Prostanoid-Mediated Vasoconstriction and Vascular Thromboxane Receptor Gene Expression.” *Journal of Hypertension* 20 (11): 2239–45. https://doi.org/10.1097/00004872-200211000-00024.

Trochu, Jean Noël, Véronique Leblais, Yohann Rautureau, Fabrizio Bévérelli, Hervé Le Marec, Alain Berdeaux, and Chantal Gauthier. 1999. “Beta 3-Adrenoceptor Stimulation Induces Vasorelaxation Mediated Essentially by Endothelium-Derived Nitric Oxide in Rat Thoracic Aorta.” *British Journal of Pharmacology* 128 (1): 69–76. https://doi.org/10.1038/sj.bjp.0702797.

Tsai, Emily J., and David A. Kass. 2009a. “Cyclic GMP Signaling in Cardiovascular Pathophysiology and Therapeutics.” *Pharmacology and Therapeutics*. https://doi.org/10.1016/j.pharmthera.2009.02.009.

Tsai, Emily J, and David A Kass. 2009b. “Cyclic GMP Signaling in Cardiovascular Pathophysiology and Therapeutics.” *Pharmacology & Therapeutics* 122 (3): 216–38. https://doi.org/10.1016/j.pharmthera.2009.02.009.

Tune, Johnathan D., Adam G. Goodwill, Daniel J. Sassoon, and Kieren J. Mather. 2017. “Cardiovascular Consequences of Metabolic Syndrome.” *Translational Research*. Mosby Inc. https://doi.org/10.1016/j.trsl.2017.01.001.

Ufer, Christoph, and Renée Germack. 2009. “Cross-Regulation between β 1- and β 3-Adrenoceptors Following Chronic β-Adrenergic Stimulation in Neonatal Rat Cardiomyocytes.” *British Journal of Pharmacology* 158 (1): 300–313. https://doi.org/10.1111/j.1476-5381.2009.00328.x.

Ukkola, Olavi, and Merja Santaniemi. 2002. “Adiponectin: A Link between Excess Adiposity and Associated Comorbidities?” *Journal of Molecular Medicine*. Springer. https://doi.org/10.1007/s00109-002-0378-7.

Unger, Thomas, Claudio Borghi, Fadi Charchar, Nadia A. Khan, Neil R. Poulter, Dorairaj Prabhakaran, Agustin Ramirez, et al. 2020. “2020 International Society of Hypertension Global Hypertension Practice Guidelines.” *Journal of Hypertension* 38 (6): 982–1004. https://doi.org/10.1097/HJH.0000000000002453.

Valerio, Alessandra, Annalisa Cardile, Valeria Cozzi, Renata Bracale, Laura Tedesco, Addolorata

Pisconti, Letizia Palomba, et al. 2006. “TNF-α Downregulates ENOS Expression and Mitochondrial Biogenesis in Fat and Muscle of Obese Rodents.” *Journal of Clinical Investigation* 116 (10): 2791–98. https://doi.org/10.1172/JCI28570.

Vanhoutte, P. M., H. Shimokawa, M. Feletou, and E. H.C. Tang. 2017. “Endothelial Dysfunction and Vascular Disease – a 30th Anniversary Update.” *Acta Physiologica*. Blackwell Publishing Ltd. https://doi.org/10.1111/apha.12646.

Vanhoutte, Paul M., Michel Feletou, and Stefano Taddei. 2005. “Endothelium-Dependent Contractions in Hypertension.” *British Journal of Pharmacology*. Wiley-Blackwell. https://doi.org/10.1038/sj.bjp.0706042.

Vanhoutte, Paul M., and Eva H.C. Tang. 2008. “Endothelium-Dependent Contractions: When a Good Guy Turns Bad!” *Journal of Physiology*. J Physiol. https://doi.org/10.1113/jphysiol.2008.161430.

Vasan, Ramachandran S. 2003. “Cardiac Function and Obesity.” *Heart* 89 (10): 1127–29. https://doi.org/10.1136/heart.89.10.1127.

Vavlukis, Marija, and Ana Vavlukis. 2020. “Statins Alone or in Combination with Ezetimibe or PCSK9 Inhibitors in Atherosclerotic Cardiovascular Disease Protection.” In *Lipid Peroxidation Research*. IntechOpen. https://doi.org/10.5772/intechopen.82520.

Vincent, Michelle A., Monica Montagnani, and Michael J. Quon. 2003. “Molecular and Physiologic Actions of Insulin Related to Production of Nitric Oxide in Vascular Endothelium.” *Current Diabetes Reports*. Current Science Ltd. https://doi.org/10.1007/s11892-003-0018-9.

Vincent, Michelle A, Lucy H Clerk, Stephen Rattigan, Michael G Clark, and Eugene J Barrett. 2005. “ACTIVE ROLE FOR THE VASCULATURE IN THE DELIVERY OF INSULIN TO SKELETAL MUSCLE.” *Clinical and Experimental Pharmacology and Physiology* 32 (4): 302–7. https://doi.org/10.1111/j.1440-1681.2005.04188.x.

Violin, Jonathan D., Aimee L. Crombie, David G. Soergel, and Michael W. Lark. 2014. “Biased Ligands at G-Protein-Coupled Receptors: Promise and Progress.” *Trends in Pharmacological Sciences*. Elsevier Ltd. https://doi.org/10.1016/j.tips.2014.04.007.

Vliet-Ostaptchouk, Jana V van, Marja-Liisa Nuotio, Sandra N Slagter, Dany Doiron, Krista Fischer, Luisa Foco, Amadou Gaye, et al. 2014. “The Prevalence of Metabolic Syndrome and Metabolically Healthy Obesity in Europe: A Collaborative Analysis of Ten Large Cohort Studies.” https://doi.org/10.1186/1472-6823-14-9.

Vykoukal, Daynene, and Mark G. Davies. 2011. “Vascular Biology of Metabolic Syndrome.” *Journal of Vascular Surgery* 54 (3): 819–31. https://doi.org/10.1016/j.jvs.2011.01.003.

Wadden, T. A., P. Hollander, S. Klein, K. Niswender, V. Woo, P. M. Hale, and L. Aronne. 2013. “Weight Maintenance and Additional Weight Loss with Liraglutide after Low-Calorie-Diet-Induced Weight Loss: The SCALE Maintenance Randomized Study.” *International Journal of Obesity* 37 (11): 1443–51. https://doi.org/10.1038/ijo.2013.120.

Walther, Cornelia, and Stephen S.G. Ferguson. 2013. “Arrestins: Role in the Desensitization,

Sequestration, and Vesicular Trafficking of g Protein-Coupled Receptors." In *Progress in Molecular Biology and Translational Science*, 118:93–113. Elsevier B.V. https://doi.org/10.1016/B978-0-12-394440-5.00004-8.

Wang, Jiali, Silvana Obici, Kimyata Morgan, Nir Barzilai, Zhaohui Feng, and Luciano Rossetti. 2001. "Overfeeding Rapidly Induces Leptin and Insulin Resistance." *Diabetes* 50 (12): 2786–91. https://doi.org/10.2337/diabetes.50.12.2786.

Wang, Lianguo, Nicole M. De Jesus, and Crystal M. Ripplinger. 2015. "Optical Mapping of Intra-Sarcoplasmic Reticulum Ca2+and Transmembrane Potential in the Langendorff-Perfused Rabbit Heart." *Journal of Visualized Experiments*, no. 103: 1–7. https://doi.org/10.3791/53166.

Wang, Tiange, Yoriko Heianza, Dianjianyi Sun, Tao Huang, Wenjie Ma, Eric B. Rimm, Joann E. Manson, Frank B. Hu, Walter C. Willett, and Lu Qi. 2018. "Improving Adherence to Healthy Dietary Patterns, Genetic Risk, and Long Term Weight Gain: Gene-Diet Interaction Analysis in Two Prospective Cohort Studies." *BMJ (Online)* 360. https://doi.org/10.1136/bmj.j5644.

Wang, Yan, Shun Qiao, De-Wu Han, Xin-Ren Rong, Yi-Xiao Wang, Jing-jing Xue, and Jing Yang. 2018. "Telmisartan Improves Insulin Resistance." *American Journal of Therapeutics* 25 (6): e642–51. https://doi.org/10.1097/MJT.0000000000000733.

Wang, Youfa, May A. Beydoun, Lan Liang, Benjamin Caballero, and Shiriki K. Kumanyika. 2008. "Will All Americans Become Overweight or Obese? Estimating the Progression and Cost of the US Obesity Epidemic." *Obesity* 16 (10): 2323–30. https://doi.org/10.1038/oby.2008.351.

Waqar, Ahmed Bilal, Tomonari Koike, Ying Yu, Tomohiro Inoue, Tadashi Aoki, Enqi Liu, and Jianglin Fan. 2010. "High-Fat Diet without Excess Calories Induces Metabolic Disorders and Enhances Atherosclerosis in Rabbits." *Atherosclerosis* 213 (1): 148–55. https://doi.org/10.1016/j.atherosclerosis.2010.07.051.

Warren, Katherine, Helena Burden, and Paul Abrams. 2016. "Mirabegron in Overactive Bladder Patients: Efficacy Review and Update on Drug Safety." *Therapeutic Advances in Drug Safety*. SAGE Publications Ltd. https://doi.org/10.1177/2042098616659412.

Wautier, Marie Paule, Olivier Chappey, Stefano Corda, David M. Stern, Ann Marie Schmidt, and Jean Luc Wautier. 2001. "Activation of NADPH Oxidase by AGE Links Oxidant Stress to Altered Gene Expression via RAGE." *American Journal of Physiology - Endocrinology and Metabolism* 280 (5 43-5). https://doi.org/10.1152/ajpendo.2001.280.5.e685.

Welsh, Jean A., Andrea Sharma, Jerome L. Abramson, Viola Vaccarino, Cathleen Gillespie, and Miriam B. Vos. 2010. "Caloric Sweetener Consumption and Dyslipidemia among US Adults." *JAMA - Journal of the American Medical Association* 303 (15): 1490–97. https://doi.org/10.1001/jama.2010.449.

Weverling-Rijnsburger, Annelies W.E., Iris J.A.M. Jonkers, Eric Van Exel, Jacobijn Gussekloo, and Rudi G.J. Westendorp. 2003. "High-Density vs Low-Density Lipoprotein Cholesterol as the Risk Factor for Coronary Artery Disease and Stroke in Old Age." *Archives of Internal Medicine* 163 (13): 1549–54. https://doi.org/10.1001/archinte.163.13.1549.

WHO. 2020. “WHO/Europe | Nutrition - Body Mass Index - BMI.” 2020. https://www.euro.who.int/en/health-topics/disease-prevention/nutrition/a-healthy-lifestyle/body-mass-index-bmi.

Wilkinson, Ian B., Stanley S. Franklin, and John R. Cockcroft. 2004. “Nitric Oxide and the Regulation of Large Artery Stiffness: From Physiology to Pharmacology.” *Hypertension*. Lippincott Williams & Wilkins. https://doi.org/10.1161/01.HYP.0000138068.03893.40.

Wilkinson, Michael J., Emily N.C. Manoogian, Adena Zadourian, Hannah Lo, Savannah Fakhouri, Azarin Shoghi, Xinran Wang, et al. 2020. “Ten-Hour Time-Restricted Eating Reduces Weight, Blood Pressure, and Atherogenic Lipids in Patients with Metabolic Syndrome.” *Cell Metabolism* 31 (1): 92-104.e5. https://doi.org/10.1016/j.cmet.2019.11.004.

Wilson, Peter W.F., Ralph B. D’Agostino, Helen Parise, Lisa Sullivan, and James B. Meigs. 2005. “Metabolic Syndrome as a Precursor of Cardiovascular Disease and Type 2 Diabetes Mellitus.” *Circulation* 112 (20): 3066–72. https://doi.org/10.1161/CIRCULATIONAHA.105.539528.

Wong, Sok Kuan, Kok-Yong Chin, Farihah Hj Suhaimi, Ahmad Fairus, and Soelaiman Ima-Nirwana. 2016. “Animal Models of Metabolic Syndrome: A Review.” *Nutrition & Metabolism* 13 (1): 65. https://doi.org/10.1186/s12986-016-0123-9.

Worthmann, Anna, Clara John, Malte C. Rühlemann, Miriam Baguhl, Femke Anouska Heinsen, Nicola Schaltenberg, Markus Heine, et al. 2017. “Cold-Induced Conversion of Cholesterol to Bile Acids in Mice Shapes the Gut Microbiome and Promotes Adaptive Thermogenesis.” *Nature Medicine* 23 (7): 839–49. https://doi.org/10.1038/nm.4357.

Xiao, Cuiying, Margalit Goldgof, Oksana Gavrilova, and Marc L. Reitman. 2015. “Anti-Obesity and Metabolic Efficacy of the B3-Adrenergic Agonist, CL316243, in Mice at Thermoneutrality Compared to 22°C.” *Obesity* 23 (7): 1450–59. https://doi.org/10.1002/oby.21124.

Xydakis, Antonios M., Christopher C. Case, Peter H. Jones, Ron C. Hoogeveen, Mine Yine Liu, E. O’Brian Smith, Kathleen W. Nelson, and Christie M. Ballantyne. 2004. “Adiponectin, Inflammation, and the Expression of the Metabolic Syndrome in Obese Individuals: The Impact of Rapid Weight Lose through Caloric Restriction.” In *Journal of Clinical Endocrinology and Metabolism*, 89:2697–2703. J Clin Endocrinol Metab. https://doi.org/10.1210/jc.2003-031826.

Yamauchi, T., J. Kamon, Y. Minokoshi, Y. Ito, H. Waki, S. Uchida, S. Yamashita, et al. 2002. “Adiponectin Stimulates Glucose Utilization and Fatty-Acid Oxidation by Activating AMP-Activated Protein Kinase.” *Nature Medicine* 8 (11): 1288–95. https://doi.org/10.1038/nm788.

Yanai, Hidekatsu, Yoshiharu Tomono, Kumie Ito, Nobuyuki Furutani, Hiroshi Yoshida, and Norio Tada. 2008. “The Underlying Mechanisms for Development of Hypertension in the Metabolic Syndrome.” *Nutrition Journal*. BioMed Central. https://doi.org/10.1186/1475-2891-7-10.

Yang, Lin, Guoxia Liu, Sergey I. Zakharov, Andrew M. Bellinger, Marco Mongillo, and Steven O. Marx. 2007. “Protein Kinase G Phosphorylates Cav1.2 A1c and B2 Subunits.” *Circulation Research* 101 (5): 465–74. https://doi.org/10.1161/CIRCRESAHA.107.156976.

Ye, J. 2009. “Emerging Role of Adipose Tissue Hypoxia in Obesity and Insulin Resistance.” *International Journal of Obesity*. NIH Public Access. https://doi.org/10.1038/ijo.2008.229.

Yin, Wu, Ester Carballo-Jane, David G. McLaren, Vivienne H. Mendoza, Karen Gagen, Neil S. Geoghagen, Lesley Ann McNamara, et al. 2012. “Plasma Lipid Profiling across Species for the Identification of Optimal Animal Models of Human Dyslipidemia.” *Journal of Lipid Research* 53 (1): 51–65. https://doi.org/10.1194/jlr.M019927.

Yoo, Hye Jin. 2014. “Adipokines as a Novel Link between Obesity and Atherosclerosis.” *World Journal of Diabetes* 5 (3): 357. https://doi.org/10.4239/wjd.v5.i3.357.

Yoshizumi, Masao, Mark A. Perrella, John C. Burnett, and Mu En Lee. 1993. “Tumor Necrosis Factor Downregulates an Endothelial Nitric Oxide Synthase MRNA by Shortening Its Half-Life.” *Circulation Research* 73 (1): 205–9. https://doi.org/10.1161/01.RES.73.1.205.

Yu, Min, Chunshui Liang, Qianran Kong, Yihan Wang, and Minmin Li. 2020. “Efficacy of Combination Therapy with Ezetimibe and Statins versus a Double Dose of Statin Monotherapy in Participants with Hypercholesterolemia: A Meta-Analysis of Literature.” *Lipids in Health and Disease* 19 (1). https://doi.org/10.1186/s12944-019-1182-5.

Yudkin, John S., Meena Kumari, Steve E. Humphries, and Vidya Mohamed-Ali. 2000. “Inflammation, Obesity, Stress and Coronary Heart Disease: Is Interleukin-6 the Link?” *Atherosclerosis*. Elsevier. https://doi.org/10.1016/S0021-9150(99)00463-3.

Zanchetti, Alberto, Micheal Hennig, Hansjoerg Baurecht, Rong Tang, Cesare Cuspidi, Stefano Carugo, and Giuseppe Mancia. 2007. “Prevalence and Incidence of the Metabolic Syndrome in the European Lacidipine Study on Atherosclerosis (ELSA) and Its Relation with Carotid Intima-Media Thickness.” *Journal of Hypertension* 25 (12): 2463–70. https://doi.org/10.1097/HJH.0b013e3282f063d5.

Zatterale, Federica, Michele Longo, Jamal Naderi, Gregory Alexander Raciti, Antonella Desiderio, Claudia Miele, and Francesco Beguinot. 2020. “Chronic Adipose Tissue Inflammation Linking Obesity to Insulin Resistance and Type 2 Diabetes.” *Frontiers in Physiology*. Frontiers Media S.A. https://doi.org/10.3389/fphys.2019.01607.

Zhang, Xiaodan, Lu Xing, Xiaona Jia, Xiaocong Pang, Qian Xiang, Xia Zhao, Lingyue Ma, et al. 2020. “Comparative Lipid-Lowering/Increasing Efficacy of 7 Statins in Patients with Dyslipidemia, Cardiovascular Diseases, or Diabetes Mellitus: Systematic Review and Network Meta-Analyses of 50 Randomized Controlled Trials.” *Cardiovascular Therapeutics*. Hindawi Limited. https://doi.org/10.1155/2020/3987065.

Zhang, Yin Hua. 2017. “Nitric Oxide Signalling and Neuronal Nitric Oxide Synthase in the Heart under Stress.” *F1000Research*. Faculty of 1000 Ltd. https://doi.org/10.12688/f1000research.10128.1.

Zhou, Ming Sheng, Ivonne H. Schulman, and Qiang Zeng. 2012. “Link between the Renin-Angiotensin System and Insulin Resistance: Implications for Cardiovascular Disease.” *Vascular Medicine (United Kingdom)* 17 (5): 330–41. https://doi.org/10.1177/1358863X12450094.

Zhu, Lin, Andrew Hayen, and Katy J.L. Bell. 2020. “Legacy Effect of Fibrate Add-on Therapy in Diabetic Patients with Dyslipidemia: A Secondary Analysis of the ACCORDION Study.” *Cardiovascular Diabetology* 19 (1): 28. https://doi.org/10.1186/s12933-020-01002-x.

Zillich, Alan J., Jay Garg, Sanjib Basu, George L. Bakris, and Barry L. Carter. 2006. “Thiazide Diuretics, Potassium, and the Development of Diabetes: A Quantitative Review.” *Hypertension* 48 (2): 219–24. https://doi.org/10.1161/01.HYP.0000231552.10054.aa.

Zimmet, Paul, Dianna Magliano, Yuji Matsuzawa, George Alberti, and Jonathan Shaw. 2005. “The Metabolic Syndrome: A Global Public Health Problem and A New Definition.” *Journal of Atherosclerosis and Thrombosis* 12 (6): 295–300. https://doi.org/10.5551/jat.12.295.

Zinman, Bernard, Stewart B. Harris, Jan Neuman, Hertzel C. Gerstein, Ravi R. Retnakaran, Janet Raboud, Ying Qi, and Anthony J.G. Hanley. 2010. “Low-Dose Combination Therapy with Rosiglitazone and Metformin to Prevent Type 2 Diabetes Mellitus (CANOE Trial): A Double-Blind Randomised Controlled Study.” *The Lancet* 376 (9735): 103–11. https://doi.org/10.1016/S0140-6736(10)60746-5.

Zreikat, Hala H., Spencer E. Harpe, Patricia W. Slattum, D’Arcy P. Mays, Paulina A. Essah, and Kai I. Cheang. 2014. “Effect of Renin-Angiotensin System Inhibition on Cardiovascular Events in Older Hypertensive Patients with Metabolic Syndrome.” *Metabolism: Clinical and Experimental* 63 (3): 392–99. https://doi.org/10.1016/j.metabol.2013.11.006.

Zuliani, Giovanni, Stefano Volpato, Alessando Blè, Stefania Bandinelli, Anna Maria Corsi, Fulvio Lauretani, Giuseppe Paolisso, Renato Fellin, and Luigi Ferrucci. 2007. “High Interleukin-6 Plasma Levels Are Associated with Low HDL-C Levels in Community-Dwelling Older Adults: The InChianti Study.” *Atherosclerosis* 192 (2): 384–90. https://doi.org/10.1016/j.atherosclerosis.2006.05.024.

Résumé

Introduction

Le syndrome métabolique (SMet), également nommé syndrome cardiométabolique, regroupe plusieurs facteurs de risque qui, lorsqu'ils sont combinés, augmentent le risque de développer des maladies cardiovasculaires. Les causes sous-jacentes du SMet sont liées à une propagation mondiale d'un mode de vie occidental. Celui-ci se caractérise par une consommation accrue d'aliments riches en calories et faibles en fibres (« fast food ») et également, par un manque d'activité physique (mode de vie sédentaire). Ce syndrome est devenu un des principaux dangers pour la santé mondiale. En plus d'être un défi clinique et de son impact sur la santé de l'individu.

Le SMet est caractérisé par une accumulation accrue d'adiposité abdominale/viscérale qui conduit à une résistance à l'insuline. Autrement dit, l'obésité globale n'est pas le principal contributeur à une résistance à l'insuline. De plus, le concept d'obésité saine est maintenant répandue dans le monde de la recherche dépendant de la manière dont la graisse est distribuée. En effet, un certain nombre d'individus obèses présentent un métabolisme sain, pour lesquels une adiposité sous-cutanée est installée, plutôt qu'une adiposité abdominale. Ainsi, l'une des erreurs courantes faites dans le domaine de la recherche, est que la plupart des études établies se concentrent sur l'obésité en tant que facteur principal dans le SMet. C'est la raison pour laquelle, il est indispensable de se concentrer également sur une autre catégorie de personnes, qui est sans aucun doute présente parmi les patients atteints de SMet. Cette catégorie inclue les patients nommés métaboliquement obèses mais sans surpoids.

Ainsi, dans notre étude, nous n'avons pas inclus l'obésité en tant que facteur du Smet, nous nous sommes focalisés sur la résistance à l'insuline. Afin d'induire une résistance à l'insuline plutôt qu'une obésité, nous avons utilisé un régime riche en graisses et en fructose (HFFD), connu pour sa capacité d'induire l'isulino-résistance (IR). Ce régime a la particularité de contenir la même quantité de calories que le régime témoin (standard) mais est moins riche en taux de protéines et de fibres. Quant au modèle animal utilisé dans cette étude, il s'agit du lapin Watanabe (Watanabe heritable hyperlipidemic (WHHL)) qui, en raison d'une mutation de son récepteur de lipoprotéines de basse densité (LDLr), développe spontanément une dyslipidémie et/ou une athérosclérose.

Dans notre étude, nous avons choisi de travailler sur deux molécules, BAY 41-2272 (stimulateur de guanylate cyclase soluble) et mirabegron (agoniste des récepteurs β3-adrénergiques). Notre choix est principalement lié à leurs effets, prometteurs dans le traitement des maladies métaboliques et cardiovasculaires, qui sont essentiellement dus à la modulation de la voie de guanosine monophosphate cyclique (GMPc). Ainsi, nous avons émis l'hypothèse que la modulation de la voie du monoxyde d'azote (NO)–GMPc, par des outils pharmacologiques, pourrait représenter une modalité thérapeutique prometteuse pour traiter le SMet et les pathologies cardiovasculaires qui y sont liées.

La FDA (Food and Drug Administration) et l'Agence européenne des médicaments (EMA), ont approuvé l'utilisation du BAY 41-2272 et du Mirabegron pour le traitement de l'hypertension artérielle pulmonaire et du syndrome de la vessie hyperactive, respectivement. En général, le processus du développement d'un médicament peut prendre jusqu'à 20 ans avant que le médicament ne soit approuvé et mis sur le marché. En effet, il faut généralement jusqu'à 15 ans pour qu'un médicament atteigne la phase d'essai clinique, qui se révèle parfois infructueuse. Par conséquent, le concept des médicaments réutilisables[30] permet aux chercheurs d'économiser du temps, de l'énergie et des ressources.

Les objectifs de notre étude sont, dans un premier temps, de mettre en place un modèle de SMet, induit expérimentalement, qui combine principalement la dyslipidémie et la résistance à l'IR chez le lapin WHHL. Dans un deuxième temps, l'exploration des effets du BAY 41-2272 et du mirabegron sur les perturbations métaboliques et cardiovasculaires associées au Smet, est effectuée. Les paramètres associés au SMet sont évalués au cours d'un protocole de 12 semaines. Le protocole est basé sur quatre groupes de lapins WHHL qui ont reçu un régime témoin, un HFFD, un HFFD avec du BAY 41-2272 et HFFD avec du Mirabegron.

[30] Les médicaments réutilisables sont des médicaments qui ont été initialement développés pour traiter une certaine maladie et qui se sont révélés avoir des effets bénéfiques prometteurs dans le traitement d'une autre maladie.

Syndrome métabolique

Définition

Le SMet, également connu sous le nom de syndrome cardiométabolique, fait référence à la co-occurrence d'un groupe de troubles métaboliques et de facteurs de risque cardiovasculaire. Ceux-ci comprennent la résistance à l'insuline/l'intolérance au glucose, l'obésité viscérale/centrale, la dyslipidémie athérogène et l'hypertension artérielle (Zimmet et al.2005)(Rochlani et al.2017). La définition du MetS a fait l'objet de débats et de controverses en raison de sa nature complexe, interdépendante et multifactorielle (Tune et al.2017).

Physiopathologie

Obésité abdominale/viscérale

Selon l'organisation mondiale de la santé (OMS), un individu est considéré comme obèse lorsque son indice de masse corporelle (IMC) est supérieur ou égal à 30. Lorsque l'IMC varie entre 25 et 34,9 kg / m^2, des seuils de tour de taille spécifiques au sexe sont utilisés en concomitance avec l'IMC, afin d'identifier les patients à risque. L'homme et la femme sont considérés comme obèses lorsque leur tour de taille dépasse respectivement 102 et 88 cm, respectivement.

La prévalence de l'obésité est principalement causée par une consommation accrue d'aliments riches en calories et une activité physique réduite, conduisant à un déséquilibre entre l'apport énergétique et la dépense énergétique, et éventuellement à une prise de poids excessive (Drenowatz 2015). L'équilibre entre la lipolyse des adipocytes et la synthèse des triglycérides, qui est habituellement régulée par les hormones et le système nerveux autonome, est perturbé chez les patients obèses (Kershaw and Flier 2004). Outre sa fonction de stockage d'énergie, le tissu adipeux est un organe endocrinien qui participe à l'homéostasie énergétique et qui permet une réponse rapide et dynamique aux altérations énergétiques. Pour s'adapter à l'excès de nutriments, le tissus adipeux peut subir une hypertrophie et hyperplasie (Halberg, Wernstedt-Asterholm, and Scherer 2008)(Sun, Kusminski, and Scherer 2011)(Longo et al. 2019). L'élargissement des adipocytes entrainerait une diminution de l'apport sanguin conduisant à une hypoxie (Ellulu et al. 2017). Il a été proposé que cette hypoxie induirait une nécrose ainsi qu'une infiltration de macrophages conduisant à une surproduction d'adipocytokines, y compris des médiateurs pro-inflammatoires

(facteur de nécrose tumorale α (TNF-α) et l'interleukine-6 (IL-6)), des acides gras libres (AGL), de la leptine, l'inhibiteur de l'activateur du plasminogène-1 (IAP-1), la protéine C-réactive (CRP) et l'angiotensinogène (Ye 2009)(Chan and Hsieh 2017). L'inflammation localisée au niveau du tissu adipeux se propage plus tard, engendrant ainsi une inflammation systémique globale de bas grade, qui par la suite entraîne d'autres complications observées dans le SMet (Zatterale et al. 2020) **(Figure 26)**.

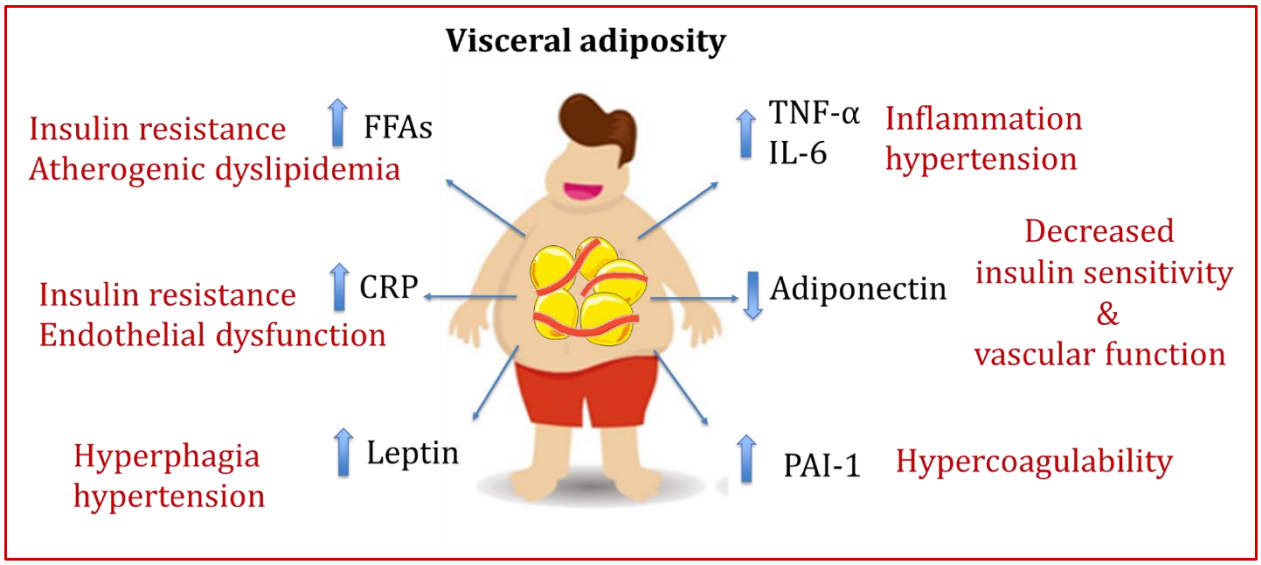

Figure 26: Rôle de l'obésité viscérale dans le développement du syndrome métabolique.

Résistance à l'insuline

La résistance à l'insuline est l'une des composantes principales et essentielles du SMet. Elle est décrite comme une baisse de réponse des tissus périphériques à l'effet de l'insuline (Kaur 2014). Pour tenter de contrebalancer cet état, la sécrétion d'insuline est augmentée, conduisant à un état d'hyperinsulinémie (Liese, Mayer-Davis, and Haffner 1998). En général, la résistance à l'insuline se caractérise par une augmentation des taux d'insuline (hyperinsulinémie), une hyperglycémie et une altération de l'évaluation du modèle homéostatique de la résistance à l'insuline (HOMA-IR) (Beilby 2004).

L'obésité abdominale et la résistance à l'insuline semblent être les deux facteurs principaux du SMet (Cornier et al. 2008)(Gallagher et al. 2010). Il semblerait également que les AGL et les

cytokines inflammatoires, non seulement, jouent un rôle central dans le développement de la résistance à l'insuline, mais constituent aussi un lien entre cette résistance et l'obésité (Kahn et al. 2006). Cependant, il est à noter que certaines personnes obèses sont métaboliquement normales avec une sensibilité à l'insuline normale; tandis que la résistance à l'insuline peut être présente chez les sujets non obèses (Ruderman et al. 1998) (Karelis et al. 2005). En effet, il existe une catégorie d'individus qui sont nommés métaboliquement obèses sans un surpoids. Ces personnes présentent une baisse de sensibilité à l'insuline ainsi que des risques élevés de développer un diabète et des maladies cardiovasculaires (Lee et al. 2015).

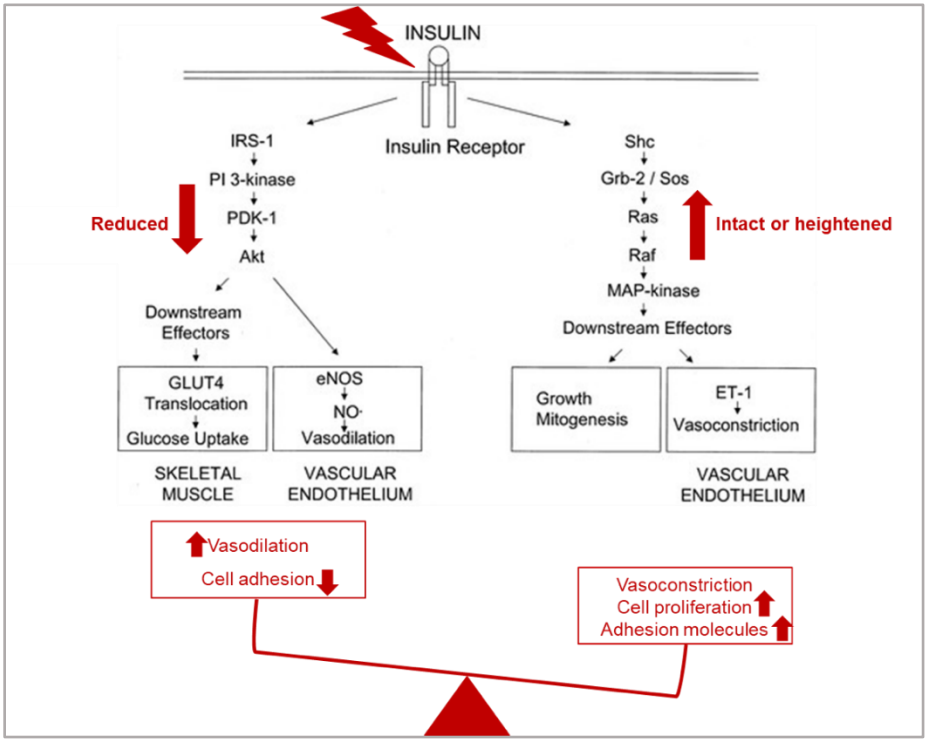

Figure 27: Un schéma représentant les conséquences du déséquilibre entre les voies IRS-PI3K-Akt et Ras protéine-mitogène-activé protéine kinase (Ras-MAPK), qui se produit au cours de la résistance à l'insuline.

Dans les états de résistance à l'insuline, tous les tissus périphériques deviennent insensibles à l'effet de l'insuline, entraînant une hyperglycémie maintenue et des effets orexigènes accrus (Kaur 2014). Seule la voie de signalisation insulin receptor substrate1- phosphoinositide 3-kinase-protein kinase B- nitic oxide (IRS1-PI3K-Akt-NO) est réduite, tandis que la voie de signalisation Ras kinase- Mitogen-activated protein kinase-endothelin1 (Ras-MAPK-ET1) reste intacte ou devient

renforcée. Le déséquilibre entre ces deux voies conduit à une dysfonction endothéliale en raison d'une diminution de la synthèse de NO. Cette diminution est caractérisée avec différents niveaux de production non affectés d'ET-1 en plus de l'expression de molécules d'adhésion des cellules vasculaires et de la prolifération des cellules musculaires lisses (Muniyappa and Sowers 2013). Par conséquent, la translocation du transporteur de glucose (GLUT4) est réduite, ce qui entraîne une diminution de l'absorption des graisses et du glucose musculaire (Kim et al. 2006) (**Figure 27**).

Les actions métaboliques et hémodynamiques de l'insuline semblent être complémentaires. Puisque, en plus de son action vasodilatatrice via l'activation de la NO synthase endothéliale (eNOS) et la production ultérieure de NO, l'insuline améliore l'apport de glucose au tissu cible par le recrutement capillaire (Barrett et al. 2011b). Lors d'une résistance à l'insuline, la vasodilatation induite par l'insuline est diminuée ou altérée, ce qui entraîne une diminution de l'apport de glucose et de l'insuline aux organes cibles. De plus, l'altération du métabolisme intracellulaire du glucose et des lipides médiée par l'insuline entraîne une augmentation des niveaux d'espèces réactives de l'oxygène (ROS) et des espèces réactives de l'azote (RNS). Ceci va entrainer une plus grande consommation de NO, et donc une nouvelle diminution de la disponibilité du NO (Cersosimo and DeFronzo 2006) (**Figure 28**).

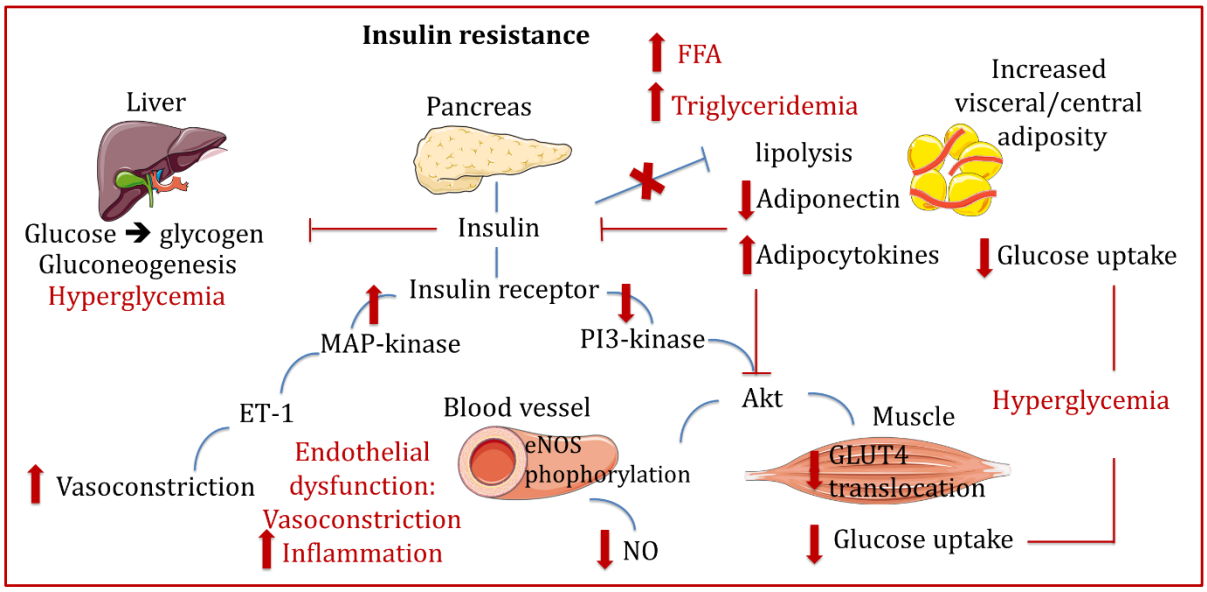

Figure 28: Rôle de la résistance à l'insuline dans la pathogenèse du syndrome métabolique.

Dyslipidémie

La dyslipidémie est caractérisée par une augmentation du taux plasmatiques des triglycérides (TG) et des lipoprotéines de basses densités (LDL-C). Elle est également caractérisée par une diminution du taux des lipoprotéines de hautes densités (HDL-C) (Grundy 2006). La résistance à l'insuline et l'obésité viscérale sont associées à la dyslipidémie athérogène (Giannini et al. 2011)(Hwang et al. 2016).

Dans des conditions physiologiques, l'insuline diminue la production et la sécrétion des triglycérides, des lipoprotéines de très basses densités (VLDL) et d'apolipoprotéine B (apoB). Elle améliore également la dégradation de de l'apolipoprotéine B (apoB) (Gonzalez-Baró, Lewin, and Coleman 2007)(Sparks, Sparks, and Adeli 2012). Dans des conditions normales, l'insuline modifie l'activité de l'apoB par les voies dépendantes du PI3K et régule l'activité de la lipoprotéine lipase, conduisant respectivement à une diminution de la production et à une augmentation de la clairance des VLDL. Puisque dans des conditions d'insulino-resistance, l'insuline est incapable d'exercer ses effets, ces deux actions sont contrariées. Ceci conduit à une augmentation du taux de VLDL. De plus, ceci amène également à une altération de la signalisation de l'insuline qui entraîne une augmentation de la lipolyse et une augmentation ultérieure des taux d'AGL (Kaur 2014).

Quelle résulte de la résistance à l'insuline elle-même ou du tissu adipeux viscéral hypertrophié, l'augmentation du flux d'acides gras libres (AGL) vers le foie entraîne une augmentation de la production et du stockage des TG. Puis, l'excès de TG est regroupé avec l'apoB et sécrété sous forme de VLDL (Lewis et al. 1995)(Lewis and Steiner 1996)(Ginsberg et al. 2005). Dans le transport inverse du cholestérol, la protéine de transport des esters de cholestérol (CETP) stimule le transfert des TG des VLDL vers les HDL et, des CETP des HDL vers les VLDL. Ainsi, des taux accrus de TG et de VLDL se traduisent par des particules de HDL enrichies en TG et de VLDL enrichies en CETP (Ginsberg et al. 2005). Les particules HDL enrichies en TG sont de meilleurs substrats pour la lipase hépatique, ce qui les rendent plus susceptible à l'elimination. Ces particules sont ensuite rapidement éliminées de la circulation, ce qui entraîne une diminution des concentrations plasmatiques de HDL et ainsi une dyslipidémie athérogène (Lamarche et al. 1999) (Kaur 2014). En effet, le HDL-C est bien connu pour ses propriétés anti-athérosclérotiques et anti-inflammatoires (Weverling-Rijnsburger et al. 2003)(Sanossian et al. 2007). Ainsi, des taux réduits en HDL sont associés à un risque cardiovasculaire accru. De plus, même si les niveaux de LDL sont parfois inchangés, le fait que les particules de LDL enrichies en TG soient petites et denses, facilite leur pénétration dans la paroi endothéliale et les rend plus sensibles à l'oxydation, augmentant encore l'athérogénicité et le risque cardiovasculaire (Lamarche et al. 1998) (Hulthe et al. 2000) (Cornier et al. 2008) **(Figure 29)**.

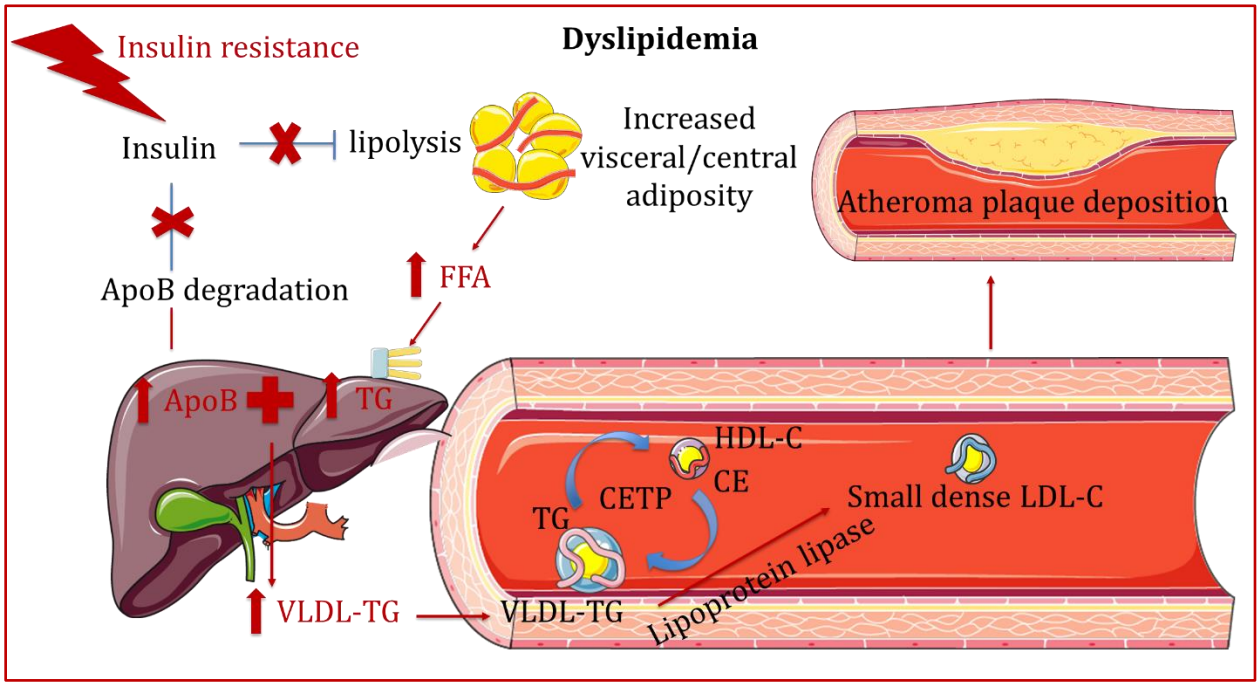

Figure 29: Dyslipidémie athérogène dans le syndrome métabolique.

Hypertension artérielle

L'hypertension est une des facteurs de risque majeurs constituant le SMet. En effet, Jusqu'à un tiers des patients hypertendus sont également atteint du SMet (Schillaci et al. 2004)(Cuspidi et al. 2004). Dans le diagnostic clinique de l'hypertension artérielle, un individu est considéré comme hypertendu lorsque la pression artérielle (PA) systolique et/ou la pression artérielle diastolique dépassent, respectivement, 130 mmHg et 85 mmHg. L'augmentation de la pression artérielle chez les patients du SMet semble être fortement associée à une augmentation de l'adiposité viscérale et de l'IR (Ferrannini et al. 1997)(Yanai et al. 2008). De multiples mécanismes sont à l'origine du développement de l'hypertension dans le SMet, tels que l'activation de la rénine angiotensine aldostérone (RAAS) et l'activité (SNS). De plus, le tissu adipeux viscéral hypertrophique est responsable de la production et de la sécrétion de nombreux adipocytokines, telles que la TNF-α, l'IL-6, l'angiotensinogène, la leptine et les AGL. Ces molécules participent à l'augmentation de la PA par différentes voies (Katagiri et al. 2007) (**Figure 30**).

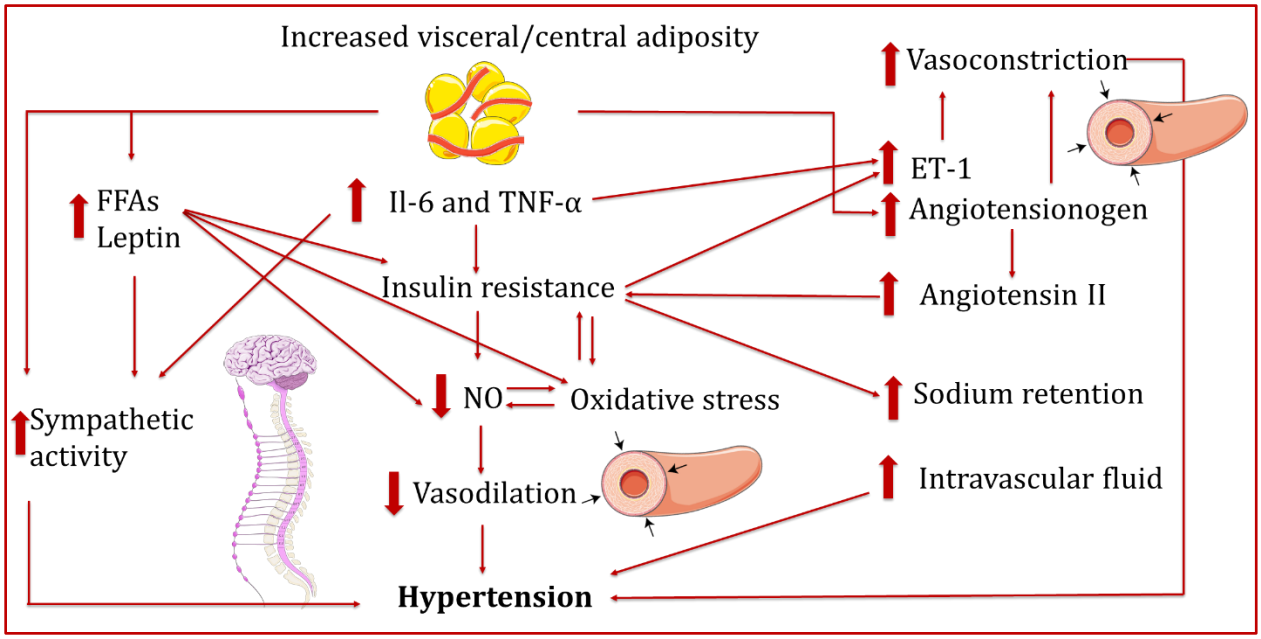

Figure 30: Un schéma qui représente les mécanismes impliqués dans le développement de l'hypertension dans le syndrome métabolique.

Objectifs de l’étude

Le SMet augmente le risque de développement d’un diabète de type 2 et de maladies cardiovasculaires, ainsi il est considéré comme une menace sanitaire et économique pour la société. Par conséquent, il est essentiel de chercher des mesures thérapeutiques et préventives afin d’améliorer la prise en charge de ce syndrome. Actuellement, la plupart des médicaments utilisés dans le traitement de ce syndrome ciblent uniquement chaque facteur de risque. Par conséquent, l'utilisation de molécules ayant des effets pléiotropes ou qui agissent sur un large spectre de cellules et de tissus, pourrait être plus efficace dans la gestion de ce syndrome multifactoriel.

De plus en plus, des études ont montré que la modulation de la signalisation au niveau de la voie de NO-GMPc, par des outils pharmacologiques, est efficace, dans des contextes de maladies métaboliques et cardiovasculaires (J.-P. Stasch et al. 2002)(Mitschke et al. 2013)(Nossaman and Kadowitz 2013)(Pfeifer et al. 2013)(Ramirez et al. 2015)(M. Park, Sandner, and Krieg 2018). Par la suite, nous avons émis l'hypothèse que l'activation pharmacologique chronique de la voie NO-sGC-cGMP pourrait représenter une thérapie pharmacologique prometteuse pour traiter la combinaison de deux composants majeurs du SMet, la dyslipidémie et la résistance à l’insuline.

Notre premier objectif était de développer et de caractériser un modèle animal expérimental de syndrome métabolique avec une dyslipidémie et une résistance à l'insuline comme principaux facteurs de risque.

Notre deuxième objectif était d'étudier l'efficacité d'un agoniste des récepteurs β3-adrénergiques (β3-AR), le Mirabegron, et d'un stimulateur sGC, le BAY 41-2272, dans l'atténuation des perturbations métaboliques associées à la combinaison dyslipidémie-IR, et ainsi dans la prévention du développement des pathologies cardiovasculaires qui lui sont associés.

Afin de répondre à ces ojectifs, nous avons utilisés les lapins Watanabe qui sont des modèles animaux d'hypercholestérolémie familiale humaine (FH) et de dyslipidémie spontanée due à un défaut génétique dans leur récepteur LDL. Notre protocole expérimental a duré 12 semaines et a inclus quatre groupes de lapins Watanabe: contrôle, HFFD, HFFD avec BAY 41-2272 et HFFD avec Mirabegron. Le régime riche en graisses en fructose (HFFD) a été utilisé pour induire l’insulino-résistance.

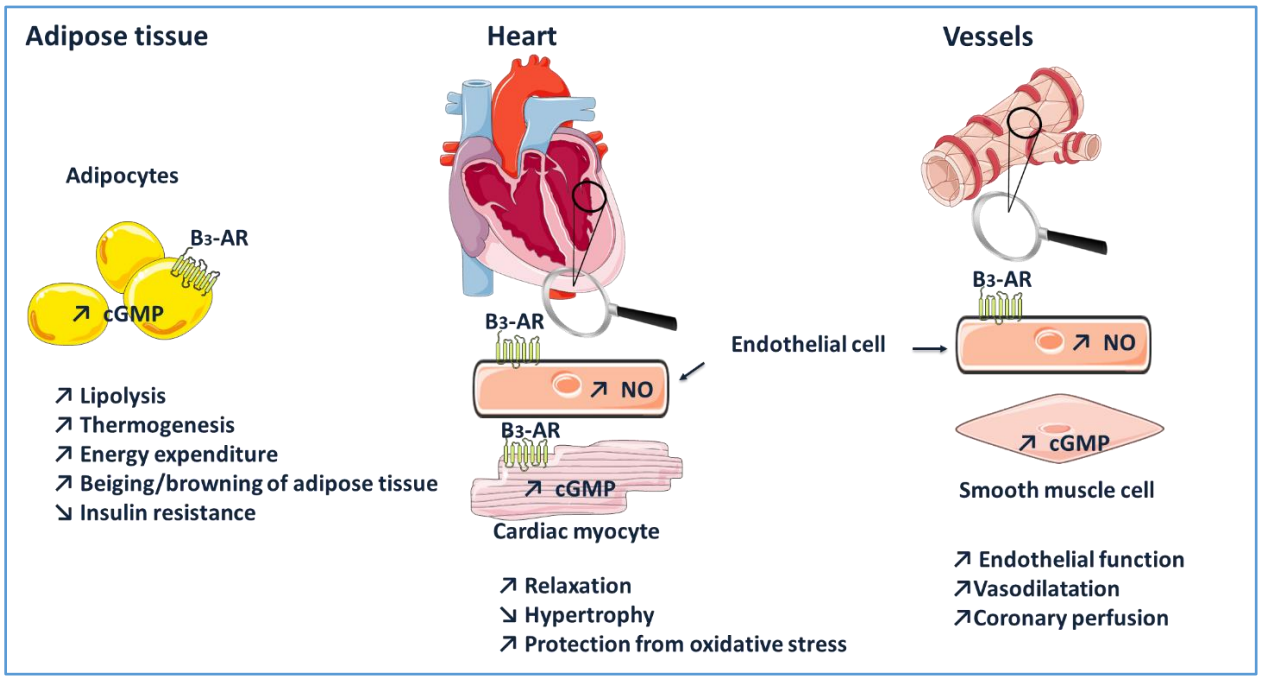

Figure 31: Effet thérapeutique du mirabegron et du BAY 41-2272 par l'activation de la voie de NO-cGMP dans les tissu adipeux, le cœur et les vaisseaux.

Le Mirabegron et BAY 41-2272 activent, respectivement, les récepteurs β_3-AR et la voie sGC-GMPc :

- Dans les adipocytes (à gauche), entraînant une augmentation de la lipolyse (tissu adipeux blanc), de la dépense énergétique (augmentation de la lipolyse et de la thermogenèse dans le tissu adipeux brun), le brunissement des adipocytes et l'amélioration de la sensibilité à l'insuline (par le passage transcapillaire de l'insuline et du glucose aux tissus cibles)
- Dans les myocytes cardiaques (centre) provoquant, des effets protecteurs antioxydants induite par les GMPc contre le remodelage ainsi qu'une meilleure relaxation.
- Dans les cellules endothéliales et cellules musculaires lisses du système vasculaire (à droite; y compris les artères coronaires), engendrant une augmentation de la vasodilatation dépendante de l'endothélium et de la perfusion myocardique (Balligand 2016)(Pouleur et al. 2018).

Design de l'étude

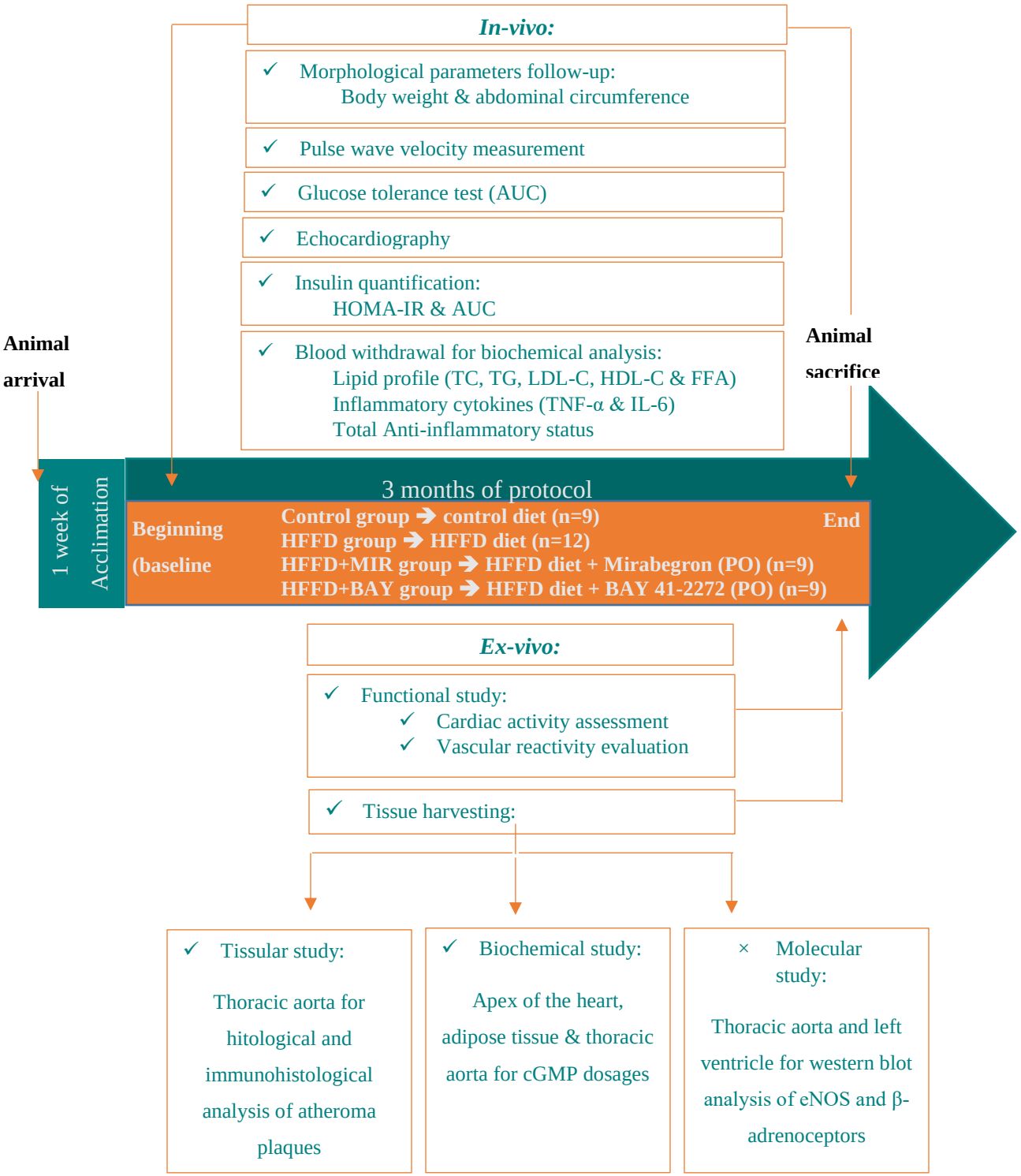

Résultats

Article numéro 1: Développement et caractérisation d'un modèle expérimental de syndrome métabolique avec la dyslipidémie et la résistance à l'insuline comme facteurs principaux chez les lapins Watanabe.

Contexte et objectif: En raison de son lien avec les maladies cardiovasculaires, le syndrome métabolique (SMet) est devenu un fardeau majeur de santé publique. Travailler sur un modèle animal approprié qui imite la maladie humaine est d'une grande importance. Cependant, jusqu'à présent, la physiopathologie de ce syndrome sans le facteur d'obésité est peu connue. Cette étude a été conçue afin d'étudier les perturbations métaboliques et cardiovasculaires associées à la combinaison de deux caractéristiques principales de ce syndrome, la dyslipidémie et la résistance à l'insuline.

Méthodes: 21 lapins Watanabe mâles et femelles (WHHL) ont été aléatoirement assignés au groupe témoin (n = 9) et HFFD (n = 12) qui ont été soumis à un régime alimentaire standard et un régime alimentaire riche en fructose et riche en graisses (HFFD), respectivement. Le protocole a duré 12 semaines, au cours desquelles le poids et la circonférence abdominale ont été surveillés; les taux plasmatiques de lipides, de glucose et d'insuline à jeun ont été mesurés et un test intraveineux de tolérance au glucose (TTG) a été réalisé. L'évaluation du modèle homéostatique de la résistance à l'insuline (HOMA-IR) a été calculé. La fonction cardiaque a été évaluée à l'aide d'approches *in vivo* (échocardiographie) et *ex vivo* (cœur isolé de Langendorff). La réactivité et l'élasticité vasculaires ont été évaluées sur des artères de carotides isolées (myographie) et en déterminant la vitesse d'onde de pouls, respectivement.

Résultats: Les lapins nourris au HFFD ont présenté une augmentation de l'insuline à jeun, de l'HOMA-IR, de l'aire sous la courbe du TTG, des triglycérides, du taux de cholestérol, des LDL-C, de la sensibilité à la phényléphrine et une diminution de la contractilité cardiaque et de la vasorelaxation induite par l'insuline.

Conclusion: Nos résultats ont montré que le HFFD induit une résistance à l'insuline et accentue la dyslipidémie; et que, lorsqu'ils sont soumis à HFFD, les lapins Watanabe pourraient devenir un

modèle animal de SMet avec deux caractéristiques principales, une dyslipidémie et une résistance à l'insuline.

Article numéro 2: Etude des effets du traitement au Mirabegron, un agoniste des récepteurs β3-adrénergiques, sur les paramètres métaboliques et cardiovasculaires d'un modèle animal de dyslipidémie et de résistance à l'insuline.

Introduction: Le syndrome métabolique (SMet) est une épidémie mondiale de santé et un fardeau économique. Il est essentiel de trouver une approche pharmacologique appropriée pour gérer ce syndrome. Nous avons exploré le potentiel du mirabegron (MIR), un agoniste β_3-adrénergique en tant qu'agent thérapeutique réutilisé pour le traitement du SMet et de ses conséquences cardiovasculaires.

Méthodes: 30 lapins Watanabe, mâles et femelles (WHHL), ont été aléatoirement reparties dans des groupes : témoins (n = 9), HFFD (n = 12) et HFFD + MIR (n = 9) qui, respectivement, ont reçu les traitements suivants: régime standard, régime HFFD (riche en fructose et en gras) et régime HFFD avec le MIR (3 mg / kg, PO). Le protocole a duré 12 semaines, au cours desquelles le poids et la circonférence abdominale ont été surveillés; les taux plasmatiques de lipides, de glucose et d'insuline à jeun ont été mesurés et un test intraveineux de tolérance au glucose (TTG) a été réalisé. L'évaluation du modèle d'homéostasie de la résistance à l'insuline (HOMA-IR) a été calculée. La fonction cardiaque a été évaluée à l'aide d'approches in vivo (échocardiographie) et ex vivo (cœur isolé de Langendorff). La réactivité vasculaire et la rigidité artérielle ont été évaluées sur des artères carotides isolées et en déterminant la vitesse d'onde pouls, respectivement.

Résultats: Les lapins soumis au HFFD ont présenté une augmentation significative de l'insuline à jeun, l' HOMA-IR, de l'aire sous la courbe du TTG, des triglycérides (TG), du cholestérol total, et des lipoprotéines de basses densités ainsi qu'une diminution de la contractilité cardiaque, par rapport au groupe témoin. Le traitement au MIR a empêché l'augmentation des taux d'insuline à jeun, d'HOMA-IR et de TG et a entrainé une augmentation significative de l'inotropie cardiaque et de la lusitropie par rapport au groupe HFFD.

Conclusion: le traitement à long terme au MIR a stabilisé le gain de poids et le taux des TG et a amélioré la sensibilité à l'insuline et la fonction cardiaque d'un modèle animal de lapin combinant deux facteurs majeurs du SMet, la dyslipidémie et la résistance à l'insuline.

Article numéro 3: Effet d'un traitement à long terme au BAY 41-2272, un stimulateur de la guanylate cyclase soluble, sur les paramètres métaboliques et cardiovasculaires d'un modèle animal de dyslipidémie et de résistance à l'insuline.

Introduction: Le syndrome métabolique (SMet) est associé à des risques accrus de diabète de type 2 et de maladies cardiovasculaires. Compte tenu du caractère multifactoriel de ce syndrome, la prise en charge de ce syndrome nécessite une approche thérapeutique pharmacologique à effet pléotropique. Nous avons exploré le potentiel d'un modulateur de la voie de guanosine monophosphate cylcic (GMPc), BAY 41-2272 (BAY), dans le traitement du SMet et de ses conséquences cardiovasculaires.

Méthodes: 30 lapins Watanabe (WHHL) ont été aléatoirement réparties dans des groupes : témoins (n = 9), HFFD (n = 12) et HFFD + BAY (n = 9) qui, respectivement, ont reçu un régime standard, un régime HFFD et un régime HFFD (riche en fructose et en gras) avec le BAY (3 mg / kg, PO). Le protocole a duré 12 semaines, au cours desquelles le poids et la circonférence abdominale ont été surveillés; les taux plasmatiques de lipides, de glucose et d'insuline à jeun ont été mesurés et un test intraveineux de tolérance au glucose (TTG) a été réalisé. L'évaluation du modèle d'homéostasie de la résistance à l'insuline (HOMA-IR) a été calculée. La fonction cardiaque a été évaluée à l'aide d'approches in vivo (échocardiographie) et ex vivo (cœur isolé de Langendorff). La réactivité vasculaire et la rigidité artérielle ont été évaluées sur des artères carotides isolées et en déterminant le PWV, respectivement.

Résultats: Les lapins nourris avec du HFFD ont présenté une augmentation significative de l'insuline à jeun, HOMA-IR, de l'aire sous la courbe du TTG, des triglycérides (TG), du cholestérol total, de la sensibilité à la phényléphrine et une diminution significative de la vasorelaxation médiée par l'insuline, par rapport au groupe témoin. Le traitement par BAY a empêché l'augmentation des taux d'insuline à jeun, de l'HOMA-IR, des TG et de l'hypersensibilité à la phényléphrine induite par le HFFD.

Conclusion: le traitement à long terme au BAY a stabilisé le gain de poids et les taux de TG, amélioré la sensibilité à l'insuline et amélioré la fonction endothéliale, en diminuant la sensibilité aux α1-adrénorécepteurs, d'un modèle animal de SMet qui combine la dyslipidémie et la résistance à l'insuline

Conclusion

Dans notre étude on a réussi:

- ✓ Dans un premier temps à induire une insulino-résistance chez un modèle animal, présentant une dyslipidémie spontanée, créant ainsi un lapin modèle de Smet avec deux facteurs principaux, la dyslipidémie et l'insulino-résistance.

- ✓ Dans un second temps, on a prouvé que la modulation de la voie de GMPc pourrait être une stratégie prometteuse dans la prise en charge du syndrome métabolique.

DOCTORAT BIOLOGIE BRETAGNE SANTE LOIRE

ÉCOLE NATIONALE VÉTÉRINAIRE, AGROALIMENTAIRE ET DE L'ALIMENTATION
SANTÉ ET ALIMENTATION AU CŒUR DE LA VIE

Titre : Effets métaboliques et cardiovasculaires de la modulation de la voie de signalisation oxyde nitrique-guanosine monophosphate cyclique (NO-GMPc): Etude dans un modèle expérimental de syndrome métabolique induit par une alimentation riche en fructose et en graisses chez le lapin Watanabe.

Mots clés : Syndrome métabolique, insulino-résistance, dyslipidémie, la voie de signalisation NO-GMPc, mirabegron, BAY-412272, lapin watanabe, HFFD.

Résumé : Le syndrome métabolique (SMet) est caractérisé par la présence chez le même individu de plusieurs anomalies parmi les suivantes: une adiposité abdominale, une insulino-résistance (IR), une intolérance au glucose, une hypertension artérielle et une dyslipidémie. Des études ont révélé que la modulation de la voie de signalisation NO/GMPc dans le SMet peut exercer des effets métaboliques et cardiovasculaires protecteurs. Nous avons exploré, dans ce contexte, l'effet du mirabegron et du BAY 41-2272, deux molécules connues pour leur capacité à activer la voie NO-GMPc. Nous avons d'abord développé un modèle animal expérimental avec deux facteurs principaux du SMet, la dyslipidémie et l'IR. Nos résultats ont montré qu'après 12 semaines d'alimentation riche en fructose et en graisses (HFFD), le lapin Watanabe (WHHL), un modèle animal de dyslipidémie spontanée, présentait une intolérance au glucose, une IR (test HOMA-IR), une aggravation de la dyslipidémie et une diminution de la contractilité cardiaque (approche *ex-vivo*). Après 12 semaines de traitement, le mirabegron et le BAY 41-2272 ont prévenu le gain de poids et l'augmentation du taux de TG et ont amélioré la sensibilité à l'insuline, la fonction endothéliale des artères carotides et la fonction cardiaque (mirabegron). Ce travail a permis de mettre en place un modèle expérimental combinant la dyslipidémie et l'IR chez le lapin WHHL. De plus, les résultats ont montré que l'activation à long terme de la voie de signalisation NO-GMPc représente une approche pharmacologique prometteuse dans la gestion des complications métaboliques et cardiovasculaires associées au SMet.

Title: Metabolic and cardiovascular effects of nitric oxide-cyclic guanosine monophosphate (NO-cGMP) signaling pathway modulation: Study in the WHHL rabbit as an experimental model of high fructose high fat diet-induced metabolic syndrome.

Keywords: Metabolic syndrome, insulin resistance, dyslipidemia, NO-cGMP signaling pathway, mirabegron, BAY41-272, WHHL rabbit, HFFD.

Abstract: Metabolic syndrome (MetS) is characterized by abdominal adiposity, insulin resistance (IR), glucose intolerance, arterial hypertension and dyslipidemia. Experimental studies have revealed that modulation of the nitric oxide-cyclic guanosine monophosphate (NO-cGMP) signaling pathway in MetS can exert protective metabolic and cardiovascular effects. In this regard, we explored the effect of mirabegron and BAY 41-2272, two molecules known for their ability to activate the NO-cGMP pathway. We first developed an experimental animal model with two main components of the MetS, dyslipidemia and IR. Our results showed that after 12 weeks of high-fructose high-fat diet (HFFD) feeding, the Watanabe heritable hyperlipidemic (WHHL) rabbit, an animal model of spontaneous dyslipidemia, exhibited glucose intolerance, IR (HOMA-IR test), an aggravation in dyslipidemia and a decrease in cardiac contractility (*ex-vivo* approach). Twelve weeks of mirabegron and BAY 41-2272 treatment prevented weight gain and the increase in TG levels and improved insulin sensitivity, carotid endothelial function, and cardiac function (mirabegron). We were able to develop an experimental model combining dyslipidemia and IR in the WHHL rabbit. Furthermore, our results showed that long-term activation of the NO-cGMP signaling pathway represents a promising pharmacological approach in the management of the MetS and its metabolic and cardiovascular consequences.